# GP130 Regulation of Breast Cancer Signaling and Bone Dissemination

By

Tolu Nelson Omokehinde

Dissertation

Submitted to the Faculty of the

Graduate School of Vanderbilt University

In partial fulfillment of the requirements

for the degree of

DOCTOR OF PHILOSOPHY

in

Cancer Biology

January 31, 2022

Nashville, Tennessee

Approved:

Julie A. Rhoades, Ph.D

Linda Sealy, Ph.D

Fiona Yull, D. Phil

Rachelle Johnson, Ph.D

To my family:

To my parents, for their unwavering support and their belief in me
To my brother, for the constant laughs and good times

To the Meyerhoff Scholars Program, for giving me the opportunity to become a scientist and building my confidence so that I can be change I want to see in the world

and

To my pristine wife and best friend, Geena, for all of her love and constant excitement in my life, if not for her support I would not have made it till the end.

# ACKNOWLEDGMENTS

The work presented in this dissertation was made possible by the financial support of the Howard Hughes Medical Institute (HHMI) Gilliam Fellowship for Advance Study, NIH award R00CA194198 (Rachelle Johnson) and DoD Breakthrough Award W81XWH-18-1-0029 (Rachelle Johnson).

First, I want to thank and acknowledge my mentor, Rachelle Johnson. Thank you for all of your support these past 5 years, but most importantly, thank you for believing in me and your endless support. All of the times I would knock on your door to ask questions, thank you for being available and taking the time for me. You have consistently advocated for me, and I will always be grateful to you for the scientist that I am today. I also would like to acknowledge my thesis committee, Julie Rhoades, Linda Sealy, and Fiona Yull. Thank you for challenging me to be a better scientist and for all your feedback and guidance throughout my graduate career.

To the past and present members of “J-Squad” aka. “Johnson Squad” aka. The Johnson lab. I would not be here today without your support both in and outside lab. You all have made graduate school enjoyable, and it’s been an honor to work beside you all. In particular, Courtney Edwards, Vera Todd, Miranda Clements, and Alec Jotte, you all have made my experience in the Johnson lab memorable. Thank you to Miranda for being our lab guru and passing down your knowledge to us. Thank you, Courtney, for not only being a lab mate but a true friend and someone I can count on (If you ever need some flow done, I got you). Lastly, thank you Vera for being day 1 Johnson lab mates together. To Jasmine Johnson and Tony (Lawrence) Vecchi III, thank you for being the best lab managers anyone could ever ask for. Your friendship and support these past few years have made lab enjoyable and without you both, this degree would not have been possible. To Alec Jotte, there are no words to describe how proud I am to have mentored you while in the Johnson lab. You are driven, hardworking, enthusiastic, and one of the most incredible people I have ever met. To me you were more than just my mentee, you were like a little brother to me, and I can’t wait to see where life takes you. To Lauren

Holtslander, you were the first undergraduate student to join the lab and you are not only driven, but an inspiring individual.

Thank you to the amazing administrators of IGP, in particular Beth Bowman and Carolyn Berry. You both made navigating the first two years of graduate school possible. The reason I choose Vanderbilt for my graduate career was because of the IMSD program. I would like to thank Christina Keeton, Linda Sealy and Roger Chalkley. To Roger and Linda, thank you being constant advocates and always being supportive of my goals since I arrived at Vanderbilt. Both of you supported me in nomination for the Gilliam Fellowship and have always advocated for the advancement of underrepresented minorities in STEM. Many of my fellow peers, including myself, would not have made it to the end of their PhD without your unwavering support and guidance. The university needs more people like you, who not only listen to graduate student needs, but act on them to make change. To Christina Keeton, I want to thank you for being more than just the administrator of ISMD, advisor and mentor. Thank you for being a close friend throughout my graduate career. In all my personal challenges in graduate school, you have been a constant ray of support. You have helped me through difficulties of graduate school, and I will be forever grateful to you.

Thank you to all my friends and IMSD family, that I met in graduate school. While we all came from different backgrounds and different parts of the world, we had a common goal in wanting to become scientists to hopefully change the world. It has been an honor to work and study alongside you all these past few years.

To my best friends from UMBC, Matthew Shirley, Kendall Queen, Jesse Smith, Catrina Johnson, Hilary Bright, and Randi Williams, thank you being my squad and closest friends anyone could ever ask for. I know we will continue to support each other no matter what and I look forward to continuing our friendship as we hold fast to dreams.

I would also like to thank the Meyerhoff Scholars Program at UMBC. For more than 30 years, the Meyerhoff Scholars program has been the pinnacle and example for fostering the growth and mentorship of underrepresented minorities that pursue terminal degrees in STEM. I stand on the shoulders of giants that came before me and I am proud to be a member of the 24$^{th}$ cohort of the Meyerhoff Scholars Program and a UMBC alum.

I would like to thank Dr. Freeman Hrabowski III, Earnestine Baker, Mistue Wiggs, Sharon Johnson, Keith Harmon, Michael Goodwyn, Ivanna Abreu, Alicia Hall and Jacqueline King for fostering my growth as an individual and believing in my success.

Finally, none of this would have been possible without the love and support of my family. To my brother, Victor Omokehinde, thank you for being a supportive younger brother and keeping me humble. To my parents, Stephen and Carol Omokehinde, thank you for being my biggest supporters and always pushing me to be the best version of myself. From the beginning, you both have always wanted my brother and I to reach for the stars. Whatever it is that we wanted to do in life, you wanted us to be the best at it so there aren't enough ways I can say "Thank You". To my wife Geena, despite the craziness of graduate school and the world, you are my moon and stars, and I cannot thank you enough for your unwavering support throughout this journey. I love you and none of this would have been possible without you.

*It takes a village.*

TABLE OF CONTENTS

Page

## LIST OF TABLES

## LIST OF FIGURES

ABBRREVIATIONS

| | |
|---|---|
| AKT | AKT serine/threonine kinase |
| AKT1 | AKT serine/threonine kinase 1 |
| AKT2 | AKT serine/threonine kinase 2 |
| ALDH1A1 | Aldehyde Dehydrogenase 1 Family, Member A1 |
| AMOT | Angiomotin |
| ATCC | American Type Culture Collection |
| ATR | ATR Serine/Threonine Kinase |
| B2M | Beta 2 microglobulin |
| BAK | BCL2 Antagonist/Killer 1 |
| bFGF | Basic Fibroblast Growth Factor |
| BIM | Bcl-2-like Protein 11 |
| BMDCs | Bone Marrow-Derived Cells |
| BMI1 | Polycomb Complex Protein BMI-1 |
| BMP | Bone Morphogenetic Protein |
| BMP7 | Bone Morphogenetic Protein 7 |
| BSA | Bovine Sereum Albumin |
| CASP3 | Caspase 3 |
| CD11b | Integrin alpha M (cluster of differentiation molecule 11B) |
| CD117 | Proto-oncogene c-KIT (cluster of differentiation 117) |
| CD155 | PVR Cell Adhesion Molecule (cluster of differentiation 155) |
| CD226 | DNAX Accessory Molecule 1 (cluster of differentiation 226) |
| CD24 | Heat Stable Antigen CD24 (cluster of differentiation 24) |
| CD4 | T-Cell Surface Glycoprotein CD4 (cluster of differentiation 4) |
| CD44 | Hematopoietic Cell E- And L-Selectin Ligand (cluster of differentiation 44) |
| CD5 | Lymphocyte Antigen T1/Leu-1 (cluster of differentiation 5) |
| CD8 | T-Lymphocyte Differentiation Antigen T8/Leu-2 (cluster of differentiation 8) |
| CD96 | T Cell-Activated Increased Late Expression Protein (cluster of differentiation 9) |
| CDKN1B | Cyclin Dependent Kinase Inhibitor 1B |
| c-Jun | Jun Proto-Oncogene, AP-1 Transcription Factor Subunit |

| | |
|---|---|
| CNTF | Ciliary Neurotrophic Factor |
| CNTFR | Ciliary Neurotrophic Factor Receptor |
| CREB | cAMP Response Element-Binding Protein |
| CSC | Cancer Stem Cells |
| CT-1 | Cardiotrophin-1 |
| CTC | Circulating Tumor Cells |
| CTLA4 | Cytotoxic T-Lymphocyte Associated Protein 4 |
| CXCL10 | C-X-C Motif Chemokine Ligand 10 |
| CXCL12 | C-X-C Motif Chemokine Ligand 12 |
| CXCL9 | C-X-C Motif Chemokine Ligand 9 |
| CXCR4 | C-X-C Motif Chemokine Receptor 4 |
| DAPI | 4',6-Diamidino-2-Phenylindole |
| DCIS | Ductal carcinoma in situ |
| DEC2 | Basic Helix-Loop-Helix Family Member E41 |
| DFOM | Deferoxamine |
| DTC | Disseminated Tumor Cell |
| EBI4 | Epstein-Barr virus induced 3 |
| EC359 | Leukemia Inhibitory Factor Receptor (LIFR) Inhibitor |
| ECM | Extracellular Matrix |
| EGFR | Epidermal Growth Factor Receptor |
| EMT | Epithelial-Mesenchymal Transition |
| ERa | Estrogen Receptor Alpha |
| ERCC1 | ERCC Excision Repair 1, Endonuclease Non-Catalytic Subunit |
| ERK | Mitogen-Activated Protein Kinase 1 |
| FBS | Fetal Bovine Serum |
| FGF | Fibroblast Growth Factors |
| FOXA1 | Forkhead Box A1 |
| GAB2 | GRB2 Associated Binding Protein 2 |
| Gapdh | Glyceraldehyde-3-Phosphate Dehydrogenase |
| GAS6 | Growth Arrest Specific 6 |
| GATA3 | GATA Binding Protein 3 |

| | |
|---|---|
| GCSF | Granulocyte Colony-Stimulating Factor |
| GLUT1 | Glucose transporter 1 |
| GMCSF | Granulocyte-Macrophage Colony-Stimulating Factor |
| GP130 | Glycoprotein 130 |
| GSK | Glycogen Synthase Kinase |
| HER2 | Erb-B2 Receptor Tyrosine Kinase 2 |
| HIF1 | Hypoxia Inducible Factor 1 |
| HIST1H2BK | Histone H2B type 1-K |
| HMEC | Human Mammary Epithelial Cells |
| HNSCC | Head and Neck Squamous Cell Carcinomas |
| HRE | Hypoxia-Response Elements |
| HSC | Hematopoietic Stem Cell |
| HSP27 | Heat Shock Protein 27 |
| IACUC | Institutional Animal Care and Use Committee |
| IDC | Invasive Ductal Carcinoma |
| IDO | Indoleamine 2,3-Dioxygenase 1 |
| IFB | Interferon Beta |
| IFN | Interferon |
| IFNAR | Interferon-α/β Receptor |
| IL-11 | Interleukin 11 |
| IL-11R | Interleukin 11 Receptor |
| IL-2 | Interleukin 2 |
| IL-27 | Interleukin 27 |
| IL-3 | Interleukin 3 |
| IL-30 | Interleukin 30 |
| IL-6 | Interleukin 6 |
| IL-6R | Interleukin 6 Receptor |
| IL6ST | GP130 |
| ILEI | Interleukin-related Protein |
| INK4A | Cyclin Dependent Kinase Inhibitor 2A |
| iNOS | Nitric oxide synthase |

| | |
|---|---|
| IRF7 | Interferon Regulatory Factor 7 |
| JAK | Janus kinase |
| JNK | c-Jun N-terminal kinases |
| KRAS | Kirsten rat sarcoma virus |
| LIF | Leukemia Inhibitory Factor |
| LIFR | Leukemia Inhibitory Factor Receptor |
| LOX | Lysyl Oxidase |
| LPS | Lipopolysaccharide |
| MAPK | Mitogen-Activated Protein Kinase |
| MAPK11 | Mitogen-Activated Protein Kinase 11 |
| MAPK14 | Mitogen-Activated Protein Kinase 14 |
| MDR1 | Multidrug Resistance Protein 1 |
| MDSC | Myeloid-Derived Suppressor Cell |
| MEK1 | Mitogen-Activated Protein Kinase Kinase 1 |
| mESC | Mouse Embryonic Stem Cells |
| miR-190 | microRNA 190 |
| MMP | Matrix metalloproteinase |
| MMP9 | Matrix Metallopeptidase 9 |
| MNC | Multinucleated Cells |
| MSC | Mesenchymal Stem Cells |
| MSI2 | Musashi-2 |
| MSK1 | Mitogen- and stress-activated kinases |
| MTCO1 | Mitochondrially Encoded Cytochrome C Oxidase I |
| mTOR | Mammalian target of rapamycin |
| NANOG | Nanog Homeobox |
| NETs | Neutrophil Extracellular Traps |
| NF-KappaB | Nuclear factor kappa-light-chain-enhancer of activated B cells |
| NK | Natural Killer Cell |
| NO | Nitric Oxide |
| NOTCH1 | Notch Receptor 1 |
| NR2F1 | Nuclear Receptor Subfamily 2 Group F Member 1 |

| | |
|---|---|
| Nras | Neuroblastoma RAS viral oncogene homolog |
| OSM | Oncostatin M |
| OSMR | Oncostatin M Receptor |
| Oct4 | POU Class 5 Homeobox 1 |
| P/S | Penicillin/streptomycin |
| P130Cas | Breast cancer anti-estrogen resistance protein 1 |
| P4HA1 | Prolyl 4-Hydroxylase Subunit Alpha 1 |
| PAD4 | Peptidyl Arginine Deiminase 4 |
| PAI1 | Serpin Family E Member 1 |
| PDCD4 | Programmed Cell Death 4 |
| PDX | Patient-Derived Xenograft |
| PHD | Prolyl hydroxylase domain proteins |
| PIK3CA | Phosphatidylinositol-4,5-Bisphosphate 3-Kinase Catalytic Subunit Alpha |
| POSTN | Periostin |
| PR | Progesterone |
| PREX1 | Phosphatidylinositol-3,4,5-Trisphosphate Dependent Rac Exchange Factor 1 |
| PROM1 | Prominin 1 (cluster of differentiation 133) |
| PTHRP | PTH-Related Peptide |
| PXN | Paxillin |
| PYGB | Glycogen Phosphorylase B |
| PyMT | Polyoma middle T antigen |
| QSOX1 | Quiescin Sulfhydryl Oxidase 1 |
| RANK | Receptor activator of nuclear factor κ B |
| RANKL | Receptor activator of nuclear factor κ B Ligand |
| RBM15 | RNA Binding Motif Protein 15 |
| RHoGAP | Rho GTPase activating protein |
| ROS | Reactive Oxygen Species |
| SBP56 | Selenium binding protein |
| SCF | Stem Cell Factor |
| SDS-PAGE | Sodium dodecyl sulfate polyacrylamide gel electrophoresis |
| SHP2 | SH2 containing protein tyrosine phosphatase-2 |

| | |
|---|---|
| shRNA | short hairpin RNA |
| siRNA | Small interfering RNA |
| SMAD1 | SMAD Family Member 1 |
| SMAD3 | SMAD Family Member 3 |
| SOCS3 | Suppressor Of Cytokine Signaling 3 |
| SOX2 | SRY-Box Transcription Factor 2 |
| SRC | SRC Proto-Oncogene, Non-Receptor Tyrosine Kinase |
| STAT | Signal Transducer And Activator Of Transcription |
| STAT1 | Signal Transducer And Activator Of Transcription 1 |
| STAT3 | Signal Transducer And Activator Of Transcription 3 |
| TERT | Telomerase Reverse Transcriptase |
| TGFB1 | Transforming Growth Factor Beta 1 |
| TGFB2 | Transforming Growth Factor Beta 2 |
| THBS1 | Thrombospondin 1 |
| TIE2 | Angiopoietin-1 |
| TNBC | Triple Negative Breast Cancer |
| TNF | Tumor Necrosis Factor |
| TPM1 | Tropomyosin 1 |
| TRAP | Tartrate-resistant acid phosphatase |
| VEGF | Vascular endothelial growth factor |
| WSX-1 | Interleukin 27 receptor |
| XTT | 2,3-Bis-(2-Methoxy-4-Nitro-5-Sulfophenyl)-2H-Tetrazolium-5-Carboxanilide |

# CHAPTER I

# INTRODUCTION

This chapter is adapted from “Dormancy in the Tumor Microenvironment” published as a book chapter in a Tumor Microenvironment book series and “GP130 Cytokines in Breast Cancer and Bone” published in *Cancers (Basel)*.

Omokehinde T., Johnson R.W. (2021) Dormancy in the Tumor Microenvironment. In: Birbrair A. (eds) Tumor Microenvironment. Advances in Experimental Medicine and Biology, vol 1329. Springer, Cham. https://doi.org/10.1007/978-3-030-73119-9_2

Omokehinde T, Johnson RW. GP130 Cytokines in Breast Cancer and Bone. Cancers (Basel). 2020 Jan 31;12(2):326. doi: 10.3390/cancers12020326.

## Overview

Breast cancer remains to be one of the most diagnosed cancers among adults in the United States, with over 280,000 estimated new cases in 2021 [1]. Breast cancer makes up approximately 30% of all new cancer cases in women and is the second leading cause of cancer-related deaths in women. There have been significant advances in the diagnosis, early detection, removal and treatment of breast cancer, and as a result, the five-year relative survival rate for breast cancer is 90% [2, 3]; however, the molecular subtype of the breast tumor can dramatically impact overall patient outcomes. The expression of three receptors (estrogen receptor (ER), progesterone receptor (PR) and human epidermal growth factor receptor 2 (HER2)) on breast tumor cells determines prognosis and overall response to medical therapy. Patients with ER+ and PR+ tumors tend to have lower histologic grade, better prognosis, and respond to targeted endocrine therapy, while patients with ER- and PR- tumors, have higher histologic grade, worse prognosis and generally do not respond to targeted therapies [4, 5]. However, it has been well established that breast cancer recurrence occurs in patients with both ER+ and ER-

tumors [6-9], although the timeline for recurrence is generally longer in patients with ER+ disease.

Despite advances in cancer therapeutics, clinical oncology and basic cancer research, patients with cancer often develop recurrent metastatic disease. Relapse is a result of malignant cells spreading from the primary tumor to distant sites and organs, and these disseminated tumor cells (DTCs) often undergo long periods of remission that range from years to even decades after initial treatment [10, 11]. Tumor dormancy can be defined as a stage in cancer progression where the residual disease is present, but DTCs are undetectable and the patients are asymptomatic [6, 11]. Tumor cells that can escape or resist conventional therapies and survive as DTCs may enter a dormant state for a period of time before reactivation by microenvironmental cues and colonization of a secondary site. The duration of tumor dormancy varies between cancer types, but often aggressive tumors have short latency periods, resulting in high relapse and mortality rates. In contrast, prolonged latency typically occurs in less aggressive disease, but once patients' relapse, the outcomes are the same [6, 12]. Differences in tumor cell behavior across tumor types make it difficult to predict when and which patients will develop overt metastases. At present, therapeutic options for overt metastases and metastatic disease are limited in efficacy due to the advanced nature of the disease [13, 14]. Understanding the mechanism by which tumor cells enter and, in particular, exit dormancy will be critical in determining the best way to therapeutically target these cells in patients at risk for recurrence.

There are two major models of tumor dormancy, with each reflecting distinct growth characteristics and signaling pathways. 'Tumor mass dormancy' involves the arrest of overall tumor growth due to a balance between proliferation and apoptosis. The prevailing models suggest that this balance can be regulated by vascular/angiogenic components (angiogenic dormancy) or immunosurveillance (immunologic dormancy). In order to grow beyond 2mm, tumor cells may induce vessel formation by secreting pro-angiogenic factors like vascular endothelial growth factor (VEGF), which recruits endothelial and pro-angiogenic immune cells [15-17]. Tumor mass dormancy can also be induced or maintained by downregulation of pro-angiogenic factors [18, 19] and increased expression of known angiogenic suppressors [20]. Immunologic dormancy consists of a

balance between immune clearance and the outgrowth of tumor cells and is observed across multiple tumor types [21-26]. DTCs can adapt to pressures from the immune system by promoting the recruitment of immunosuppressive cells like myeloid derived suppressor cells (MDSCs) and T-regulatory cells (Tregs) or promote inflammatory responses that support DTC outgrowth [27, 28]. ‘Cellular dormancy’ occurs when a DTC enters a state of quiescence similar to G0/G1 cell cycle arrest [12]. This arrest can be induced by several factors including mitogens, microenvironmental stresses and key pro-dormancy factors secreted by cells within the various bone niches (osteogenic and stem-cell driven dormancy) [29]. In addition, evidence has pointed to DTCs exhibiting stem-like properties which are inherent to the dormancy phenotype and are thought to be governed by internal and external microenvironmental cues. Cancer stem cells (CSCs) are a subset of cancer cells with increased tumor initiating and metastatic properties, but most notably, CSCs can adopt a dormancy phenotype to aid in therapeutic resistance, resulting in latent recurrence [30-33]. Expression of C-X-C chemokine receptor type 4 (CXCR4) by DTCs not only facilitates bone metastasis, but promotes stemness, plasticity and CSC properties [34, 35].

Within each model of tumor dormancy, the local microenvironment of the primary tumor and the metastatic site profoundly regulate tumor cell dissemination, dormancy status and resistance to conventional therapies, and will be discussed in the following sections.

**Hypoxia in tumor dormancy**

Hypoxia, or low oxygen tensions, is oftentimes present in solid tumors as a result of the unstable and leaky vasculature [36]. In response to this physiological stress, cells within the tumor will up-regulate and release pro-angiogenic factors, including VEGF and FGFs, which can stimulate endothelial cells to proliferate. This results in the inhibition of THBS1 [19], allowing for new blood vessels to form and the tumor mass to expand beyond 1-2mm through the expression of HIF-1 [19, 37-39]. HIF-1 is a heterodimeric protein that consists of two proteins, HIF-1α and HIF-1β, which activate the transcription of many genes involved in angiogenesis, metabolism, proliferation, survival, invasion and metastasis [36]. Hypoxia and activation of HIF-1 have been shown to promote tumor

progression and metastasis to various distant sites across several different tumor types [40-46]. In the context of angiogenesis, it has been shown that HIF-1 will bind to hypoxia response elements (HREs) to drive the expression of VEGF signaling in endothelial cells, resulting in sprouting, formation of new blood vessels, and support of tumor growth [47, 48].

Hypoxia negatively regulates leukemia factor receptor (LIFR), which confers a dormant phenotype in bone-disseminated breast cancer cells. LIFR also functions as a known tumor suppressor and metastasis suppressor in breast cancer [49, 50]. Hypoxia downregulates LIFR expression in MCF7 and SUM159 human breast cancer cells *in vitro* and is negatively correlated with LIFR mRNA expression levels in patient samples [50]. The effect of hypoxia on LIFR expression was demonstrated to be through epigenetic modulation of LIFR, rather than a HIF-dependent mechanism. However, HIF signaling in breast cancer cells has been shown to promote the activation of lysyl oxidase (LOX) a hypoxia induced pro-metastasis factor that plays a role in dissemination of tumor cells to distant sites. Studies have reported that LOX secreted from primary breast tumor cells results in remodeling of the extracellular matrix (ECM) in the lungs of orthotopically inoculated mice, leading to the invasion of bone marrow-derived cells (BMDCs), which are necessary for metastatic niche formation [51, 52]. Mechanistically, LOX has known

roles in cross-linking collagens and elastins in the ECM [53]. Thus, secretion of LOX by hypoxic tumor cells promotes BMDC invasion by cross-linking collagen IV, as evidenced by increased adhesion of $CD11b^+$ $CD117^+$ immature myeloid cells in mouse lung tissue pre-incubated with LOX *ex vivo* [52]. In contrast, inhibition of LOX either through genetic knockdown or HIF inhibitors (digoxin or acriflavine) on breast cancer cells blocks collagen cross-linking, prevents BMDC recruitment to the lung ECM, and reduces metastatic outgrowth [51, 52].Overall, hypoxia is associated with numerous pro-tumorigenic properties, and has been shown to downregulate pro-dormancy signaling pathways (Figure 1).

It has also been reported that hypoxia can induce tumor dormancy in disseminated tumor cells. Induction of tumor hypoxia using desferrioxamine (DFOM), which is a hypoxia mimicking agent that causes activation of HIF-1α, has been shown to preferentially select

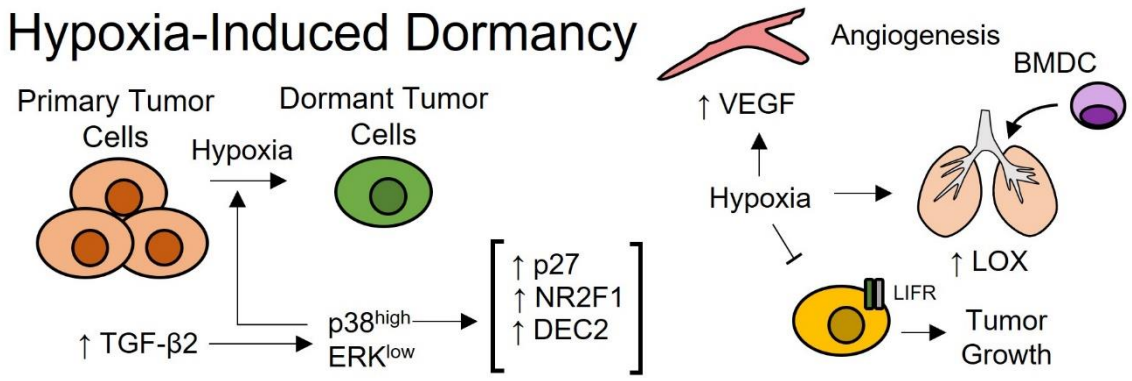


**Figure 1. Hypoxia can both negatively regulate and induce tumor dormancy.** TGF-β2 in tumor cells activates p38, which is a stress-activated kinase that plays a key role in tumor suppression and dormancy. A high ratio of p38 to ERK expression is a feature of dormant tumor cells because these cells have higher expression of pro-dormancy genes (NR2F1, DEC2, p27). Similarly, usage of the hypoxia mimicking agent DFOM, which activates HIF-1, upregulates these same genes. In contrast, hypoxia also negative regulates dormancy by downregulating LIFR, increasing tumor dissemination to bone and osteolytic bone destruction. Hypoxia has been shown to upregulate LOX in the lungs, increasing the presence of BMDCs, and allows for the remodeling of the ECM priming the area for metastatic niche formation. Lastly, hypoxia through HIF-1 activation has been shown to drive expression of VEGF in endothelial cells to support tumor growth.

for a population of DTCs that express pro-dormancy genes such as nuclear receptor subfamily 2 group F, member 1 (NR2F1) and basic helix-loop-helix family, member e41 (DEC2), cyclin-dependent kinase inhibitor 1B (p27) and hypoxia genes HIF-1α and glucose transporter 1 (GLUT1) in MDA-MB-231 breast cancer cells and T-HEp3 head and neck squamous cell carcinoma (HNSCC) cells [54]. Upregulation of NR2F1 has been linked to a dormancy phenotype found in models of HNSCC and has been linked to prostate cancer patients harboring dormant disease [55, 56]. Interestingly, DFOM treated tumor cells that activate a NR2F1 dormancy phenotype are resistant to cisplatin treatment, and have significantly more quiescent tumors, suggesting that hypoxia signaling can induce the formation of chemo-resistant dormant tumor cells that have the potential to persist long-term. In conjunction with the NR2F1 dormancy phenotype, p38 is a stress activated kinase that plays a key role in tumor suppression and the induction of tumor dormancy. Activated downstream of transforming growth factor-beta 2 (TGF-β2) signaling, the ratio of ERK to p38 can influence the dormancy profile of HNSCC cells, where a low ERK and high p38 ratio was characteristic of dormant tumor cells [57]. This is further supported where p38 activation seems to affect several pro-dormancy genes including NR2F1 [55, 58]. Hypoxia appears to have a dual role in tumor dormancy, where tumor cells may adopt specific programming to remain in a dormant state but may also drive tumor cells out of dormancy in the bone marrow through downregulation of LIFR and other pro-dormancy genes like THBS1.

**Immunologic Dormancy**

The role of the immune system in influencing cancer growth has been extensively reviewed in recent years [11, 59-61]. A current model explaining the role of the immune system in dormancy consists of three main stages: elimination, equilibrium and escape. “Elimination’ is when cancer cells are recognized and eliminated by the immune system, and escape is when tumors are no longer kept in check by the immune system. In the context of tumor dormancy, several groups hypothesize that immunologic dormancy takes place at the ‘equilibrium’ state which is a less-well defined process where the immune system controls cancer outgrowth but doesn’t completely eliminate the tumor. This is possible because the summation of pro-tumor and immune-anti-tumor pathways

are both active. An imbalance in these pathways can result in immune escape, which is believed to be driven by immune modulatory signals that are produced by tumor cells or the microenvironment [59, 60, 62].

It has been noted that cytokines and chemokines produced by the tumor or tumor microenvironment can modulate immune responses to tumor cells (Figure 2). Interferon (IFN) signaling has been shown to mediate metastasis specifically in breast cancer cells. $ER^-$ breast cancer cells that survive neoadjuvant chemotherapy elicit a state of immunological dormancy due to the prevalence of upregulated type I IFN genes. This dormant phenotype is proposed to be through the sustained activation of interferon regulatory factor 7 (IRF7)/interferon beta (IFN-β)/interferon alpha and beta receptor (IFNAR) signaling axis, which when upregulated promotes chemoresistance, reduces cell growth and induces a switch from myeloid derived suppressor-dominated immune response to a $CD4^+$/$CD8^+$ T-cell-dependent anti-tumor response [63]. Furthermore, silencing of IRF7, blocking IFNAR signaling using anti-IFNAR1 antibodies or downregulation of IFN-β, reverses the dormant state and promotes spontaneous escape from dormancy in breast cancer cells. This effect is also observed in mouse studies when comparing primary 4T1 mammary carcinoma cells and spine metastatic variants. Targets of the IRF7/IFN-β/IFNAR signaling axis are significantly suppressed in a bone metastatic variant of the 4T1 tumor cells and restoration of IRF7/IFN-β/IFNAR signaling reduces bone metastases and prolongs survival in mice [64]. In both studies, these pro-dormancy effects elicited by the IRF7/IFN-β/IFNAR signaling axis are mediated by natural killer (NK) cells and $CD4^+$/$CD8^+$ T-cell responses [63, 64] but even earlier works have identified the connected role between IFN, T cells and immune-mediated dormancy [65]. $CD8^+$ T-cells and NK cell activity are necessary to elicit anti-tumor responses to cancer outgrowth. In the RET.AAD melanoma model, the control of metastatic outgrowth in distant sites requires $CD8^+$ T-cells and depletion of these cells accelerates metastatic growth in the lungs and the reproductive tract [26]. NK cells have also been shown to promote anti-tumor responses. CD96 expression on NK cells has been identified to compete with CD226 for CD155 binding, which negatively regulates NK cell functions[66]. Recently, CD96 blockade has been identified to enhance control of metastatic outgrowth in the lungs of mice, but this suppression is reliant on the

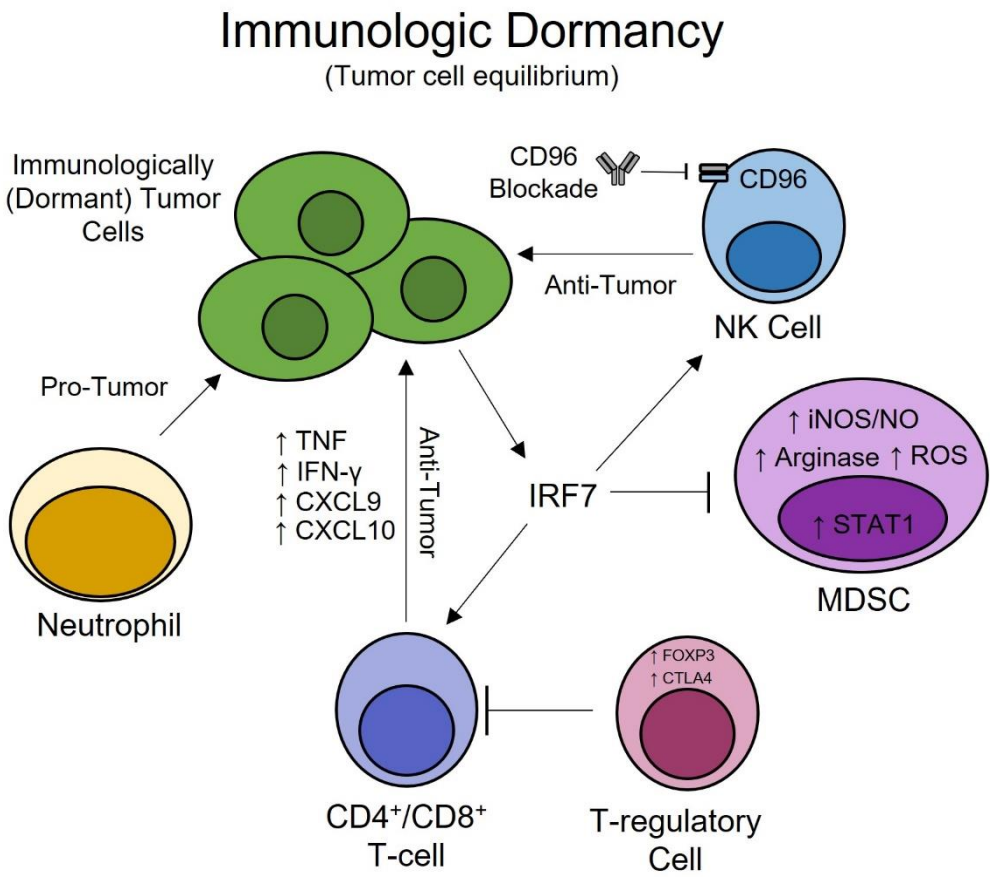


**Figure 2. Crosstalk between different immune cells supports tumor dormancy.** Immunologic dormancy occurs when there is an 'equilibrium' state where the immune system controls cancer outgrowth but doesn't completely eliminate the tumor cells. After neoadjuvant chemotherapy, tumor cells can elicit a state of immunologic dormancy due to the activation and secretion of IRF7. Through the IRF7:IFN-β:IFNAR signaling axis, tumor cells became more chemo-resistant and promote the expansion of NK cells and $CD4^+/CD8^+$ T-cells while suppressing MDSC and Treg recruitment. Supported by TNF, IFN-γ, and CD96, NK cells and $CD8^+$ T-cells elicit anti-tumor responses that maintain and control tumor growth. CXCL9 and CXCL10 are potent angiogenic inhibitors produced by $CD4^+$ T-cells that elicit anti-tumor effects by stimulating Th1 polarization, producing IFN-γ and TNF while also enhancing anti-tumor responses by NK cells and $CD8^+$ T-cells.

presence of NK cells [67]. In conjunction, depletion of NK cells using antibodies results in permissive outgrowth of breast and lung cancer cells in various metastatic sites including the bones, lung and brain.

T-cell-induced dormancy may involve crosstalk with endothelial cells and possibly overlap with angiogenic dormancy. In pancreatic cancer, tumor necrosis factor receptor 1 (TNFR1) and IFN-γ arrests tumor growth through the injection of $CD4^+$ T cells, preventing activation of $a_v\beta_3$ integrin, tumor angiogenesis and further cancer progression [68]. These anti-tumor mediated effects are due to release of CXCL9 and CXCL10, potent angiogenic inhibitors [69, 70]. The anti-tumor effects of CXCL9 and CXCL10 can be seen in several pre-clinical tumor models including colon [71], lung [71, 72], kidney [73], melanoma [74], myeloma [75], and glioma [76]. CXCL9 and CXCL10 stimulate immune cells through type 1 T helper (Th1) polarization and activation. Th1 cells produce IFN-γ, IL-2 and TNF-β and enhance anti-tumor immunity by stimulating $CD8^+$ T-cells, NK cells and macrophages [77-79].

In the tumor microenvironment, it has been shown that Tregs and MDSCs promote immune suppression and tumor progression in numerous types of cancer including colorectal [80-82], head and neck [83-85], ovarian [86-88], gastric [89, 90] and breast [91, 92]. By expression of forkhead box P3 (FOXP3) and cytotoxic T-lymphocyte-associated protein 4 (CTLA-4), Tregs are able to suppress the secretion of IFN-γ and IL-2 by $CD8^+$ T cells, while also inhibiting the expansion of $CD4^+$/$CD8^+$ T cells [88]. In addition, oxygen sensing-prolyl-hydroxylase (PHD) proteins promote Treg expansion while also suppressing IFN-γ production by $CD8^+$ T-cells, allowing for the colonization of tumor cells into the lungs of mice [93]. MDSCs represent a population of cells that consist of immature monocytes (the exact cell surface markers have not been uniformly agreed upon in the field) that potently suppress T-cell mediated actions through cell-cell contact or activation of signal transducer and activation of transcription 1 (STAT1), leading to the secretion of arginase, cytokine-inducible nitric oxide synthase (iNOS), NO, and reactive oxygen species (ROS) [27]. Using a wounding model to mimic surgical resection, one group has shown that following surgery a global induction and mobilization of inflammatory cytokines and myeloid cells contributes to the outgrowth of once dormant DTCs [94]. The number

of infiltrating $CD11b^+$ myeloid cells is negatively correlated with the number of $CD8^+$ T-cells present in the tumor while the number of tumor cells present positively correlates with the number of $CD11b^+$ cells, suggesting that the myeloid cells may promote tumor outgrowth by countering or suppressing cytotoxic T-cell responses. Several groups have also shown that MDSCs can contribute to tumor angiogenic escape because of their increased expression of MMPs [95], but specifically the secretion of MMP9 has been associated with promoting the bioavailability of VEGF [96]. Some evidence indicates that myeloid cells can also enter metastatic sites and elicit anti-tumor activity. Upon shedding of circulating tumor cells (CTC) from the primary site into the blood, phagocytosing-myeloid cells accumulate in the lungs to interact with CTCs to confer anti-metastatic protection [97]. In a separate study, sustained nasal instillation of lipopolysaccharide (LPS) has been shown to induce lung inflammation, which leads to aggressive lung metastasis of dormant tumor cells, facilitated by neutrophil extracellular traps (NETs) [98]. Using a protein arginine deiminase 4 (PAD4) inhibitor, NET formation was blocked, preventing tumor cells from exiting dormancy and highlighting the role of inflammation in tumor dormancy. The above data suggest that in certain situations the immune system mediates several signaling pathways that affect tumor dormancy and suppress residual tumor cell expansion. At the same time tumor cells can mediate these same signaling pathways to favor an immune escape phenotype. It is important to note that many of the genes that promote exit from dormancy may intersect the other ‘forms’ of dormancy to coordinate the ability of tumor cells to evade the immune system.

**Vascular / Angiogenic Dormancy**

It has long been established that tumors are dependent on the formation of new vasculature to sustain their growth [99, 100]. When a tumor mass expands beyond 1-2 mm it relies on the formation of new vasculature in order to acquire oxygen and other nutrients for growth by inducing expression of various factors such as the transcription factor hypoxia-inducible factor-1 (HIF-1) [39]. Since the bone marrow compartment is heavily vascularized, angiogenic dormancy may overlap with dormancy driven by the osteogenic or HSC niche. Angiogenic dormancy results from the balance between pro- and anti-angiogenic factors such as vascular endothelial growth factor (VEGF) and

thrombospondin-1 (THBS1). Through genetic ablation, VEGF has been demonstrated as critical for the differentiation of endothelial cells [101], morphogenesis of vasculature [102] and vascular homeostasis [103]. THBS1 has previously been identified as a tumor suppressor, where expression of THBS1 in human breast cancer cell lines resulted in reductions in primary tumor growth, metastatic potential and angiogenesis [104]. Using proteomics to analyze proteins in microvascular niches, THBS1 was identified as an endothelium-derived tumor suppressor that stabilizes the microvasculature to maintain tumor dormancy in breast cancer cells [19]. However, this effect is negated by sprouting endothelial tips, and pro-angiogenic factors secreted during neovascularization results in reduced THBS1 expression and increased expression of transforming growth factor beta 1 (TGF-β1) and periostin (POSTN), which promote proliferation of DTCs [19]. In addition, heat shock 27 (HSP27) has been shown to regulate angiogenesis directly by inducing VEGF and fibroblast growth factor (FGF) [18]. Downregulation of HSP27 results in significant reductions in pro-angiogenic factors in human breast cancer cell lines, while overexpression results in expansive tumor growth. Taken together, a delicate balance between pro- and anti-angiogenic factors results in angiogenic dormancy of tumor cells (Figure 3). Over time and through multiple mechanisms the tumor mass may expand, resulting in the recruitment of endothelial cells, which only occurs after the metastases undergo a ‘switch’ from a non-angiogenic dormant phenotype to an angiogenic phenotype [38]. Often called the angiogenic switch, the change in angiogenic phenotype is driven by increased expression of VEGF and FGF by both the tumor cells and endothelial cells, and decreased expression of angiogenesis inhibitors like THBS1 [37]. In leukemic cells, direct cellular contact with endothelial cells has been shown to support their survival and proliferation. Release of pro-angiogenic factors (i.e., VEGF), which activates endothelial cells to secrete cytokines such as IL-6, IL-3, granulocyte-CSF (G-CSF), granulocyte-macrophage-CSF (GM-CSF) and nitric oxide (NO), was shown to promote leukemic cell and prostate cancer cell proliferation, highlighting the role of activated angiogenic endothelial cells in tumor cells escaping dormancy [105-109].

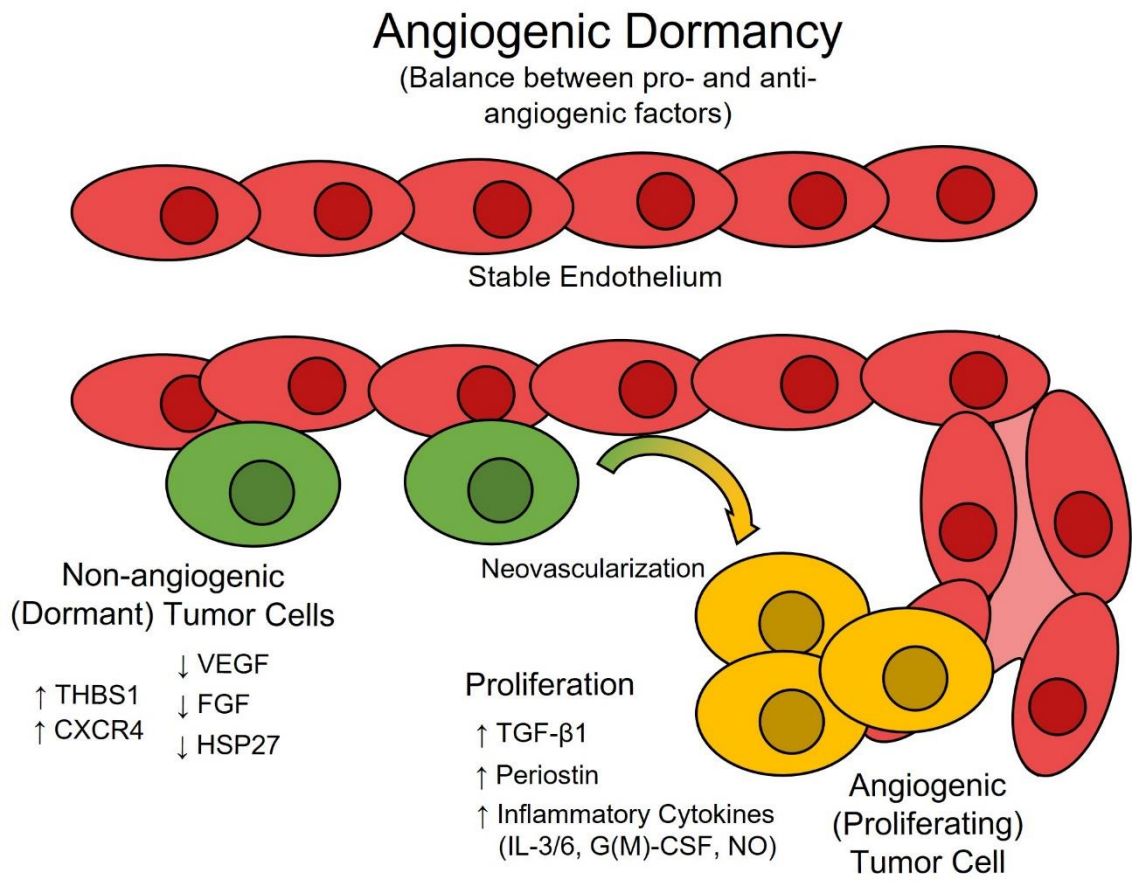


**Figure 3. Angiogenic dormancy requires the balance of pro-/anti- angiogenic factors.** Endothelial cells from stable endothelium will secrete anti-angiogenic factors (THBS1, CXCR4) to reduce metastatic outgrowth and maintain tumor dormancy. In contrast, tumor cells and endothelial cells can express pro-angiogenic factors (VEGF, FGF, HSP27) that can tip the balance between pro-and anti-angiogenic factors. This angiogenic 'switch' can result in neovascularization leading to tumor cells switch from a non-angiogenic state to an angiogenic state and expression of TGF-β1 and periostin. Subsequently, VEGF activation results in endothelial cells secretion of inflammatory cytokines (IL-3, IL-6, G-CSF, GM-CSF, NO) which promote tumor cell proliferation.

**Osteogenic and Stem Cell-Driven Dormancy**

Bone is the most common site of metastasis for a number of solid tumor types, including breast and prostate [110-112], and the bone marrow microenvironment plays a critical role in disease spread during metastatic growth. This process begins when tumor cells disseminate into the bone marrow compartment and engage with specialized microenvironments that support bone resident cell maturation and hematopoietic stem cell (HSC) maintenance [112]. The endosteal niche, which is rich in bone-resident cells including osteoblasts and bone lining cells, is localized to both the trabecular and endocortical bone surfaces. Bone resident cells have been shown to interact with HSCs by directly binding to them using adherens junction molecules (Figure 4). In the absence of bone morphogenetic protein (BMP), which promotes osteogenesis, the number of N-cadherin$^{+}$ osteoblast-lineage cells directly correlates with the number of HSCs present, and N-cadherin and β-catenin are localized to the border between osteoblasts and long-term HSCs, highlighting the importance of osteoblast-lineage cells as a key component of this HSC supportive niche [113]. The perivascular niche contains blood vessel lining endothelial cells and mesenchymal stem cells (MSCs) that are key to supporting HSC maintenance [114-117]. Some of these signals include stem cell factor (SCF) [116, 118], CXC chemokine ligand 12 (CXCL12) [119-122], Notch signaling [123, 124], interleukin-6 (IL-6) [125], and E-selectin [126]. Both of these niches contain cells that are key producers of pro-survival, quiescence and self-renewal signals that maintain the HSC population. DTCs interact with their microenvironment to survive and evade the immune system while remaining dormant for extensive periods of time. It has been proposed that bone-DTCs interact with bone marrow resident cells and compete with HSCs in the endosteal and perivascular niche. Multiple studies have established the CXCL12:CXC chemokine receptor 4 (CXCR4) signaling axis as a mechanism for tumor cell chemotaxis and invasion into distant sites like lymph nodes, lung and bone [127-130]. Interestingly, in multiple myeloma, prostate and breast cancer, inhibition of CXCR4 results in a ‘release’ of cancer cells from the bone microenvironment, increasing their sensitivity to chemotherapeutic agents [131-133]. Osteogenic cells of the endosteal niche have been reported to promote early-stage bone colonization of disseminated breast cancer cells

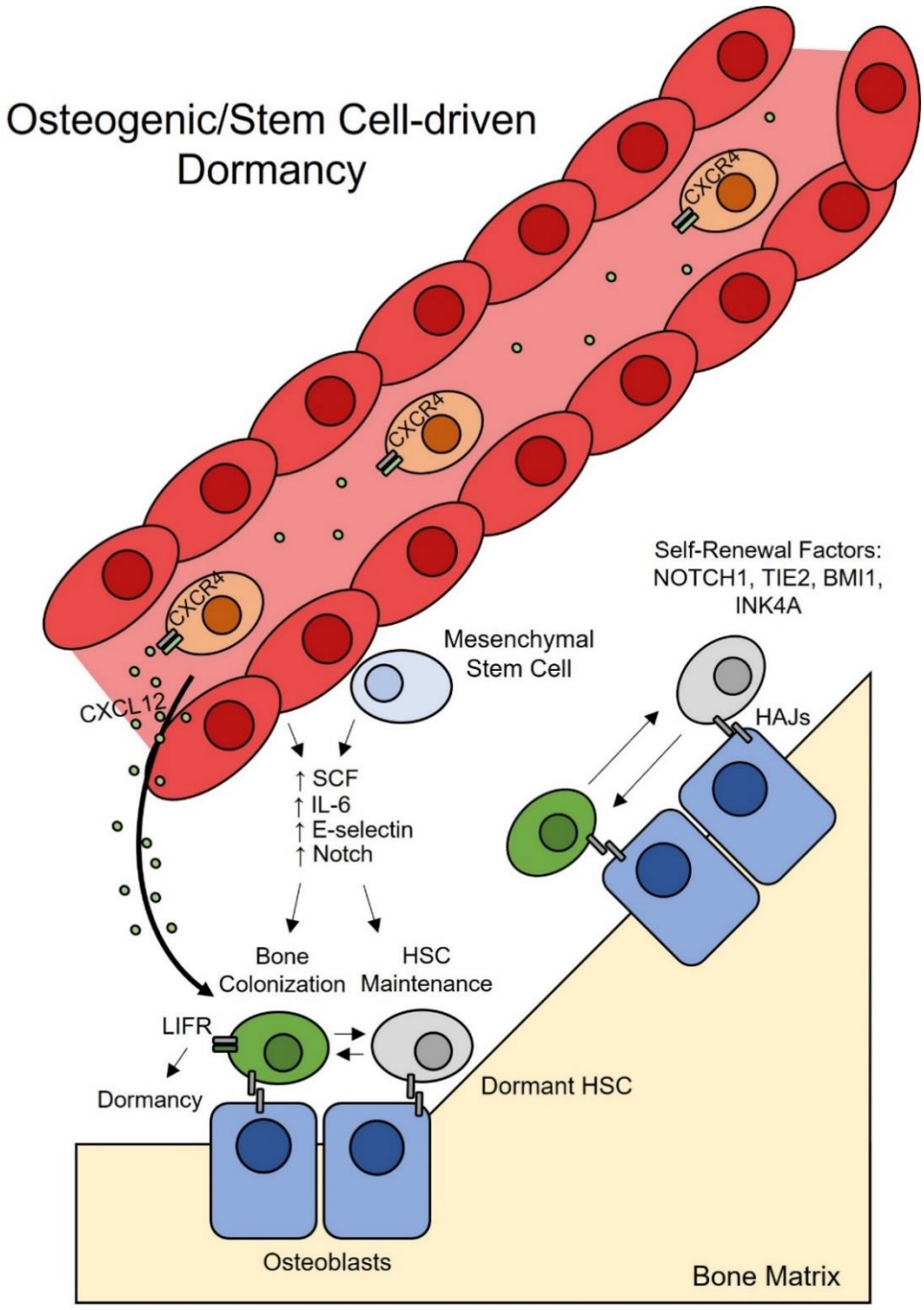


**Figure 4. Osteogenic/stem cell niche supports bone colonization and DTC survival and dormancy.** CXCL12 acts as a 'homing beacon' for tumor cells that express CXCR4, allowing tumor cells to traffic to the bone marrow. Osteoblast and osteoblast-lineage cells can support the dormancy of HSCs through the secretion of self-renewal and pro-survival factors (NOTCH1, TIE2, BMI1, INK4A). Along with these factors, mesenchymal stem cells and endothelial cells secrete SCF, IL-6, E-selectin and Notch to support HSC maintenance, bone colonization, and dormancy of tumor cells.

through co-localization by the formation of heterotypic adheren junctions between cancer cells expressing E-cadherin and osteogenic cells expressing N-cadherin [134]. These heterotypic adheren junctions also confer proliferative signals though the activation of the mTOR pathway and ablation of either E-cadherin, N-cadherin or the mTOR signaling axis results in delayed bone colonization and a reduction in osteogenic cell-conferred proliferative effects [134]. Others have shown that prostate cancer cells target the endosteal niche during metastasis by competitively binding to osteoblasts, outcompeting HSC-osteoblast interactions, and targeting niche-adhesion molecules and HSC self-renewal factors such as NOTCH1, TIE2, BMI1, and INK4A [135]. Overall, it is evident that osteogenic and stem-cell driven factors affect the ability of tumor cells to disseminate into the bone marrow and regulate the dormancy status of DTCs. Many of the factors produced by bone-resident cells act by directly interacting with tumor cells to modulate their proliferative properties while supporting their survival in a new microenvironment.

**Interleukin-6 (IL-6) / gp130 cytokine family**

Upon dissemination into the bone marrow, breast cancer cells and other tumor types encounter a rigid [136], hypoxic [137] microenvironment containing bone-resident immune and stromal cell populations. It is hypothesized that disseminated tumor cells (DTCs) compete for the hematopoietic stem cell niche and are thus maintained in a quiescent state by interactions with osteoblast lineage cells [135] for an indefinite period of time. Bone-DTCs secrete factors [e.g. parathyroid-hormone-related protein (PTHrP)] that stimulate the receptor activator of NFκB (RANK)-RANK ligand (RANKL) axis and promote osteoclastogenesis [138]. These factors may enable tumor cells to overcome quiescence [139], but it remains unclear whether some breast cancer cells begin secreting these factors prior to dissemination or during circulation, or whether the bone microenvironment induces breast cancer cells to stimulate osteoclasts. Increased osteoclastogenesis gives rise to localized bone resorption and the release of cytokines and growth factors from the bone matrix that stimulate tumor cell growth and further enhance the RANK-RANKL signaling cascade to promote bone resorption [138], resulting in overt tumor-induced bone disease.

Cytokines and cytokine receptors have a wide range of physiological functions and biological activities in many tissues and cell types [140]. The interleukin-6 (IL-6) / glycoprotein130 (gp130) cytokine family has been implicated not only in inflammation and immune response, but also in hematopoiesis, neuronal regeneration, bone remodeling, and cancer [141, 142]. In this review we will focus primarily on the role for the gp130 cytokines in cancer and bone.

The gp130 co-receptor is expressed in almost all major organs of the human body [143], and is the key signaling transducer that unites the IL-6 cytokine family. Each of the cytokines in the family binds to a cytokine-specific receptor and will complex with at least one subunit of gp130 to form its cell surface receptor complex. Targeted deletion of *Il6st* (the gp130 mouse gene) in mice resulted in embryonic lethality, with greatly reduced numbers of hematopoietic progenitors, impaired development of red blood cells, and defects in heart development [144]. *Il6st* null mice also exhibited poor bone development, reduced osteoblast number and function [145]. While osteoclast number was increased with gp130 deletion [145, 146], osteoclasts had poorly developed ruffled borders and the mice were slightly hypocalcemic, suggesting a defect in osteoclast activity. These data highlight the importance of gp130 in development, bone homeostasis, hematopoiesis, cell survival and growth. All of the IL-6 cytokines are dependent upon gp130 to induce downstream signaling pathways to affect a wide range of biological processes (Figure 5). When IL-6 binds to IL-6 receptor (IL-6R) it triggers a homodimeric association with gp130 to form its receptor complex [147], allowing signal transduction to occur in the target cell. Similar results have been shown for interleukin-11 (IL-11) when binding to IL-11 receptor (IL-11R), and other gp130 family members induce the recruitment of cytokine specific receptor chains [148]. An example of this is leukemia inhibitory factor (LIF) receptor (LIFR), which is required for signal transduction induced by the ligands LIF, cardiotrophin-1 (CT-1), and ciliary neurotrophic factor (CNTF). LIF signals by first binding to its cytokine-specific receptor LIFR and then recruits gp130, forming a heterodimeric receptor complex. CT-1 also signals by binding to LIFR and inducing heterodimerization with gp130, but there is evidence of a third receptor involved in signaling for CT-1, forming a possible heterotrimeric receptor complex [149]. Signal transduction for CNTF requires that it binds to CNTF receptor (CNTFR) first, then recruits LIFR and gp130, forming a

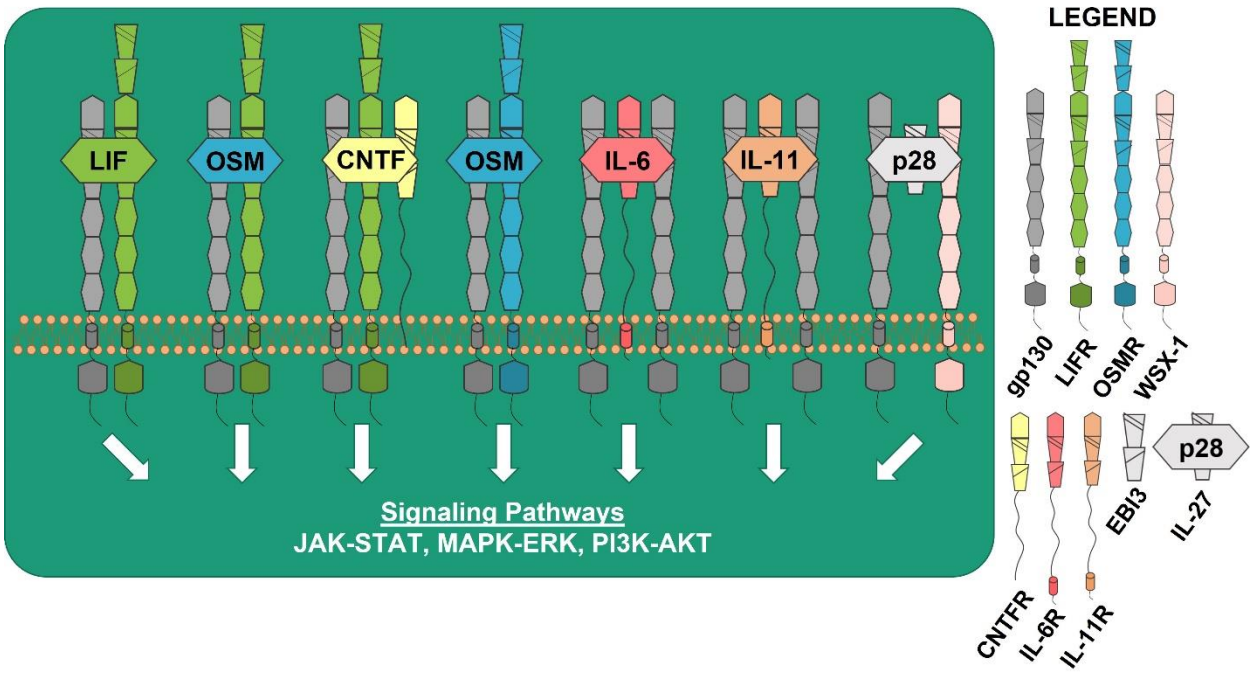


**Figure 5. gp130 cytokines and receptors activate downstream signaling pathways.** Receptors: dark gray=glycoprotein130 (gp130) co-receptor, green=leukemia inhibitory factor (LIF) receptor (LIFR), blue=oncostatin M (OSM) receptor (OSMR), light pink=WSX-1 (interleukin 27 receptor subunit alpha), yellow=ciliary neurotrophic factor (CNTF) receptor (CNTFR), dark pink=interleukin-6 (IL-6) receptor (IL-6R), orange=interleukin-11 (IL-11) receptor (IL-11R), light gray= Epstein-Barr virus induced 3 (EBI3); EBI3+IL-27p28 (IL-30) = interleukin-27 (IL-27). LIF, OSM, CNTF, IL-6, Il-11, and IL-27 bind to their cytokine specific receptors to activate major downstream signaling pathways: the Janus-activated kinase (JAK) – signal transducer and activation of transcription (STAT) pathway, the Ras-Raf mitogen-activated protein kinase (MAPK, MEK/ERK) signaling cascade, and the phosphatidylinositol 3-kinase-dependent (PI3K/AKT) pathway.

heterotrimeric receptor complex. Oncostatin M (OSM) is unique because it can form two different heterodimeric receptor complexes, where OSM first binds to gp130, then recruits either OSM receptor (OSMR) or LIFR [150]. IL-27, which consists of IL-27p28 (p28) and Epstein-Barr virus induced 3 (EBI3), is known to signal through a receptor complex of WSX-1 (also referred to as interleukin 27 receptor subunit alpha) and gp130 to induce downstream signal transduction and activation of STAT3 [142, 151, 152]. When IL-27p28 signals and forms complexes independent of EBI3 it is referred to as IL-30 [153].

Signal transduction through gp130 by any of the IL-6 family cytokines generally results in the activation of three major downstream pathways: the Janus-activated kinase (JAK) – signal transducer and activation of transcription (STAT) pathway, the Ras-Raf mitogen-activated protein kinase (MAPK, MEK/ERK) signaling cascade, and the phosphatidylinositol 3-kinase-dependent (PI3K/AKT) pathway [154-157]. The HIPPO-YAP pathway has also been shown to be negatively regulated downstream of LIFR [49]. However, in the osteoblast lineage it has been shown that OSM activates distinct signaling pathways depending upon whether it complexes with OSMR or LIFR [158], suggesting that these cytokines and their specific receptor complexes may induce specific downstream signals in bone-resident cells. Despite the similar sequence homology, structure, and intron-exon and promoter elements between OSM and LIF [159], the individual IL-6 cytokines do have differing roles in cancer and bone biology. This may be in part due to tissue specificity for ligand and receptor expression or due to activation of different downstream signals. A comprehensive comparison of the downstream pathways activated by the different cytokines after binding to breast cancer cells will be discussed in the following chapters.

**gp130 in physiological bone remodeling**

Bone-resident osteoblasts (bone-forming cells), osteocytes (mechano-sensing terminally differentiated osteoblasts), and osteoclasts (bone-resorbing cells) maintain bone homeostasis and health through the tightly regulated process of bone formation and bone resorption [160]. The gp130 cytokines are recognized as key regulators of bone remodeling. Il-6, Il-11, and Osm have been shown to promote bone formation by increasing alkaline phosphatase activity on mouse pre-osteoblast MC3T3 cells and

primary mouse calvarial cells [161], and Osm [162], CT-1 [163], Lif [164], and Il-6 [165] stimulate bone formation *in vivo*. Importantly, it has been demonstrated that Il-6 [166, 167], Il-11 [168], Osm [162], Lif [169, 170], and Cntf [171, 172], are expressed by osteoblast-lineage cells and that CT-1 is expressed by osteoclasts [163], suggesting that tumor cells that home to the bone marrow will encounter these signals in the physiological bone marrow microenvironment. Many of these factors are also expressed in skeletal muscle [173-175], suggesting they may act in a paracrine manner on the adjacent bone.

The mechanisms by which these cytokines induce bone formation varies. Osm, in addition to Lif and Ct-1, can complex with Lifr/gp130 to inhibit production of sclerostin, a potent inhibitor of bone formation [176], in late differentiated osteoblasts and osteocytes. Osm can also act through Osmr/gp130 to promote osteoblast differentiation and increase Rankl production [162]. Thus, Osm acting through Lifr/gp130 results in increased Wnt signaling and bone formation, while Osm acting through Osmr/gp130 increases osteoclastogenesis. *In vitro* and *in vivo* evidence suggests that this is due to differential activation of STAT3 signaling over STAT1 signaling [158]. In physiological bone remodeling, mouse genetic knockout studies of the receptors have revealed the importance of these cytokines in physiological bone remodeling. Mice deficient for gp130 [145] and Lifr [177] have increased osteoclast numbers, low trabecular bone mass, various bone abnormalities, and impaired bone formation. Knockout of Lif [178], and Ct-1 [163] give rise to a similar phenotype, with impaired osteoblast function and large osteoclasts both in neonate and adult mice. In contrast, deletion of Osmr [162] and Il-11R [179] resulted in suppressed osteoclast differentiation, high trabecular bone volume, number, and thickness. The observed increase in bone volume in Osmr knockout mice is likely due to its negative regulation of sclerostin [162, 180]. The mechanism for increased bone volume in Il-11r knockout mice remains unclear.

Il-6 [181-183], Il-11 [181, 184], Lif [181-183], Ct-1 [163, 182] and Osm [181-183] are also known to induce pro-osteoclast effects by acting on osteoblast lineage cells to produce Rankl. Il-6, Lif, Osm and Ct-1 induce the formation of tartrate resistant acid phosphatase (TRAP) positive multinucleated cells (MNC) and enhance osteoclast activity *in vitro* [181, 182]. However, the role of these cytokines *in vivo* shows cytokine-specific phenotypic variations [185]. Gp130 null mice were observed to have very high osteoclast

numbers, but also have embryonic and hematopoietic defects [145]. Conditional knockout of gp130 in late osteoblasts and osteocytes [180], as well as osteoclasts [186] resulted in reduced osteoblast numbers and bone formation, but no change in osteoclasts. Similar to gp130 deletion, genetic deletion of Ct-1, Lif, and Lifr also produced an increase in osteoclast formation. Ct-1 null mice had increased osteoclast formation and many large osteoclasts, but with abnormalities in their function, making the bones abnormally dense [163]. Knockout of Lif or Lifr resulted in an increase in large osteoclasts with activity clustered near the growth plate in young mice [177, 178].

These cytokines orchestrate bone remodeling to maintain bone homeostasis; however, bone-DTCs can hijack bone remodeling to alter the environment and make a more suitable environment for tumors to grow. Breast cancer cells induce osteolytic destruction to support their own growth and survival. By expressing and releasing cytokines such as IL-6 and IL-11, they promote their own growth through autocrine signaling and stimulate osteoclastic bone resorption through paracrine signaling. Importantly, breast cancer cells can also respond to these cytokines produced by the bone-resident cells since they express gp130 and many of the cytokine-specific receptors [187-189]. In this regard, understanding the role for gp130 cytokines in normal bone remodeling is essential to understand the impact of gp130 cytokines and signaling in bone-DTCs.

**gp130 cytokines in breast cancer**

Breast cancer is commonly categorized by hormone receptor expression and can be classified into distinct groups: estrogen receptor positive (ER+), human epidermal growth factor receptor 2 positive (HER2+), progesterone receptor positive (PR+), or triple-negative breast cancer (TNBC) [190]. Approximately 65-75% of breast cancer cases are ER+, 25-30% have HER2 gene amplified, and 10-20% of cases involve triple-negative breast cancer (TNBC), one of the most aggressive forms of the disease [190-193]. Similarly, breast cancer cell lines can also be distinguished by their hormone receptor expression, with phenotypes similar to the clinical counterpart (e.g. TNBC breast cancer cell lines are highly metastatic in mouse models, readily colonizing the lung or bone

marrow after intravenous inoculation, while ER+ MCF7 cells do not readily colonize and exhibit slow or no growth in distant metastatic sites following inoculation [50, 194]).

In the context of the gp130 cytokines, IL-6 has been reported by numerous groups to play a role in breast cancer progression, and these effects correspond with hormone receptor expression. ER+ breast cancer patients tended to have lower levels of sIL-6R when compared to ER- patients, and increased levels of sIL-6R were associated with increased recurrence when compared to patients with lower levels of sIL-6R [195]. Interestingly, *in silico* modeling and *in vitro* testing of two selective estrogen receptor modulators (SERMs), raloxifene and bazedoxifene, revealed that they are able to bind to gp130, selectively downregulate IL-6 mediated STAT3 phosphorylation, and significantly inhibit STAT3 activity in ER- SUM159 breast cancer cells [196]. In contrast to ER+ breast cancer, both HER2+ and TNBC have elevated levels of IL-6, causing an autocrine feedback loop through IL-6-activated STAT3 [197, 198]. Inhibition of IL-6 by use of an IL-6 antagonist, tocilizumab, or through shRNA resulted in decreased tumor growth, reduced CSCs and suppression of colony formation in HER2+ and TNBC studies [197, 199].

While a large body of work has focused on the connection between hormone receptor status and the IL-6/gp130 signaling axis, there have been few studies that focused on LIF/LIFR and OSM/OSMR in connection with hormone receptor status. Dhingra et al. reported that LIFR expression in patient tumors was significantly correlated with the presence of estrogen receptor [200] and LIFR expression and function is typically highest in ER+ breast cancer cells lines [50], although ER- SUM159 cells also possess an active LIFR capable of inducing downstream signals in response to ligand [49, 50]. Recent work by Li et al. reported that nuclear p21-activated kinase 4 (nPAK4) co-localized with endogenous ER-alpha (ERα) in the nucleus of ER+ MCF7 and ZR-75-30 breast cancer cells, resulting in the recruitment of the PAK4-ERα complex to estrogen response elements (EREs) upstream of the LIFR promoter, inhibiting the expression of LIFR and promoting bone metastasis [201]. the context of OSM/OSMR signaling, high levels of OSM and OSMR mRNA expression was associated with low expression of ESR1 (ER) and ER-regulated genes in a breast cancer gene expression data set. That same study also noted that recombinant OSM potently suppressed ER protein and mRNA expression *in vitro* and that loss of ER expression was necessary for OSM-mediated signal

transduction and migratory effects in ER+ MCF7 and T47D breast cancer cells [188]. Overall, these studies did not show a correlative trend in regard to the hormone receptor status and the expression of the gp130 cytokines, but these studies do suggest that ER may negatively regulate both LIFR and OSMR in breast cancer cells. Highlighted in the next section, we will discuss the often-contradictory effects of some of the gp130 cytokines in relation to breast cancer, and how these correspond to hormone receptor status.

*IL-6:* Of all the gp130 cytokines, IL-6 is perhaps the most well-studied. Many groups since the 1980s have demonstrated that recombinant IL-6 slows proliferation of breast cancer cells in 2D culture, with most of these studies focusing on ER+ human breast cancer cell lines like MCF7, T47D, and ZR-75-1 cells [202-207]. While there are a few reports that IL-6 cytokines do not affect MCF7 tumor cell proliferation *in vitro* [208, 209] , these studies typically looked at early time points (e.g. 48-72 hours of treatment). It is important to note that across all of these studies, the source of IL-6 was either not reported, came from different commercial vendors, or was produced in house. Of those that reported a commercial source for IL-6, none of these came from the same vendor. Thus, while there is a large amount of variation in the extent to which IL-6 inhibits proliferation, the overwhelming body of evidence suggests that IL-6 inhibits breast cancer cell proliferation in 2D culture. It is also worth noting that while IL-6 appears to inhibit proliferation, it was also found to promote motility of MCF7, T47D, and ZR-75-1 cells [205, 206], suggesting that it is not an entirely benign factor. IL-6 requires the expression of gp130 and the IL-6 receptor (either expressed on the cell surface or in soluble form) in order to elicit intracellular signaling, but the vast majority of these studies did not examine expression and contribution of the receptors [202, 203, 205-207]. Chiu et al, which reported that IL-6 inhibits MCF7, T47D, and ZR-75-1 cell proliferation, determined that all three cell lines secrete soluble IL-6 receptor and express gp130 [204], but did not test whether adding additional soluble IL-6 receptor enhanced or changed this effect. In contrast, Jiang et al reported no effect of IL-6 on MCF7 cell proliferation treated with either IL-6 or soluble IL-6 receptor, but did not test the combination of IL-6 and soluble IL-6 receptor or examine whether IL-6 receptor or gp130 is expressed on MCF7 cells in their hands [209]. This may be of importance since the MCF7 cell line is notoriously

heterogeneous in nature [210]. It is therefore possible that the effects of these cytokines on proliferation may be in part dependent upon the expression and availability of the receptors, but difficult to say with certainty given that most studies have not examined receptor expression.

It is also important to note that there is one study that suggests IL-6 stimulates proliferation of ER+ MCF7 and BT474 cells [211], and that this study had two notable differences from the aforementioned studies. First, the assay was conducted with a fluorescence reporter, in contrast to the thymidine incorporation and cell count studies that were previously used, and second, the cells were grown in a 3D tumor culture system. This key difference may reveal important differences in the effect of IL-6 on tumor cell proliferation *in vitro* and suggests that the ability of IL-6 to promote proliferation is dependent upon the environment of the tumor cell. Expression or secretion of IL-6 receptor and gp130 was not evaluated in this study, so it is not clear whether tumor cells cultured in 3D expressed different levels of the receptors compared to cells cultured in 2D. It is worth noting that the observed inconsistencies in IL-6-induced proliferation are not due to cell line hormone receptor status, since the same ER+ cell lines were used across multiple studies.

In the context of bone, IL-6 is well known to stimulate mesenchymal progenitor differentiation towards the osteoblast lineage while also promoting RANKL expression in osteoblasts and osteoblast lineage cells [183, 185, 212, 213]. Interestingly, tumor cells cultured *in vitro* with recombinant RANKL increased IL-6 expression in response to RANKL, and similar results were found with co-culture of mouse primary osteoblasts with breast cancer cells or conditioned media from breast cancer cells [214, 215], suggesting that IL-6 and RANKL form a feed-forward loop in bone-DTCs. These studies suggest that breast cancer cells within the bone microenvironment may interact with osteoblast lineage cells to produce cytokines like IL-6 to either promote tumor growth or induce bone resorption. These data are also more consistent with the *in vitro* 3D study that suggests IL-6 enhances tumor cell proliferation [211] than the numerous 2D studies that suggest opposing effects on proliferation [202-207]. Treatment of mice with anti-IL-6R antibodies resulted in similar cellular growth inhibition in prostate cancer, reduced osteolytic lesions and a reduction in serum RANKL levels *in vivo* [141]. Since IL-6 signaling in bone-

disseminated tumor cells might be driven by *cis*- or *trans*-IL-6 signaling [27], future studies investigating the efficacy of these neutralizing antibodies on both types of signaling are of interest. Additionally, shRNA targeting of RANKL in breast and prostate cancer, and shRNA targeting of IL-6 in breast cancer, each resulted in smaller osteolytic lesions, reduced bone turnover and reduced osteoclast numbers in inoculated mice. These data suggest that RANKL secreted by osteoblasts in response to IL-6 from tumor cells contributes to the preservation of RANKL-induced osteoclast activity. Furthermore, tumor cells exposed to osteoblast-derived RANKL increase their IL-6 output [215]. This was corroborated by a separate study that found RANK (the receptor for RANKL) knockdown in MDA-MB-231 (TNBC) cells reduces osteolytic bone destruction [216]. The IL-6 results were further confirmed in another study by an independent group, where senescent osteoblasts stimulated the production of IL-6, which increased osteoclast number and activity, promoting a metastatic 'niche' for breast tumor cells to home, and bone colonization was reduced following treatment with an IL-6 neutralizing antibody [217]. Taken together, these data indicate a pro-tumorigenic role for IL-6 expressed by bone-DTCs through their interactions with the bone microenvironment. Expression of IL-6 can also be driven by IL27-p28 (IL-30), which has tumor-promoting effects in prostate cancer [218, 219] and in breast cancer is enriched for and associated with the TNBC subtype. In breast cancer, the source of IL-30 was stromal leukocytes, and IL-30 stimulated proliferation of breast cancer cells in a gp130/IL-6R and STAT1/STAT3-mediated mechanism [220]. These studies were carried out in the context of the primary tumor and not metastatic disease, but these data are consistent with the observed tumor-promoting effects of IL-6 on bone-disseminated tumor cells and it is therefore possible that some of these effects may be mediated through IL-30- driven IL-6 signaling.

*LIF:* The LIF receptor (LIFR) was identified as a breast tumor suppressor by a shRNA screen [221] and shown to function as a breast cancer lung metastasis suppressor by a second laboratory [49]. In SUM159 human breast cancer cells, knockdown of LIFR dramatically increased the ability of tumor cells to colonize the lungs, while ectopic LIFR expression in 4T1 mouse mammary carcinoma cells significantly reduced the ability of these cells to colonize the lungs [49]. Breast cancer cell lines with low metastatic potential, defined by their lack of colonization of the lung or bone marrow

following intravenous inoculation, (e.g. MCF7, SUM159, and D2.0R cells) abundantly express LIFR and initiate downstream signals in response to recombinant LIF, but highly metastatic breast cancer cell lines (e.g. MDA-MB-231b, 4T1BM2 and D2A1 cells) do not express a functional LIFR and are unresponsive to recombinant LIF treatment [50], suggesting the ability of cells to respond to LIF corresponds with their metastatic potential. Interestingly, restoration of LIFR in highly aggressive MDA-MB-231 cells by treatment with a histone deacetylase inhibitor restores STAT3 signaling downstream of LIF:LIFR, which has been proposed to promote drug resistance by breast cancer cells [222]. When evaluating metrics of tumor dormancy, the MCF7 breast cancer cell line has been used by our group and others as a model of tumor dormancy because of their limited growth in the bone microenvironment [19, 50, 223]. Knockdown of LIFR in MCF7 cells increased invasion, downregulated dormancy genes, and increased osteolytic bone destruction [50]. Furthermore, PTHrP overexpression in MCF7 cells, which effectively enables the cells to exit dormancy in the bone marrow and become aggressively osteolytic [224], also down-regulates LIFR and suppressor of cytokine signaling 3 (SOCS3) [50] independent of cAMP signaling [139]. These data are consistent with the role for LIFR as a metastasis suppressor [49]. However, it remains unclear whether LIF in fact drives the metastasis suppressor actions of LIFR, since most data suggest that LIF is tumor promoting. Several other ligands (OSM and CNTF included) are also able to bind to LIFR, which may mediate the tumor suppressive actions of LIFR. Recently, interleukin-like epithelial-mesenchymal transition (EMT) inducer (ILEI) has emerged as a new cytokine that can activate STAT3 and drive both EMT and breast cancer stem cell formation through LIFR [225]. It is important to also note that acetylation of LIFR on its juxtamembrane domain appears to be responsible for LIF-mediated STAT3 activation and that phosphorylation of LIFR suppresses LIF signaling [226, 227]. Previous work has demonstrated that LIF can induce STAT3 signaling in breast cancer cells [50, 222], and STAT3 has been previously identified as pro-dormancy factor in ER+ breast cancer cells [223] and prevents colonization of the bone by disseminated tumor cells [50]. Thus, while *in vitro* treatment with LIF may stimulate tumor cell proliferation, its ability to stimulate STAT3 signaling in the context of the bone microenvironment may still promote tumor dormancy, although the mechanism is unresolved. Further studies will be required to examine the mechanism

of action for LIF effects on breast cancer cells in the context of the bone microenvironment.

The role for LIF signaling in cancer progression appears to be tumor-type dependent, although this does not resolve all of the controversy. In breast cancer, numerous studies point to a tumor-promoting role for LIF. LIF increased proliferation and colony formation of MCF7 [228] and T-47D cells in a dose-dependent manner *in vitro*, and this effect was reversed when cells were treated with anti-LIF antibodies [229]. LIF also stimulated migration and invasion in ER+ MCF7, T-47D, and MDA-MB-231 TNBC cells *in vitro* using trans-well assays, and overexpression of LIF in these cell lines increased the number of lung metastases and distant metastases *in vivo* [230]. However, since these studies made use of the MDA-MB-231 breast cancer cell line, which several groups have shown do not express a functional LIFR [50, 222], it is unclear how LIF may stimulate migration and invasion of these cells *in vitro*. LIF effects on metastasis were ablated through the use of shRNA knockdown of LIF in the MDA-MB-231 cells [230], but given the absence of a functional LIFR in these cells, the effects observed *in vivo* would most likely be mediated through paracrine LIF signaling from the tumor cells to the microenvironment.

In contrast to the pro-tumorigenic effects of LIF identified in MDA-MB-231 TNBC cells, two independent groups have demonstrated that LIF can have a mild inhibitory effect on proliferation *in vitro*. ER+ MCF7 cells, which do have a functional LIFR [50], had significant growth reduction following treatment with exogenous LIF [50, 187, 231], a decrease in the number of cells in S phase [231], and reduced clonogenic potential [187]. Thus, LIF treatment on MCF7 cells is reported to have both positive and negative effects on cellular proliferation in two different clonogenic assays [187, 228, 229], but the differential effects may arise from the types of soft agar used and the chemical make-up of these assays. Other methods have been used to determine the role of LIF on cellular proliferation *in vitro* such as XTT assays [50], absolute cell counts [230, 231], and flow cytometry [231], but the growth promoting or inhibitory effects may stem from the limitations of each test. A more standardized approach to *in vitro* clonogenic assays [232] has been heavily used by a number of groups and may be useful to address the discrepancy in previous studies. The differential effects of LIF treatment across several

studies also may be due to varying sources and activity of the recombinant cytokine used by each group. Several groups have also reported using a wide range of concentrations, anywhere between 6 – 200 ng/mL, which when coupled with the different sources of the recombinant cytokine, could explain why the results are paradoxical. The mixed outcomes of these studies demonstrate that LIF signaling in breast cancer is controversial and at this time it is unclear whether this is associated with hormone receptor status.

*OSM:* Early studies into OSM effects on breast cancer cell proliferation suggested a growth inhibitory role for this cytokine. Breast cancer cells treated with OSM had reductions in DNA synthesis (($^{3}$H)thymidine incorporation) in a dose dependent manner [233], decreased absolute cell counts [231] and a reduction in the number of cells in S phase [231, 234]. In support of these findings, another group has published that OSM inhibits the growth of MCF7 and MDA-MB-231 cells [235] as well as human breast epithelial cells [234, 236]. More recently, several studies have focused on OSM's role in EMT and invasion. Treatment with OSM resulted in morphological redistribution of β-catenin, enhanced mammosphere formation in T-47D and MCF7 cells, suppressed E-cadherin expression and increased expression of N-cadherin in MCF7 cells [237], suggesting that OSM promotes EMT; however, these findings have not been tested *in vivo*. Other studies have pointed to OSM inducing morphological changes necessary to enhance the metastatic characteristics of various breast cancer cells. In the presence of OSM, T-47D cells exhibited decreased intercellular contact [238], and increased cellular detachment and invasiveness [239]. In patient data, high OSM expression has also been correlated with decreased patient survival, pointing to its possible role in metastatic disease [240]. In the context of breast cancer bone metastasis, one group has shown that OSM knockdown in 4T1 mouse mammary carcinoma cells reduced spontaneous metastasis to the spine as assessed by qPCR analysis following orthotopic injections, and less osteolytic bone destruction following intratibial injections [241]. This group also demonstrated that global knockdown of OSM in Balb/c mice reduced the formation of spontaneous lung metastases [242]. These data suggest that autocrine OSM promotes bone metastasis, and paracrine OSM signaling promotes lung metastasis, but the mechanism by which OSM acts *in vivo* to stimulate metastasis remains unclear.

While direct stimulation of OSM on breast cancer cells results in a growth inhibitory phenotype [231, 233-235], OSM has also been shown to enhance the invasiveness and metastasis of tumor cells. However, OSM can signal through both LIFR and OSMR to induce downstream signaling [150, 162], and the function of OSM:LIFR and OSM:OSMR signaling in breast cancer cells has not been fully explored [238]. Previous studies have shown that STAT3 is abundantly phosphorylated in response to OSM across a number of breast cancer cells lines with no correlation to their status of LIFR or the metastatic phenotype [50]. Since the status of OSMR on breast cancer cell lines has not been fully elucidated yet, the effects of OSM could be delineated between the expression and functionality of OSMR and LIFR in such cell lines. Interestingly, OSMR expression was associated with shorter recurrence-free survival and overall survival in breast cancer patients [188], suggesting a connection to disease progression in breast cancer.

*Activation of downstream signaling by the gp130 family:* Upon binding to gp130 and their cytokine specific receptor on tumor cells, the gp130 ligands are known to activate the JAK/STAT, MAPK/MEK/ERK, and PI3K/AKT signaling pathways [154-157]. While there has not been a comprehensive comparison of the downstream pathways activated by each ligand in breast cancer, many mechanistic studies have identified STAT3 as the key downstream mediator of IL-6 [243] and OSM [240, 244, 245] tumor-promoting effects. Signal transduction by IL-6, LIF, and OSM is initiated after dimer formation between the cytokine specific receptors (e.g. IL-6R, LIFR and OSMR) and gp130, resulting in the phosphorylation of STAT3 by JAK [150, 246, 247]. Phosphorylated STAT3 undergoes dimerization and translocates into the nucleus resulting in transcription of target genes [243]. An extensive body of literature has established a role for STAT3 in the induction of pro-inflammatory cytokines, tumor progression, initiation, metastasis, chemoresistance, and immune evasion [243, 248]. STAT3 has also been shown to cross-talk with Ras signaling to further promote oncogenic transformation of human mammary epithelial cells [249], and recent studies in ovarian cancer has pointed to STAT3's ability to promote metastasis, chemoresistance, and EMT via MAPK/PI3K/AKT signaling downstream of p53/Ras signaling [250].

It is therefore not surprising that ectopic expression of IL-6 or treatment with recombinant IL-6 in ER+ breast cancer cells significantly increases expression of EMT

related genes through STAT3, leading to increases in tumor cell proliferation in orthotopic xenograft models [251]. IL-6 has been shown to promote breast cancer metastasis by upregulating C-X-C chemokine receptor type 4 (CXCR4) through c-Jun, STAT3 and nuclear factor kappa B (NF-kappaB) [2, 252], and facilitate angiogenesis through STAT3 by upregulating vascular endothelial growth factor (VEGF), matrix metallopeptidase 9 (MMP9) and basic fibroblast growth factor (bFGF) in the tumor microenvironment [253, 254]. OSM induces similar pro-tumorigenic changes in breast cancer cells. Long-term exposure of OSM to human mammary epithelial cells (HMEC) in culture drove EMT changes and resulted in the generation of cancer stem cells (CSC) by inducing STAT3/SMAD3 signaling [255]. This effect was ablated using a TGFβRI inhibitor or expression of SMAD7 (inhibitor of SMAD3 phosphorylation). This study also noted that several gp130 cytokines (IL-6, LIF, CT-1 and CNTF) were able to significantly increase the CSC population in HMECs, pointing to their potential role as microenvironmental cytokines capable of promoting tumor progression through STAT3. OSM has also been shown to induce IL-6 in a STAT3-dependent manner in ER- breast cancer cells [240].

Interestingly, while LIF is known to activate the same downstream signaling pathways as OSM and IL-6, STAT3 appears to play a contradictory role in the context of tumor cell dormancy in the bone. In ER+ MCF7 breast cancer cells, pharmacological inhibition of MAPK/MEK/ERK or PI3K/AKT signaling had no effect on dormancy markers, while a STAT3 inhibitor reduced pro-dormancy genes [50]. These data were confirmed *in vivo*, where knockdown of STAT3 phenocopied knockdown of LIFR and led to tumor cell exit from dormancy. STAT3 is up-regulated in dormant tumor cells and was one of only six genes that was highly expressed in ER+ breast cancer cell lines with higher dormancy scores [223]. The downstream mechanism for these effects remains unclear but is intriguing as it has been observed across multiple independent dormancy studies. These data suggest that inhibition of STAT3 in the primary site is critical to reduce tumor cell growth, but in distant metastatic sites such as the bone marrow, STAT3 inactivation could lead to the awakening of dormant tumor cells. In contrast to this, the small molecule inhibitor EC359, which has been shown to directly interact with LIFR to block its interactions with LIF, OSM, CNTF, and CT-1, reduced LIFR-mediated activation of multiple gene targets, STAT3 activity and downstream target genes, and suppressed

TNBC xenograft and PDX tumor growth *in vivo* [256]. While ER+ breast cancer cell lines were used in the initial screens for LIF and LIFR in these studies, functional studies were all carried out in TNBC cell lines, so it is unclear whether EC359 would have had similar effects on ER+ tumor progression *in vivo*.

While the predominant signaling pathway activated by the gp130 cytokines is the JAK-STAT signaling axis, OSM has been shown to suppress ER protein and mRNA expression in ER+ breast cancer cells through the MAPK-ERK pathway [188]. The MAPK inhibitor U0126 blocked morphological changes in ER+ breast cancer cell lines, confirming MAPK as a downstream mediator of the pro-migratory phenotype induced by OSM. In combination with the STAT3 studies above, this points to OSM activating multiple signaling pathways to promote breast cancer progression. While OSM, LIF, and IL-6 can induce STAT3, AKT, and ERK signaling in breast cancer cells, in the absence of studies using combinations of STAT3, AKT, and ERK inhibitors it is difficult to determine which is the dominant downstream mediator. Current literature suggests that LIF and IL-6 elicit functions primarily through STAT3 activation, while OSM may act through both STAT3 and ERK.

**IL-6 cytokines and cancer stem cells**

Recently, several groups have proposed that tumor cells that reside in a dormant state do so through adoption of a cancer stem cell (CSC) phenotype [112, 257]. It has been proposed that CSCs are a subset of cancer cells that undergo self-renewal [258], are responsible for tumor initiation, progression, and metastases [258-261], and persist long term [257], but this has not been well studied with regards to bone metastasis. CSC populations have also been associated with poor prognosis and increased resistance to chemo/radio-therapies [262-264]. Certain cytokines are already known to stimulate the expression of CSC features, including TGF-β by activating Wingless (Wnt) signaling in breast cancer cells [265]. The self-renewal properties of CSCs can also be regulated by a network of regulatory and signaling pathways such as Notch [266], Hedgehog [267, 268], transforming growth factor-beta (TGF-β) [269], estrogen/progesterone (ER/PR) [270], epidermal growth factor/receptor (EGF/EGFR) [271], and LIF [272]. Overexpression of several of these signaling pathways is known to increase the stem cell

and CSC pool [267, 273]. Of these ligands, LIF has known functions as a pro-stemness factor by maintaining pluripotency in mouse embryonic stem cells [274, 275]. For the culture of mESCs, LIF and other gp130 cytokines, such as OSM, CNTF and CT-1 can enable self-renewal and promote stem-ness by activating pluripotency associated genes through STAT3 [276-282]. In pancreatic cancer, blockade of LIF:LIFR:STAT3 signaling resulted in a decrease in expression of CSC-associated markers (CD133, CD24, and CD44), a reduction in tumor initiation and formation, and an overall less aggressive phenotype [283]. In addition, long-term stimulation by OSM on transformed-human mammary epithelial cells (HMECs) resulted in an increase in $CD44^{High}/CD24^{Low}$ expression, upregulation of CSC/EMT associated genes and promoted stem cell plasticity both *in vitro* and *in vivo* [255, 284], suggesting that long-term OSM exposure may promote a CSC phenotype.

It has been previously established that LIFR expression on breast cancer cells promotes tumor dormancy in the bone marrow and that several of the gp130 cytokines (LIF, OSM, and CNTF) are able to signal through LIFR. Because LIF, OSM, and CNTF are present in the bone marrow, bone-DTCs may receive these signals in the endosteal niche to remain in a dormant state (Figure 6); however, given that these cytokines can also promote stemness, it will be important to determine whether LIF, OSM, and CNTF induce dormancy by promoting a CSC phenotype in which the cells are more quiescent but have the potential for self-renewal.

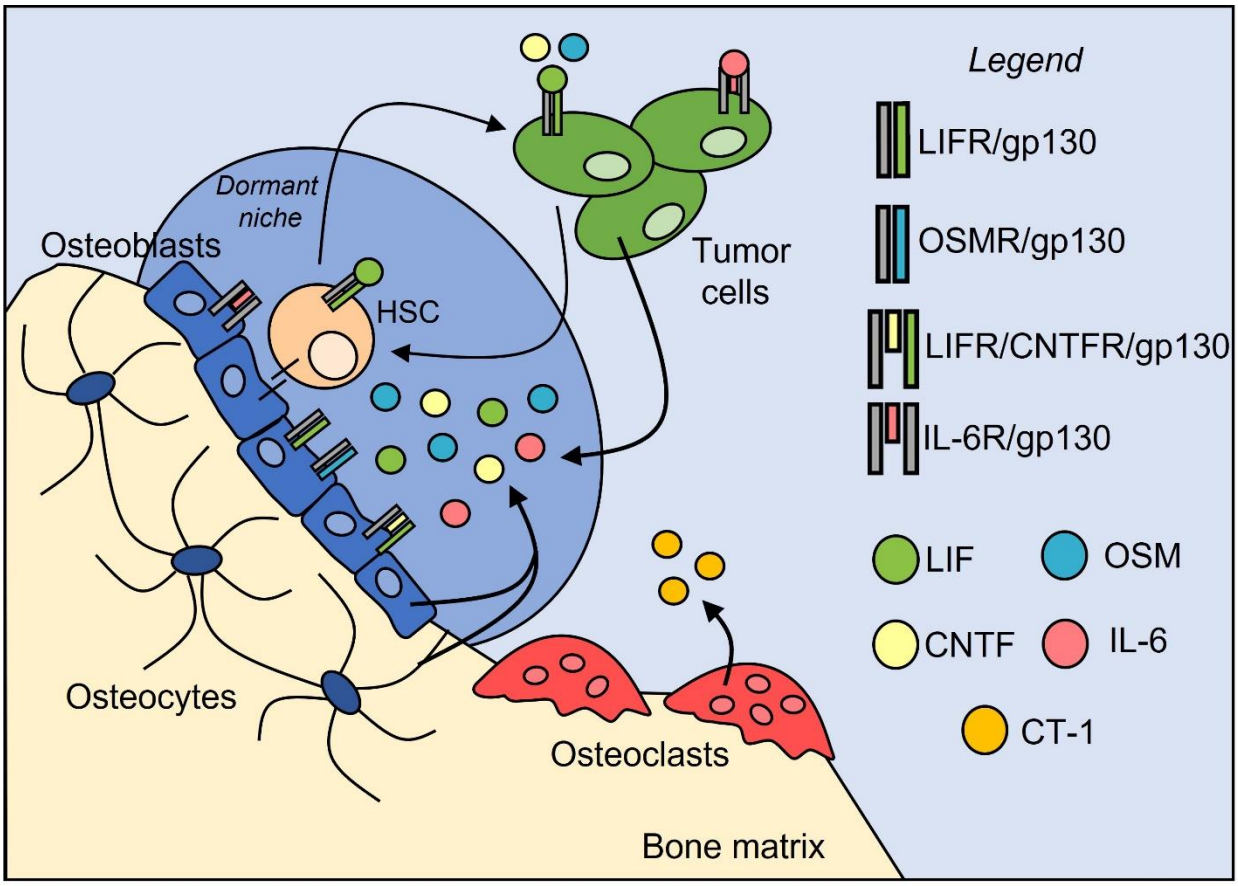


**Figure 6. Bone disseminated tumor cells compete with hematopoietic stem cells (HSCs) in the endosteal niche, where they encounter pro-dormancy cytokines in the microenvironment.** Tumor cells that disseminate into the bone marrow are proposed to compete with HSCs for the endosteal niche, which maintains dormancy through cell-cell interactions and secreted factors, including the gp130 cytokines. These cytokines normally send pro-dormancy signals to the HSCs to maintain their quiescence, and when tumor cells compete for this niche are likely to encounter the same cytokine milieu. Both HSCs and breast cancer cells express LIFR, although LIFR is markedly down-regulated in more aggressive breast cancer cells [69]. This suggests that both HSCs and breast cancer cells are capable of responding to LIF, OSM, and CNTF secreted within the bone marrow microenvironment. The source of these cytokines in the pro-dormancy niche are bone-lining osteoblasts and osteocytes embedded within the bone matrix. Osteoclasts do not express most of the gp130 cytokines, but do express CT-1, which can also bind to LIFR. It is unclear how this might contribute to the pro-dormancy niche along the quiescent osteoblast-lined surface.

**Summary and study aims**

As the dormancy field continues to expand and develop better models and tools for studying occult disseminated tumor cells, our understanding of the cellular and molecular mechanisms that regulate dormancy will likewise grow. However, currently our mechanistic understanding of bone dissemination and metastatic outgrowth remains poorly understood. While it is well established that the gp130 cytokine family regulates a plethora of biological processes that affect bone remodeling, cancer progression and metastasis, questions remain as to the exact role these cytokines play in tumor dormancy. Despite the body of literature defining the numerous roles for the gp130 cytokine family members, there are still mechanisms of action that remain unknown, particularly with regards to the contradictory effects of OSM and LIF on breast cancer cells. These cytokines can form a complex with LIFR on breast cancer cells, which promotes dormancy in bone-disseminated tumor cells, and are therefore highly relevant to the pathogenesis of bone-disseminated breast cancer cells.

We sought to present findings that will address some of the current gaps within the field pertaining to the role of the gp130 cytokines in ER+ breast cancer, the signaling pathways activated by the cytokine family, and whether specific cytokines induce CSC properties. Chapter II describes the materials and research methods used in the studies from Chapter III and Chapter IV. In Chapter III, we characterize the basal expression level of the gp130 cytokines and receptors using a panel of nine different breast cancer cell lines differing in molecular subtype, metastatic potential, and species, and link these findings to survival outcomes in breast cancer patients. We also establish the role for OSM and CNTF in ER+ breast cancer dissemination to bone and reveal distinct signaling pathways stimulated by the gp130 cytokines in breast cancer cells. Chapter IV explores whether OSM enriches for breast cancer CSCs as a potential mechanism of enhanced tumor dissemination to the bone and establishes OSM as a regulator of CD44 expression. Finally, Chapter V discusses the future implications of this work.

# CHAPTER II

## MATERIALS AND METHODS

**Cells and cell culture reagents.** Human breast cancer cells MCF7, T47D, and MDA-MB-231, were acquired from ATCC. Bone-tropic MCF7 (MCF7b) were generated in the Johnson Lab and created as previously described [285]. The bone metastatic variant of the MDA-MB-231 cells (MDA-MB-231b) cells were donated to our lab but was previously established as described [286-288]. D2.0R and D2A1 mouse mammary carcinoma cells were donated by the J. Green laboratory at the National Cancer Institute. Polyoma middle T (PyMT)-derived mouse mammary carcinoma cells were acquired and created by the Anderson laboratory at the Peter MacCallum Cancer Centre. 4T1 mouse mammary carcinoma cells were acquired from ATCC and the bone metastatic variant (4T1BM2) as described [289], were obtained as a gift from the Pouliot laboratory at the Peter MacCallum Cancer Centre. All cell lines were cultured in DMEM with 10% fetal bovine serum (FBS) and penicillin/streptomycin (P/S) as previously described [287, 290]. Human breast cancer cell line SUM159, were obtained as a gift from the Rutgers Cancer Institute of New Jersey and were cultured in Ham's F12 medium supplemented with 5% FBS, 5 μg $mL^{-1}$ and 1 μg $mL^{-1}$ hydrocortisone. Human T47D breast cancer cells were cultured in RPMI-1640 medium and supplemented with 10% FBS. All human cell lines were authenticated by ATCC and all cells were regularly tested for mycoplasma contamination.

**shRNA knockdown.** Knockdown experiments were performed as previously described [287]. For shRNA experiments 293T cells were transfected with GIPZ lentiviral-LIFR targeting vectors to produce lentivirus. MCF7 cells were transduced with virus using 5 μg $mL^{-1}$ polybrene followed by selection with 1μg/mL puromycin for 3 days.

**Stable and Transient Overexpression.** MCF7 cells with empty vector and OSM/CNTF overexpression were established by transduction using these expression plasmids: pCMV3-C-GFPSpark Vector (Sino Biologcial, Catalog Number CV026), pCMV3-C-OSM-GFP (Sino Biologcial, Catalog Number HG10452-ACG), pCMV6-AC-GFP (Origene,

Catalog Number PS100010) and pCMV6-AC-CNTF-GFP (Origene, Catalog Number RG222331). Cells were selected using hygromycin (OSM) and neomycin (CNTF). MDA-MB-231 parental and bone metastatic cells transiently overexpressing OSM and CNTF were established using previously mentioned expression vectors. Cells were transfected using Lipofectamine LTX with Plus Reagent (Thermo Fisher, Catalog Number 15338030) and harvested 36 hours later.

**RNA Extraction.** Intact femurs and cells were harvested in TRIzol (Life Technologies), extracted, DNA digested (TURBO DNA-free Kit, Life Technologies), and cDNA synthesized (iScript cDNA Synthesis Kit, Bio-Rad) using the manufacturer's instructions. Real-time PCR was performed using iTaqTM Universal SYBR Green Supermix (Bio-Rad) on a QuantStudio 5 (Thermo Fisher) with the conditions previously described [290]. For each biological replicate, three technical replicates were pipetted onto the qPCR plate and averaged for each gene analyzed. Primers for *B2M, B2m, LIFR, SOCS3*, *THBS1*, *TPM1*, *AMOT*, *TGF-β2*, *P4HA1*, *H2BK*, *IGFBP5*, *miR-190*, *SBP56, ALDH1A1*, *NOTCH1*, *CASP3*, *TERT*, *SOX2*, *OCT4*, and *NANOG* were all previously published were all previously published [287]. Primers for *QSOX1* [291], *PDCD4* [292], and *CDKN1B* [292] were previously published by other groups. The primer for mouse *gp130* was also previously published [293].

The following gene primers were designed using PrimerBlast (NCBI) against the human genome (Homo sapiens) and mouse genome (mus musculus) and validated by dissociation: *CNTF*, *Cntf*, *CNTFR*, *Cntfr*, *GP130*, *Gp130*, *LIF*, *Lif*, *OSM*, *Osm*, *OSMR*, and *Osmr*. *For* the *in vitro* studies, each target gene was normalized to the expression of the average B2M (human) or *B2m* (mouse) expression within the same sample. For the detection of human cells in mouse samples B2M was normalized to the expression of the average *Gapdh* expression within the same sample. Other primers were obtained from the MGH PrimerBank (https://pga.mgh.harvard.edu/primerbank/citation.html). Primer pairs were selected and tested for specificity using BLAST (NCBI) and validated by dissociation. For the *in vitro* studies, each target gene was normalized to the expression of the average B2M (human) expression within the same sample. PCR primer sequences are compiled in Table 1 and 2.

**Table 1. Real-Time PCR primer sequences for human genes.**

| Gene Name | Forward Primer Sequence | Reverse Primer Sequence |
|---|---|---|
| ABCG2 | TGAGCCTACAACTGGCTTAGA | CCCTGCTTAGACATCCTTTTCAG |
| ALDH1A1 | CAAGATCCAGGGCCGTACAA | CAGTGCAGGCCCTATCTTCC |
| AMOT | GGCATGCCACCCCAATCT | TTGTAGCAAGGGCAAGGACC |
| B2M | GAGTATGCCTGCCGTGTGAA | TGCGGCATCTTCAAACCTCC |
| BMP7 | TCAACCTCGTGGAACATGACA | CTTGGAAAGATCAAACCGGAACT |
| CASP3 | GCGGTTGTAGAAGAGTTTCGTG | CTCACGGCCTGGGATTTCAA |
| CD24 | CTCCTACCCACGCAGATTTATTC | AGAGTGAGACCACGAAGAGAC |
| CD44 | CCAGAAGGAACAGTGGTTTGGC | ACTGTCCTCTGGGCTTGGTGTT |
| CDKN1B | TCAAACGTGAGAGTGTCTAACG | CCGGGCCGAAGAGATTTCTG |
| CNTF | GAAGATTCGTTCAGACCTGACTG | AAGGTTCTCTTGGAGTCGCTC |
| CNTFR | TTATGGTCTGTGAGAAGGACCC | GCATTGCTGACACTTATGGAGA |
| FOXA1 | GCAATACTCGCCTTACGGCT | TACACACCTTGGTAGTACGCC |
| GAS6 | GGTAGCTGAGTTTGACTTCCG | GACAGCATCCCTGTTGACCTT |
| GATA3 | GCCCCTCATTAAGCCCAAG | TTGTGGTGGTCTGACAGTTCG |
| GP130 | GGAGTGAAGAAGCAAGTGGGA | AGGCAATGTCTTCCACACGA |
| HIST1H2BK | CAAGGCCGTCACCAAGTACA | GAAGGCAATTGTGCTTCTTTTGA |
| LIF | CCAACGTGACGGACTTCC | TACACGACTATGCGGTACAGC |
| MAPK11 | AAGCACGAGAACGTCATCGG | TCACCAAGTACACTTCGCTGA |
| MAPK14 | CCCGAGCGTTACCAGAACC | TCGCATGAATGATGGACTGAAAT |
| MDR1 | TTGCTGCTTACATTCAGGTTTCA | AGCCTATCTCCTGTCGCATTA |
| miR-190 | GCAGGCCTCTGTGTGATATGT | GGCAAGACACTGTAGGAATATGT |
| MSK1 | TTCCTTTGTTGCTCCTTCCATC | CAACATTTGTCACTCCAGGACG |
| NANOG | CTAAGAGGTGGCAGAAAAACA | CTGGTGGTAGGAAGAGTAAAGG |
| NOTCH1 | AGCCTCAACGGGTACAAGTG | CACACGTAGCCACTGGTCAT |
| OCT4 | AGAAGCTGGAGCAAAACCCG | ACCTTCCCAAATAGAACCCCCA |
| OSM | GGCAGCTGCTCGAAAGAGTA | ATAGGGGTCCAGGAGTCTGC |
| OSMR | ATGCCATCATGACCTGGAAGG | CCTTCACCATGGAGTTCAATCTG |
| P4HA1 | GTACATGACCCTGAGACTGGA | GGGGTTCATACTGTCCTCCAA |
| PDCD4 | AAGCGGAAAGACAGTGTGTG | GGCTTCATATACAAGCTCGTGG |
| PROM1 | GCTTAGCAGCAGTCTGACCA | AGGGATTGATAGCCCTGTTGG |
| QSOX1 | GACCTGACGAGTTGGT | AATCAAGCATGTGTAAGGCAC |
| SBP56 | AAGTGCGAACTGGCCTTTCT | CCCATCCAGCAGCACAAAAC |
| SOCS3 | GCTCCAAGAGCGAGTACCAG | CTGTCGCGGATCAGAAAGGT |
| SOX2 | ACCAGCGCATGGACAGTTAC | CCGTTCATGTAGGTCTGCGA |
| TERT | CTTGCGGAAGACAGTGGTGA | GTCCGGGCATAGCTGGAGTA |
| TGF-β2 | GGCCAGATCCTGTCCAAGC | GTGGGTTTCCACCATTAGCAC |
| THBS1 | TCCCCATCCAAAGCGTCTTC | ACCACGTTGTTGTCAAGGGT |
| TPM1 | TCTCAGAAGGCCAAGTCCGA | CAAACTCAGCCCGAGTCTCA |

**Table 2. Real-Time PCR primer sequences for mouse genes.**

| Gene Name | Forward Primer Sequence | Reverse Primer Sequence |
|---|---|---|
| B2m | TTCACCCCCACTGAGACTGAT | GTCTTGGGCTCGGCCATA |
| B2m | TTCACCCCCACTGAGACTGAT | GTCTTGGGCTCGGCCATA |
| Cntf | GCATTTCACCCCGACTGAAG | CGCCATTAACTCCTCTAGCTG |
| Cntfr | TGTCTACACGCAGAAACACAG | CCCAGACGCTCATACTGCAC |
| Gapdh | AGGTCGGTGTGAACGGATTTG | GGGGTCGTTGATGGCAACA |
| Gp130 | AGAAGCCATAGTCGTGCCTGTGT | AAAGCAGAACAAGACGCCCAGCA |
| Lif | AACCAGATCAAGAATCAACTGGC | TGTTAGGCGCACATAGCTTTT |
| Lifr | CTTGCAATGTGCCACTCACT | CGAGCACCACTTTGTCTTGA |
| Osm | TCATCCTGAGCATGGCACTG | CGTGAGGTTCGCCTGATTCT |
| Osmr | AAACATGATATTTCAGATAGAGATC AGTAGACT | CTTATGAAATGTTTGACACACTCCAA |

**Recombinant proteins.** Recombinant human LIF (R&D Systems), human OSM (R&D Systems), human CNTF (R&D Systems), human CNTFsR (R&D Systems), human IL-6 (R&D Systems), and human IL-6Rα (R&D Systems) were reconstituted in PBS + 0.1% bovine serum albumin (BSA) at 10–50 μg $mL^{-1}$ and aliquoted for storage at −80°C. For all experiments, human recombinant proteins were used on human cell lines. Before cytokine treatment, breast cancer cells were serum starved in DMEM supplemented with 2% FBS overnight and cytokine treatment was made up in fresh media under serum starved conditions.

**Western Blot and Densitometry Analysis.** Cells grown in a monolayer on 100mm cell culture dish were rinsed with 1X PBS and harvested for protein in RIPA buffer supplemented with protease and phosphatase inhibitor. Protein concentration was determined by BCA assay and 18-20μg protein was loaded onto an SDS-PAGE gel and transferred to nitrocellulose membranes using standard techniques. Membranes were probed with antibodies against LIFR (Santa Cruz Biotechnology, C-19, Catalog Number sc-659, 1:1000), pSTAT3 Y705 (Cell Signaling, Catalog Number 9131, 1:1000), STAT3 (Cell Signaling, clone 124H6, Catalog Number 9139, 1:1000), pSTAT1 (Cell Signaling, Catalog Number 9172, 1:1000), STAT1 (Cell Signaling, Catalog Number pAKT Ser473 (Cell Signaling, Catalog Number 9271, 1:1000), AKT (Cell Signaling, Catalog Number 9272S, 1:1000), pERK1/2 Thr202/Tyr204 (Cell Signaling, Catalog Number 9101, 1:1000), ERK1/2 (Cell Signaling, Catalog Number 9102, 1:1000), GAPDH (Cell Signaling, Catalog Number 2118S, 1:1000), alpha-tubulin (Antibody & Protein Resource at Vanderbilt University, Catalog Number VAPRTUB, 1:5000), and vinculin (Millipore, Catalog Number AB6039, 1:10,000). All western blot images were converted to a histogram rendering for each lane and peaks were converted to the relative percentage for each blot. Peaks were quantified as adjusted relative density after the relative percentage for proteins of interest were normalized to the relative percentage of the loading control for the respective lanes. These values were then plotted and defined as relative protein expression.

**Animals.** All experiments were performed in accordance with the guidelines and regulations of the Animal Welfare Act and the Guide for the Care and Use of Laboratory

Animals and were approved by the Institutional Animal Care and Use Committee (IACUC) at Vanderbilt University. Experiments were conducted using 4-6-week-old female athymic nude mice (Jackson, Cat #7850). Mice were implanted subcutaneously with 17β-estradiol pellets as described [285]. The next day, 1 x $10^6$ tumor cells in 50μL volume of sterile PBS + 50% Matrigel (Fischer Scientific) were injected into the fourth mammary fat pad (n=10 mice/group). Tumor volume was assessed by caliper measurements. Several mice were found dead or had to be sacrificed early due to estrogen toxicities and were removed from the final analysis; all other mice were euthanized 28 days post-inoculation of tumor cells. For the study, final analysis included n=10 MCF7-pCMV3 (Empty Vector) inoculated mice and n=9 MCF7-pCMV3-OSM (OSM overexpression), n=9 MCF7-pCMV6 (Empty Vector) and n=9 MCF7-pCMV6-CNTF (CNTF overexpression).

**Flow Cytometry**

***Bone Marrow CD298 Stain.*** One hindlimb was crushed with a mortar and pestle to obtain the bone marrow. PBS (1mL) was added to the crushed bone marrow and were spun down and washed with PBS to remove bone debris. Bone marrow (5 x $10^5$ cells) was stained in 100μL of PBS with LIVE/DEAD™ Fixable Green Dead Cell Stain Kit @488nm (Thermo Fisher Scientific, Catalog Number L34970, 1:1000) for 15 minutes on ice at 4°C in the dark. Cells were washed with PBS and resuspended with 100μL of 1% BSA in PBS with CD298 antibody (BioLegend, Cat #341704) for 30 minutes on ice at 4°C in the dark.

***CSC CD44 and CD24 Stain.*** Breast cancer cells treated with recombinant cytokine or PBS for 24 hours were washed with PBS and trypsinized and resuspended in 100μL of 1% PBS/BSA. Samples were stained in 100μL of 1% PBS/BSA with PE Mouse Anti-Human CD44 (BD Biosciences, Catalog Number 561858) and BV711 Mouse Anti-Human CD24 (BD Biosciences, Catalog Number 563371) for 1 hour on ice at 4°C in the dark. Cells were washed with PBS and resuspended in 1μg/mL of DAPI (Sigma, Catalog D9542-1MG) mixed with PBS and incubated for 10 minutes at 4°C in the dark.

**Flow Cytometry Analysis.** Flow cytometry experiments were performed in the VUMC Flow Cytometry Shared Resource using the 5-laser BD LSRII and 4-laser BD Fortessa

LSRII. Data was analyzed using FlowJo software (FlowJo, LLC) where bone marrow samples were gated based on forward scatter and side scatter geometry and PE-CD298 (+) cells were gated using live cells (LIVE/DEAD-Green negative). MCF7 breast cancer cells were used as a positive control for CD298 stain. Breast cancer cells were gated based on forward scatter, side scatter geometry and PE-CD44 (high) / BV711 CD24 (low) cells were gated using live cells (DAPI negative). Dead cells (DAPI positive) were gated out and not included in the representative plots or analysis. MDA-MB-231b breast cancer cells were used as a positive control for $CD44^{High}CD24^{Low}$.

**KM-Plotter and GSE Datasets.** KM-Plotter graphs were directly produced using the online bioinformatics tool (https://kmplot.com/) specifically for breast cancer [294].The specific Affymetrix ID for the probes of interest were LIF (205266_at), OSM (214637_at), CNTF (208597_at), LIFR (205876_at), OSMR (205729_at), CNTFR (205723_at), and GP130 (IL6ST-212195_at). Patients were split using the automated best-selection-cutoff analysis provided by the KM-Plotter and median survival between cohorts was computed. No restrictions on analysis were included except for ER status as indicated by microarray [294] in the stratified analysis. A total of n=4929 patients were included in the unstratified analysis and in the ER status analysis, n=3768 ER+ and n=2009 ER- patients were included. The analysis tool has had subsequent updates since its initial creation, culminating to an increase in the number of patients within the database [295, 296] and the integration of several tools for more in-depth patient sample analysis [297-300]. Overall, the KM-Plotter total breast cancer patient database includes patient samples from GSE2603, GSE17705, GSE21653, GSE16446, GSE17907 and GSE19615, with a grand total of 7830 patient samples.

For the analysis of the GEO datasets, GSE14548 [301] had a total of 66 samples from fresh-frozen biopsies obtained from the Massachusetts General Hospital. Informed consent was not applicable because specific patient characteristics and data were unavailable to the authors of the study. GSE29044 [302] had a total of 124 samples that were collected from the normal tissue and primary tumors of 109 patients between the ages of 20-62 who underwent treatment and surgery at the King Faisal Specialist Hospital and Research Center of Saudi Arabia. The authors of the study focused on breast cancer

patients diagnosed with infiltrating ductal carcinoma (IDC) and ductal carcinoma *in situ* (DCIS). Patient cohorts were stratified by tissue type (normal versus tumor), tumor grade, receptor status, tumor type (IDC versus DCIS) and age. The probes for each cytokine and receptor that were available are listed in Table 3 for GSE29044 and in Table 4 for GSE14548; we analyzed all of the probes for each sample, and all probes had a similar trend of expression across both GSE datasets. Specific probes were chosen to be displayed in Figure 22, 23, 24, 25, 26, 27 because they are representative of the larger probe set for each gene of interest.

**Statistics and reproducibility**

For all studies, the scatter dot plots indicate the mean of each group and error bars indicate the standard error of the mean (SEM). All graphs and statistical analyses were generated using Prism software (Graphpad). All *in vitro* assays were performed at least three independent times, and the replicates for each graph contains one replicate from each independent study. If technical replicates were plated these data were averaged prior to statistical analysis. Data were analyzed for statistical significance using a one-way ANOVA with Dunnett's multiple comparisons test or a two-way ANOVA with Tukey's multiple comparisons test. For *in vitro* assays, no statistical method was used to predetermine sample size. For all analyses $p<0.05$ was considered statistically significant, and *$p<0.05$, **$p<0.01$, ***$p<0.001$, ****$p<0.0001$.

**Table 3. Probeset for GSE29044.**

| GSE29044 | |
|---|---|
| **Gene** | **Probes** |
| LIF | 205266_at, |
| OSM | 230170_at, 230170_at, 214637_at |
| CNTF | 208597_at |
| LIFR | 225575_at, 225571_at, 227771_at, 205876_at, 229185_at, 1559986_at |
| OSMR | 226621_at, 1554008_at, 205729_at |
| CNTFR | 205723_at, 1561590_a_at, 1556771_a_at |
| GP130 (IL6ST) | 212195_at, 204863_s_at, 212196_at |

**Table 4. Probeset for GSE14548.**

| GSE14548 | |
|---|---|
| **Gene** | **Probes** |
| LIF | g6006018_3p_at |
| OSM | Hs.134435.0.A1_3p_a, Hs.248156.0.S2_3p_at |
| CNTF | - |
| LIFR | Hs.23767.2.A2_3p_at, Hs.23767.2.A1_3p_x_at, Hs.23767.2.A1_3p_at, g6042197_3p_at, Hs2.280369.1.S1_3p_at, Hs.124963.0.A1_3p_at, Hs.23767.1.A1_3p_at |
| OSMR | Hs2.238648.2.S1_3p_at, g4557039_3p_at |
| CNTFR | Hs2.147590.2.S1_3p_s_at, Hs.129966.0.A1_3p_at, g4502930_3p_at |
| GP130 (IL6ST) | Hs.82065.0.A1_3p_a_at, g4504674_3p_a_at, Hs.71968.0.A1_3p_x_at, Hs.283974.0.S1_3p_a, Hs.71968.0.A2_3p_at, Hs.283974.0.A1_3p_at, 212196_3p_at, Hs.71968.0.A1_3p_at |

**Reverse Phase Protein Array.** MCF7 breast cancer cells were seeded at 1 x $10^6$ cells per dish (Eppendorf) in a 100mm plate cultured overnight. The next day, cells were washed with PBS and plates were reconstituted with DMEM with 2% FBS for serum starvation prior to cytokine treatment as described in the previous section. After 30 minutes of cytokine treatment, cells were washed with PBS and 100µLof RIPA buffer (Sigma) with PhosStop (Phosphatase Inhibitor, Roche, Catalog Number 04-906-845-001) and Protease Inhibitor (Roche/Sigma, Catalog Number 4693159001) and incubated for 30 minutes at 4°C on a plate shaker. Protein concentration was determined by BCA (Thermo Fisher), adjusted to 1.5µg/µL, mixed with (4X SDS and beta-mercaptoethanol) and boiled for 5 minutes. Samples remained at -80°C until sent to MD Anderson Cancer Center where the samples were processed and analyzed by the RPPA Core facility. RPPA date sets were analyzed and fold change was determined using the normalized linear expression (Table 5).

## Table 5. Fold Change of normalized linear RPPA data from MCF7 cells treated with recombinant gp130 cytokines.

| Antibody Name | Antibody Origin | Gene Name | Validation Status | Probabilities (QC Score) | PBS (FC) | LIF (FC) | OSM (FC) | CNTF (FC) | CNTFsR (FC) |
|---|---|---|---|---|---|---|---|---|---|
| **14-3-3-beta** | R | YWHAB | V | 0.853254 | 1 | 1.122866 | 1.02535 | 1.030219 | 1.62561 |
| **14-3-3-epsilon** | M | YWHAE | C | 0.843027 | 1 | 1.274003 | 1.216989 | 1.285792 | 1.236142 |
| **14-3-3-zeta** | R | YWHAZ | V | 0.946832 | 1 | 1.044594 | 0.985914 | 0.913493 | 1.016667 |
| **4E-BP1** | R | EIF4EBP1 | V | 0.95298 | 1 | 1.198839 | 1.024961 | 1.056834 | 0.840564 |
| **4E-BP1_pS65** | R | EIF4EBP1 | V | 0.965572 | 1 | 1.037249 | 0.970142 | 1.023826 | 0.915956 |
| **4E-BP1_pT37_T46** | R | EIF4EBP1 | V | 0.965878 | 1 | 1.171584 | 1.058873 | 1.051052 | 0.956105 |
| **53BP1** | R | TP53BP1 | V | 0.966571 | 1 | 1.046702 | 1.068097 | 1.073217 | 0.984907 |
| **A-Raf** | R | ARAF | V | 0.964164 | 1 | 1.103687 | 1.154195 | 0.978409 | 0.92562 |
| **A-Raf_pS299** | R | ARAF | C | 0.882715 | 1 | 0.939028 | 1.124351 | 1.205901 | 1.210732 |
| **ACC1** | R | ACACA/ACACB | C | 0.957725 | 1 | 1.11175 | 0.965605 | 1.085672 | 0.979203 |
| **ACC_pS79** | R | ACACA/ACACB | V | 0.95095 | 1 | 1.033128 | 1.056671 | 1.192157 | 1.010616 |
| **AceCS1** | R | ACSS2 | V | 0.952558 | 1 | 0.887202 | 1.063114 | 1.193032 | 0.940076 |
| **ACLY_pS455** | R | ACLY | V | 0.92798 | 1 | 0.610793 | 1.289718 | 1.823109 | 1.861653 |
| **ACSL1** | R | ACSL1 | V | 0.820758 | 1 | 1.041691 | 1.06297 | 1.390154 | 1.309305 |
| **ACVRL1** | R | ACVRL1 | C | 0.892758 | 1 | 0.616327 | 0.627434 | 0.644421 | 0.600745 |
| **ADAR1** | M | ADAR | V | 0.93084 | 1 | 0.96 | 0.830243 | 0.904348 | 0.993312 |
| **Akt** | R | AKT1/2/3 | V | 0.922976 | 1 | 0.977946 | 0.979408 | 0.901351 | 1.004274 |
| **Akt1** | R | AKT1 | V | 0.960845 | 1 | 0.997562 | 0.976108 | 0.936885 | 1.043949 |
| **Akt1_pS473** | R | AKT1 | V | 0.925483 | 1 | 1.166644 | 2.65338 | 1.037035 | 1.195435 |
| **Akt2** | R | AKT2 | V | 0.966292 | 1 | 0.953809 | 0.911502 | 0.987004 | 1.010538 |
| **Akt2_pS474** | R | AKT2 | C | 0.933762 | 1 | 1.075871 | 1.58658 | 0.887301 | 0.737759 |
| **Akt_pS473** | R | AKT1/2/3 | V | 0.927901 | 1 | 0.950393 | 2.645211 | 1.134715 | 0.985829 |
| **Akt_pT308** | R | AKT1/2/3 | V | 0.966771 | 1 | 0.885452 | 1.000971 | 1.058135 | 0.961451 |
| **Ambra1_pS52** | R | AMBRA1 | C | 0.95758 | 1 | 1.019186 | 1.040284 | 1.04512 | 1.068598 |
| **AMPK-a2_pS345** | R | PRKAA2 | V | 0.95002 | 1 | 1.180593 | 1.064863 | 1.160891 | 1.203758 |
| **AMPKa** | R | PRKAA1/2 | C | 0.968907 | 1 | 1.038816 | 1.01706 | 1.06137 | 1.006925 |
| **AMPKa_pT172** | R | PRKAA1/2 | C | 0.971398 | 1 | 0.96525 | 0.937475 | 1.062319 | 1.012914 |
| **Annexin-I** | M | ANXA1 | V | 0.928212 | 1 | 1.046702 | 1.068097 | 1.073217 | 0.984907 |
| **Annexin-VII** | M | ANXA7 | V | 0.928532 | 1 | 0.997067 | 0.96367 | 0.970973 | 1.079005 |
| **AR** | R | AR | V | 0.918332 | 1 | 0.932656 | 0.918288 | 1.004264 | 1.009575 |
| **ARID1A** | R | ARID1A | C | 0.969672 | 1 | 0.88822 | 0.906832 | 1.027825 | 0.836095 |
| **ASNS** | R | ASNS | V | 0.960677 | 1 | 0.817472 | 0.851764 | 1.004959 | 0.811543 |
| **Atg3** | R | ATG3 | V | 0.888056 | 1 | 1.032791 | 0.95409 | 0.921772 | 0.716095 |
| **Atg4B** | R | ATG4B | C | 0.947458 | 1 | 1.032791 | 0.945871 | 0.868424 | 0.993934 |
| **Atg5** | R | ATG5 | C | 0.956495 | 1 | 1.067937 | 0.974552 | 0.963766 | 1.077006 |
| **Atg7** | R | ATG7 | V | 0.926862 | 1 | 0.743205 | 1.021529 | 0.99825 | 0.98918 |
| **ATM** | R | ATM | V | 0.959904 | 1 | 0.960568 | 0.995911 | 1.303874 | 1.010367 |
| **ATM_pS1981** | R | ATM | V | 0.810835 | 1 | 1.064346 | 1.062479 | 1.008807 | 1.01198 |
| **ATP5H** | R | ATP5PD | V | 0.910278 | 1 | 1.046702 | 1.068097 | 1.073217 | 0.988478 |
| **ATR** | R | ATR | V | 0.935709 | 1 | 0.993709 | 1.013915 | 1.018507 | 1.064221 |
| **ATRX** | R | ATRX | C | 0.95754 | 1 | 1.072594 | 1.093227 | 1.128754 | 0.913169 |
| **ATR_pS428** | R | ATR | C | 0.948833 | 1 | 0.921643 | 1.081397 | 0.91891 | 1.18753 |
| **Aurora-A** | R | AURKA | C | 0.954452 | 1 | 0.836358 | 0.895991 | 1.239075 | 0.73704 |
| **Aurora-ABC_pT288_pT232_pT198** | R | AURKA-C | C | 0.928326 | 1 | 0.974797 | 0.976185 | 1.237917 | 1.022733 |
| **Aurora-B** | R | AURKB | V | 0.950832 | 1 | 0.901644 | 1.097155 | 1.250486 | 0.923796 |
| **Axl** | R | AXL | V | 0.956735 | 1 | 0.651184 | 0.666212 | 1.226201 | 1.152905 |
| **b-Actin** | R | ACTB | C | 0.86349 | 1 | 1.045452 | 1.066814 | 1.07193 | 0.992784 |
| **b-Catenin** | R | CTNNB1 | V | 0.944569 | 1 | 1.03316 | 0.903671 | 1.080472 | 0.951422 |

| | | | | | | | | | |
|---|---|---|---|---|---|---|---|---|---|
| **b-Catenin_pT41 S45** | R | CTNNB1 | V | 0.953338 | 1 | 1.173931 | 0.983916 | 1.207571 | 1.053938 |
| **B-Raf** | R | BRAF | C | 0.96641 | 1 | 1.046702 | 1.068097 | 1.073217 | 0.984907 |
| **B-Raf_pS445** | R | BRAF | V | 0.968277 | 1 | 1.10109 | 0.998931 | 1.147781 | 1.03929 |
| **B7-H3** | R | CD276 | C | 0.910507 | 1 | 0.931456 | 0.900741 | 0.90627 | 1.049141 |
| **B7-H4** | R | VTCN1 | C | 0.946749 | 1 | 1.033432 | 0.817874 | 0.789934 | 0.993524 |
| **Bad_pS112** | R | BAD | V | 0.962365 | 1 | 1.333397 | 1.092991 | 1.076076 | 0.94913 |
| **Bak** | R | BAK1 | C | 0.946323 | 1 | 0.973593 | 0.779406 | 0.97623 | 0.820378 |
| **BAP1** | M | BAP1 | V | 0.931419 | 1 | 1.107284 | 1.027264 | 0.971308 | 0.763331 |
| **Bax** | R | BAX | V | 0.956911 | 1 | 1.032508 | 0.857676 | 0.980913 | 0.89902 |
| **Bcl-xL** | R | BCL2L1 | V | 0.967914 | 1 | 1.027251 | 0.973987 | 1.155404 | 0.927946 |
| **Bcl2** | R | BCL2 | V | 0.871443 | 1 | 1.025061 | 1.665541 | 1.453038 | 1.217943 |
| **BCL2A1** | R | BCL2A1 | V | 0.933498 | 1 | 0.943382 | 0.881889 | 0.962615 | 0.83575 |
| **Beclin** | R | BECN1 | C | 0.933009 | 1 | 1.059541 | 1.097149 | 0.958517 | 1.095879 |
| **Bid** | R | BID | C | 0.959366 | 1 | 0.991568 | 0.828181 | 1.055703 | 0.946509 |
| **Bim** | R | BCL2L11 | V | 0.964666 | 1 | 0.989293 | 0.825235 | 0.992224 | 0.855317 |
| **BiP-GRP78** | M | HSPA5 | C | 0.836859 | 1 | 1.046702 | 1.105831 | 1.073217 | 0.984907 |
| **BMK1-Erk5_pT218_Y220** | R | MAPK7 | V | 0.951909 | 1 | 1.044415 | 1.012692 | 0.963178 | 1.105856 |
| **BRCA1** | M | BRCA1 | C | 0.878204 | 1 | 1.046702 | 1.068097 | 1.073217 | 0.984907 |
| **BRD4** | R | BRD4 | V | 0.957973 | 1 | 0.700889 | 0.813385 | 1.061639 | 0.734545 |
| **c-Abl** | R | ABL1 | V | 0.963053 | 1 | 0.726445 | 0.882017 | 0.979511 | 0.899458 |
| **c-Abl_pY412** | R | ABL1 | C | 0.885537 | 1 | 0.981304 | 0.917781 | 0.883012 | 1.036638 |
| **c-IAP2** | R | BIRC3 | C | 0.93658 | 1 | 1.18704 | 1.137067 | 1.026249 | 0.907283 |
| **c-Jun_pS73** | R | JUN | V | 0.891427 | 1 | 0.825843 | 1.322506 | 1.179661 | 0.935671 |
| **c-Kit** | R | KIT | V | 0.918384 | 1 | 1.158008 | 1.061238 | 1.137254 | 1.028811 |
| **c-Met_pY1234_Y1235** | R | MET | V | 0.929112 | 1 | 0.880203 | 0.979411 | 0.836806 | 0.996177 |
| **c-Myc** | R | MYC | C | 0.962021 | 1 | 0.855585 | 0.808542 | 0.86555 | 0.939209 |
| **C-Raf** | R | RAF1 | C | 0.959886 | 1 | 1.152944 | 1.141339 | 1.058308 | 0.819021 |
| **C-Raf_pS338** | R | RAF1 | V | 0.954235 | 1 | 1.100265 | 1.233588 | 1.054151 | 0.945968 |
| **CA9** | R | CA9 | C | 0.861262 | 1 | 1.080845 | 0.940287 | 0.995495 | 1.098415 |
| **Calnexin** | R | CANX | V | 0.878782 | 1 | 1.036022 | 2.007026 | 1.062247 | 0.983639 |
| **Caspase-3-cleaved** | R | CASP3 | C | 0.824713 | 1 | 1.131072 | 0.95877 | 0.891149 | 0.896935 |
| **Caspase-7-cleaved-** | R | CASP7 | C | 0.959214 | 1 | 0.798754 | 0.877989 | 0.889698 | 0.760348 |
| **Caspase-8** | M | CASP8 | Q | 0.919531 | 1 | 0.962398 | 0.922949 | 0.950516 | 1.023297 |
| **Caveolin-1** | R | CAV1 | V | 0.954263 | 1 | 0.935923 | 0.969948 | 1.115363 | 1.099812 |
| **CD134** | R | TNFRSF4 | V | 0.913458 | 1 | 0.960648 | 1.083104 | 1.055377 | 1.126942 |
| **CD171** | M | L1CAM | V | 0.928009 | 1 | 1.108774 | 1.046563 | 1.016452 | 0.834129 |
| **CD20** | R | MS4A1 | C | 0.851345 | 1 | 1.046702 | 1.068097 | 1.073217 | 0.984907 |
| **CD26** | R | DPP4 | V | 0.888119 | 1 | 1.019565 | 0.970337 | 1.215113 | 1.174481 |
| **CD31** | M | PECAM1 | V | 0.8907 | 1 | 1.069866 | 0.782753 | 0.835403 | 1.083823 |
| **CD38** | R | CD38 | C | 0.881975 | 1 | 1.046702 | 1.068097 | 1.073217 | 0.984907 |
| **CD4** | R | CD4 | V | 0.873875 | 1 | 1.055528 | 1.018354 | 1.026578 | 0.934776 |
| **CD44** | R | CD44 | C | 0.907603 | 1 | 0.763433 | 0.872812 | 0.851166 | 0.785657 |
| **CD45** | M | PTPRC | V | 0.84114 | 1 | 0.737545 | 0.750076 | 0.881917 | 0.614689 |
| **CD49b** | M | ITGA2 | V | 0.938161 | 1 | 1.048258 | 0.943054 | 0.932543 | 0.998431 |
| **CD5** | M | CD5 | C | 0.890262 | 1 | 1.027068 | 0.839569 | 0.917334 | 1.089698 |
| **CD68** | M | CD68 | C | 0.923256 | 1 | 0.90523 | 0.861099 | 0.879733 | 0.920807 |
| **CD86** | R | CD86 | C | 0.913368 | 1 | 1.046702 | 1.068097 | 1.073217 | 0.984907 |
| **cdc25C** | R | CDC25C | V | 0.975828 | 1 | 0.873186 | 0.860836 | 0.949529 | 1.067017 |
| **cdc2_pY15** | R | CDK1 | C | 0.938987 | 1 | 0.939577 | 0.920979 | 0.845259 | 1.005109 |
| **Cdc42** | R | CDC42/RAC1 | C | 0.897637 | 1 | 0.882173 | 0.803605 | 1.033399 | 1.370133 |
| **Cdc6** | R | CDC6 | V | 0.936572 | 1 | 0.71117 | 0.980562 | 1.246506 | 1.032026 |
| **CDK1_pT14** | R | CDK1/2/3 | C | 0.957667 | 1 | 0.656227 | 0.829841 | 1.059825 | 0.942143 |
| **CDT1** | R | CDT1 | V | 0.805419 | 1 | 1.058181 | 1.271171 | 2.401288 | 1.517529 |
| **CHD1L** | R | CHD1L | V | 0.96997 | 1 | 1.058009 | 1.190053 | 1.103955 | 0.876815 |
| **Chk1** | M | CHEK1 | C | 0.954515 | 1 | 0.941183 | 0.964544 | 0.993931 | 1.059298 |
| **Chk1_pS296** | R | CHEK1 | V | 0.94057 | 1 | 0.86582 | 0.907715 | 0.839379 | 1.124324 |
| **Chk1_pS345** | R | CHEK1 | C | 0.968845 | 1 | 0.974591 | 0.850578 | 0.829733 | 0.983057 |
| **Chk2** | M | CHEK2 | V | 0.94303 | 1 | 1.012736 | 0.925351 | 0.970954 | 0.983202 |
| **Chk2_pT68** | R | CHEK2 | C | 0.946388 | 1 | 1.380662 | 0.788781 | 1.091449 | 0.970507 |

| | | | | | | | | | |
|---|---|---|---|---|---|---|---|---|---|
| **CIITA** | R | CIITA | C | 0.904888 | 1 | 0.915712 | 0.974331 | 0.994049 | 1.130053 |
| **Claudin-7** | R | CLDN7 | V | 0.821421 | 1 | 1.010158 | 0.93227 | 0.998994 | 1.111975 |
| **Collagen-VI** | R | COL6A1 | V | 0.966983 | 1 | 0.958682 | 0.927965 | 0.829646 | 0.981896 |
| **Complex-II-Subunit** | M | SDHB | V | 0.945384 | 1 | 1.172282 | 1.238231 | 1.128463 | 1.016454 |
| **Connexin-43** | R | GJA1 | C | 0.921194 | 1 | 0.791173 | 0.930942 | 1.107033 | 0.82934 |
| **Coup-TFII** | R | NR2F2 | C | 0.952689 | 1 | 1.017681 | 1.074607 | 1.051433 | 0.864277 |
| **Cox-IV** | R | COX4I1 | V | 0.949611 | 1 | 0.989142 | 0.932272 | 0.880676 | 0.990301 |
| **Cox2** | R | PTGS2 | C | 0.94813 | 1 | 0.831546 | 0.810549 | 1.06258 | 0.86458 |
| **Creb** | R | CREB1 | C | 0.892543 | 1 | 1.143224 | 0.996822 | 0.944805 | 0.918334 |
| **CREB_pS133** | R | CREB1 | C | 0.965058 | 1 | 1.070785 | 1.80497 | 1.387733 | 1.09727 |
| **CSK** | R | CSK | C | 0.884717 | 1 | 1.05747 | 1.068097 | 1.073217 | 1.014503 |
| **CtIP** | R | RBBP8 | V | 0.854544 | 1 | 0.887839 | 0.989812 | 0.924655 | 0.937229 |
| **Cyclin-B1** | R | CCNB1 | V | 0.969237 | 1 | 0.991824 | 0.946053 | 1.132767 | 0.946934 |
| **Cyclin-D1** | R | CCND1 | C | 0.894801 | 1 | 0.79514 | 1.253776 | 1.52361 | 1.049533 |
| **Cyclin-D3** | M | CCND3 | V | 0.926778 | 1 | 1.043288 | 0.949085 | 0.958399 | 1.022295 |
| **Cyclin-E1** | R | CCNE1 | V | 0.952159 | 1 | 0.957531 | 1.334391 | 1.635921 | 1.201785 |
| **Cyclophilin-F** | M | PPIF | V | 0.952877 | 1 | 1.19557 | 1.162824 | 1.054742 | 0.809739 |
| **D-a-Tubulin** | R | TUBA4A/ TUBA3C | V | 0.922649 | 1 | 0.711206 | 0.840594 | 1.254099 | 0.711642 |
| **DAPK1_pS308** | M | DAPK1 | C | 0.908557 | 1 | 1.046702 | 1.068097 | 1.073217 | 0.984907 |
| **DAPK2** | R | DAPK2 | C | 0.965953 | 1 | 1.003404 | 0.985023 | 0.915652 | 0.994271 |
| **DDB-1** | R | DDB1 | V | 0.965558 | 1 | 1.056537 | 0.950362 | 0.89204 | 1.034135 |
| **DDR1** | R | DDR1 | V | 0.94166 | 1 | 0.734204 | 0.775368 | 1.453156 | 1.05931 |
| **DDR1_pY513** | R | DDR1 | C | 0.923987 | 1 | 1.321974 | 1.053623 | 1.598021 | 1.005643 |
| **DJ1** | R | PARK7 | V | 0.964635 | 1 | 0.91637 | 0.954404 | 0.892097 | 1.002062 |
| **DM-Histone-H3** | R | HIST1H3A-J | V | 0.878538 | 1 | 0.851176 | 0.920403 | 0.943579 | 1.082824 |
| **DNA-Ligase-IV** | R | LIG4 | C | 0.933019 | 1 | 1.033412 | 1.064557 | 1.059529 | 0.972345 |
| **DNA_POLG** | R | POLG | V | 0.942754 | 1 | 0.722078 | 1.144288 | 0.897687 | 0.788483 |
| **DNMT1** | R | DNMT1 | V | 0.971727 | 1 | 1.009701 | 1.05815 | 1.199263 | 1.019341 |
| **DRP1** | R | DNM1L | V | 0.952426 | 1 | 1.107684 | 1.085139 | 1.065965 | 0.912813 |
| **DUSP4** | R | DUSP4 | V | 0.963061 | 1 | 0.812596 | 0.883074 | 1.437459 | 1.088546 |
| **DUSP6** | R | DUSP6 | C | 0.961288 | 1 | 1.046702 | 1.068097 | 1.073217 | 0.984907 |
| **Dvl3** | R | DVL3 | V | 0.975652 | 1 | 0.917394 | 0.959634 | 0.962868 | 1.137255 |
| **E-Cadherin** | R | CDH1 | V | 0.828459 | 1 | 0.939074 | 0.929657 | 0.864099 | 1.018707 |
| **E2F1** | R | E2F1 | V | 0.920989 | 1 | 1.046702 | 1.068097 | 1.073217 | 0.984907 |
| **eEF2** | R | EEF2 | C | 0.939449 | 1 | 0.986858 | 0.913962 | 0.924529 | 1.038949 |
| **eEF2K** | R | EEF2K | V | 0.960327 | 1 | 0.980269 | 0.905513 | 0.807794 | 0.990081 |
| **EGFR** | R | EGFR | V | 0.939755 | 1 | 0.909154 | 0.941011 | 0.94486 | 1.027357 |
| **EGFR_pY1173** | R | EGFR | V | 0.954826 | 1 | 1.035348 | 0.845775 | 0.99541 | 0.863671 |
| **eIF4E** | R | EIF4E | V | 0.945364 | 1 | 1.058323 | 1.004555 | 0.968314 | 1.085393 |
| **eIF4E_pS209** | R | EIF4E | V | 0.96733 | 1 | 0.794688 | 0.819158 | 0.823094 | 0.91856 |
| **eIF4G** | R | EIF4G1 | C | 0.949515 | 1 | 0.860324 | 1.032192 | 0.907241 | 0.854302 |
| **Elk1_pS383** | R | ELK1 | C | 0.957955 | 1 | 0.979725 | 1.075312 | 1.142093 | 1.029372 |
| **EMA** | M | MUC1 | C | 0.91796 | 1 | 0.968576 | 0.996542 | 0.927049 | 0.855644 |
| **Enolase-1** | R | ENO1 | V | 0.93758 | 1 | 1.018731 | 1.193148 | 1.378237 | 1.140395 |
| **Enolase-2** | R | ENO2 | V | 0.938284 | 1 | 1.020581 | 1.157392 | 1.148758 | 1.024906 |
| **ENY2** | M | ENY2 | C | 0.895145 | 1 | 0.988682 | 0.95205 | 0.796258 | 0.967296 |
| **EphA2** | R | EPHA2 | V | 0.946685 | 1 | 0.859431 | 0.953326 | 1.276811 | 1.199007 |
| **EphA2_pS897** | R | EPHA2 | C | 0.93667 | 1 | 0.777103 | 1.126717 | 1.462555 | 0.924403 |
| **EphA2_pY588** | R | EPHA2 | C | 0.95175 | 1 | 1.321545 | 1.447642 | 1.455207 | 1.272572 |
| **ER-a** | R | ESR1 | V | 0.959007 | 1 | 1.01889 | 0.914887 | 0.823306 | 1.13518 |
| **ER-a_pS118** | R | ESR1 | V | 0.893972 | 1 | 1.155979 | 1.316552 | 1.026595 | 0.808837 |
| **ERCC1** | M | ERCC1 | V | 0.901718 | 1 | 1.316252 | 0.980124 | 1.079985 | 0.986892 |
| **ERCC5** | R | ERCC5 | C | 0.967448 | 1 | 1.247731 | 1.124519 | 1.291249 | 1.080216 |
| **Erk5** | R | MAPK7 | V | 0.867279 | 1 | 0.784358 | 1.042908 | 1.093839 | 0.962001 |
| **ERRalpha** | R | ESRRA | V | 0.943391 | 1 | 0.884696 | 1.065213 | 0.937191 | 1.066567 |
| **Ets-1** | R | ETS1 | V | 0.954272 | 1 | 0.898177 | 0.914462 | 0.87143 | 0.968792 |
| **EVI1** | R | MECOM | V | 0.953302 | 1 | 1.046702 | 1.068097 | 1.073217 | 0.984907 |
| **FABP5** | R | FABP5 | C | 0.892383 | 1 | 1.202844 | 0.898468 | 0.983323 | 1.022778 |
| **FAK** | R | PTK2 | C | 0.895643 | 1 | 1.046702 | 1.109371 | 1.112285 | 0.984907 |

| | | | | | | | | | |
|---|---|---|---|---|---|---|---|---|---|
| **FAK_pY397** | R | PTK2 | V | 0.959845 | 1 | 0.949774 | 1.026158 | 0.931131 | 1.043519 |
| **FASN** | R | FASN | V | 0.970641 | 1 | 1.082222 | 0.99859 | 1.022196 | 0.828643 |
| **FGF-basic** | R | FGF2 | C | 0.958683 | 1 | 1.040986 | 1.062321 | 1.067381 | 1.012909 |
| **Fibronectin** | R | FN1 | V | 0.946611 | 1 | 0.88974 | 0.903997 | 0.954242 | 0.916156 |
| **FN14** | R | TNFRSF12A | C | 0.937934 | 1 | 1.057588 | 1.005283 | 0.894791 | 1.133718 |
| **FOXM1** | R | FOXM1 | V | 0.964815 | 1 | 1.046702 | 1.068097 | 1.073217 | 1.065181 |
| **FOXO3** | R | FOXO3 | V | 0.972874 | 1 | 1.217707 | 1.168622 | 1.086056 | 1.094482 |
| **FoxO3a_pS318_S321** | R | FOXO3 | C | 0.951095 | 1 | 0.984555 | 0.995138 | 1.095439 | 1.038284 |
| **FRS2-alpha_pY196** | R | FRS2 | V | 0.968762 | 1 | 0.950282 | 0.8214 | 0.899369 | 0.902294 |
| **G6PD** | R | G6PD | V | 0.918957 | 1 | 0.962934 | 0.901454 | 0.895354 | 1.06023 |
| **Gab2** | R | GAB2 | V | 0.962889 | 1 | 0.820761 | 0.884494 | 0.91241 | 1.024195 |
| **GATA3** | M | GATA3 | V | 0.929393 | 1 | 0.953314 | 0.848654 | 0.864884 | 1.003071 |
| **GATA6** | R | GATA6 | V | 0.875915 | 1 | 0.810874 | 1.653336 | 1.602094 | 0.662487 |
| **GCLC** | R | GCLC | C | 0.947091 | 1 | 0.918241 | 0.940912 | 0.903378 | 0.951956 |
| **GCLM** | R | GCLM | C | 0.969805 | 1 | 0.916766 | 0.911767 | 0.912355 | 0.990623 |
| **GCN5L2** | R | KAT2A | V | 0.953996 | 1 | 0.766944 | 0.859841 | 0.943799 | 0.875914 |
| **GGPS1** | M | GGPS1 | V | 0.913924 | 1 | 1.205683 | 1.422592 | 1.315942 | 1.013361 |
| **Gli1** | R | GLI1 | C | 0.903229 | 1 | 0.853591 | 0.88177 | 1.15376 | 0.901504 |
| **Gli3** | R | GLI3 | C | 0.926517 | 1 | 0.499977 | 0.576257 | 0.680569 | 0.566202 |
| **Glutamate-D1-2** | R | GLUD1 | V | 0.95924 | 1 | 1.043159 | 1.099751 | 1.072467 | 0.874555 |
| **Glutaminase** | R | GLS | C | 0.945574 | 1 | 0.629624 | 0.739554 | 1.158384 | 0.879995 |
| **Granzyme-B** | R | GZMB | V | 0.902588 | 1 | 1.046702 | 1.068097 | 1.073217 | 1.041674 |
| **GRB7** | R | GRB7 | V | 0.910313 | 1 | 0.907937 | 1.122789 | 1.243127 | 1.152827 |
| **Grp75** | R | HSPA9 | C | 0.926066 | 1 | 0.933739 | 1.125622 | 1.205579 | 0.878935 |
| **GSK-3a-b** | M | GSK3A/GSK3B | V | 0.907375 | 1 | 1.010188 | 0.959274 | 0.936737 | 0.927767 |
| **GSK-3a-b_pS21_S9** | R | GSK3A/GSK3B | V | 0.952251 | 1 | 0.931598 | 1.175172 | 1.025543 | 0.976603 |
| **GSK-3B** | R | GSK3B | C | 0.973941 | 1 | 1.130117 | 1.044597 | 1.086107 | 0.88473 |
| **Gys** | R | GYS1 | V | 0.941593 | 1 | 0.894203 | 0.84114 | 0.943075 | 1.016192 |
| **Gys_pS641** | R | GYS1 | V | 0.904528 | 1 | 0.983449 | 1.00335 | 1.019527 | 0.979387 |
| **H2AX_pS139** | R | H2AFX | C | 0.918016 | 1 | 1.397486 | 1.040351 | 1.642656 | 1.879768 |
| **H2AX_pS140** | M | H2AFX | C | 0.937794 | 1 | 1.016402 | 1.055555 | 0.908781 | 0.939816 |
| **HER2** | M | ERBB2 | V | 0.915816 | 1 | 0.749629 | 1.242934 | 1.337924 | 1.456954 |
| **HER2_pY1248** | R | ERBB2 | C | 0.940618 | 1 | 1.001676 | 0.976227 | 1.117591 | 1.022404 |
| **HER3** | R | ERBB3 | V | 0.957411 | 1 | 0.902925 | 0.871599 | 0.845378 | 1.067027 |
| **HER3_pY1289** | R | ERBB3 | C | 0.963959 | 1 | 0.952618 | 0.977394 | 0.893236 | 1.063731 |
| **Heregulin** | R | NRG1 | V | 0.951136 | 1 | 0.976511 | 1.003623 | 0.91496 | 1.073469 |
| **HES1** | R | HES1 | V | 0.950344 | 1 | 0.818781 | 0.816359 | 0.980446 | 1.016571 |
| **Hexokinase-I** | R | HK1 | C | 0.95431 | 1 | 0.808649 | 0.855147 | 1.058709 | 1.169889 |
| **Hexokinase-II** | R | HK2 | V | 0.941476 | 1 | 1.236986 | 1.146092 | 1.121756 | 0.967932 |
| **Hif-1-alpha** | R | HIF1A | C | 0.95668 | 1 | 0.711163 | 0.437884 | 0.775218 | 0.779422 |
| **Histone-H3_pS10** | R | HIST1H3A-J | V | 0.900003 | 1 | 0.675587 | 1.097068 | 1.379237 | 1.105714 |
| **HLA-DR-DP-DQ-DX** | R | HLA-DRA | C | 0.917187 | 1 | 0.87508 | 0.828387 | 1.174298 | 1.054662 |
| **HMHA1** | R | ARHGAP45 | V | 0.910498 | 1 | 1.046702 | 1.068097 | 1.073217 | 0.984907 |
| **HNRNPK** | R | HNRNPK | V | 0.963384 | 1 | 0.894314 | 0.99588 | 0.894199 | 0.991716 |
| **HSP27** | M | HSBP1 | C | 0.907767 | 1 | 0.907592 | 0.885126 | 1.026727 | 1.042305 |
| **HSP27_pS82** | R | HSBP1 | V | 0.943979 | 1 | 1.064286 | 2.098401 | 1.040901 | 0.991625 |
| **HSP60** | R | HSPD1 | V | 0.908015 | 1 | 1.035099 | 1.056188 | 1.061266 | 0.979631 |
| **HSP70** | R | HSPA1A | C | 0.962709 | 1 | 1.080515 | 0.960263 | 1.041998 | 0.928164 |
| **IDO** | R | IDO1 | C | 0.847927 | 1 | 0.782828 | 0.94226 | 0.867921 | 0.985798 |
| **IGF1R_pY1135_Y1136** | R | IGF1R/INSR | V | 0.951282 | 1 | 0.820996 | 0.827772 | 1.244531 | 1.199401 |
| **IGFBP2** | R | IGFBP2 | V | 0.933911 | 1 | 1.021963 | 0.951566 | 1.072813 | 0.911152 |
| **IGFBP3** | M | IGFBP3 | V | 0.870969 | 1 | 1.023846 | 0.98724 | 0.994109 | 1.023338 |
| **IGFRb** | R | IGF1R | C | 0.935294 | 1 | 1.075775 | 1.016726 | 1.002431 | 0.852678 |
| **IL-6** | R | IL6 | C | 0.908126 | 1 | 0.832628 | 0.898485 | 0.949404 | 1.070315 |
| **INPP4b** | R | INPP4B | C | 0.965499 | 1 | 0.947091 | 0.944973 | 0.901809 | 1.048219 |

| | | | | | | | | | |
|---|---|---|---|---|---|---|---|---|---|
| **IR-b** | R | INSR | C | 0.965593 | 1 | 0.919075 | 0.802329 | 0.939491 | 0.845119 |
| **IRF-1** | R | IRF1 | C | 0.947307 | 1 | 1.025297 | 1.038589 | 1.047681 | 1.208631 |
| **IRS2** | R | IRS2 | C | 0.967804 | 1 | 0.874102 | 0.931978 | 1.258205 | 1.004599 |
| **JAB1** | M | COPS5 | C | 0.885489 | 1 | 1.309447 | 1.268058 | 0.985641 | 0.904537 |
| **Jagged1** | R | JAG1 | V | 0.938773 | 1 | 0.980034 | 0.986436 | 1.32594 | 0.85539 |
| **Jak2** | R | JAK2 | V | 0.919858 | 1 | 1.035727 | 1.023695 | 0.986968 | 0.855779 |
| **JNK2** | R | MAPK9 | V | 0.93613 | 1 | 0.91629 | 0.540571 | 0.557114 | 0.951433 |
| **JNK_pT183_Y185** | R | MAPK8 | C | 0.904361 | 1 | 1.623311 | 3.292004 | 1.845288 | 1.66986 |
| **KAP1** | R | TRIM28 | V | 0.957706 | 1 | 1.026586 | 0.96886 | 1.017218 | 1.148039 |
| **LAD1** | R | LAD1 | V | 0.964047 | 1 | 1.39481 | 1.158627 | 1.45098 | 1.028908 |
| **Lasu1** | R | HUWE1 | V | 0.939439 | 1 | 0.983057 | 0.939244 | 1.007857 | 1.067847 |
| **LC3A-B** | R | MAP1LC3A/B | C | 0.929351 | 1 | 0.808568 | 0.962222 | 0.991105 | 0.892502 |
| **Lck** | R | LCK | V | 0.965516 | 1 | 0.974847 | 1.098949 | 1.142775 | 0.946908 |
| **LRP6_pS1490** | R | LRP6 | V | 0.944054 | 1 | 0.986742 | 0.994257 | 1.235865 | 0.873046 |
| **Lyn** | R | LYN | V | 0.856157 | 1 | 0.980541 | 1.360754 | 1.040956 | 1.256549 |
| **MAPK_pT202_Y204** | R | MAPK1/MAPK3 | C | 0.953752 | 1 | 1.238378 | 7.047357 | 0.963065 | 1.274599 |
| **Mcl-1** | R | MCL1 | V | 0.966994 | 1 | 1.100955 | 1.026461 | 1.014854 | 0.846686 |
| **MCT4** | R | SLC16A3 | V | 0.945105 | 1 | 1.046702 | 1.068097 | 1.073217 | 0.984907 |
| **MDM2_pS166** | R | MDM2 | V | 0.969895 | 1 | 0.935861 | 0.99698 | 1.029166 | 0.861222 |
| **MEK1** | R | MAP2K1 | V | 0.950361 | 1 | 1.046446 | 0.873074 | 1.143018 | 0.820506 |
| **MEK1_p_S217_S221** | R | MAP2K1/MAP2K2 | V | 0.941529 | 1 | 1.031948 | 1.293164 | 1.013267 | 1.069535 |
| **MEK2** | R | MAP2K2 | V | 0.942467 | 1 | 0.970873 | 0.815291 | 1.268283 | 0.827034 |
| **MelanA** | R | MLANA | C | 0.927138 | 1 | 0.871689 | 1.046843 | 0.983221 | 1.069774 |
| **Melanoma-gp100** | R | PMEL | C | 0.827726 | 1 | 1.078499 | 1.167348 | 1.22131 | 1.086242 |
| **MERIT40** | R | BABAM1 | C | 0.911125 | 1 | 0.997856 | 0.909734 | 0.915383 | 0.996797 |
| **MERIT40_pS29** | R | BABAM1 | V | 0.965451 | 1 | 0.792355 | 0.868453 | 0.882365 | 0.889572 |
| **Merlin** | R | NF2 | C | 0.96116 | 1 | 1.042699 | 1.000321 | 0.936937 | 0.971533 |
| **MIF** | R | MIF | C | 0.936827 | 1 | 1.057266 | 1.01879 | 0.883224 | 1.006432 |
| **MIG6** | M | ERRFI1 | V | 0.945725 | 1 | 0.867252 | 0.916986 | 0.897328 | 0.911432 |
| **Mitofusin-1** | R | MFN1 | V | 0.930246 | 1 | 1.003251 | 1.133438 | 1.022846 | 1.138214 |
| **Mitofusin-2** | R | MFN2 | V | 0.963423 | 1 | 0.889496 | 0.888641 | 1.006712 | 1.11887 |
| **MLH1** | M | MLH1 | V | 0.884123 | 1 | 1.451035 | 0.962569 | 0.944323 | 1.020715 |
| **MLKL** | R | MLKL | V | 0.956394 | 1 | 0.965843 | 0.917786 | 0.937489 | 1.060538 |
| **MMP14** | R | MMP14 | V | 0.963384 | 1 | 0.883119 | 0.902275 | 1.340962 | 1.10612 |
| **MMP2** | R | MMP2 | V | 0.960083 | 1 | 1.083322 | 1.211079 | 1.097833 | 1.064064 |
| **Mnk1** | R | MKNK1 | V | 0.941914 | 1 | 0.882066 | 0.92127 | 0.861249 | 0.885303 |
| **MR1** | M | MR1 | C | 0.901419 | 1 | 1.058673 | 1.221628 | 1.278367 | 0.958562 |
| **MRAP** | R | MRAP | C | 0.921114 | 1 | 0.819016 | 1.133816 | 1.50635 | 0.919093 |
| **MSH2** | R | MSH2 | C | 0.963325 | 1 | 1.081592 | 1.058939 | 1.032056 | 0.926588 |
| **MSH6** | R | MSH6 | C | 0.958349 | 1 | 0.912174 | 0.986143 | 0.934028 | 0.966442 |
| **MSI2** | R | MSI2 | C | 0.946316 | 1 | 0.844724 | 0.870175 | 0.849395 | 0.903306 |
| **MTCO1** | M | MT-CO1 | V | 0.911608 | 1 | 0.893991 | 0.889588 | 1.276029 | 0.994012 |
| **mTOR** | R | MTOR | V | 0.97455 | 1 | 1.029415 | 0.936299 | 1.072811 | 0.839931 |
| **mTOR_pS2448** | R | MTOR | C | 0.971665 | 1 | 1.129969 | 1.038418 | 1.042329 | 0.90576 |
| **MTSS1** | M | MTSS1 | C | 0.817041 | 1 | 0.866197 | 0.902785 | 0.908787 | 0.98277 |
| **MYH11** | R | MYH11 | C | 0.947895 | 1 | 0.969294 | 1.070667 | 1.035592 | 1.060681 |
| **Myosin-IIa** | R | MYH9 | C | 0.864436 | 1 | 1.046702 | 1.068097 | 1.073217 | 0.984907 |
| **Myosin-IIa_pS1943** | R | MYH9 | V | 0.951078 | 1 | 1.279198 | 1.068097 | 1.073217 | 0.984907 |
| **Myt1** | R | PKMYT1 | C | 0.948625 | 1 | 1.143265 | 0.837652 | 0.833316 | 1.118923 |
| **N-Cadherin** | R | CDH2 | V | 0.920639 | 1 | 1.038272 | 1.159008 | 0.938179 | 0.930104 |
| **N-Ras** | M | NRAS | V | 0.92038 | 1 | 0.920078 | 1.023181 | 1.370988 | 0.82381 |
| **NAPSIN-A** | R | NAPSA | C | 0.933718 | 1 | 1.046348 | 1.09935 | 1.16306 | 0.972571 |
| **NDRG1_pT346** | R | NDRG1 | V | 0.956335 | 1 | 0.931454 | 1.195598 | 1.262271 | 0.960822 |
| **NDUFB4** | R | NDUFB4 | V | 0.872541 | 1 | 1.314211 | 1.214911 | 1.155247 | 1.170801 |
| **NF-kB-p65_pS536** | R | RELA | C | 0.9718 | 1 | 1.183289 | 1.038262 | 1.229199 | 1.026799 |
| **Notch1** | R | NOTCH1 | V | 0.963732 | 1 | 1.046702 | 1.068097 | 1.073217 | 1.013516 |
| **Notch1-cleaved** | R | NOTCH1 | V | 0.93784 | 1 | 0.928968 | 0.883163 | 0.832145 | 0.901813 |
| **Notch3** | R | NOTCH3 | C | 0.927879 | 1 | 1.002536 | 0.851475 | 0.844369 | 0.954095 |
| **NRF2** | R | NFE2L2 | C | 0.920794 | 1 | 0.994325 | 0.955705 | 0.894705 | 1.173814 |
| **Oct-4** | R | POU5F1 | C | 0.950687 | 1 | 0.793477 | 0.704231 | 0.890614 | 0.910948 |
| **P-Cadherin** | R | CDH3 | C | 0.957715 | 1 | 1.147947 | 1.068097 | 1.238497 | 0.984907 |
| **p21** | R | CDKN1A | C | 0.937894 | 1 | 1.127949 | 1.050107 | 0.99399 | 0.769804 |
| **p27-Kip1** | R | CDKN1B | V | 0.953855 | 1 | 0.935888 | 0.929104 | 0.926987 | 1.069971 |

| | | | | | | | | | |
|---|---|---|---|---|---|---|---|---|---|
| **p27_pT157** | R | CDKN1B | C | 0.96343 | 1 | 1.003053 | 0.938845 | 1.014347 | 1.111313 |
| **p27_pT198** | R | CDKN1B | V | 0.951423 | 1 | 1.040343 | 0.854307 | 0.82519 | 0.842582 |
| **p38-a** | M | MAPK14 | V | 0.947565 | 1 | 0.95538 | 0.894463 | 0.912924 | 1.018996 |
| **p38-MAPK** | R | MAPK14/ 11/12 | V | 0.967943 | 1 | 1.079821 | 0.959275 | 1.00787 | 0.832249 |
| **p38-MAPK-_pT180_Y182** | R | MAPK11/ 13/12/14 | V | 0.899217 | 1 | 1.375864 | 1.173524 | 1.115408 | 1.172512 |
| **p44-42-MAPK** | R | MAPK1/ MAPK3 | V | 0.950155 | 1 | 0.992665 | 0.953432 | 0.954915 | 1.034517 |
| **p53** | R | TP53 | C | 0.942795 | 1 | 0.712894 | 0.729683 | 1.193336 | 1.155702 |
| **p70-S6K1** | R | RPS6KB 1 | V | 0.960281 | 1 | 1.12497 | 1.052652 | 0.966836 | 0.814494 |
| **p70-S6K_pT389** | R | RPS6KB 1 | V | 0.961136 | 1 | 1.196725 | 2.062808 | 1.122358 | 1.064567 |
| **p90RSK_pT573** | R | RPS6KA 1 | C | 0.972396 | 1 | 1.027568 | 1.051797 | 1.05368 | 0.966977 |
| **PAI-1** | M | SERPIN E1 | V | 0.958787 | 1 | 0.838881 | 0.827563 | 0.919788 | 0.960343 |
| **PAICS** | R | PAICS | C | 0.966902 | 1 | 1.105088 | 1.021048 | 1.05545 | 0.948498 |
| **PAK1** | R | PAK1 | V | 0.950816 | 1 | 1.046702 | 1.068097 | 1.073217 | 0.984907 |
| **PAK4** | R | PAK4 | V | 0.940358 | 1 | 0.992039 | 0.862201 | 0.946929 | 0.712333 |
| **PAR** | R | [PAR Modification] | C | 0.941175 | 1 | 1.017395 | 1.081618 | 1.108957 | 1.00919 |
| **PARG** | R | PARG | C | 0.897347 | 1 | 1.046702 | 1.068097 | 1.073217 | 0.984907 |
| **PARP** | R | PARP1 | V | 0.949651 | 1 | 1.046702 | 1.068097 | 1.073217 | 0.984907 |
| **Patched** | R | PTCH1 | C | 0.87747 | 1 | 0.734613 | 1.174558 | 1.006177 | 0.754582 |
| **PAX6** | R | PAX6 | V | 0.865319 | 1 | 0.955675 | 0.945713 | 0.972193 | 0.913808 |
| **PAX8** | R | PAX8 | C | 0.966344 | 1 | 0.965027 | 1.090733 | 1.943847 | 1.215461 |
| **Paxillin** | R | PXN | C | 0.966396 | 1 | 1.007706 | 0.918816 | 1.12538 | 0.976048 |
| **PCNA** | M | PCNA | C | 0.90826 | 1 | 1.046753 | 0.952931 | 0.949802 | 0.970264 |
| **PD-1** | R | PDCD1 | V | 0.896127 | 1 | 1.114077 | 0.982829 | 1.037911 | 0.993966 |
| **PD-L1** | R | CD274 | C | 0.90107 | 1 | 0.828685 | 0.901083 | 0.924839 | 1.066859 |
| **Pdcd4** | R | PDCD4 | C | 0.95981 | 1 | 0.947131 | 1.081071 | 0.899488 | 1.094937 |
| **PDGFR-b** | R | PDGFR | V | 0.877761 | 1 | 0.900031 | 0.990743 | 1.012865 | 0.948574 |
| **PDH** | M | DLAT | V | 0.891234 | 1 | 0.844705 | 0.871178 | 0.967718 | 1.131538 |
| **PDHA1** | R | PDHA1 | V | 0.950285 | 1 | 1.0133 | 0.991655 | 0.966016 | 1.002897 |
| **PDHK1** | R | PDK1 | C | 0.909079 | 1 | 1.060775 | 0.989687 | 0.96441 | 1.059971 |
| **PDK1** | R | PDPK1 | V | 0.937728 | 1 | 0.958976 | 0.950626 | 1.067052 | 0.879931 |
| **PDK1_pS241** | R | PDPK1 | V | 0.96803 | 1 | 1.062921 | 0.935418 | 0.974427 | 0.829185 |
| **PEA-15** | R | PEA15 | V | 0.962983 | 1 | 0.980714 | 0.975485 | 0.921882 | 0.997997 |
| **PEA-15_pS116** | R | PEA15 | V | 0.948077 | 1 | 1.045932 | 1.032295 | 0.979342 | 1.118698 |
| **PERK** | R | EIF2AK3 | V | 0.975481 | 1 | 1.146231 | 1.084035 | 1.041212 | 0.880569 |
| **PHGDH** | R | PHGDH | C | 0.920889 | 1 | 0.783582 | 0.920608 | 1.416729 | 1.14693 |
| **PHLPP** | R | PHLPP1 | V | 0.967192 | 1 | 0.954702 | 0.895755 | 1.192018 | 0.813117 |
| **PI3K-p110-a** | R | PIK3CA | C | 0.959011 | 1 | 1.002886 | 0.822895 | 0.874283 | 0.981398 |
| **PI3K-p110-b** | M | PIK3CB | C | 0.907491 | 1 | 1.145208 | 1.216798 | 0.984107 | 0.843925 |
| **PI3K-p85** | R | PIK3R1 | V | 0.971626 | 1 | 1.11296 | 1.027792 | 1.007384 | 0.905549 |
| **PKA-a** | R | PRKAR1A | V | 0.973479 | 1 | 0.989158 | 0.905711 | 0.86623 | 1.002794 |
| **PKC-a-b-II_pT638_T641** | R | PRKCA/ PRKCB | V | 0.865151 | 1 | 0.894266 | 1.437875 | 1.334532 | 0.904041 |
| **PKC-b-II_pS660** | R | PRKCA/ B/D/E/H/ Q | V | 0.940738 | 1 | 0.754754 | 1.22847 | 1.39863 | 0.993274 |
| **PKC-delta_pS664** | R | PRKCD | V | 0.965257 | 1 | 0.965148 | 0.876253 | 0.921971 | 0.961888 |
| **PKCa** | R | PRKCA | V | 0.963905 | 1 | 0.768056 | 0.851086 | 0.941033 | 0.989019 |
| **PKM2** | R | PKM | C | 0.966736 | 1 | 0.921872 | 0.896992 | 0.934156 | 1.017685 |
| **PLC-gamma1** | R | PLCG1 | V | 0.958735 | 1 | 1.011056 | 0.887552 | 0.89606 | 1.009148 |
| **PLK1** | R | PLK1 | C | 0.974639 | 1 | 0.989645 | 0.903684 | 0.924113 | 1.112341 |
| **PMS2** | R | PMS2 | V | 0.967257 | 1 | 0.829621 | 1.060698 | 1.39565 | 1.24739 |
| **Porin** | M | VDAC1 | V | 0.92422 | 1 | 1.101367 | 0.921832 | 0.791284 | 1.008614 |
| **PR** | R | PGR | V | 0.954413 | 1 | 0.84071 | 0.930671 | 1.402162 | 1.116799 |
| **PRAS40** | M | AKT1S1 | C | 0.882763 | 1 | 1.083688 | 0.968633 | 0.930371 | 1.016669 |
| **PRAS40_pT246** | R | AKT1S1 | V | 0.941509 | 1 | 1.022314 | 0.873361 | 0.821213 | 1.087817 |
| **PRC1_pT481** | R | PRC1 | C | 0.926537 | 1 | 0.816786 | 0.932938 | 1.113696 | 0.898885 |

| | | | | | | | | | |
|---|---|---|---|---|---|---|---|---|---|
| **PREX1** | R | PREX1 | V | 0.946925 | 1 | 1.024303 | 0.998128 | 1.08348 | 0.859097 |
| **PTEN** | R | PTEN | V | 0.942024 | 1 | 1.122697 | 1.016869 | 1.058022 | 0.850437 |
| **PTPN12** | R | PTPN12 | V | 0.957561 | 1 | 1.046702 | 1.068097 | 1.073217 | 0.984907 |
| **Puma** | R | BBC3 | C | 0.938314 | 1 | 0.927842 | 0.797316 | 1.020083 | 0.992684 |
| **PYGB** | R | PYGB | V | 0.892747 | 1 | 0.909472 | 0.970441 | 1.725196 | 1.503177 |
| **PYGM** | M | PYGM | C | 0.892219 | 1 | 1.046702 | 1.068097 | 1.073217 | 0.984907 |
| **Pyk2_pY402** | R | PTK2B | C | 0.938558 | 1 | 0.724693 | 0.891719 | 1.446345 | 0.806166 |
| **Rab11** | R | RAB11A/B | C | 0.934117 | 1 | 0.876297 | 0.869503 | 0.845736 | 0.957378 |
| **Rab25** | R | RAB25 | V | 0.958923 | 1 | 1.019024 | 1.057828 | 1.19157 | 1.056878 |
| **Rad23A** | R | RAD23A | C | 0.941408 | 1 | 0.922302 | 0.953622 | 0.910964 | 0.932313 |
| **Rad50** | R | RAD50 | V | 0.966492 | 1 | 0.620355 | 0.750387 | 0.947883 | 0.614725 |
| **Rad51** | R | RAD51 | C | 0.931263 | 1 | 1.09051 | 1.03036 | 1.145853 | 1.397606 |
| **Raptor** | R | RPTOR | V | 0.959773 | 1 | 0.997137 | 1.387488 | 1.388743 | 1.206514 |
| **Rb** | M | RB1 | Q | 0.933345 | 1 | 1.006747 | 0.867139 | 0.9142 | 1.024541 |
| **RBM15** | R | RBM15 | V | 0.963574 | 1 | 0.968354 | 1.184242 | 1.119171 | 1.708035 |
| **Rb_pS807_S811** | R | RB1 | V | 0.958005 | 1 | 1.15315 | 1.093645 | 1.001974 | 0.772088 |
| **Rheb** | M | RHEB | C | 0.846632 | 1 | 1.010309 | 0.990531 | 0.995111 | 0.996521 |
| **Rictor** | R | RICTOR | C | 0.972454 | 1 | 0.988421 | 1.159645 | 1.17777 | 0.963073 |
| **Rictor_pT1135** | R | RICTOR | V | 0.96661 | 1 | 1.265888 | 1.52385 | 1.4101 | 1.300156 |
| **RIP** | R | RIPK1 | C | 0.920428 | 1 | 0.991843 | 1.01592 | 1.017193 | 0.967406 |
| **RIP3** | R | RIPK3 | C | 0.808054 | 1 | 1.008382 | 1.008353 | 1.014292 | 1.038654 |
| **RPA32** | R | RPA2 | V | 0.941669 | 1 | 1.030113 | 0.955782 | 0.975454 | 0.820599 |
| **RRM1** | R | RRM1 | C | 0.922834 | 1 | 1.092973 | 0.873834 | 0.911406 | 0.924609 |
| **RRM2** | R | RRM2 | C | 0.964421 | 1 | 0.921757 | 0.921296 | 0.950045 | 1.024847 |
| **RSK** | R | RPS6KA1/2/3 | C | 0.969285 | 1 | 0.898394 | 0.863282 | 0.882089 | 1.050007 |
| **RSK1** | R | RPS6KA1 | V | 0.973208 | 1 | 1.037813 | 1.234626 | 1.102643 | 1.173188 |
| **S6** | M | RPS6 | V | 0.948408 | 1 | 0.864318 | 0.822186 | 0.982957 | 1.222454 |
| **S6_pS235_S236** | R | RPS6 | V | 0.943652 | 1 | 1.157464 | 1.178967 | 1.130286 | 0.892291 |
| **S6_pS240_S244** | R | RPS6 | V | 0.958995 | 1 | 1.233427 | 1.184868 | 1.059505 | 0.709576 |
| **SCD** | M | SCD | V | 0.936656 | 1 | 1.179976 | 1.211926 | 1.05678 | 0.916521 |
| **SDHA** | R | SDHA | V | 0.959701 | 1 | 1.129121 | 0.947047 | 1.134992 | 1.22082 |
| **SF2** | M | SRSF1 | V | 0.865748 | 1 | 0.953646 | 0.949621 | 0.89919 | 0.964712 |
| **SFRP1** | R | SFRP1 | C | 0.920617 | 1 | 0.951396 | 0.965341 | 0.972331 | 0.960532 |
| **SGK1** | R | SGK1 | V | 0.89756 | 1 | 0.656657 | 0.779354 | 0.624118 | 0.618791 |
| **SGK3** | R | SGK3 | V | 0.909854 | 1 | 0.968902 | 1.583 | 1.105987 | 0.86979 |
| **Shc_pY317** | R | SHC1 | V | 0.956989 | 1 | 1.081101 | 0.406987 | 0.438319 | 0.612083 |
| **SHP-2_pY542** | R | PTPN11 | C | 0.967624 | 1 | 1.354537 | 2.971859 | 1.353537 | 1.095391 |
| **SHP2** | R | PTPN11 | V | 0.86425 | 1 | 0.652989 | 0.836415 | 0.937141 | 0.840586 |
| **SLC1A5** | R | SLC1A5 | C | 0.933401 | 1 | 1.008471 | 1.037238 | 1.152272 | 1.156176 |
| **Slfn11** | G | SLFN11 | C | 0.911678 | 1 | 1.046702 | 1.068097 | 1.09188 | 0.990409 |
| **Smac** | M | DIABLO | Q | 0.951761 | 1 | 0.9592 | 0.948182 | 0.866496 | 1.011682 |
| **Smad1** | R | SMAD1 | V | 0.969097 | 1 | 1.003332 | 0.793511 | 0.906473 | 0.972573 |
| **Smad3** | R | SMAD3 | V | 0.952493 | 1 | 1.064144 | 0.948884 | 0.886554 | 1.027931 |
| **Smad4** | R | SMAD4 | V | 0.955026 | 1 | 0.861045 | 0.782971 | 1.128925 | 1.385272 |
| **Snail** | M | SNAI1 | Q | 0.936918 | 1 | 0.977523 | 0.96898 | 0.86726 | 1.021728 |
| **SOD1** | M | SOD1 | V | 0.901731 | 1 | 0.915108 | 1.004026 | 0.937711 | 1.027248 |
| **SOD2** | R | SOD2 | V | 0.932395 | 1 | 0.857285 | 0.903309 | 0.812865 | 1.159156 |
| **Sox17** | R | SOX17 | V | 0.958821 | 1 | 0.725856 | 0.87903 | 1.320379 | 0.998966 |
| **Sox2** | R | SOX2 | V | 0.927831 | 1 | 0.899713 | 0.868643 | 0.857633 | 0.987271 |
| **Src** | M | SRC | V | 0.946031 | 1 | 0.79813 | 0.859118 | 0.849574 | 0.973827 |
| **Src_pY416** | R | SRC | V | 0.949365 | 1 | 0.997467 | 1.01832 | 1.041461 | 1.073741 |
| **Src_pY527** | R | SRC | V | 0.968122 | 1 | 1.396165 | 1.344916 | 1.226328 | 1.01137 |
| **Stat3** | R | STAT3 | C | 0.95847 | 1 | 0.829745 | 0.631763 | 1.041272 | 0.857718 |
| **Stat3_pY705** | R | STAT3 | C | 0.947947 | 1 | 1.118164 | 1.703216 | 1.103035 | 0.940036 |
| **Stat5a** | R | STAT5A | V | 0.958907 | 1 | 1.062225 | 1.010837 | 1.130088 | 0.934117 |
| **Stathmin-1** | R | STMN1 | V | 0.947942 | 1 | 0.773841 | 0.806253 | 1.030881 | 1.130799 |
| **STING** | R | TMEM173 | V | 0.954977 | 1 | 1.046702 | 1.068097 | 1.073217 | 0.984907 |
| **Syk** | M | SYK | V | 0.949739 | 1 | 1.135169 | 1.111188 | 1.164296 | 1.036671 |
| **Tau** | M | MAPT | C | 0.933643 | 1 | 0.99437 | 1.037529 | 0.981312 | 1.060028 |
| **TAZ** | R | WWTR1 | V | 0.966486 | 1 | 0.852413 | 0.876976 | 0.939464 | 1.070323 |
| **TFAM** | R | TFAM | V | 0.967684 | 1 | 1.002718 | 0.955782 | 1.138426 | 1.054521 |
| **TFRC** | R | TFRC | V | 0.892649 | 1 | 1.30183 | 1.159573 | 1.11791 | 0.916071 |
| **TIGAR** | R | TIGAR | V | 0.865762 | 1 | 1.017253 | 0.924538 | 0.937824 | 0.991442 |
| **Transglutaminase** | M | TGM2 | V | 0.928416 | 1 | 1.262693 | 1.294123 | 0.988047 | 0.89268 |

| | | | | | | | | | |
|---|---|---|---|---|---|---|---|---|---|
| **TRAP1** | M | TRAP1 | V | 0.936607 | 1 | 1.00386 | 0.935991 | 0.85293 | 0.94286 |
| **TRIM25** | R | TRIM25 | C | 0.954724 | 1 | 1.082385 | 0.96238 | 0.95499 | 1.062614 |
| **TRIP13** | R | TRIP13 | V | 0.944625 | 1 | 0.863242 | 0.829775 | 1.41774 | 1.149965 |
| **TSC1** | R | TSC1 | C | 0.955584 | 1 | 1.080015 | 1.14898 | 1.068733 | 0.995835 |
| **TTF1** | R | NKX2-1 | V | 0.892336 | 1 | 0.98432 | 1.012399 | 1.009508 | 1.030552 |
| **Tuberin** | R | TSC2 | V | 0.966187 | 1 | 1.011316 | 0.938089 | 0.992859 | 0.880969 |
| **Tuberin_pT1462** | R | TSC2 | V | 0.955572 | 1 | 0.9008 | 0.988962 | 1.037603 | 0.92896 |
| **TUFM** | R | TUFM | V | 0.963506 | 1 | 0.983532 | 0.885777 | 1.030088 | 0.871901 |
| **Twist** | M | TWIST1 | C | 0.908618 | 1 | 1.302695 | 1.308053 | 1.174813 | 1.373133 |
| **Tyro3** | R | TYRO3 | V | 0.962494 | 1 | 1.008458 | 1.021109 | 1.016649 | 0.817502 |
| **UBAC1** | R | UBAC1 | V | 0.957252 | 1 | 0.980827 | 0.91373 | 1.031697 | 0.879766 |
| **UBQLN4** | M | UBQLN4 | C | 0.913087 | 1 | 0.82953 | 1.238881 | 1.368281 | 1.081684 |
| **UGT1A** | M | UGT1A1/ 3-5/7-10 | V | 0.923708 | 1 | 1.018455 | 1.138642 | 0.949246 | 0.992803 |
| **ULK1_pS757** | R | ULK1 | C | 0.936697 | 1 | 0.981146 | 1.027837 | 0.979669 | 1.146488 |
| **UQCRC2** | M | UQCRC2 | C | 0.805063 | 1 | 1.046702 | 1.068097 | 1.073217 | 1.09655 |
| **UVRAG** | R | UVRAG | C | 0.893756 | 1 | 0.775193 | 0.7508 | 1.010261 | 0.891976 |
| **VASP** | R | VASP | V | 0.962417 | 1 | 0.992091 | 0.887215 | 1.014456 | 0.907583 |
| **VAV1** | R | VAV1 | C | 0.912644 | 1 | 0.898331 | 0.972322 | 1.078481 | 1.147484 |
| **VEGFR-2** | R | KDR | V | 0.956295 | 1 | 1.104346 | 1.026391 | 1.074375 | 0.956383 |
| **VEGFR-2_pY1175** | R | KDR | C | 0.965139 | 1 | 0.867927 | 1.208351 | 1.418373 | 0.932735 |
| **VHL** | R | VHL | C | 0.933657 | 1 | 1.085342 | 1.253458 | 1.099368 | 1.000051 |
| **VHL-EPPK1** | M | EPPK1 | C | 0.869249 | 1 | 1.132412 | 1.049512 | 1.566239 | 1.663442 |
| **Vinculin** | M | VCL | V | 0.94515 | 1 | 0.937355 | 0.913842 | 1.028848 | 1.151017 |
| **Wee1** | R | WEE1 | C | 0.927052 | 1 | 1.000232 | 1.017009 | 1.021818 | 1.036046 |
| **Wee1_pS642** | R | WEE1 | C | 0.940848 | 1 | 0.996729 | 1.076722 | 1.022184 | 1.007241 |
| **WIPI1** | R | WIPI1 | C | 0.940177 | 1 | 1.046702 | 1.068097 | 1.073217 | 0.984907 |
| **WIPI2** | R | WIPI2 | C | 0.865282 | 1 | 0.972369 | 0.995452 | 0.955263 | 1.404758 |
| **XBP-1** | G | XBP1 | C | 0.930965 | 1 | 1.305267 | 1.133363 | 1.112924 | 0.879439 |
| **XIAP** | R | XIAP | C | 0.95882 | 1 | 1.068016 | 1.077694 | 0.846694 | 1.02996 |
| **XPA** | M | XPA | V | 0.95192 | 1 | 1.046702 | 1.068097 | 1.073217 | 0.984907 |
| **XPF** | R | ERCC4 | C | 0.963757 | 1 | 1.103338 | 1.05802 | 0.998784 | 1.05862 |
| **XRCC1** | R | XRCC1 | C | 0.9131 | 1 | 0.943111 | 0.969502 | 0.976744 | 0.967147 |
| **YAP** | R | YAP1 | C | 0.958027 | 1 | 0.788136 | 0.832152 | 1.467755 | 1.451732 |
| **YAP_pS127** | R | YAP1 | V | 0.959953 | 1 | 0.950655 | 0.969919 | 0.990572 | 0.998716 |
| **YB1_pS102** | R | YBX1 | V | 0.968572 | 1 | 0.868918 | 0.996364 | 0.863764 | 1.018027 |
| **YES1** | R | YES1 | V | 0.939784 | 1 | 1.00169 | 0.968146 | 0.926313 | 0.910682 |
| **ZAP-70** | R | ZAP70 | C | 0.937022 | 1 | 0.683869 | 1.395873 | 0.831671 | 0.672465 |
| **ZEB1** | R | ZEB1 | V | 0.902648 | 1 | 1.08421 | 1.216655 | 1.416789 | 1.257024 |

# CHAPTER III

# GP130 CYTOKINES ACTIVATE NOVEL SIGNALING PATHWAYS AND ALTER BONE DISEMMINATION IN ER+ BREAST CANCER CELLS

The work presented in this chapter is published and adapted from:
Omokehinde T, Jotte A, Johnson RW. gp130 Cytokines Activate Novel Signaling Pathways and Alter Bone Dissemination in ER+ Breast Cancer Cells. J Bone Miner Res. 2021 Sep 3. doi: 10.1002/jbmr.4430.

**Summary**

Breast cancer cells frequently home to the bone marrow, where they encounter signals that promote survival and quiescence or stimulate their proliferation. The interleukin-6 (IL-6) cytokines signal through the co-receptor glycoprotein130 (gp130) and are abundantly secreted within the bone microenvironment. Breast cancer cell expression of leukemia inhibitory factor (LIF) receptor (LIFR)/STAT3 signaling promotes tumor dormancy in the bone, but it is unclear which, if any of the cytokines that signal through LIFR, including LIF, oncostatin M (OSM), and ciliary neurotrophic factor (CNTF), promote tumor dormancy and which signaling pathways are induced. We first confirmed that LIF, OSM, and CNTF and their receptor components were expressed across a panel of breast cancer cell lines, although expression was lower in estrogen receptor negative bone metastatic clones compared to parental cell lines. In estrogen receptor positive (ER+) cells, OSM robustly stimulated phosphorylation of known gp130 signaling targets STAT3, ERK and AKT, while CNTF activated STAT3 signaling. In ER- breast cancer cells, OSM alone stimulated AKT and ERK signaling. Overexpression of OSM, but not CNTF, reduced dormancy gene expression and increased ER+ breast cancer bone dissemination. Reverse-phase protein array revealed distinct and overlapping pathways stimulated by OSM, LIF, and CNTF with known roles in breast cancer progression and metastasis. In breast cancer patients, downregulation of the cytokines or receptors was associated with reduced relapse-free survival, but OSM was significantly elevated in patients with invasive disease and distant metastasis. Together these data indicate that

the gp130 cytokines induce multiple signaling cascades in breast cancer cells, with a potential pro-tumorigenic role for OSM and pro-dormancy role for CNTF.

## Introduction

Breast cancer cells frequently metastasize to the bone marrow, which increases patient risk of developing skeletal related events such as fracture, hypercalcemia, and spinal cord compression, and increases mortality [303, 304]. Upon dissemination into the bone marrow, breast cancer cells may either induce osteolysis or enter a latent period in which they remain quiescent before emerging as a clinically detectable metastasis [136, 305, 306]. While patients with both estrogen receptor positive (ER+) and estrogen receptor negative (ER-) disease develop bone metastases with similar frequency (~50%) [8], the risk of recurrence is different between the two subtypes; in ER- tumors, most skeletal recurrence occurs within the first 5 years after diagnosis, while extended periods of tumor dormancy (8-10 years) prior to skeletal recurrence are more common in ER+ breast cancer [7, 9].

One of the signaling molecules identified as a key regulator of tumor dormancy in the bone is leukemia inhibitory factor (LIF) receptor (LIFR) [287], which is also a breast tumor suppressor and metastasis suppressor [49, 221]. Breast cancer patients with lower LIFR levels in the primary tumor have significantly worse overall survival [221, 287], and breast cancer patients who develop bone metastases have significantly lower LIFR levels in the primary tumor [287]. When LIFR is down-regulated in ER+ breast cancer cells that lie dormant *in vivo*, the tumor cells proliferate and colonize the bone marrow [287]. This is thought to occur through loss of STAT3 signaling, since loss of STAT3 phenocopies tumor cell exit from dormancy in the bone [287] and was previously identified as a pro-dormancy gene in ER+ breast cancer cells [287, 307]. LIFR is a member of the interleukin-6 family of cytokines, which induce signaling through the common co-receptor glycoprotein130 (gp130).

There are multiple ligands that form a complex with and initiate downstream signaling through the LIFR/gp130: LIF, oncostatin M (OSM), and ciliary neurotrophic factor (CNTF). LIF and OSM can both form a complex with LIFR/gp130, but OSM can also bind to its cytokine-specific receptor OSM receptor (OSMR). CNTF forms a complex

with LIFR/gp130 and its cytokine-specific, soluble receptor CNTF receptor (CNTFR) [308]. While these cytokines are produced in the bone microenvironment [162, 170-172, 309] and are well documented to induce STAT3 signaling in breast cancer cells [222, 240, 255, 287, 310], it is unclear which, if any, of these cytokines provide signaling cues to induce tumor dormancy. Similarly, while LIF and OSM are known to induce STAT3 signaling [154, 255, 287, 310, 311], MAPK/ERK [154, 155, 157, 312], and AKT signaling [157, 230, 255], it is unknown whether these cytokines have differential effects on downstream pathways in breast cancer, and the effect of CNTF on breast cancer cells has not been studied at all.

This study therefore sought to establish the baseline expression of the LIFR-binding cytokines and their receptors in both ER+ and ER- breast cancer cells and their correlation with patient outcomes, identify differentially activated downstream signaling pathways, and determine their effect on tumor growth and dissemination to bone.

## Results

***LIFR-binding ligands and receptors are expressed at variable levels in breast cancer cells and reduced in bone metastatic breast cancer.*** To determine the endogenous expression levels of gp130 cytokines in breast cancer cells, we examined a panel of breast cancer cell lines inclusive of multiple molecular subtypes and species (human and mouse). The human breast cancer cell lines MCF7 (dormant / low metastatic potential *in vivo*, estrogen receptor positive, ER+), SUM159 (dormant / low metastatic potential *in vivo*, estrogen receptor negative, ER-), and MDA-MB-231 (high metastatic potential *in vivo*, ER-) all expressed *LIF*, *OSM* and *CNTF* (Figure 7A-C) at variable levels. Similarly, mouse mammary carcinoma cell lines (low metastatic potential: D2.0R and PyMT-derived; high metastatic potential: 4T1 and D2A1) expressed *Lif, Osm,* and *Cntf* (Figure 7D-F).

Since all the breast cancer cell lines we examined are able to disseminate to the bone marrow [285, 286, 288, 289, 313, 314], and LIFR is a metastasis suppressor [49] and prevents tumor colonization of bone [287], we examined whether there were differences in cytokine expression between parental and bone-metastatic variants. In comparison to their parental counterparts, there was no significant difference in *LIF* or

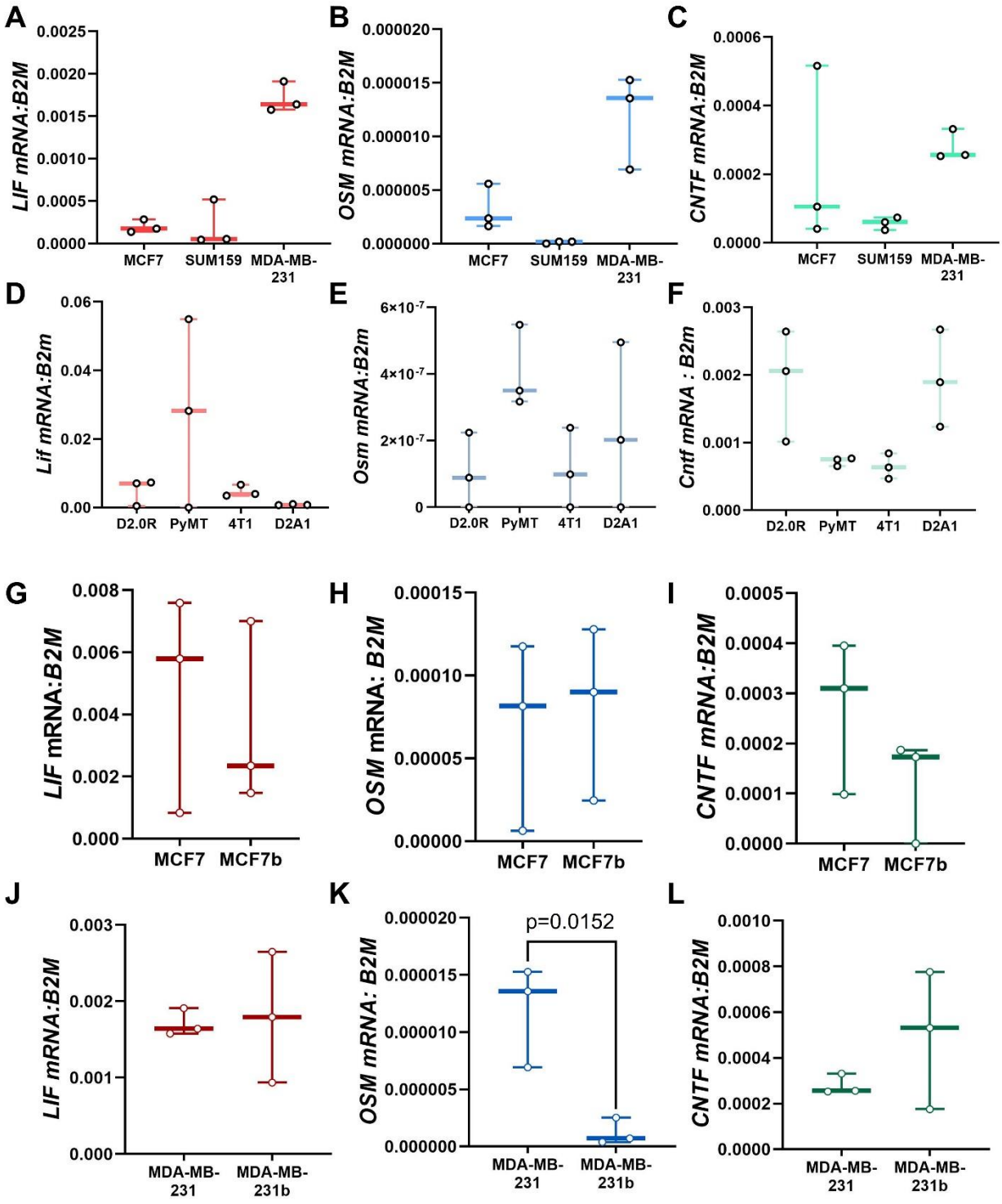
A
LIF mRNA:B2M
0.0025
0.0020
0.0015
0.0010
0.0005
0.0000
MCF7
SUM159
MDA-MB-231
B
OSM mRNA:B2M
0.000020
0.000015
0.000010
0.000005
0.000000
MCF7
SUM159
MDA-MB-231
C
CNTF mRNA:B2M
0.0006
0.0004
0.0002
0.0000
MCF7
SUM159
MDA-MB-231
D
Lif mRNA:B2m
0.06
0.04
0.02
0.00
D2.0R
PyMT
4T1
D2A1
E
Osm mRNA:B2m
6×10-7
4×10-7
2×10-7
0
D2.0R
PyMT
4T1
D2A1
F
Cntf mRNA : B2m
0.003
0.002
0.001
0.000
D2.0R
PyMT
4T1
D2A1
G
LIF mRNA:B2M
0.008
0.006
0.004
0.002
0.000
MCF7
MCF7b
H
OSM mRNA: B2M
0.00015
0.00010
0.00005
0.00000
MCF7
MCF7b
I
CNTF mRNA:B2M
0.0005
0.0004
0.0003
0.0002
0.0001
0.0000
MCF7
MCF7b
J
LIF mRNA:B2M
0.003
0.002
0.001
0.000
MDA-MB-231
MDA-MB-231b
K
OSM mRNA: B2M
p=0.0152
0.000020
0.000015
0.000010
0.000005
0.000000
MDA-MB-231
MDA-MB-231b
L
CNTF mRNA:B2M
0.0010
0.0008
0.0006
0.0004
0.0002
0.0000
MDA-MB-231
MDA-MB-231b

**Figure 7. Relative expression of the gp130 cytokines across multiple breast cancer cell lines.** (A-C) qPCR analysis of parental MCF7, SUM159 and MDA-MB-231 human breast cancer cells for (A) *LIF*, (B) *OSM*, and (C) *CNTF* mRNA levels normalized to *B2M* (housekeeping gene). (D-F) qPCR analysis of parental D2.0R, PyMT, 4T1, D2A1 mouse mammary carcinoma cells for (D) *Lif*, (E) *Osm*, and (F) *Cntf* mRNA levels normalized to *B2m* (housekeeping gene). (G-L) qPCR analysis of *LIF*, *OSM*, and *CNTF* mRNA levels for (G-I) parental MCF7 and MCF7b cells (bone metastatic variant) and (J-L) parental MDA-MB-231 and MDA-MB-231b cells (bone metastatic variant). G-L: Student's unpaired t-test. n=three independent biological replicates. Boxplots represent mean + interquartile range.

*CNTF* expression in the bone metastatic variants of the MCF7 cell line (MCF7b) [285] or MDA-MB-231 cells (MDA-MB-231b) [286, 288] in comparison to the parental cell lines (Figure 7G, I, J, L), but OSM was significantly lower in MDA-MB-231b compared to parental cells (Figure 7K; 90%, p=0.0152) and unchanged in MCF7b cells (Figure 7H). The bone-metastatic variants for human breast cancer cell line MDA-MB-231 were run concurrently with the parental cell lines, which were re-plotted in Figure 1J-L for comparison to the bone metastatic lines. In contrast, *Lif* (82%, p=0.0299), *Osm* (86%, p=0.0271), and *Cntf* (58%, p=0.0076) were all significantly down-regulated in the bone metastatic variant of the 4T1 mouse mammary carcinoma cell line (4T1BM2) [289] compared to the 4T1 parental line (Figure 8A-C). Thus, each breast cancer cell line that was investigated expressed the gp130 ligands at the mRNA level and may therefore be capable of gp130 autocrine signaling.

Since the tumor cell lines expressed the gp130 cytokines, we next examined the endogenous receptor levels across all cell lines to determine whether each component of the LIFR/gp130, OSMR/gp130, and LIFR/CNTFR/gp130 complex is expressed in the breast cancer cells. In the parental human breast cancer cell lines, *GP130*, the co-receptor subunit for not only *LIFR*, *OSMR*, and *CNTFR* but also IL-6 and IL-11 signaling [315-317], was abundantly expressed in MCF7, SUM159, and MDA-MB-231 cells (Figure 9A), and *LIFR, OSMR*, and *CNTFR* were all expressed in the human breast cancer cell lines (Figure 9B-D), although *CNTFR* expression was much lower across all cell lines. All the mouse mammary carcinoma cell lines also expressed gp130 and the cytokine specific receptors, again with particularly low CNTFR expression across all cell lines (Figure 9E-H).

Upon examination of the bone-metastatic cell lines, MCF7b cells had no significant change in *GP130, LIFR*, *OSMR*, or *CNTFR* (Figure 9I-L), nor did MDA-MB-231b cells compared to the parental cell line (Figure 9M-P). In 4T1BM2 cells, *gp130* was unchanged (Figure 2Q), but *Lifr* (85%, p=0.0081), *Osmr* (73%, p=0.0344), and *Cntfr*(82%, p=0.0036) were all significantly reduced (Figure 8D-F). Thus, all of the receptors required for LIFR signaling are expressed in breast cancer cell lines, although some of the receptors are expressed at lower levels in bone-metastatic cells. ER- cell lines, there was no significant change in the expression of *LIF, OSM, CNTF* or *GP130* (Figure 10A-D) between ER+

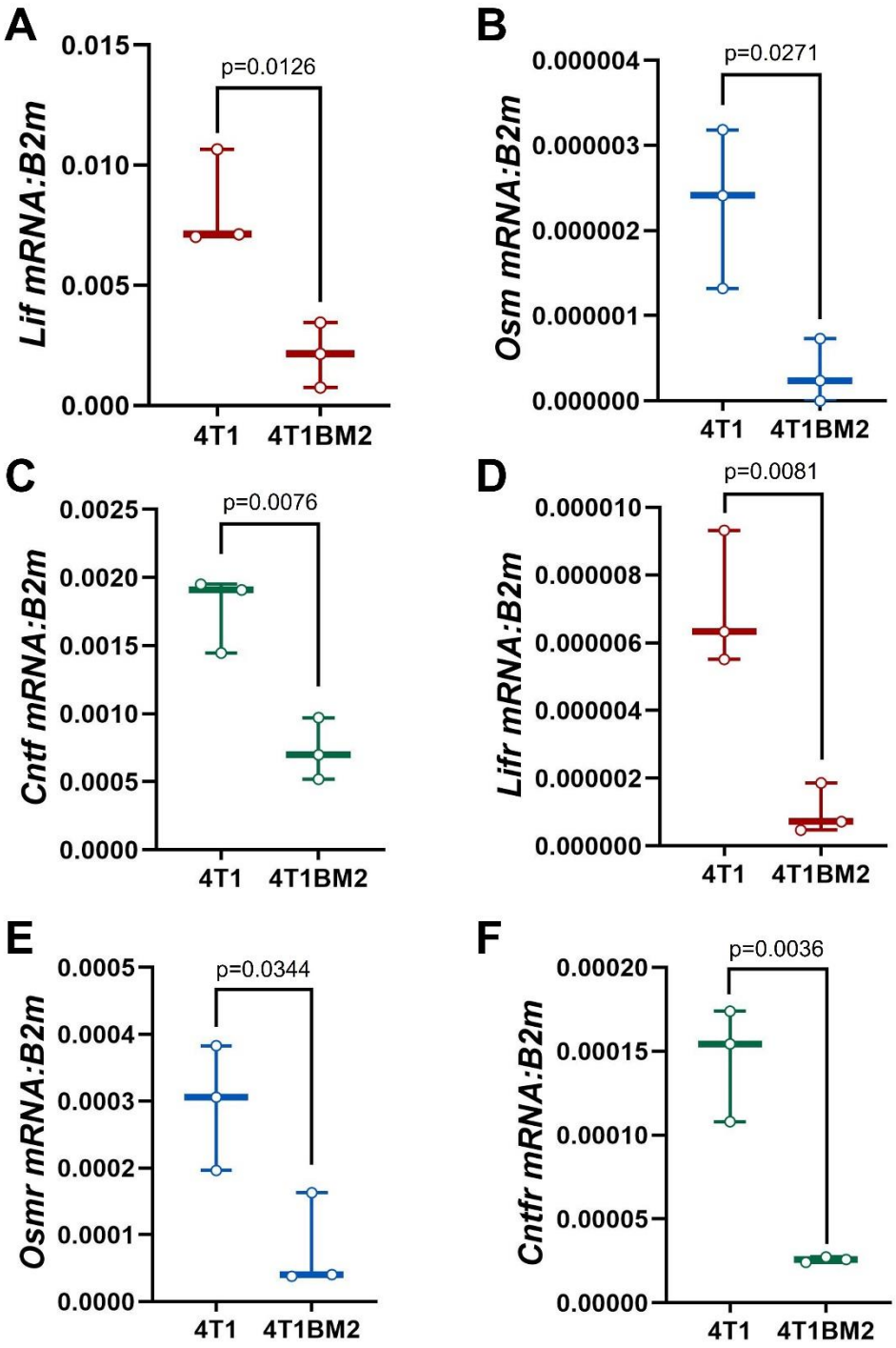


**Figure 8. Comparison of the relative expression of the gp130 ligands in parental and bone metastatic variants of 4T1 breast cancer cell lines.** (A-F) qPCR analysis of parental 4T1 and 4T1BM2 cells (bone metastatic) (A) *Lif*, (B) *Osm*, (C) *Cntf*, (D) *Lifr*, (E) *Osmr*, and (F) *Cntfr* mRNA levels normalized to *B2M* (housekeeping gene). Student's unpaired t-test. n=three independent biological replicates. Boxplots represent mean + interquartile range.

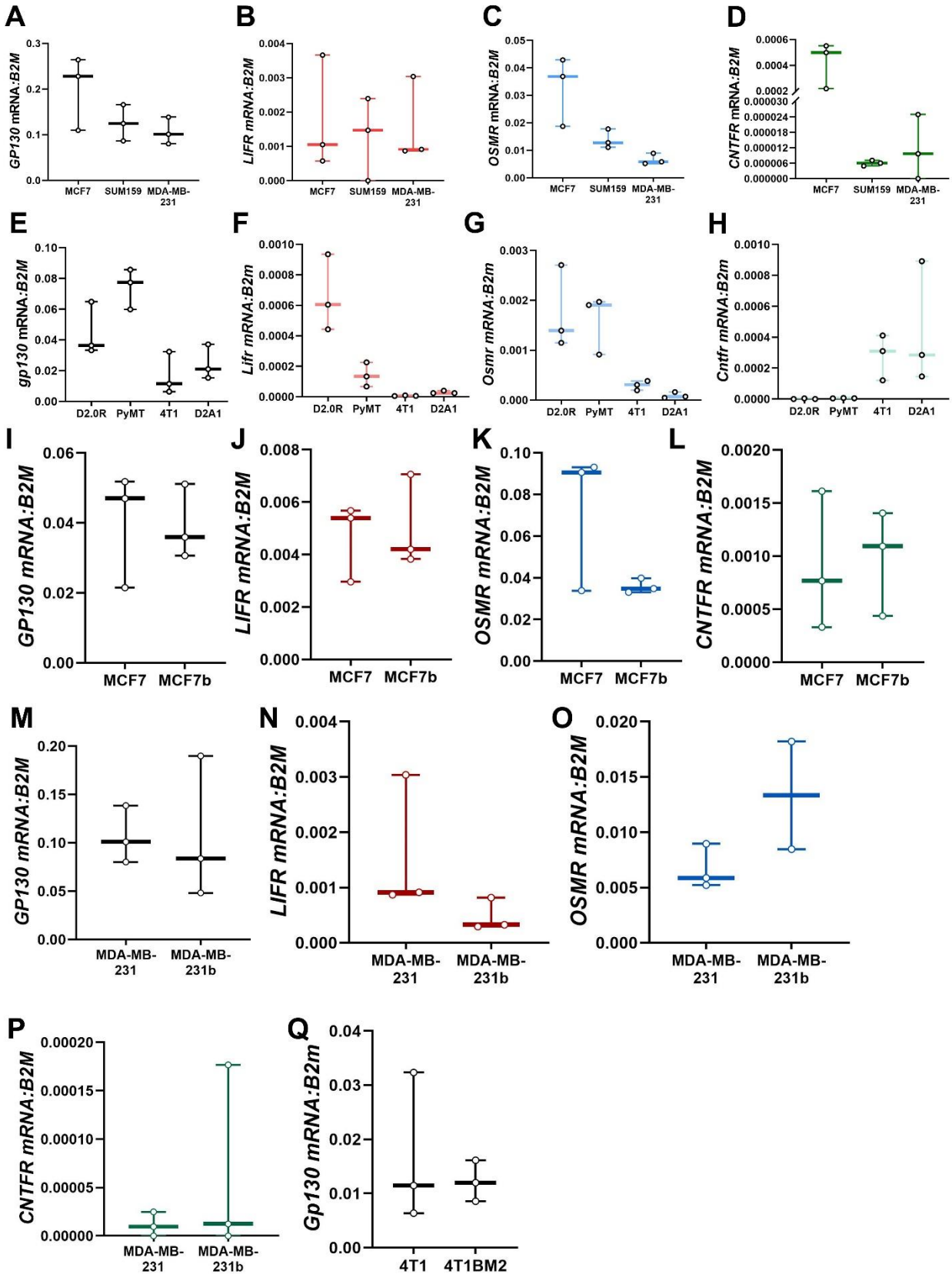
A
GP130 mRNA:B2M
0.3
0.2
0.1
0.0
MCF7
SUM159
MDA-MB-231
B
LIFR mRNA:B2M
0.004
0.003
0.002
0.001
0.000
MCF7
SUM159
MDA-MB-231
C
OSMR mRNA:B2M
0.05
0.04
0.03
0.02
0.01
0.00
MCF7
SUM159
MDA-MB-231
D
CNTFR mRNA:B2M
0.0006
0.0004
0.0002
0.000030
0.000024
0.000018
0.000012
0.000006
0.000000
MCF7
SUM159
MDA-MB-231
E
gp130 mRNA:B2M
0.10
0.08
0.06
0.04
0.02
0.00
D2.0R
PyMT
4T1
D2A1
F
Lifr mRNA:B2m
0.0010
0.0008
0.0006
0.0004
0.0002
0.0000
D2.0R
PyMT
4T1
D2A1
G
Osmr mRNA:B2m
0.003
0.002
0.001
0.000
D2.0R
PyMT
4T1
D2A1
H
Cntfr mRNA:B2m
0.0010
0.0008
0.0006
0.0004
0.0002
0.0000
D2.0R
PyMT
4T1
D2A1
I
GP130 mRNA:B2M
0.06
0.04
0.02
0.00
MCF7
MCF7b
J
LIFR mRNA:B2M
0.008
0.006
0.004
0.002
0.000
MCF7
MCF7b
K
OSMR mRNA:B2M
0.10
0.08
0.06
0.04
0.02
0.00
MCF7
MCF7b
L
CNTFR mRNA:B2M
0.0020
0.0015
0.0010
0.0005
0.0000
MCF7
MCF7b
M
GP130 mRNA:B2M
0.20
0.15
0.10
0.05
0.00
MDA-MB-231
MDA-MB-231b
N
LIFR mRNA:B2M
0.004
0.003
0.002
0.001
0.000
MDA-MB-231
MDA-MB-231b
O
OSMR mRNA:B2M
0.020
0.015
0.010
0.005
0.000
MDA-MB-231
MDA-MB-231b
P
CNTFR mRNA:B2M
0.00020
0.00015
0.00010
0.00005
0.00000
MDA-MB-231
MDA-MB-231b
Q
Gp130 mRNA:B2m
0.04
0.03
0.02
0.01
0.00
4T1
4T1BM2

**Figure 9. Relative expression of the gp130 cytokine specific receptors across a panel of breast cancer cell lines.** (A-D) qPCR analysis of parental MCF7, SUM159 and MDA-MB-231 human breast cancer cells for (A) *GP130*, (B) *LIFR*, (C) *OSMR*, and (D) *CNTFR* mRNA levels normalized to *B2M* (housekeeping gene). (E-H) qPCR analysis of parental D2.0R, PyMT, 4T1, D2A1 mouse mammary carcinoma cells for (E) *Gp130*, (F) *Lifr*, (G) *Osmr*, and (H) *Cntfr* mRNA levels normalized to *B2m* (housekeeping gene). (I-L) qPCR analysis of parental MCF7 and MCF7b cells (bone metastatic variant) for (I) *GP130*, (J) *LIFR*, (K) *OSMR*, and (L) *CNTFR* mRNA levels normalized to *B2M*. (M-P) qPCR analysis of parental MDA-MB-231 and MDA-MB-231b cells (bone metastatic variant) for (M) *GP130*, (N) *LIFR*, (O) *OSMR*, and (P) *CNTFR* mRNA levels normalized to *B2M*. (Q) qPCR analysis of *Gp130* mRNA levels normalized to *B2m* for parental 4T1 and 4T1BM2 cells (bone metastatic variant). I-T: Student's unpaired t-test. n=three independent biological replicates. Boxplots represent mean + interquartile range.

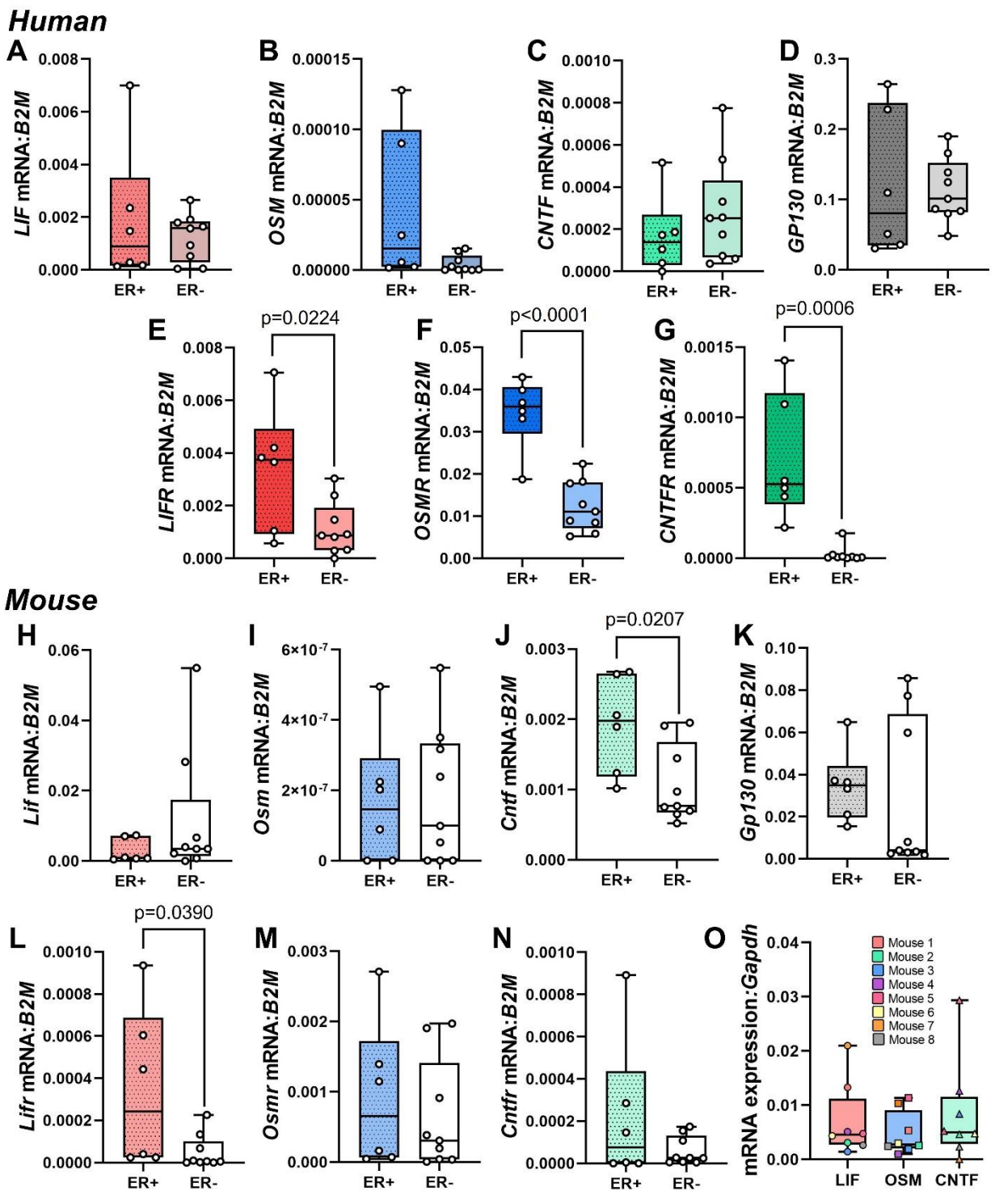
Human
A
LIF mRNA:B2M
0.008
0.006
0.004
0.002
0.000
ER+
ER-
B
OSM mRNA:B2M
0.00015
0.00010
0.00005
0.00000
C
CNTF mRNA:B2M
0.0010
0.0008
0.0006
0.0004
0.0002
0.0000
D
GP130 mRNA:B2M
0.3
0.2
0.1
0.0
E
LIFR mRNA:B2M
p=0.0224
F
OSMR mRNA:B2M
p<0.0001
0.05
0.04
0.03
0.02
0.01
0.00
G
CNTFR mRNA:B2M
p=0.0006
0.0015
0.0010
0.0005
0.0000
Mouse
H
Lif mRNA:B2M
0.06
0.04
0.02
0.00
I
Osm mRNA:B2M
6×10-7
4×10-7
2×10-7
0
J
Cntf mRNA:B2M
p=0.0207
0.003
0.002
0.001
0.000
K
Gp130 mRNA:B2M
0.10
0.08
0.06
0.04
0.02
0.00
L
Lifr mRNA:B2M
p=0.0390
0.0010
0.0008
0.0006
0.0004
0.0002
0.0000
M
Osmr mRNA:B2M
0.003
0.002
0.001
0.000
N
Cntfr mRNA:B2M
0.0010
0.0008
0.0006
0.0004
0.0002
0.0000
O
mRNA expression:Gapdh
0.04
0.03
0.02
0.01
0.00
Mouse 1
Mouse 2
Mouse 3
Mouse 4
Mouse 5
Mouse 6
Mouse 7
Mouse 8
LIF
OSM
CNTF

**Figure 10. Relative expression of the gp130 cytokines and receptors clustered by ER status in both human and mouse cell lines.** (A-G) Expression values from qPCR analysis of (A) *LIF*, (B) *OSM*, (C) *CNTF*, (D) *GP130*, (E) *LIFR*, (F) *OSMR*, and (G) *CNTFR* mRNA levels in human breast cancer cell lines are clustered based on ER status. (H-N) Expression values from qPCR analysis of (A) *Lif*, (B) *Osm*, (C) *Cntf*, (D) *Gp130*, (E) *Lifr*, (F) *Osmr*, and (G) *Cntfr* mRNA levels in mouse mammary carcinonoma cell lines are clustered based on ER status. (O) qPCR analysis of homogenized mouse femora for *Lif*, *Osm* and *Cntf* to validate expression of the gp130 cytokines within the bone microenvironment. n=three independent biological replicates. Boxplots represent mean and interquartile range + min/max.

and ER- human breast cancer cell lines. In contrast, the cytokine specific receptors *LIFR* (66%, p=0.0224)*, OSMR* (64%, p<0.0001) *and CNTFR* (96%, p=0.0006) were all significantly reduced in the human ER- breast cancer cell lines when compared to the ER+ cell lines (Figure 10E-G). In mouse cell lines, *Cntf* (44%, p=0.0207) and *Lifr* (85%, p=0.0390) were significantly lower in ER- compared to ER+ cell lines, with no significant changes in *Lif*, *Osm*, *gp130*, *Osmr*, or *Cntfr* (Figure 10H-N). The expression of gp130, LIFR, OSMR, and CNTFR in breast cancer cells suggests that breast cancer cells possess all of the machinery to induce downstream signaling in response to both autocrine and paracrine-secreted gp130 ligands. Breast cancer cells have been shown to colonize the osteogenic niche, and it was previously reported that osteoblast lineage cells express LIF [170, 309], OSM [162], and CNTF [171, 172], along with hematopoietic cell lineages and stromal cells [318] suggesting that bone-disseminated tumor cells in the osteogenic niche may be exposed to these signals. We have confirmed that these cytokines are also expressed at the transcript level in homogenized mouse femora, which include bone marrow (Figure 10O).

***OSM activates STAT3, ERK, and AKT signaling in MCF7 cells.*** Since breast cancer cells express the necessary signal transduction machinery for LIFR signaling, we next examined whether the cytokines induce known gp130 downstream signaling pathways. LIF, OSM, and CNTF have all been previously reported to activate AKT, ERK, and STAT signaling [154, 155, 157, 222, 230, 240, 255, 287, 310, 312, 319, 320], but the relative induction of these downstream signaling pathways, and in response to CNTF in particular, has not been explored in breast cancer. While the MCF7 cells have low basal phosphorylated AKT (pAKT) and ERK (pERK), OSM dramatically activated AKT (up to a 9-fold increase, p<0.0001) and ERK (up to a 5-fold increase, p=0.0542-0.0001) signaling, while LIF only activated ERK signaling (up to a 3-fold increase, p=0.0025) above baseline (Figure 11A-C). CNTF alone did not activate either pathway, as indicated by pAKT and pERK expression, but modestly increased ERK signaling (p=0.0130) when combined with its soluble receptor CNTFR (sR), which has been reported to mediate downstream CNTF signaling in osteoblasts [172]. In contrast, LIF, OSM, and CNTF all robustly activated the STAT3 signaling pathway, as indicated by up to a 37-fold increase in phosphorylated

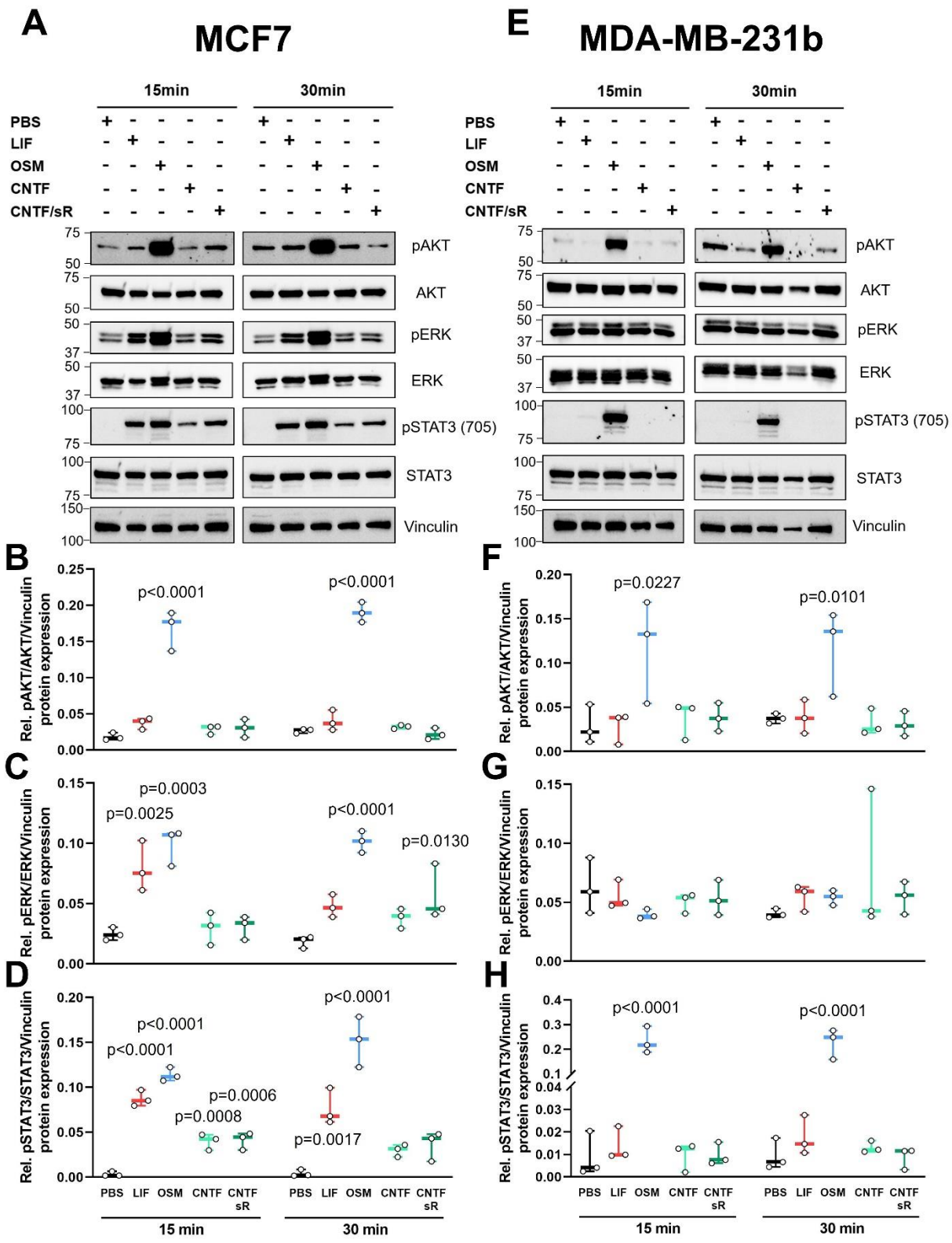
A
MCF7
15min
30min
PBS
LIF
OSM
CNTF
CNTF/sR
pAKT
AKT
pERK
ERK
pSTAT3 (705)
STAT3
Vinculin
E
MDA-MB-231b
B
Rel. pAKT/AKT/Vinculin protein expression
p<0.0001
p<0.0001
F
p=0.0227
p=0.0101
C
Rel. pERK/ERK/Vinculin protein expression
p=0.0003
p=0.0025
p<0.0001
p=0.0130
G
D
Rel. pSTAT3/STAT3/Vinculin protein expression
p<0.0001
p<0.0001
p=0.0006
p=0.0008
p<0.0001
p=0.0017
H
p<0.0001
p<0.0001
PBS LIF OSM CNTF CNTF sR
15 min
30 min

**Figure 11. LIFR-binding ligands activate AKT, ERK, and STAT3 signaling pathways in MCF7 and MDA-MB-231 cells.** (A-H) Western blot analysis for $pAKT^{S473}$, total AKT, $pERK^{T202-204}$, total ERK, $pSTAT3^{Y705}$, total STAT3 and vinculin (loading control) after 15 or 30 minute treatment with PBS, recombinant LIF, recombinant OSM, recombinant CNTF at 50 ng $mL^{-1}$ and a 1:10 ratio of CNTF and its soluble receptor CNTF (50:500 µg $mL^{-1}$) in (A-D) MCF7 and (E-H) MDA-MB-231b breast cancer cells. (A, E) Representative western blot images for MCF7 and MDA-MB-231b cells treated with the respective cytokines. (B-D, F-H) Densitometry analysis from western blot images developed from 3 biological replicates of MCF7 and MDA-MB-231b cells treated with the respective cytokines. One-way ANOVA with Sidak's multiple comparisons. n=three independent biological replicates. Boxplots represent mean + interquartile range.

STAT3 (pSTAT3$^{Y705}$) when compared to PBS control (Figure 11A, D; p=0.0001 – 0.0017). CNTF and CNTF+sR (CNTFsR) activation of STAT3 signaling was only significant at 15 minutes (Figure 11D), but still induced pSTAT3 signaling well above baseline at 30 minutes (Figure 11A). Thus, OSM is the most potent signal transducer of AKT, ERK, and STAT3 signaling in ER+ breast cancer cells.

***OSM activates STAT3 and AKT signaling in MDA-MB-231b cells.*** We and others have previously reported that MDA-MB-231 and MDA-MB-231b cells express LIFR at the protein level, but that it is non-functional, since treatment with LIF does not activate downstream STAT3 signaling [222, 287]. While OSM activated AKT in MDA-MB-231 cells, with up to a 4-fold increase in pAKT, neither LIF, CNTF nor CNTF/CNTFsR treatment induced pAKT (Figure 11E, F; p=0.0101 – 0.0227). Since MDA-MB-231 cells have constitutive ERK activation [312], we saw no further enhancement of ERK signaling by any of the ligands (Figure 11E, G). As previously demonstrated, recombinant LIF did not activate STAT3 signaling, while OSM dramatically activated STAT3 signaling (Figure 11E, H; up to 2.41-fold increase, p<0.0001). MDA-MB-231b cells were unresponsive to CNTF and CNTFsR (Figure 11E-H), consistent with the need for a functional LIFR, which both the MDA-MB-231 and MDA-MB-231b cells lack [222, 287]. Despite LIFR being non-functional in the MDA-MB-231b cells, OSM was still able to activate STAT3 signaling, suggesting that OSM specifically may still be able to induce downstream signaling through LIFR in breast cancer cells, or that OSM may be able to signal through the OSMR, which was expressed in both MDA-MB-231 and MDA-MB-231b cells (Figure 10O). Collectively these data indicate that OSM is the most potent inducer of downstream signaling in ER- and ER+ breast cancer cells.

***LIFR is required for LIF but not OSM induction of downstream signaling.*** Given that MCF7 cells express both OSMR and LIFR, we next aimed to determine whether MCF7 cells retain their responsivity to OSM and LIF when LIFR is knocked down. When compared to MCF7 non-silencing control (NSC) cells, two distinct MCF7 shLIFR cell lines (generated from pooled populations of two different shRNAs) had reduced expression of LIFR (Figure 12A-C), as expected. It is important to note that while each cell line is

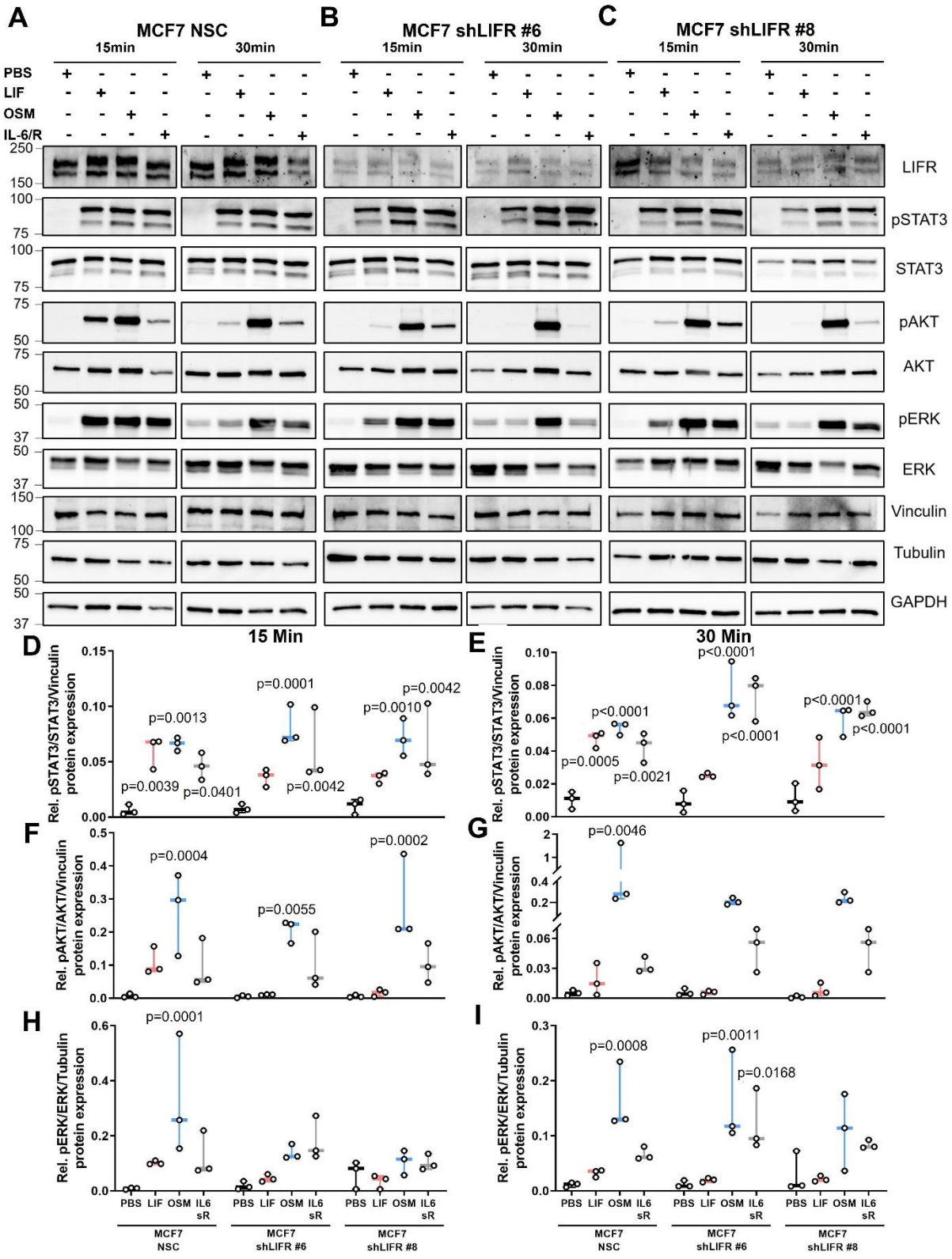
A
MCF7 NSC
B
MCF7 shLIFR #6
C
MCF7 shLIFR #8
15min
30min
PBS
LIF
OSM
IL-6/R
LIFR
pSTAT3
STAT3
pAKT
AKT
pERK
ERK
Vinculin
Tubulin
GAPDH
D
15 Min
Rel. pSTAT3/STAT3/Vinculin protein expression
p=0.0013
p=0.0039
p=0.0401
p=0.0001
p=0.0042
p=0.0010
p=0.0042
E
30 Min
p<0.0001
p<0.0001
p=0.0005
p=0.0021
p<0.0001
p<0.0001
p<0.0001
F
Rel. pAKT/AKT/Vinculin protein expression
p=0.0004
p=0.0055
p=0.0002
G
p=0.0046
H
Rel. pERK/ERK/Tubulin protein expression
p=0.0001
I
p=0.0008
p=0.0011
p=0.0168
PBS
LIF
OSM
IL6 sR
MCF7 NSC
MCF7 shLIFR #6
MCF7 shLIFR #8

**Figure 12. OSM induces downstream signaling independent of LIFR knockdown.** (A-C) Representative western blot images for LIFR, pSTAT3$^{Y705}$, total STAT3, pAKT$^{S473}$, total AKT, pERK$^{T202-204}$, total ERK, Vinculin, α-Tubulin, and GAPDH after 15 or 30 minute treatment with PBS, recombinant LIF, recombinant OSM at 50 ng mL$^{-1}$ recombinant IL-6 and its soluble receptor IL-6R a 1:10 ratio (50:500 µg mL$^{-1}$). (D-I) Densitometry analysis for (D, E) STAT3, (F, G) AKT and (H, I) ERK from western blot images developed from 3 biological replicates of MCF7 NSC, MCF7 shLIFR #6 and MCF7 shLIFR #8. One-way ANOVA with Sidak's multiple comparisons test. *p<0.05, **p<0.01, ***p<0.001, ****p<0.0001. n=three independent biological replicates. Boxplots represent mean + interquartile range.

represented by its own blot, all blots were developed simultaneously for NSC and shLIFR cell lines at 15 and 30 minutes. LIF (78-89% increase, p=0.0005 – 0.0039), OSM (81-90% increase, p<0.0001 – 0.0013) and IL-6 (75-86% increase, p=0.0021 – 0.0401), which was included as a control since it does not require LIFR to signal, significantly activated STAT3 signaling in MCF7 NSC cells as indicated by pSTAT3 (Y705) levels (Figure 12A, D, E). However, in MCF7 shLIFR cells, LIF activation of STAT3 signaling was no longer significant (Figure 12D, E). LIF activation of AKT and ERK was similarly dampened in the MCF7 shLIFR cells (Figure 12A-C, F-I). In contrast, OSM robustly activated STAT3 and AKT signaling up to a 72-fold increase, regardless of LIFR knockdown (Figure 12A-I; p=0.0001 – 0.0055). OSM induction of ERK was significantly dampened with LIFR knockdown (Figure 12A-C, H; p=0.2290 – 0.8960). As expected and similar to IL-6 activation of STAT3, IL-6 stimulation resulted in an increase in AKT (83-95% increase) and ERK (37%-93% increase) activation when compared to the PBS control, regardless of LIFR knockdown (Figure 12A-C, F-I). OSM therefore remains a potent inducer of downstream signaling even when LIFR expression is reduced.

***OSM promotes spontaneous dissemination of MCF7 cells to the bone.*** To determine whether autocrine gp130 signaling alters tumor progression and known dormancy-promoting genes [287], we constitutively over-expressed OSM, LIF, and CNTF in MCF7 cells. We chose the MCF7 model for these experiments since they are ER+ and patients with ER+ disease typically have much longer latency (dormancy) periods prior to recurrence than patients with ER- disease (5-10 years compared to <5 years) [8, 9], and patients with ER+ breast cancers are also more likely to develop bone-only metastases [321]. We and others have also published that MCF7 tumor cells remain dormant in distant sites including the lung and bone marrow following inoculation [285, 287, 290, 314, 322]. The OSM and CNTF overexpression plasmids had unique plasmid backbones (OSM: pCMV3, CNTF: pCMV6) and were each compared to their respective control cell lines expressing the empty vector. We were unable to generate stable LIF overexpressing cells (data not shown), which we hypothesize may be due to dormancy induction within the LIF-overexpressing clones. Overexpression of OSM and CNTF was confirmed by qPCR (Figure 13A, B; 107-fold - p<0.0079, 4000-fold - p<0.0003) in MCF7

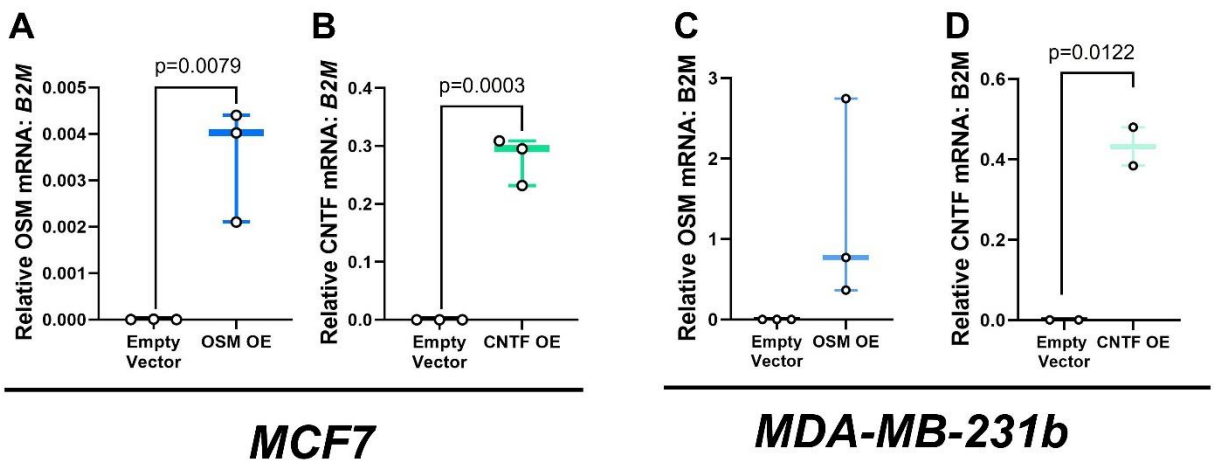


**Figure 13. Validation of OSM and CNTF expression plasmids.** (A-B) MCF7 cells with constitutive expression of OSM or CNTF confirmed by qPCR analysis. (C-D) MDA-MB-231b cells with transient expression of OSM or CNTF confirmed by qPCR analysis. n=3 independent biological replicates. A-D: Student's unpaired t-test. n=three independent biological replicates. Boxplots represent mean + interquartile range.

cells (OSM-OE and CNTF-OE). Utilizing these overexpression cells, we sought to determine the role of OSM and CNTF in primary tumor growth *in vivo*, OSM-OE and CNTF-OE or control MCF7 cells were inoculated into the mammary fat pad of mice with estradiol supplementation (n=10 mice/group). Over-expressing cells were re-validated for OSM and CNTF overexpression at the time of inoculation. Overexpression of OSM resulted in a modest but significant increase in primary tumor volume at end point with a trend toward an increase in tumor weight (Figure 14A&B). We also examined whether tumor dissemination to bone was impacted by OSM overexpression, using previously published techniques to detect ultra-low levels of bone-disseminated tumor cells [290]. Assessment of tumor burden by qPCR for the human housekeeping gene *B2M* did not yield any detectable expression in the femurs of mice inoculated with either empty vector or OSM-overexpressing cells (Figure 14C) but more sensitive flow cytometric analysis of bone-disseminated CD298+ tumor cells [290] revealed a significant increase in the number and percentage of CD298+ tumor cells in the bone in mice inoculated with OSM-overexpressing tumor cells, regardless of whether tumor burden was normalized to primary tumor weight at sacrifice (Figure 14D-G; p=0.0009 – 0.0401). Overexpression of CNTF did not significantly alter primary tumor volume but modestly increased primary tumor weight at the endpoint of the study. (Figure 15A, B). There was no change in bone-disseminated tumor burden in mice inoculated with CNTF-overexpressing tumor cells by either qPCR or flow cytometric analysis, regardless of whether the data were normalized to primary tumor weight (Figure 15C-H). Of note, a slight trend in increased bone dissemination in CNTF overexpressing cells was observed; however, this effect was reversed when normalized to final tumor weight (Figure 15E&G). Thus, OSM, but not CNTF promotes ER+ tumor dissemination to bone.

***Constitutive expression of OSM, but not CNTF, reduces pro-dormancy genes in ER+ breast cancer cells.*** To determine whether the OSM-induced increase in bone-disseminated tumor cells may be due to cells exiting dormancy, we examined expression of pro-dormancy genes in OSM and CNTF-overexpressing cells. Overexpression of OSM in MCF7 cells (OSM-OE) significantly reduced the expression of 6/21 pro-dormancy genes [287], including *MAPK11* (p38β), *BMP7*, *FOXA1*, *IGFBP5*, *PDCD4*, and *TGFB2*

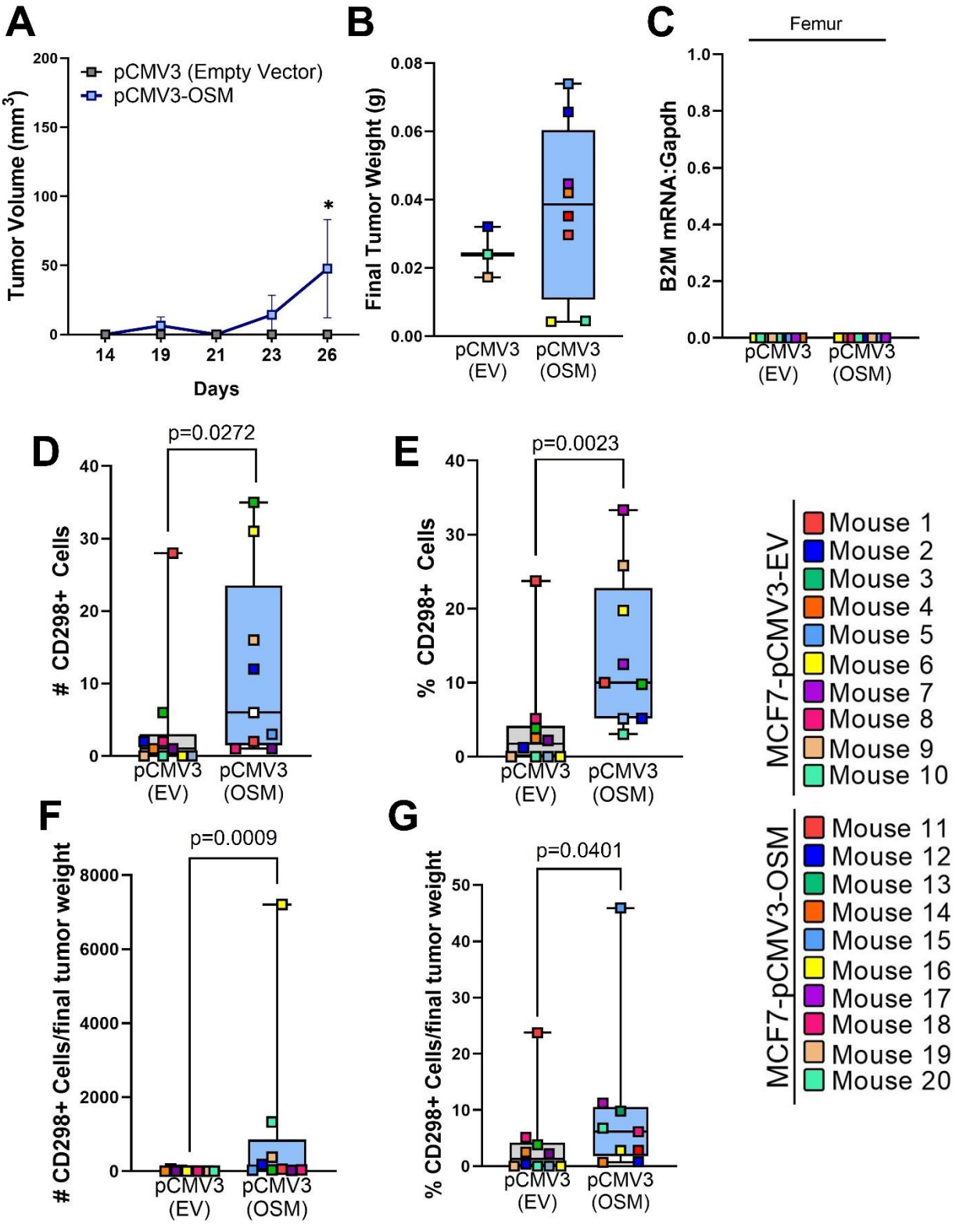
A
pCMV3 (Empty Vector)
pCMV3-OSM
Tumor Volume (mm3)
Days
B
Final Tumor Weight (g)
pCMV3 (EV)
pCMV3 (OSM)
C
Femur
B2M mRNA:Gapdh
D
p=0.0272
# CD298+ Cells
E
p=0.0023
% CD298+ Cells
F
p=0.0009
# CD298+ Cells/final tumor weight
G
p=0.0401
% CD298+ Cells/final tumor weight
MCF7-pCMV3-EV
Mouse 1
Mouse 2
Mouse 3
Mouse 4
Mouse 5
Mouse 6
Mouse 7
Mouse 8
Mouse 9
Mouse 10
MCF7-pCMV3-OSM
Mouse 11
Mouse 12
Mouse 13
Mouse 14
Mouse 15
Mouse 16
Mouse 17
Mouse 18
Mouse 19
Mouse 20

**Figure 14. Overexpression of OSM promotes spontaneous dissemination of MCF7 cells to the bone.** (A-G) *In vivo* analysis of MCF7 OSM/CNTF overexpressing cells. n=10 mice/group for MCF7-pCMV3, n=9 mice/group for MCF7-pCMV3-OSM. (A) Tumor volume by caliper measurements over 26 days following injection of MCF7-pCMV3 (empty vector), MCF7-pCMV3-OSM (OSM over-expression). (B) Final tumor weight after sacrifice. (C) qPCR analysis of *B2M* expression in homogenized femur from inoculated mice normalized to mouse *Gapdh* (housekeeping gene). (D, E) Quantification of the total number (D) and percentage (E) of CD298+ tumor cells detected by flow cytometry in the bone marrow of inoculated mice. (F, G) Normalization of total number (F) and percentage (G) of CD298+ cells to final tumor weight. A: Two-way ANOVA with Tukey's multiple comparisons test. B-G: Mann-Whitney Test. n=three independent biological replicates. Boxplots represent mean + interquartile range.

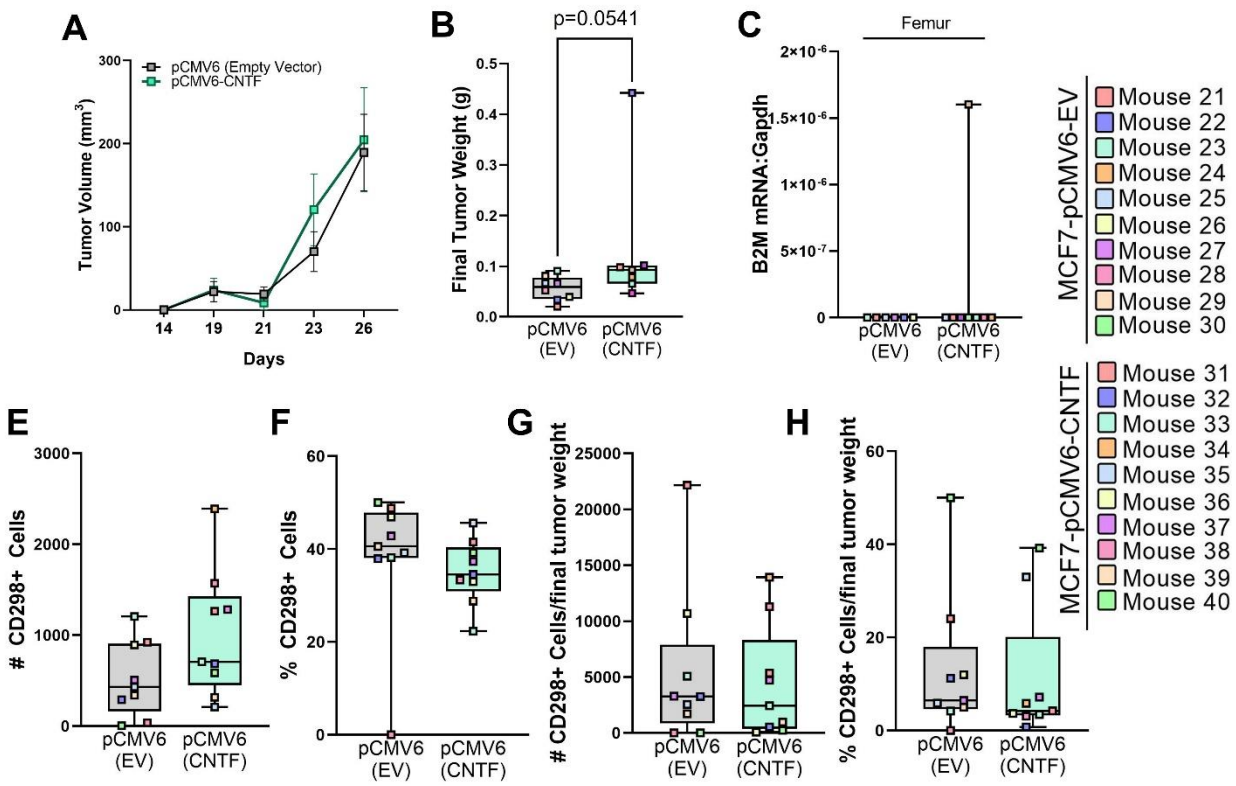


**Figure 15. CNTF expression plasmids and CNTF overexpression in bone dissemination.** (A-B) MCF7 cells with constitutive expression of OSM or CNTF confirmed by qPCR analysis. (C-D) MDA-MB-231b cells with transient expression of OSM or CNTF confirmed by qPCR analysis. n=3 independent biological replicates. A-D: Student's unpaired t-test. n=three independent biological replicates. Boxplots represent mean + interquartile range. (E-K) *In vivo* analysis of MCF7 CNTF overexpressing cells. n=10 mice/group for MCF7-pCMV6, n=9 mice/group for MCF7-pCMV6-CNTF. (E) Tumor volume by caliper measurements over 26 days following injection of MCF7-pCMV6 (empty vector), MCF7-pCMV6-CNTF (CNTF over-expression). (F) Final tumor weight after sacrifice. (G) qPCR analysis of *B2M* expression in homogenized femur from inoculated mice normalized to mouse *Gapdh* (housekeeping gene). (H, I) Quantification of the total number (H) and percentage (I) of CD298+ tumor cells detected by flow cytometry in the bone marrow of inoculated mice. (J, K) Normalization of total number (F) and percentage (G) of CD298+ cells to final tumor weight. E: Two-way ANOVA with Tukey's multiple comparisons test. F-K: Mann-Whitney Test. n=three independent biological replicates. Boxplots represent mean + interquartile range.

when compared to the empty vector expressing control cell line (Figure 16A; 41-97.5%, p<0.05-0.0001). In contrast, one gene, *BMP7*, was significantly reduced in CNTF-over-expressing MCF7 (CNTF-OE) cells (Figure 16B; 20%, p=0.0223). Using the same expression vectors, we transiently over-expressed OSM and CNTF in MDA-MB-231 parental and bone-metastatic cells to determine if gp130 signaling alters dormancy related genes in ER- breast cancer cell lines. Overexpression of OSM (2500-fold, p=0.0188) in MDA-MB-231 parental cells significantly reduced *GAS6* expression (p=0.0064; Figure 17A&C); CNTF overexpression (2400-fold, p=0.0100) did not alter any of the dormancy genes (Figure 17B&D). Overexpression of OSM (32,000-fold) in MDA-MB-231b cells significantly increased *SOCS3* (p=0.0417) and *MAPK11* (p38β, p=0.0211) (Figure 16C, 17C), but CNTF overexpression (626-fold, p=0.0122) had no effect on any dormancy genes (Figure 16D, 17D). It is therefore possible that OSM reduces pro-dormancy genes to promote the outgrowth of tumor cells in the bone.

***The gp130 cytokines activate novel signaling pathways in breast cancer cells.*** Previous studies have demonstrated that loss of LIFR in ER+ MCF7 cells leads to tumor outgrowth in the bone [287], but our data indicates that OSM is the most potent signal transducer and promotes tumor dissemination while repressing dormancy. To further understand how OSM may be acting as a pro-metastatic factor, we examined the complex downstream signaling activated by the gp130 cytokines by performing molecular reverse phase protein array (RPPA) profiling of MCF7 cells treated with recombinant LIF, OSM, CNTF or CNTF+sR (50ng/ml) for 15 minutes. Of the 496 phospho-specific and total antibodies tested, 38 proteins were significantly altered in the presence of one of the gp130 cytokines compared to PBS controls. Our findings highlight the cascade of signaling pathways activated by the GP130 cytokines *LIF*, *OSM*, *CNTF*, *CNTF:CNTF+sR* and the interconnectivity between the downstream signaling proteins in ER+ breast cancer cells (Figure 18A-F, 19A-D). We also analyzed the relative induction of downstream signaling pathways by one-way ANOVA with multiple comparisons, which yielded 13 protein targets (Figure 19D). OSM specifically activated major downstream mediators of the AKT, STAT, and ERK signaling pathways (Figure 20A-D), consistent with our findings in Figure 2, as well as mediators of the mTOR, HSP27, and Src signaling

## *MCF7*

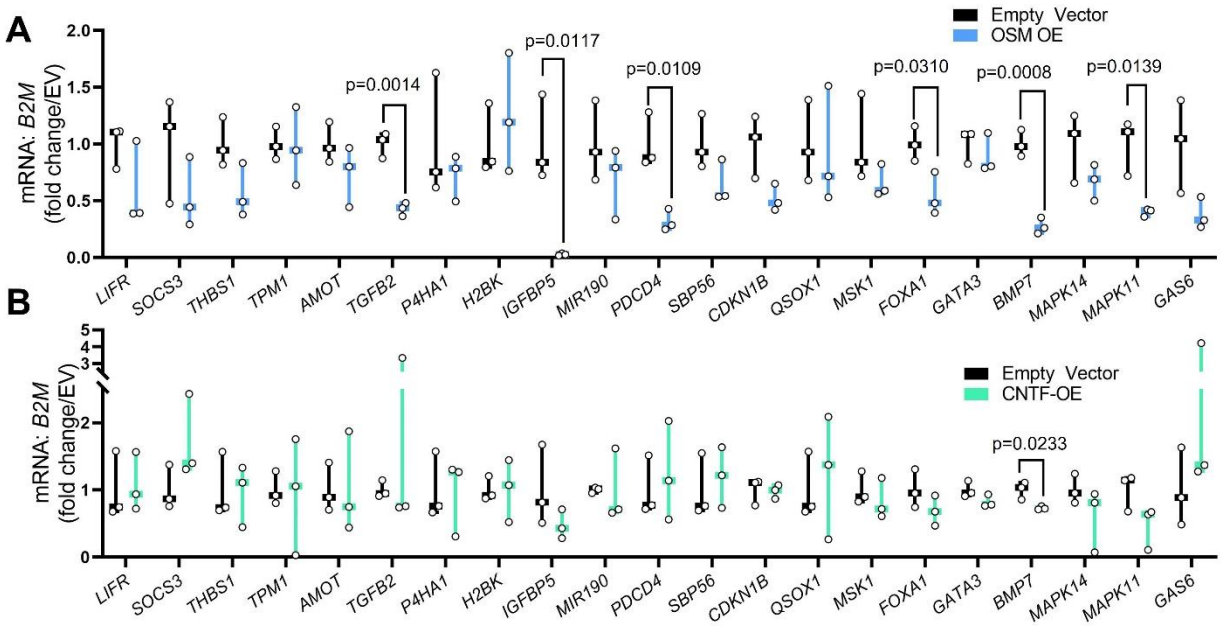


## *MDA-MB-231b*

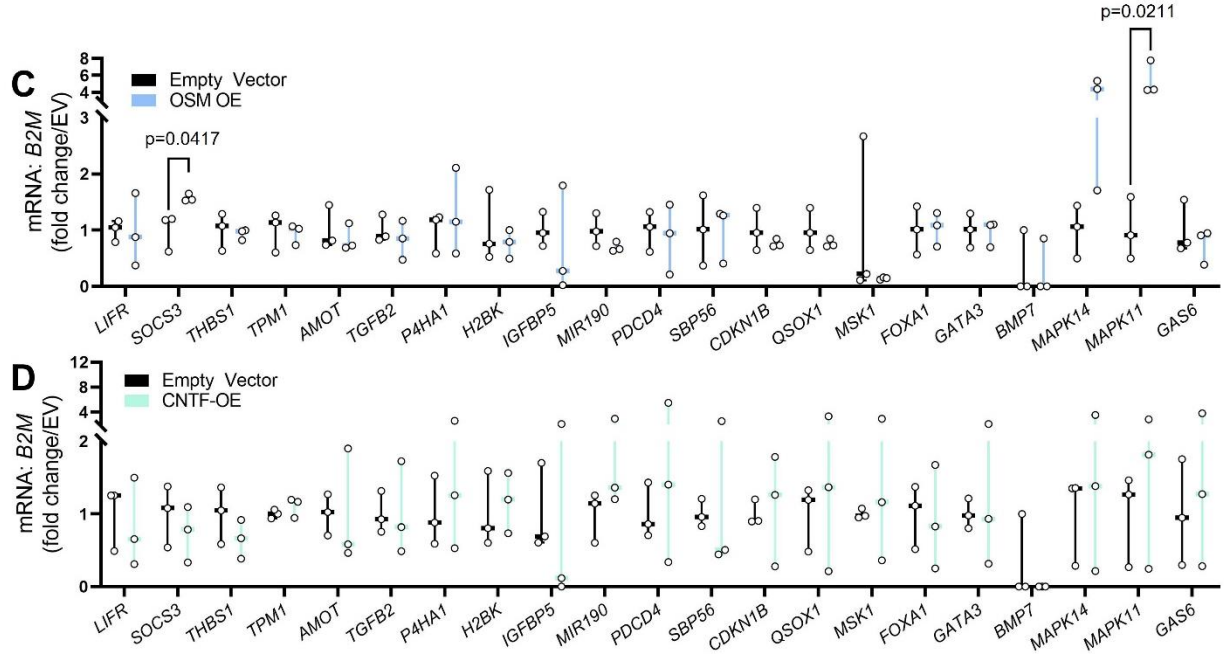

**Figure 16. Overexpression of OSM downregulates the expression of several dormancy genes in MCF7 but not MDA-MB-231 breast cancer cells.** (A, B) MCF7 cells with constitutive expression of OSM or CNTF were assessed for mRNA expression levels of genes associated with dormancy. (C, D) MDA-MB-231b cells with transient expression of OSM or CNTF were assessed for mRNA expression levels of genes associated with dormancy. n=3 independent biological replicates. A-H: Student's unpaired t-test. n=three independent biological replicates. Boxplots represent mean + interquartile range.

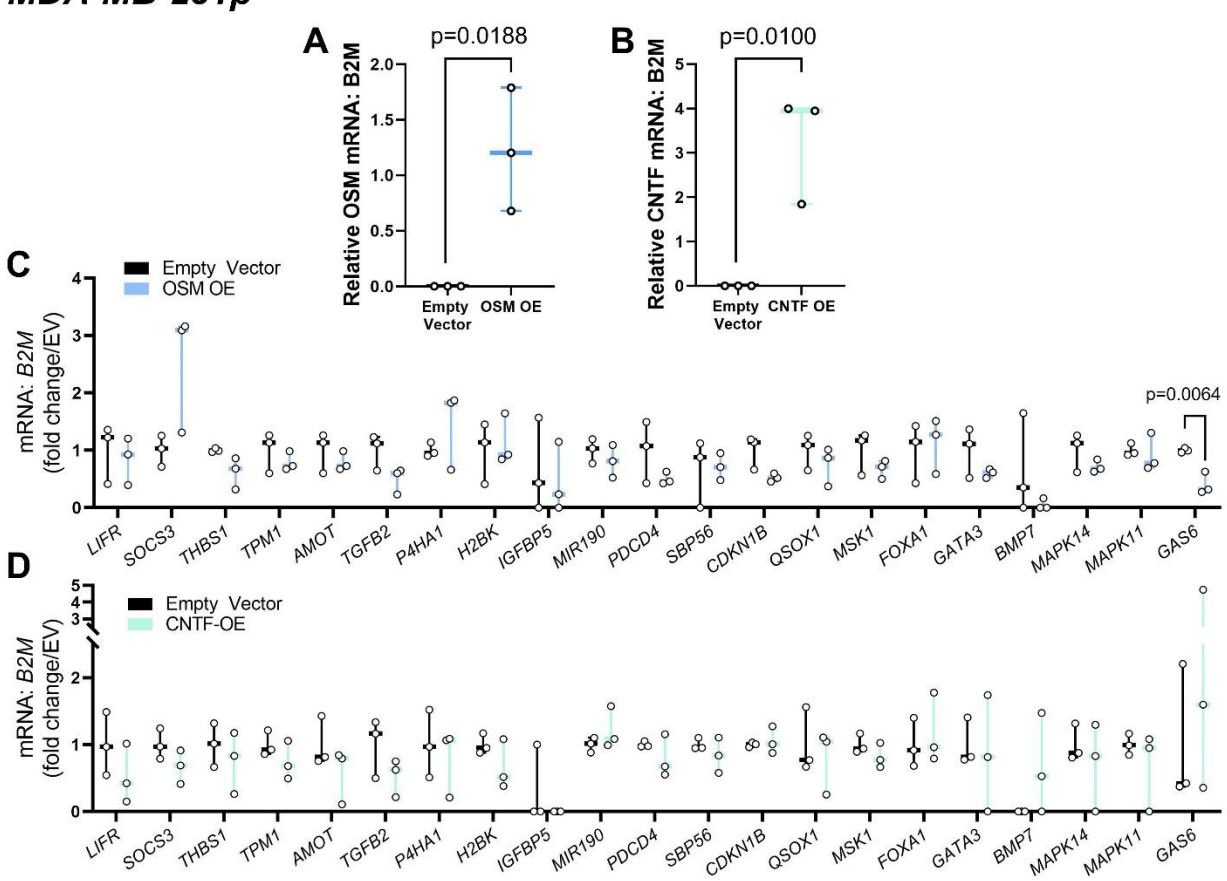


**Figure 17. OSM or CNTF overexpression in MDA-MB-231 parental breast cancer cells and STRING analysis in MCF7 cells.** (A-D) MDA-MB-231p cells with transient overexpression of OSM or CNTF confirmed by qPCR analysis (A, B) were assessed for mRNA expression levels of genes associated with dormancy (C, D). n=3 independent biological replicates. A-D: Student's unpaired t-test. n=three independent biological replicates. Boxplots represent mean + interquartile range.

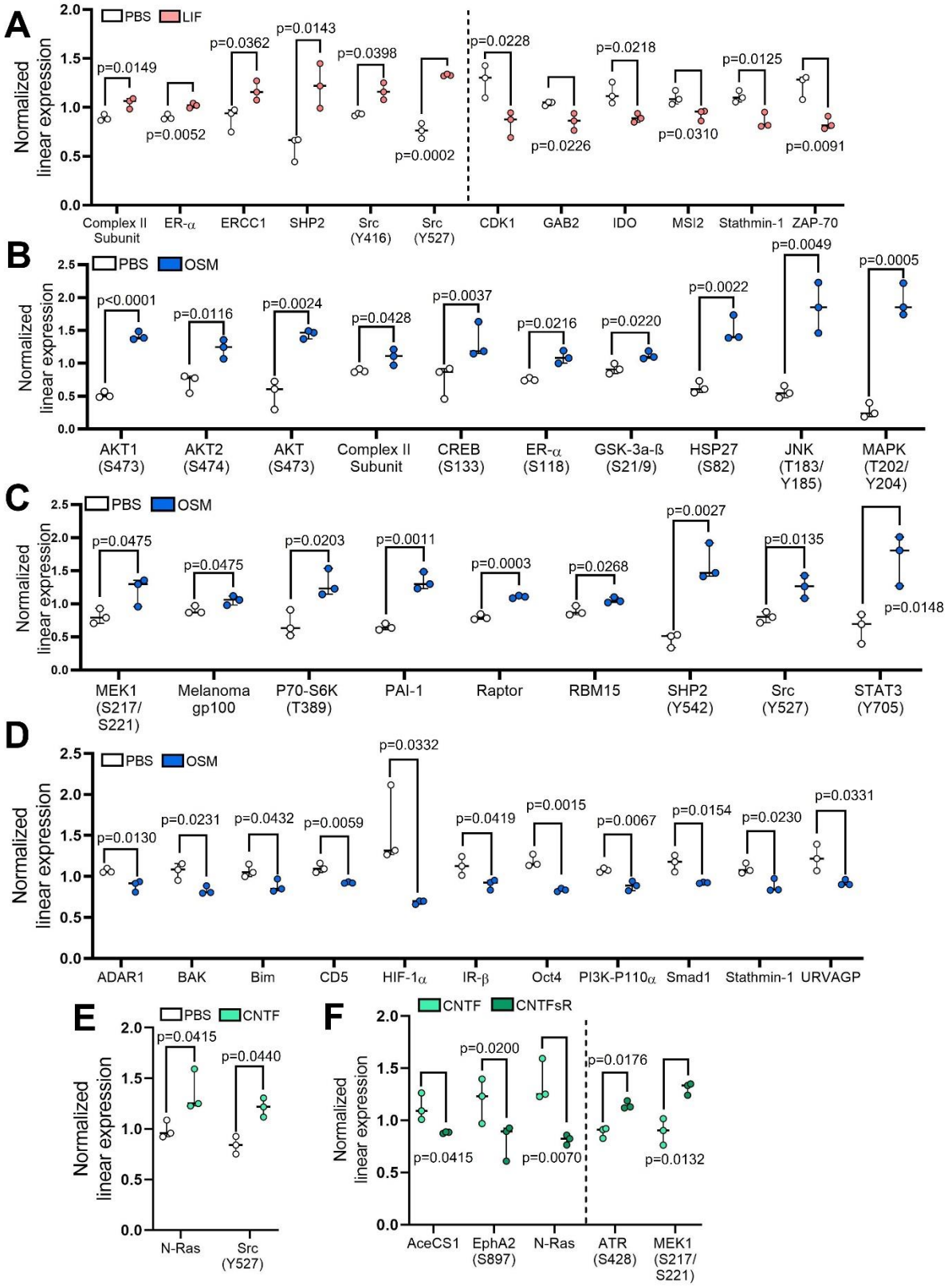
A
PBS
LIF
Normalized linear expression
p=0.0149
p=0.0052
p=0.0362
p=0.0143
p=0.0398
p=0.0002
p=0.0228
p=0.0226
p=0.0218
p=0.0310
p=0.0125
p=0.0091
Complex II Subunit
ER-α
ERCC1
SHP2
Src (Y416)
Src (Y527)
CDK1
GAB2
IDO
MSI2
Stathmin-1
ZAP-70
B
PBS
OSM
p<0.0001
p=0.0116
p=0.0024
p=0.0428
p=0.0037
p=0.0216
p=0.0220
p=0.0022
p=0.0049
p=0.0005
AKT1 (S473)
AKT2 (S474)
AKT (S473)
Complex II Subunit
CREB (S133)
ER-α (S118)
GSK-3a-ß (S21/9)
HSP27 (S82)
JNK (T183/ Y185)
MAPK (T202/ Y204)
C
PBS
OSM
p=0.0475
p=0.0475
p=0.0203
p=0.0011
p=0.0003
p=0.0268
p=0.0027
p=0.0135
p=0.0148
MEK1 (S217/ S221)
Melanoma gp100
P70-S6K (T389)
PAI-1
Raptor
RBM15
SHP2 (Y542)
Src (Y527)
STAT3 (Y705)
D
PBS
OSM
p=0.0130
p=0.0231
p=0.0432
p=0.0059
p=0.0332
p=0.0419
p=0.0015
p=0.0067
p=0.0154
p=0.0230
p=0.0331
ADAR1
BAK
Bim
CD5
HIF-1α
IR-β
Oct4
PI3K-P110α
Smad1
Stathmin-1
URVAGP
E
PBS
CNTF
p=0.0415
p=0.0440
N-Ras
Src (Y527)
F
CNTF
CNTFsR
p=0.0415
p=0.0200
p=0.0070
p=0.0176
p=0.0132
AceCS1
EphA2 (S897)
N-Ras
ATR (S428)
MEK1 (S217/ S221)

**Figure 18. The gp130 cytokines activate multiple signaling pathways in breast cancer cells.** (A-E) Proteins significantly altered by the gp130 cytokine family evaluated by RPPA in MCF7 cells treated for 30 minutes with PBS, recombinant LIF, recombinant OSM, recombinant CNTF at 50 ng $mL^{-1}$ and a 1:10 ratio of CNTF and its soluble receptor CNTF (50:500 µg $mL^{-1}$). Normalized linear protein expression of the significantly regulated proteins by (A) *LIF*, (B,C,D) *OSM*, (E) *CNTF*, and (F) *CNTFsR* treatment. One-way ANOVA with Sidak's multiple comparisons test. n=three independent biological replicates. Boxplots represent mean + interquartile range.

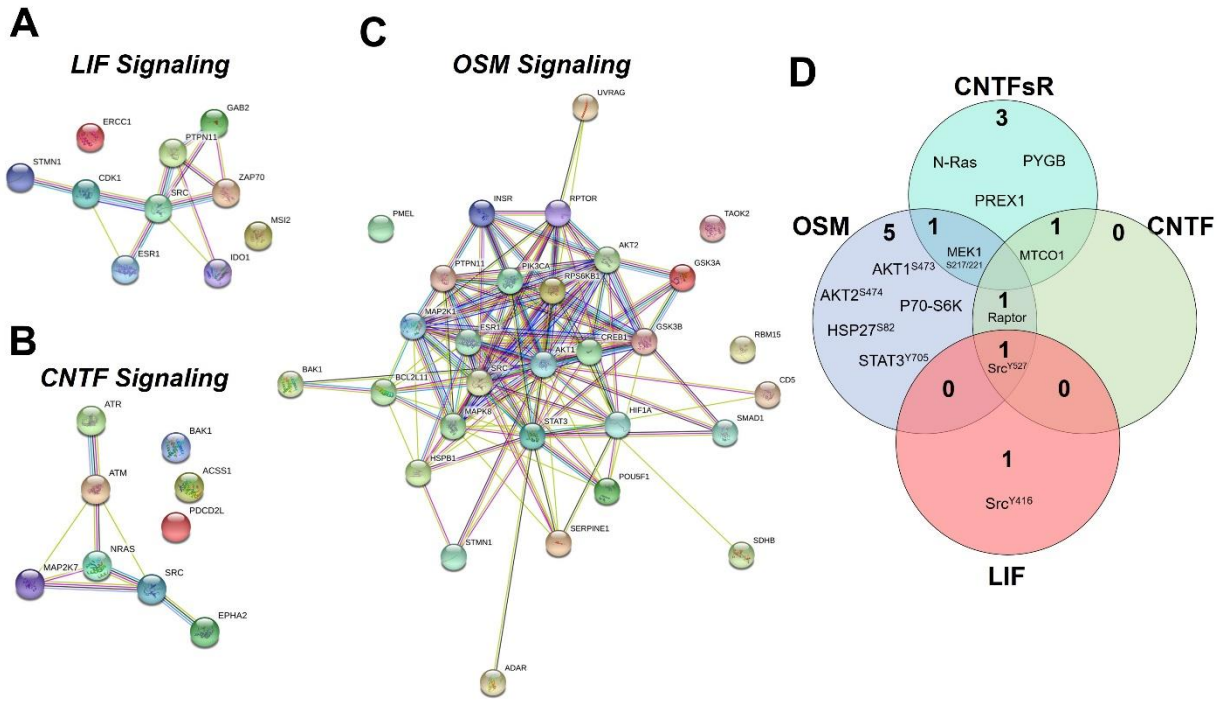


**Figure 19. STRING analysis in MCF7 cells stimulated by the gp130 cytokines.** (E-G) STRING (functional protein association interaction network maps) analysis of proteins significantly regulated by (E) LIF, (F) CNTF, (G) OSM evaluated by RPPA in MCF7 cells treated for 30 minutes with PBS, recombinant LIF, recombinant OSM, recombinant CNTF at 50 ng $mL^{-1}$ and a 1:10 ratio of CNTF and its soluble receptor CNTF (50:500 µg $mL^{-1}$). (H) Venn-diagram representing the number of proteins significantly regulated by one or more cytokines in the gp130 cytokine family.

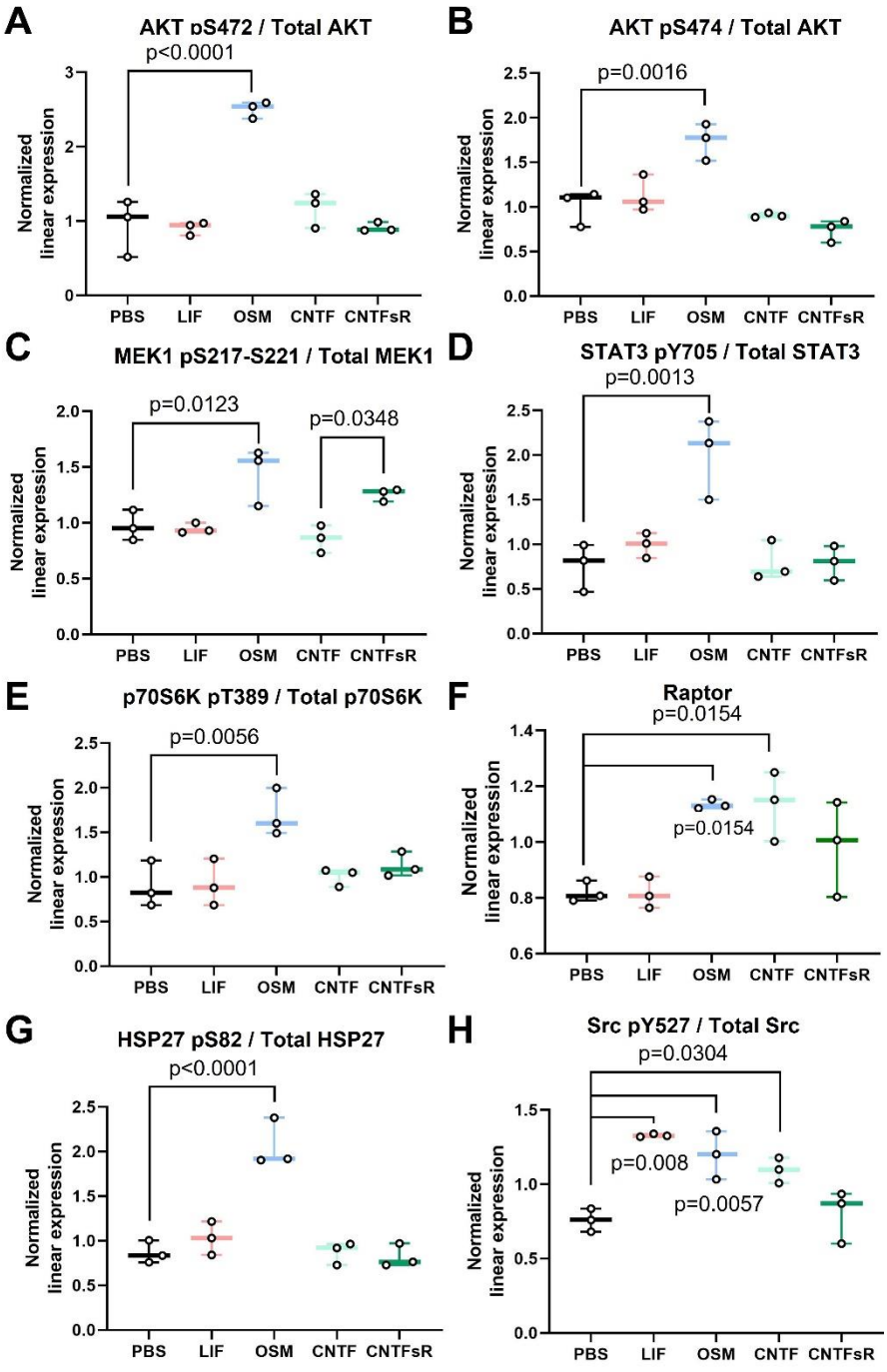


.

**Figure 20. OSM activates several downstream signaling pathways in breast cancer cells.** (A-H) Normalized linear protein expression of the significantly regulated proteins in MCF7 cells by OSM. (A) AKT (p<0.0001), (B) AKT2 (p=0.0016), (C) MEK1 (p=0.0123), (D) STAT3 (p=0.0013), (E) p70-S6K (p=0.0056), (F) Raptor (p=0.0154), (G) HSP27 (p<0.0001), and (H) Src (p=0.0057) were all significantly upregulated by OSM treatment. One-way ANOVA with Sidak's multiple comparisons test. n=three independent biological replicates. Boxplots represent mean + interquartile range.

pathways (Figure 20E-H). LIF also stimulated the Src signaling pathway (Figure 20H, 21A), while CNTF activated mTOR (Figure 20F), Src (Figure 20H) and MTCO1 (Figure 21B) downstream signaling. Interestingly, there were several pathways that were negatively regulated by the addition of sCNTFR, including MTCO1, NRAS, PREX1, and PYGB (Figure 21B-E). Of note, Src signaling was activated by all three cytokines both in the one-way ANOVA and by the individual cytokine analysis, suggesting this is a key signaling pathway activated downstream of gp130 in breast cancer. We therefore examined Src expression and several downstream signaling targets in the GSE14548 (Figure 22) and GSE29044 (Figure 23) datasets. Not all targets were available for both datasets; however, in both datasets, *c-SRC* and *KRAS* were significantly increased in invasive tumors. p190RhoGAP and NRAS were also significantly increased in the GSE14548 dataset. Interestingly, p38α (*MAPK14*) was significantly elevated in both datasets in the invasive tumors, and STAT3 was increased in GSE14548, both pro-dormancy factors [287, 307] that are downstream of Src signaling [323-326].

***Expression of the gp130 cytokines and receptors is associated with increased survival in breast cancer patients.*** Lastly, we examined whether the expression of these cytokines and receptors were associated with clinical outcomes in breast cancer patients. Kaplan Meier (KM) Plotter analysis revealed that relapse-free survival (RFS) was significantly reduced in all breast cancer patients with lower expression levels of the gp130 ligands or receptors, including OSM and OSMR, (Figure 24; $p<0.0001$), regardless of whether patients had ER+ or ER- tumors (Figure 25; $p<0.0001$). Analysis from two additional independent datasets (GSE14548 and GSE29044 [285]) demonstrated that *LIFR* mRNA expression, but not *LIF*, was significantly reduced in patients with both non-invasive ductal carcinoma *in situ* (DCIS) and invasive ductal carcinoma (IDC) (Figure 26A-B, 27A-B; $p<0.0001 – 0.0085$). OSMR expression was unchanged in DCIS and IDC patient samples in the GSE29044 dataset (Figure 26C), but OSM was increased in the GSE29044 dataset (Figure 26D), and OSM and OSMR were significantly increased in DCIS and invasive carcinoma in the GSE14548 dataset Figure 27C, D; $p=0.0006 – 0.0216$). gp130 expression was also reduced in patients with

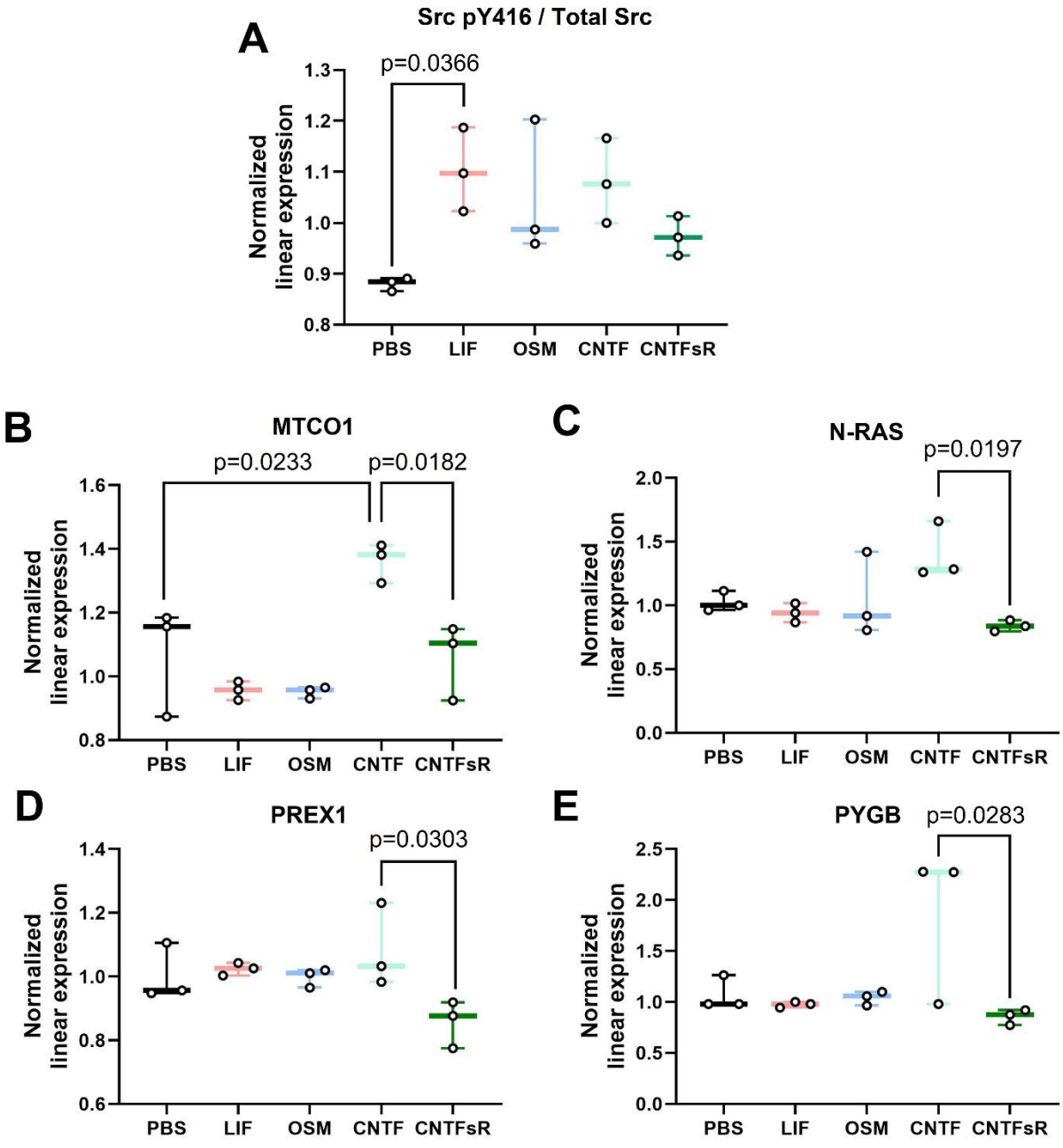


**Figure 21. LIF activates Src$^{Y416}$ and novel CNTF/CNTFsR signaling activates several previously unknown downstream effectors in breast cancer cells.** (A-E) Normalized linear protein expression of the significantly regulated proteins in MCF7 cells by LIF and CNTF/CNTFsR. (A) Src$^{Y416}$ (p=0.0366) was the only protein upregulated by LIF alone. (B) MTCO1 (p=0.0233), (C) N-Ras (p=0.0197), (D) PREX1 (p=0.0303), and (E) PYGB (p=0.0283) were significantly downregulated by CNTFsR signaling. One-way ANOVA with Sidak's multiple comparisons test. n=three independent biological replicates. Boxplots represent mean + interquartile range.

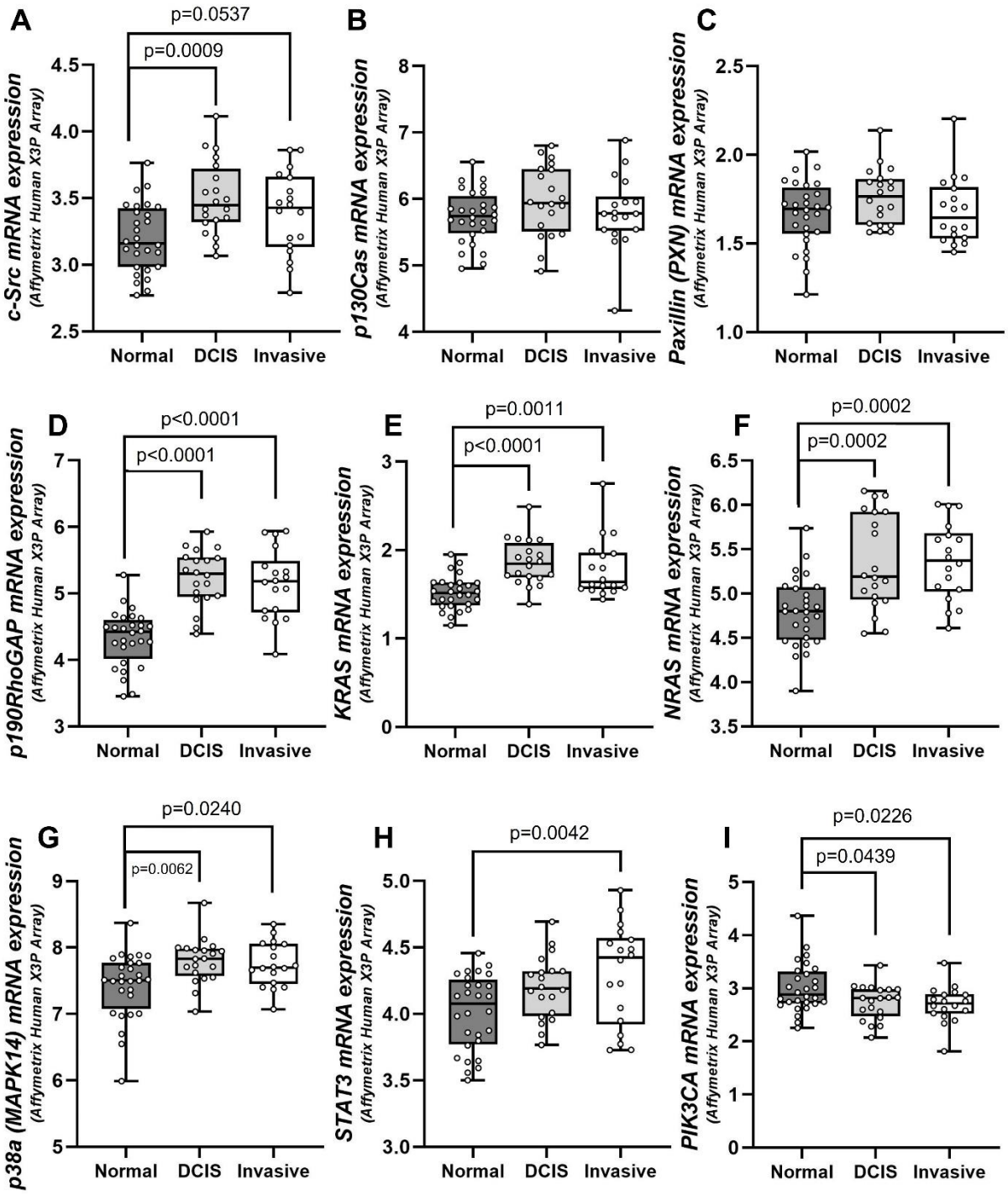


**Figure 22. GSE14548: mRNA expression of Src downstream effectors.** (A-I) c-Src, p130Cas, Paxillin, p190Rho GAP, KRAS, NRAS, MAPK14 (p38α), STAT3 and PIK3CA mRNA expression in normal, ductal carcinoma in situ (DCIS) and invasive ductal carcinoma (IDC) patient samples from GSE14548. A-I: One-way ANOVA with Sidak's multiple comparisons test. GSE14548: n= (Normal: 28, DCIS: 20, Invasive: 18). Boxplots represent mean and interquartile range + min/max.

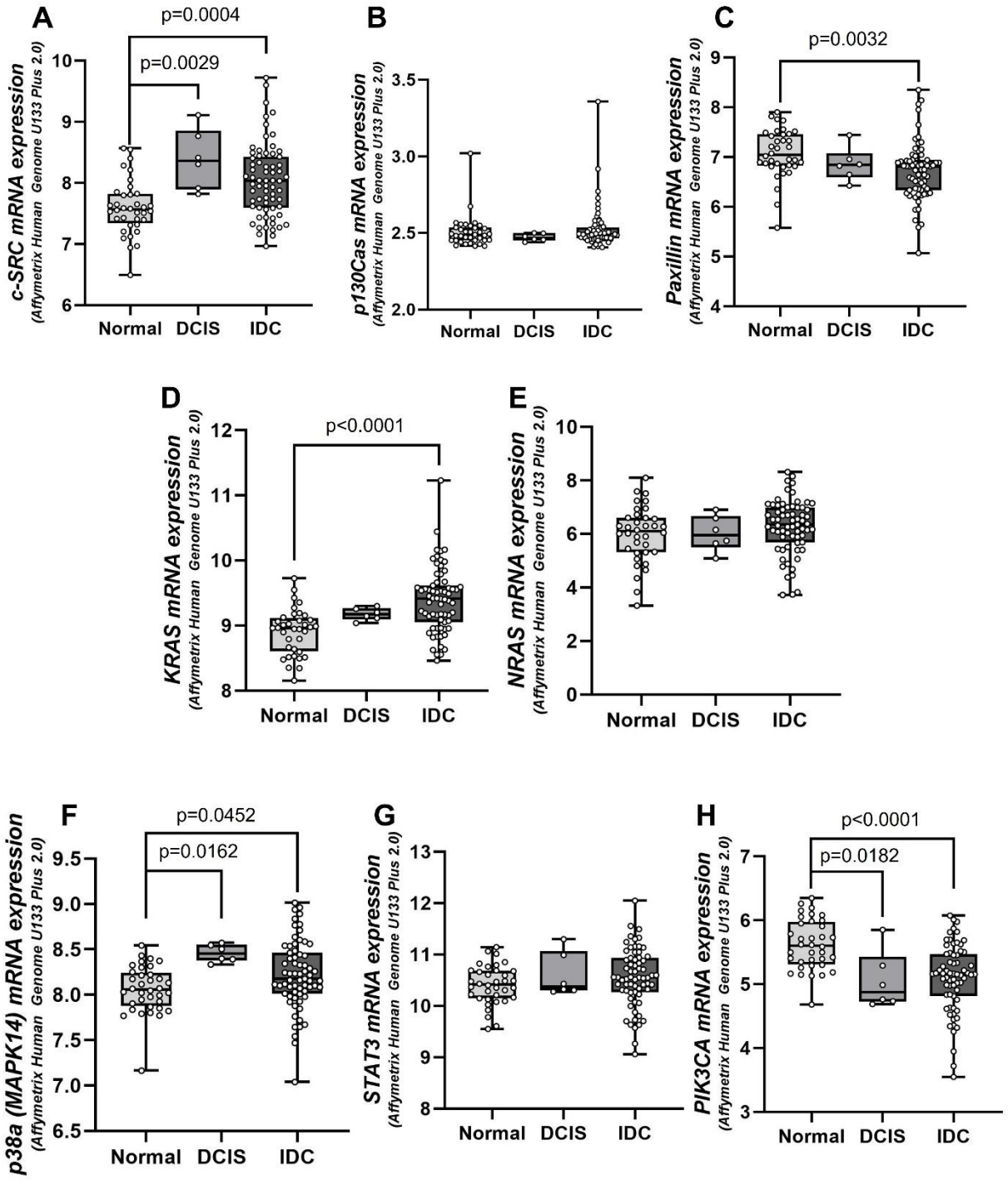


**Figure 23. GSE29044: mRNA expression of Src downstream effectors.** (A-I) c-Src, p130Cas, Paxillin, KRAS, NRAS, MAPK14 (p38α), STAT3 and PIK3CA mRNA expression in normal, ductal carcinoma in situ (DCIS) and invasive ductal carcinoma (IDC) patient samples from GSE29044. A-I: One-way ANOVA with Sidak's multiple comparisons test. GSE29044: n= (Normal: 36, DCIS: 6, IDC: 67). Boxplots represent mean and interquartile range + min/max.

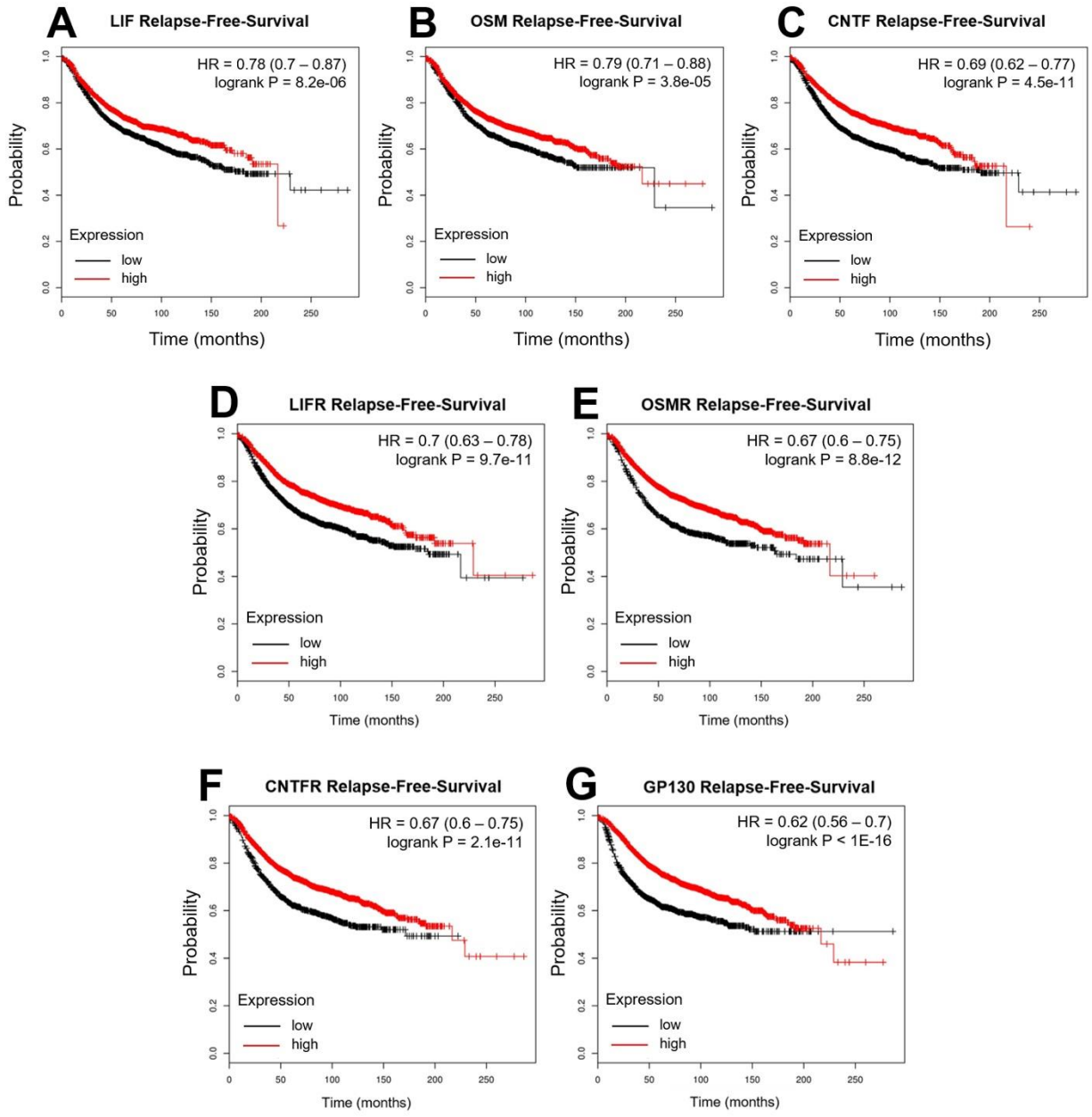


**Figure 24. Down-regulation of the gp130 cytokines and receptors is associated with decreased RFS.** (A-G) Survival plots generated using mRNA microarray data from clinical datasets analyzed with the online tool KM-plotter to evaluated relapse-free survival (RFS) for (A) LIF, (B) OSM, (C) CNTF (D) LIFR, (E) OSMR, (F) CNTFR, and (G) GP130. n=4929 patients.

## *ER+ Tumors*

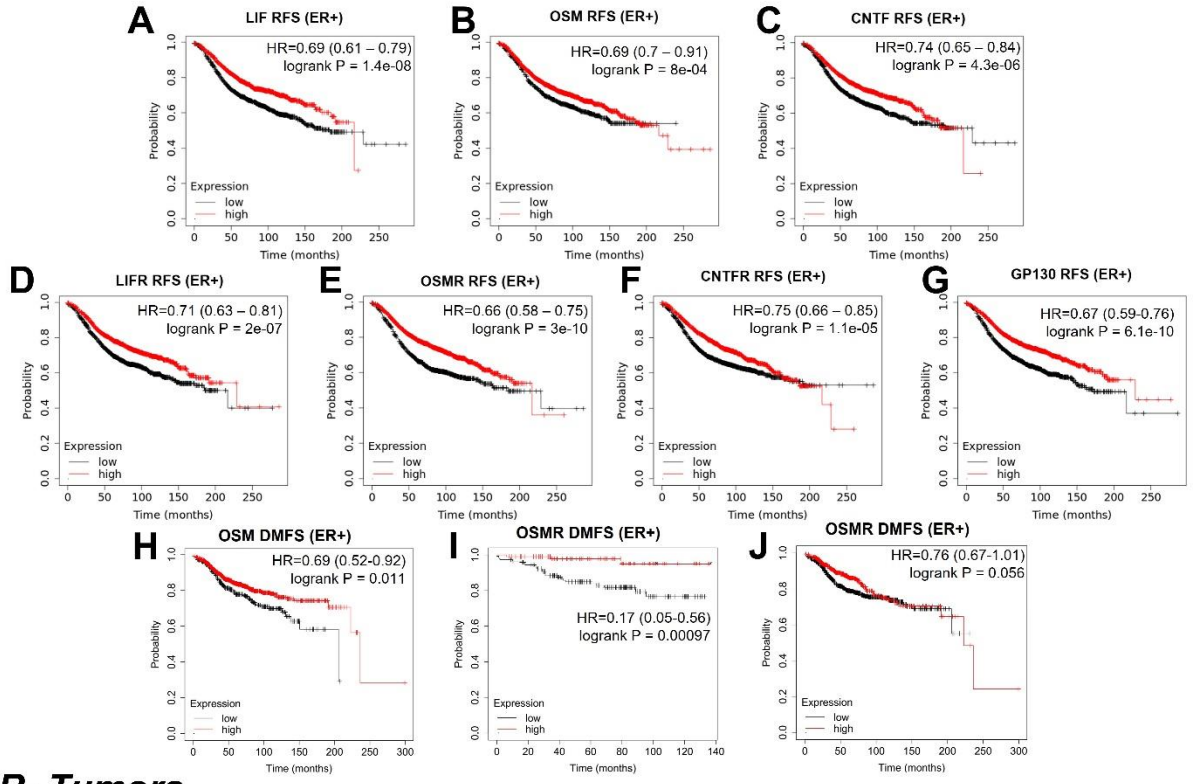


## *ER- Tumors*

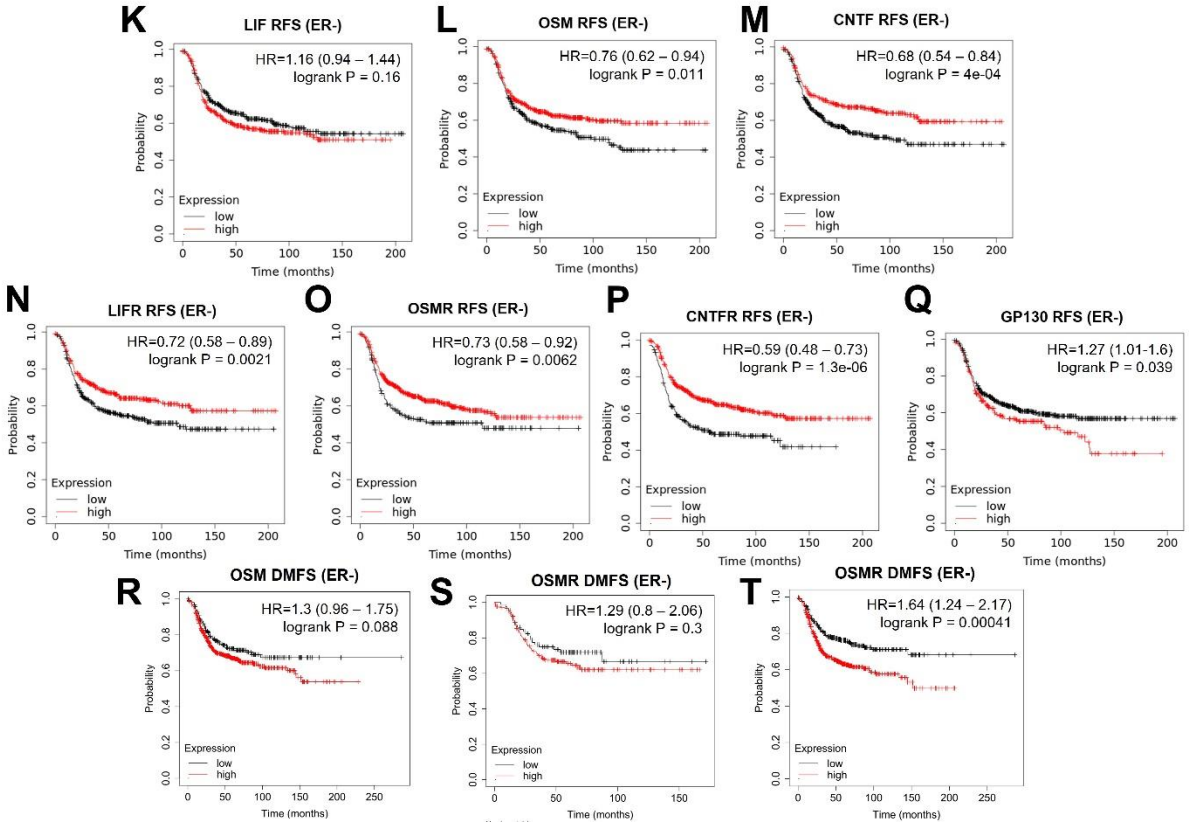

**Figure 25. Survival plots for the gp130 cytokines and receptors stratified by ER status.** (A-J) Survival plots generated using mRNA microarray data from clinical datasets analyzed with the online tool KM-plotter to evaluate RFS and distant metastasis-free survival in patients with ER+ tumors. RFS was evaluated for (A) LIF, (B) OSM, (C) CNTF (D) LIFR, (E) OSMR, (F) CNTFR, and (G) GP130 in patients with ER+ tumors. (H-J) Survival plots generated using KM-plotter to evaluate DMFS for (H) OSM, (I, J) OSMR in patients with ER+ tumors. (K-T) Survival plots generated using the online tool KM-plotter to evaluate RFS and DMFS in patients with ER- tumors. RFS was evaluated for (K) LIF, (L) OSM, (M) CNTF (N) LIFR, (O) OSMR, (P) CNTFR, and (Q) GP130. (R-T) Survival plots were generated using KM-plotter to evaluate DMFS for (R) OSM, (S, T) OSMR in patients with ER- tumors. n=3768 ER+ and n=2009 ER- patients.

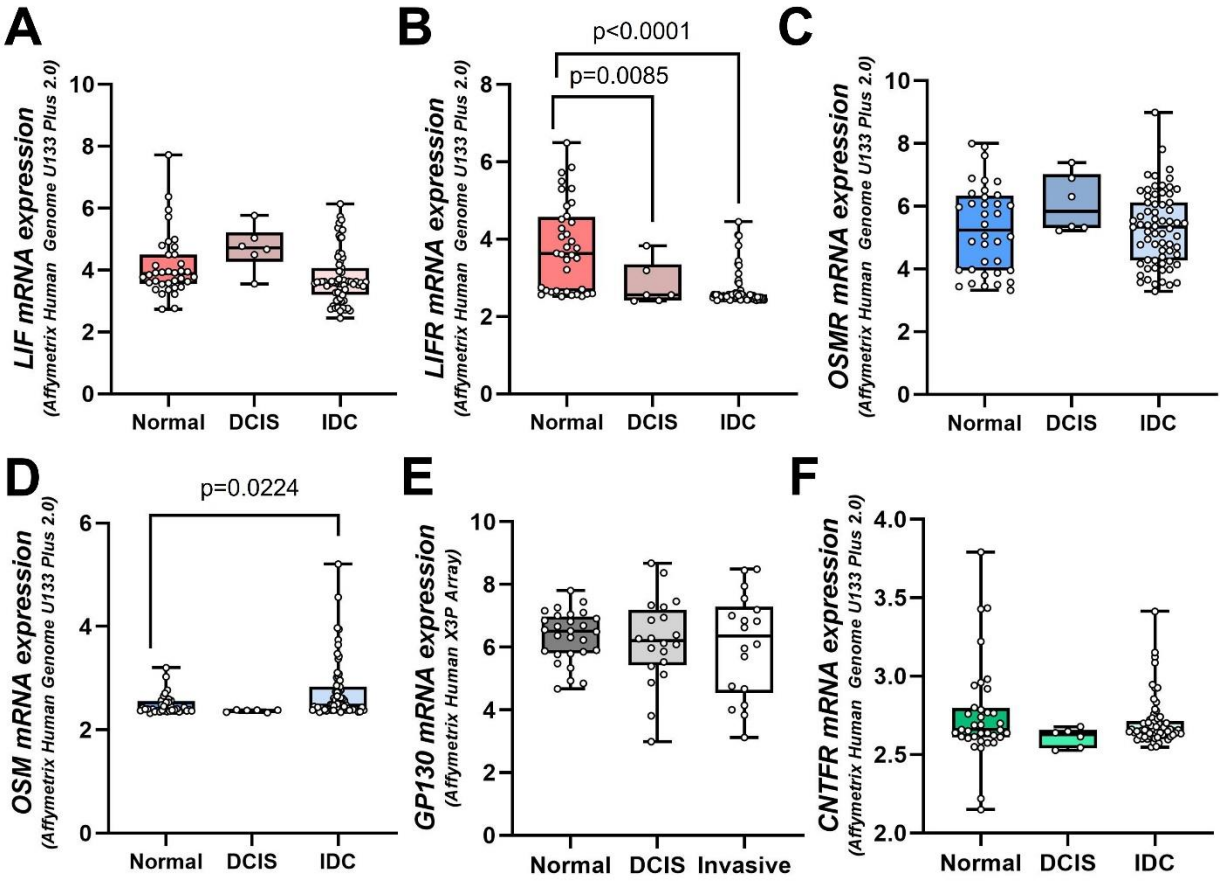


**Figure 26. gp130 cytokines and receptor mRNA expression levels in GSE29044 dataset.** (A-F) *LIF*, *LIFR*, *OSMR*, *OSM*, *GP130*, and *CNTFR* mRNA expression in normal, ductal carcinoma in situ (DCIS) and invasive ductal carcinoma (IDC) patient samples from GSE29044 One-way ANOVA with Sidak's multiple comparisons test. GSE29044: n= (Normal: 36, DCIS: 6, IDC: 67). Boxplots represent mean and interquartile range + min/max.

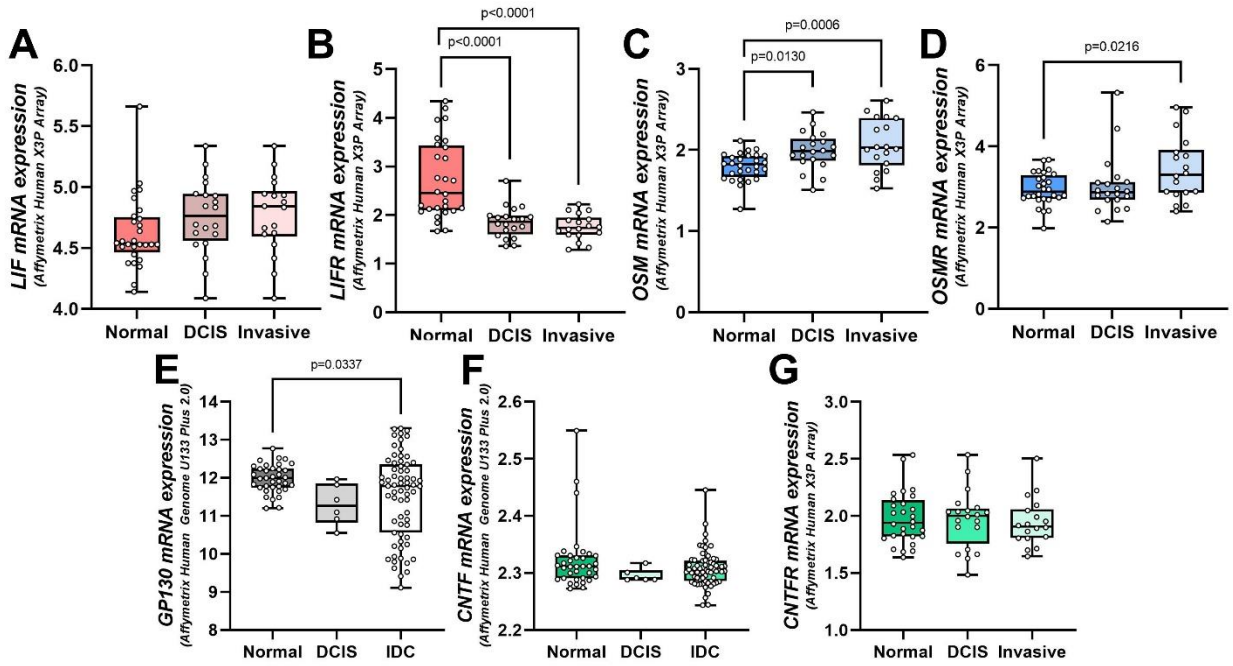


**Figure 27. Differential expression of the gp130 cytokines and receptors in clinical patient data sets.** (A-G) LIF, LIFR, OSM, OSMR, GP130, CNTF and CNTFR mRNA expression in normal, ductal carcinoma in situ (DCIS) and invasive ductal carcinoma (IDC) patient samples from GSE14548 (A, B, C, D, F, G) and GSE29044 (E). A-G: One-way ANOVA with Sidak's multiple comparisons test. GSE14548: n= (Normal: 28, DCIS: 20, Invasive: 18). GSE29044: n= (Normal: 36, DCIS: 6, IDC: 67). n=three independent biological replicates. Boxplots represent mean + interquartile range.

IDC (Figure 27E; p=0.0337) from the GSE29044 data set, but not in the GSE14548 dataset (Figure 26E). CNTF and CNTFR levels were unchanged with breast cancer stage (Figure 27F-G, 26F); CNTF was not included in the GSE29044 dataset.

**Discussion**

This study explores and characterizes the function of the gp130 cytokines in several breast cancer cell lines and patient datasets by highlighting the relative expression of the ligands and cytokine specific receptors, identifying novel signaling pathways activated by the cytokine family, and assessing the *in vivo* outcomes of breast cancer bone colonization. We utilized a panel of breast cancer cell lines with varying molecular characteristics to assess the expression of the gp130 cytokines across multiple subtypes, including highly metastatic cell lines (e.g. MDA-MB-231, 4T1) and cell lines that are considered dormant (e.g. MCF7, D2.0R), given the lack of growth and colonization of distant metastatic sites following inoculation [287, 307, 314, 327]. Our data indicate that all of the cytokines and receptors that are required for autocrine or paracrine OSM, LIF, and CNTF signaling are present in all breast cancer subtypes at the transcript level; however, we can conclude that expression of the receptors (LIFR, OSMR, CNTFR, and gp130) is considerably lower in ER- compared to ER+ disease, suggesting that loss of the gp130-related receptors (not just LIFR, as we previously reported), may be associated with more aggressive disease. These data are consistent with our previously published work demonstrating that LIFR signaling is lower across cells with high metastatic potential [287], which tend to be ER-.

OSM has been shown to induce metastatic characteristics of ER+ breast cancer cells [239], and is associated with EMT and the detachment of tumor cells [328]. In 4T1 triple negative breast cancer (TNBC) cells, (which lack ER, progesterone receptor/PR, and HER2), OSM knockdown reduces osteolytic bone destruction and spontaneous metastasis to the spine [241]. Our study suggests that OSM also promotes dissemination of ER- cells to the bone, but loss of OSM signaling may increase proliferation of bone-disseminated tumor cells, as evidenced by lower DMFS and the lower expression of OSM we observed in the bone metastatic clones of both TNBC breast cancer cell lines. While the mechanism by which OSM downregulation promotes tumor outgrowth remains unknown, OSM increased SOCS3 and p38 signaling specifically in the bone-metastatic

MDA-MB-231 cells, suggesting loss of these signaling pathways as potential mechanisms to explore. Our data also suggests there may be an inverse correlation between OSM expression in the primary tumor and bone metastases in patients with TNBC.

In ER+ breast cancer, our data indicate a pattern similar to ER- breast cancer: OSM drives bone dissemination, but loss of OSM promotes tumor outgrowth in the bone. However, our data indicate that OSM may be downregulated more frequently in ER- compared to ER+ breast cancer. Thus, while OSM drives dissemination to bone and reduces pro-dormancy genes in ER+ breast cancer, our data indicate that ER+ breast cancer cells frequently retain OSM expression and remain dormant in the bone.

The question therefore remains how OSM and LIFR signal together to regulate tumor progression and dormancy. OSM is a ligand for the LIFR, which acts as a tumor suppressor [49, 221] and pro-dormancy factor in bone [287], and OSM appears to be the most potent signal transducer of all the gp130 cytokines in breast cancer cells. However, OSM promotes bone dissemination and activates multiple pro-tumorigenic signaling pathways. How, then, does LIFR suppress tumor progression and emergence from dormancy with OSM inducing these pro-tumorigenic signaling pathways? The clinical data suggest that OSM expression is beneficial for long-term patient outcomes. Of note, OSM robustly induces ERK, AKT, and STAT3 signaling, and STAT3 is a part of an ER+ dormancy signature [307] and promotes dormancy of ER+ breast cancer cells in the bone [287]. Thus, OSM induction of STAT3 may be the dominant signaling pathway in ER+ tumor cells once they have disseminated to bone. In the primary tumor, as in our model reported here, the balance may be tipped toward ERK and AKT or the other pro-tumorigenic pathways we identified, with suppression of pro-dormancy genes helping to fuel tumor proliferation. It also cannot be ruled out that our *in vivo* findings may be impacted by the immunodeficient mouse model or estradiol treatment that is required for ER+ xenograft models. Follow-up studies in syngeneic models will shed light on this, but it is important to note that our studies are consistent with previous findings that OSM promotes bone colonization in a syngeneic immunocompetent mouse model [241].

Our findings demonstrate that LIF, OSM, and CNTF all robustly phosphorylate Src (Y527), but the significance of this is unclear given that the three cytokines do not appear to have the same effect on tumor dissemination to bone (OSM promotes, CNTF has no

effect, and LIF is unknown). Despite being in a ‘closed’ confirmation [329-331], $Src^{Y527}$ overexpression in MDA-MB-231 breast cancer cells results in increased bone and lung dissemination, and osteolytic bone destruction [332]. In patient studies, high $Src^{Y527}$ expression is significantly associated with metastatic disease, poor progression-free survival, and significantly worse bone metastasis-free survival [333, 334]. This suggests that OSM in particular may promote metastasis through activation of a $Src^{Y527}$ signaling axis; however, given that the pro-dormancy factor p38α and STAT3 expression were elevated in invasive disease alongside Src signaling factors, further studies will be necessary to determine the role for Src signaling downstream of the gp130 cytokines in breast cancer progression and metastasis.

While there are multiple reports of OSM promoting tumor proliferation and bone metastasis [239-242, 328], there is relatively little known about the role for OSMR in bone metastasis. OSM can form a complex with either LIFR/gp130 or OSMR/gp130 [319], and therefore the effects of OSM and activation of downstream signaling pathways such as STAT3, ERK, AKT, and Src signaling in breast cancer cells may be mediated through either LIFR or OSMR, but previous studies have not determined which receptor is responsible. Our data from shLIFR knockdown cells suggest that OSM may activate STAT3 and AKT signaling through the OSMR, but activates ERK signaling through both the LIFR and OSMR; however, LIFR knockdown was incomplete in our model and OSM may therefore continue to signal through residual LIFR. Indeed, LIF modestly induced STAT3 signaling in shLIFR cells, and although this did not reach statistical significance, it suggests some active, residual LIFR persists. Future studies examining the role for OSMR in tumor progression and whether it is required for OSM induction of downstream signaling will be of interest.

CNTF has been widely studied for its role in the nervous system and neurite outgrowth [335] and effects on bone formation [171, 172]. The data presented here is the first to report the effects of CNTF on breast cancer signaling and tumor progression and suggest that CNTF may prevent tumor progression and bone metastasis in patients with ER- but not ER+ disease. However, we cannot rule out potential effects of CNTF on later stages of metastatic progression in ER+ disease, such as regulation of bone colonization by disseminated tumor cells. Since CNTF preferentially activates STAT3 over AKT or

ERK signaling in ER+ cells, and we previously reported that STAT3 induces dormancy in the bone [287], this suggests that CNTF may be the most likely of the three cytokines to induce dormancy. This may also point to a potential role for CNTF/CNTFR in preventing colonization of bone in more aggressive or later stages of bone metastatic disease.

In conclusion, the gp130 cytokines play a nuanced role in tumor progression and bone dissemination and activate multiple signaling pathways in breast cancer cells. Our findings also suggest a potential stimulatory role for OSM in ER+ breast cancer bone dissemination and a potential inhibitory effect of CNTF on bone metastasis in ER- breast cancer and emergence from dormancy in ER+ breast cancer (Figure 28). Continued study of these signaling pathways in breast cancer may uncover novel ways to prevent tumor progression and the formation of bone metastases.

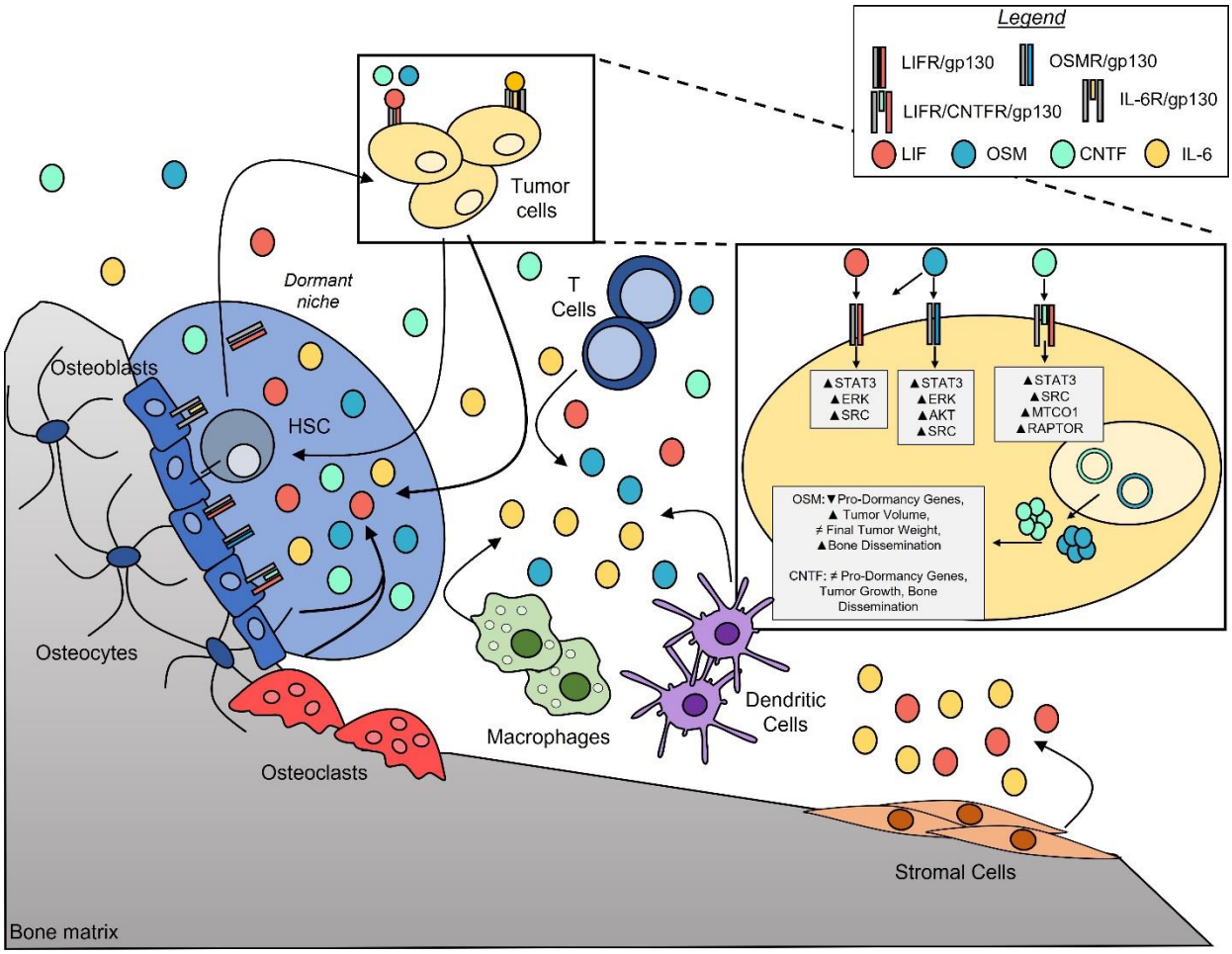


**Figure 28. Mechanistic overview of gp130 cytokines.** Tumor cells that metastasize and colonize the bone marrow, invade and establish within the endosteal niche resulting in increased interaction with dormant hematopoietic stem cells (HSCs). Our group and other propose that these tumor cells outcompete HSCs for important self-renewal and dormancy-related factors pertinent for HSC maintenance and survival. In conjunction, gp130 cytokines are expressed and produced by hemotopoietic lineage cells, osteoblast lineage cells, and stromal cells, suggesting that tumor cells encounter the cytokines via paracrine cytokine signaling. These signals then activate STAT3, ERK, AKT, and Src signaling, among other cytokine-specific pathways, to regulate tumor progression and bone dissemination.

# CHAPTER IV

# OSM INCREASES CD44 EXPRESSION BUT DOES NOT ALTER THE CANCER STEM CELL POPULATION IN ER+ BREAST CANCER


## Summary

Cancer stem cells (CSCs) are a population of tumor cells that undergo self-renewal and differentiation. Previous studies suggest that CSCs drive the progression, metastasis, and recurrence of cancer. Oncostatin M (OSM), a member of the of the interleukin-6 (IL-6) / glycoprotein130 (gp130) cytokine family, has been reported to function as a pro-stemness factor by maintaining pluripotency and the self-renewal of mouse embryonic stem cells. Previous studies demonstrate that overexpression of OSM increases bone tumor burden in estrogen receptor (ER) positive (ER+) disease; however, the mechanism of enhanced bone tumor burden has not been fully elucidated. We therefore sought to determine whether OSM induces cancer stemness as a potential mechanism for its role in promoting dissemination. In ER+ breast cancer cells, OSM stimulation resulted in a moderate increase in CD44 expression, but no significant expansion of $CD44^{High}/CD24^{Low}$ expressing cells. Consistent with recombinant OSM stimulation, OSM overexpression did not promote the expansion of CSCs, but significantly down-regulated several CSC-associated genes. Together these data indicate that expression and signal activation by OSM does not lead to an expansion of typical CSC markers.


## Introduction

Despite advancements in the diagnosis, detection, removal, and treatment of breast cancer, it remains the second deadliest cancer among women [1]. Metastatic relapse often occurs within months, years, or decades marked by the absence of clinical symptoms. Breast cancer cells commonly metastasize to the bone, where they may induce osteolysis, leading to increased fracture risk [303, 305, 306]. However, bone-disseminated breast cancer cells may also enter a period of quiescence prior to inducing bone destruction [136, 306, 336]. Different subtypes of breast cancer exhibit distinct

metastatic characteristics, but patients with estrogen receptor positive (ER+) disease, which accounts for over 70% of breast cancer diagnoses, frequently experience extended periods of tumor dormancy before skeletal recurrence [7, 9].

Recent studies suggest that dormant disseminated tumor cells survive in the foreign microenvironment of the metastatic site through the adoption of a cancer stem cell (CSC) phenotype [112, 257, 337-340]. CSCs are a population of cells capable of tumorigenesis [258, 259, 261, 341] and self-renewal [258], leading to cancer progression and metastasis [338, 342-346]. Previous work has demonstrated that CSCs not only drive metastasis but contribute to chemoresistance [30-33, 346-348]. Multiple cytokines have been shown to alter CSC properties in breast cancer. Of these cytokines, several groups have demonstrated that oncostatin M (OSM) and leukemia inhibitory factor (LIF), both members of the interleukin-6 (IL-6) / glycoprotein130 (gp130) cytokine family, can function as pro-stemness factors by maintaining pluripotency in mouse embryonic stem cells [274, 275, 277, 281, 349]. Other studies have demonstrated that additional gp130 cytokines, including ciliary neurotrophic factor (CNTF) [280] and cardiotrophin-1 (CT-1) [282], facilitate self-renewal and promote stem-ness by activating pluripotency-associated genes through STAT3 [274, 276, 278, 279, 311].

We previously demonstrated that OSM promotes bone dissemination and induces a multitude of signaling cascades in ER+ breast cancer cells [350], and others have demonstrated that OSM overexpression promotes bone colonization by ER negative (ER-) breast cancer cells. STAT3 signaling is one of the many signaling pathways induced by OSM in breast cancer cells and is known to induce pluripotency of mouse embryonic stem cells [281, 349]. Long-term stimulation by OSM on human mammary epithelial cells (HMECs) increases expression of CSC-associated genes and promotes stem cell plasticity [255]. Thus, a long-standing question in the field is whether OSM may similarly up-regulate stemness markers in breast cancer cells.

Since OSM expression increases ER+ breast cancer cell dissemination to the bone, this study aimed to evaluate whether OSM expression expands the CSC population *in vitro* in ER+ breast cancer cells.

## Results

**ER+ breast cancer cell lines have low CSC population frequency.** Previous studies have indicated that breast cancer cells with $CD44^{High}/CD24^{Low}$ expression have high tumorigenic properties and can give rise to tumors [258]. We therefore examined the baseline levels of $CD44^{High}/CD24^{Low}$ cells in human unstimulated ER+ (MCF7 and T47D) and ER- (SUM159 and MDA-MB-231) breast cancer cell lines to determine which cell lines would be appropriate for evaluating potential OSM-induced increases in CSC properties. To examine whether OSM and other gp130 cytokines induce a CSC phenotype, we preferred a cell line that intrinsically had a low CSC population. The ER+ MCF7 and T47D cell lines had low baseline levels of $CD44^{High}/CD24^{Low}$ cells (<10%), while the ER- SUM159 and MDA-MB-231 parental and bone metastatic cell lines had high baseline levels of $CD44H^{igh}/CD24^{Low}$ cells (>90%; Figure 29A-E). When we directly compared the percent parent population of ER+ compared to the ER- breast cancer cell lines, the ER+ cell lines had significantly lower baseline levels of $CD44^{High}/CD24^{Low}$ cells ($p<0.0001$, Figure 29F). We therefore utilized the MCF7 cells for subsequent studies since they had low baseline expression of this population (5-10%), but high enough population levels to detect potential OSM-induced decreases. T47D breast cancer cells were used as an additional validation, but baseline expression of $CD44^{High}/CD24^{Low}$ cells was so low (<1%) it would not be possible to detect a decrease in this population.

**Paracrine OSM does not increase the percentage of $CD44^{High}/CD24^{Low}$ cells in ER+ breast cancer cells.** Since several members of the gp130 cytokines have been reported to function as pro-stemness factors by maintaining pluripotency and the self-renewal of mESCs [275, 276, 280-282, 311], we next examined whether these cytokines increase the number of CSCs in ER+ breast cancer cells. MCF7 and T47D cells were treated for 24 hours with recombinant LIF, OSM, CNTF, or CNTF with its soluble receptor (CNTF+sR), which facilitates CNTF signaling in osteoblasts [172, 175] and can result in differential downstream pathway activation from CNTF alone in breast cancer cells [350]. Flow cytometric analysis revealed no significant difference in the number of $CD44^{High}/CD24^{Low}$ cells following cytokine stimulation with LIF, OSM, CNTF, or CNTF+sR in either MCF7 (Figure 30A-F) or T47D cells (Figure 31A-F). However, OSM treatment

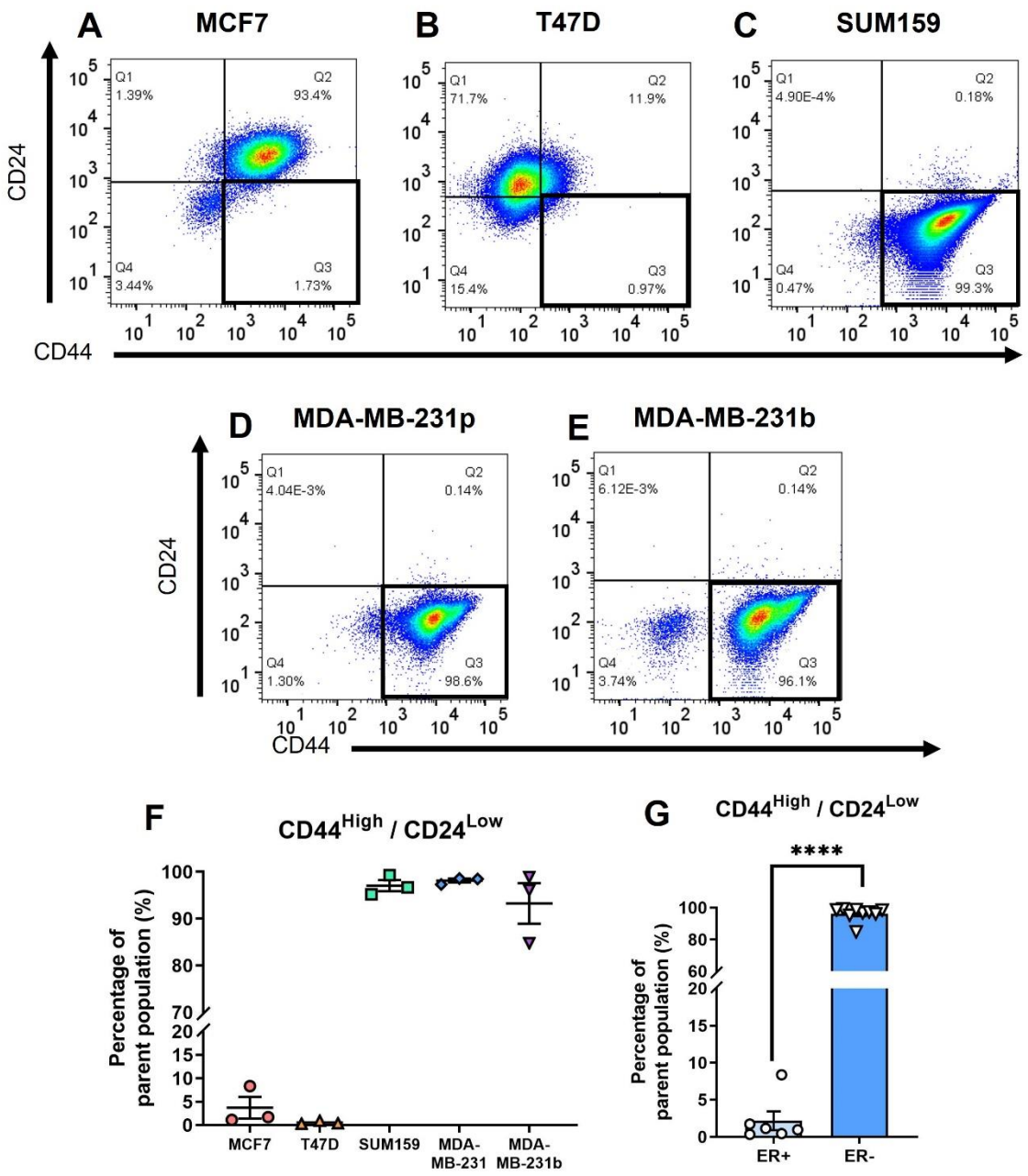


**Figure 29. Cell surface markers CD44/CD24 expression on a panel of human breast cancer cell lines.** (A-D) Representative plots from flow cytometry analysis of CD44/CD24 cell surface markers on (A) MCF7, (B) T47D, (C) SUM159, (D) MDA-MB-231p, and (E) MDA-MB-231b. Gating was set to unstained, CD44 positive cells, and CD24 positive control cells. (F) The percentage of $CD44^{High}/CD24^{Low}$ cells from the parent population of each cell line. (G) Comparative percentage of $CD44^{High}/CD24^{Low}$ cells from ER+ (MCF7, T47D) and ER- (SUM159, MDA-MB-231p/b) breast cancer cell lines. n=three independent biological replicates. Graph represent mean per group and error bars represent SEM, ****p<0.0001.

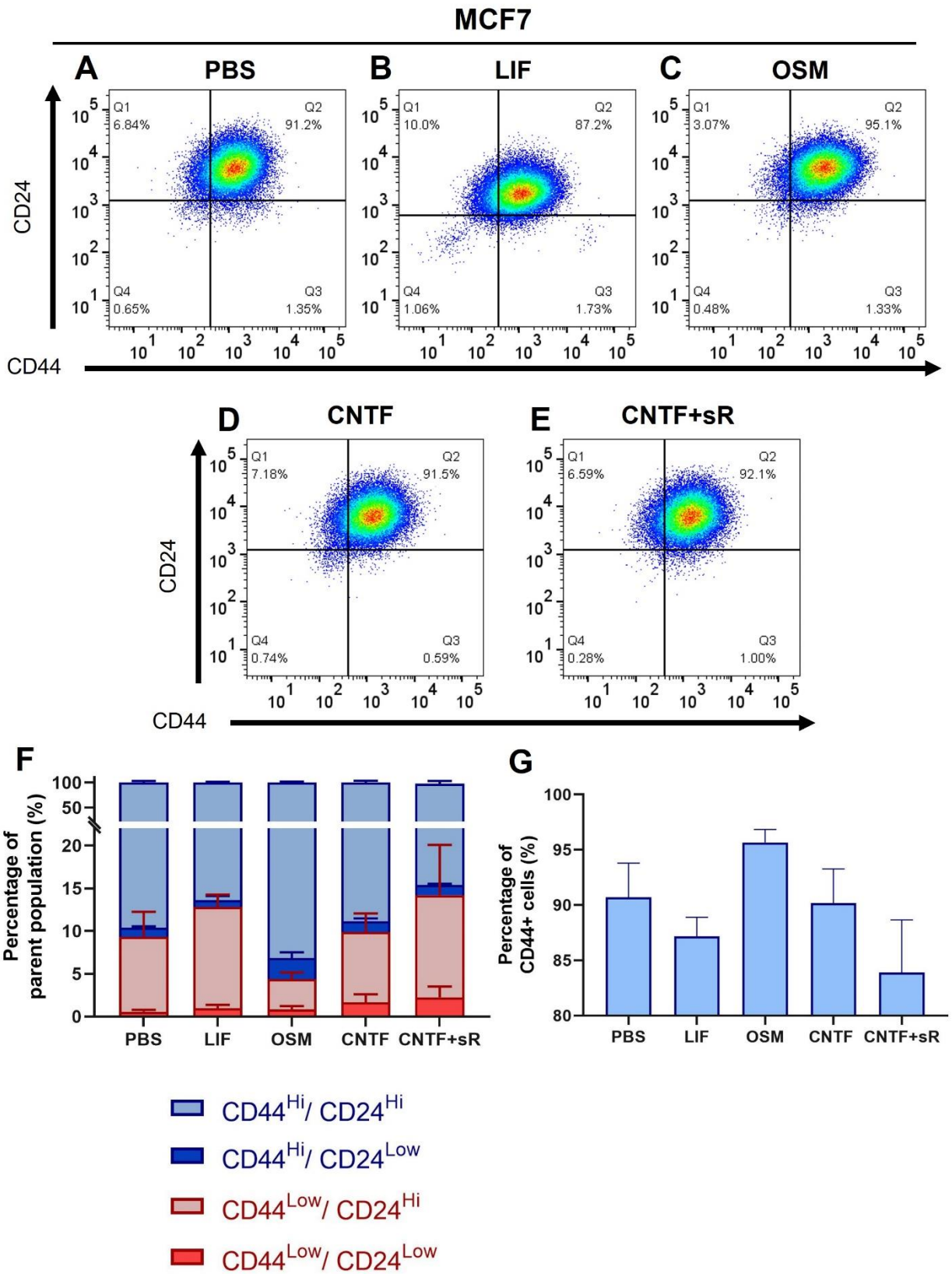
MCF7
A
PBS
Q1 6.84%
Q2 91.2%
Q4 0.65%
Q3 1.35%
B
LIF
Q1 10.0%
Q2 87.2%
Q4 1.06%
Q3 1.73%
C
OSM
Q1 3.07%
Q2 95.1%
Q4 0.48%
Q3 1.33%
CD24
CD44
D
CNTF
Q1 7.18%
Q2 91.5%
Q4 0.74%
Q3 0.59%
E
CNTF+sR
Q1 6.59%
Q2 92.1%
Q4 0.28%
Q3 1.00%
F
Percentage of parent population (%)
PBS
LIF
OSM
CNTF
CNTF+sR
G
Percentage of CD44+ cells (%)
CD44Hi/ CD24Hi
CD44Hi/ CD24Low
CD44Low/ CD24Hi
CD44Low/ CD24Low

**Figure 30. Changes in CD44 and CD24 expression in MFC7s treated with recombinant gp130 cytokines.** (A-E) Representative plots from flow cytometry analysis of CD44/CD24 cell surface markers on (A) PBS, (B) LIF, (C) OSM, (D) CNTF, and (E) CNTF+sR. Gating was set to unstained, CD44 positive cells, and CD24 positive control cells. (F) Comparative analysis of CD44 and CD24 expression from each distinct expression profile. Light Blue = $CD44^{High}/CD24^{High}$, Dark Blue = $CD44^{High}/CD24^{Low}$, Light Red = $CD44^{Low}/CD24^{High}$, Red = $CD44^{Low}/CD24^{Low}$. (G) The percentage of CD44 positive (+) cells from each treatment group. n=three independent biological replicates. Graph represent mean per group and error bars represent SEM.

Figure 3

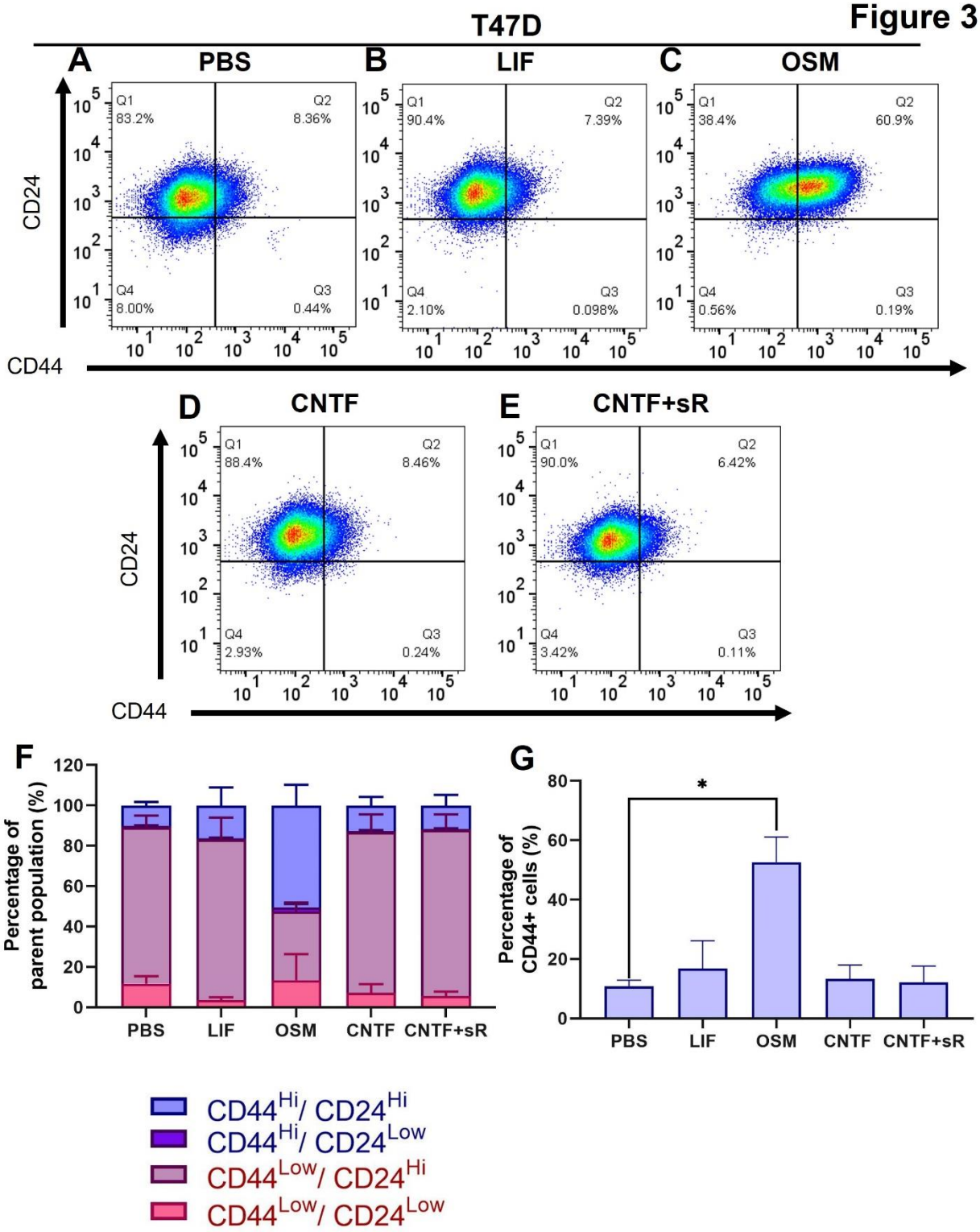
T47D
A
PBS
Q1 83.2%
Q2 8.36%
Q4 8.00%
Q3 0.44%
B
LIF
Q1 90.4%
Q2 7.39%
Q4 2.10%
Q3 0.098%
C
OSM
Q1 38.4%
Q2 60.9%
Q4 0.56%
Q3 0.19%
CD24
CD44
D
CNTF
Q1 88.4%
Q2 8.46%
Q4 2.93%
Q3 0.24%
E
CNTF+sR
Q1 90.0%
Q2 6.42%
Q4 3.42%
Q3 0.11%
CD24
CD44
F
Percentage of parent population (%)
PBS
LIF
OSM
CNTF
CNTF+sR
G
Percentage of CD44+ cells (%)
*
PBS
LIF
OSM
CNTF
CNTF+sR
CD44Hi/ CD24Hi
CD44Hi/ CD24Low
CD44Low/ CD24Hi
CD44Low/ CD24Low

**Figure 31. Changes in CD44 and CD24 expression in T47Ds treated with recombinant gp130 cytokines.** (A-E) Representative plots from flow cytometry analysis of CD44/CD24 cell surface markers on (A) PBS, (B) LIF, (C) OSM, (D) CNTF, and (E) CNTF+sR. Gating was set to unstained, CD44 positive cells, and CD24 positive control cells. (F) Comparative analysis of CD44 and CD24 expression from each distinct expression profile. Light Purple = $CD44^{High}/CD24^{High}$, Dark Purple = $CD44^{High}/CD24^{Low}$, Light Magenta = $CD44^{Low}/CD24^{High}$, Magenta= $CD44^{Low}/CD24^{Low}$. (G) The percentage of CD44 positive (+) cells from each treatment group. n=three independent biological replicates. Graph represent mean per group and error bars represent SEM, *$p<0.05$.

resulted in a modest increase (5% average) in the number of $CD44^+$ cells compared to PBS control in MCF7 cells (Figure 30G) and a significant increase (40%, $p<0.0183$) in CD44+ cells in T47D breast cancer cells (Figure 31G). These data indicate that while paracrine OSM may increase CD44 expression on ER+ breast cancer cells, it does not increase the percentage of $CD44^{High}/CD24^{Low}$ ER+ breast cancer cells.

**Autocrine OSM does not increase the percentage of $CD44^{High}/CD24^{Low}$ cells in ER+ breast cancer cells.** We previously reported that OSM overexpression in MCF7 cells promotes spontaneous dissemination of MCF7 cells to the bone marrow [350]. Utilizing the MCF7s with constitutive OSM expression [350], we analyzed the expression of CD44 and CD24 using flow cytometry to determine whether autocrine OSM signaling increases the $CD44^{High}/CD24^{Low}$ cell population. OSM overexpression increased the number of $CD44^{High}/CD24^{Low}$ cells, but the difference was not statistically significant (Figure 32A; 97% increase). In contrast to recombinant OSM treatment, which increased CD44 expression, particularly in T47D cells, the overall percentage of $CD44^+$ cells were not significantly changed with OSM overexpression (11% increase, Figure 32B). Taken together these data suggest that in some cases OSM regulates CD44 expression, but OSM autocrine or paracrine actions do not result in a major shift in the CSC population frequency in ER+ breast cancer cells.

**OSM overexpression reduces CSC-associated genes.** We next determined whether OSM expression impacts the expression of CSC-associated genes. Overexpression of OSM in MCF7 cells significantly reduced the expression of 3/12 CSC-associated genes, including *NOTCH1*, *CASP3* and *OCT4* when compared to the empty vector control cell line (Figure 33; 38-57%, $p<0.05$). *SOX2*, *MDR1* and *ABCG2* were non-significantly increased with OSM overexpression, but overall, 7/12 CSC-associated genes were lower with OSM overexpression. Of note, neither of the CSC markers *ALDH1A1* nor CD133 (gene name *PROM1*) were significantly altered with OSM overexpression. These data suggest that OSM has no effect on, or negatively regulates, CSC-associated genes.

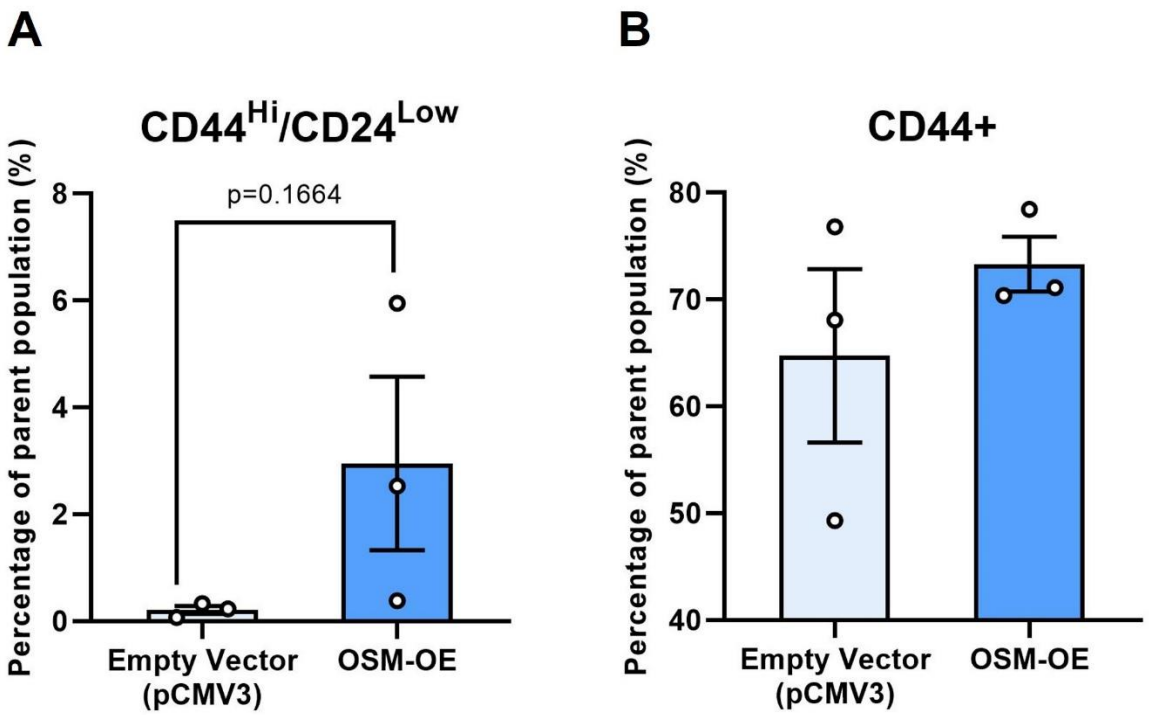


**Figure 32. Overexpression of OSM modestly increased the percentage of CD44$^{+}$ cells.** (A) MCF7 cells with constitutive expression of OSM were assessed for expression of cell surface markers CD44 and CD24. (A) *In vitro* analysis of the percentage of CD44$^{High}$/CD24$^{Low}$ cells from MCF7 empty vector control cells and OSM overexpressing cells. (B) The percentage of CD44 positive (+) cells from empty vector and OSM overexpressing cells. n=three independent biological replicates. Graph represent mean per group and error bars represent SEM.

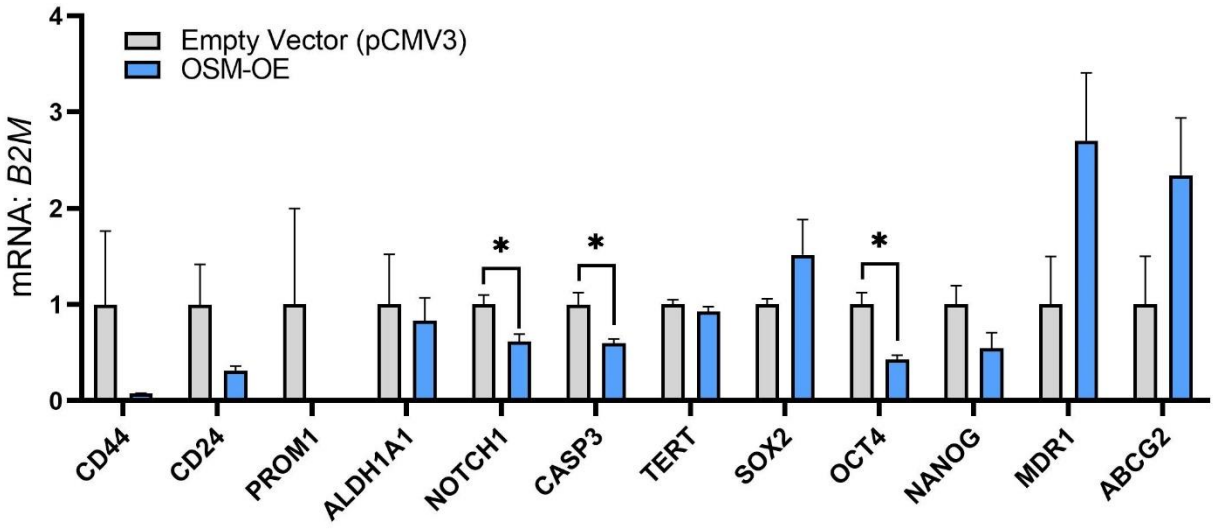


**Figure 33. Overexpression of OSM downregulates the expression of several CSC-associated genes in MCF7 breast cancer cells.** MCF7 cells with constitutive expression of OSM or CNTF were assessed for mRNA expression levels of genes associated with CSCs. n=3 independent biological replicates. A-H: Student's unpaired t-test. n=three independent biological replicates. Graph represent mean per group and error bars represent SEM, *p<0.05.

## Discussion

In breast cancer, early investigation into CSCs identified CD44 and CD24 expression as key cell surface markers to identify these tumorigenic cells, specifically $CD44^{High}/CD24^{Low}$ cells [258]. CD44 plays a prominent role in cell adhesion [351, 352], signaling, and migration [353-356] and has been implicated as a regulator of cancer progression [357, 358], angiogenesis [359, 360], invasion [351, 354, 359, 361, 362], and metastasis [351, 363-365]. Our data herein indicate that OSM increases CD44 expression since it was significantly elevated in T47D cells and modestly elevated in MCF7 cells, suggesting a potential mechanism by which OSM promotes ER+ breast cancer cell dissemination to bone [350]. This finding is consistent with previous studies demonstrating that OSM induces expression of CD44 [328, 366] and that long-term OSM stimulation results in human mammary epithelial cell (HMEC) adoption of a CSC phenotype [255]. Before HMECs adopt the $CD44^{High}/CD24^{Low}$ expression profile, the cells initially shift towards higher CD44 expression. Similar to the results in our study, cells within 2-3 days of prolonged cytokine stimulation moderately (5-15%) increased the percentage of $CD44^{High}$ cells [255] before eventually adopting the CSC expression profile. Interestingly, overexpression of OSM did not significantly increase CD44 expression, suggesting that paracrine, but not autocrine/intracrine, OSM signaling regulates CD44 expression. This may be of particular importance for bone-disseminated tumor cells, which are likely to encounter OSM, LIF, and CNTF that are produced in the bone microenvironment [162, 171, 172, 350]. However, there was high variability in the percentage of $CD44^{High}/CD24^{Low}$ cells in the OSM overexpressing cell line, which may have masked significant differences in the percentage of $CD44^{High}/CD24^{Low}$ cells between wildtype and OSM overexpressing breast cancer cells. It is therefore possible that autocrine/intracrine OSM signaling may still promote a shift toward $CD44^{High}/CD24^{Low}$ CSCs. The variability in these data further suggest that an additional factor beyond OSM alone may be required to “push” the cells from high CD44 expression to a true $CD44^{High}/CD24^{Low}$ CSC phenotype.

Together with CD44, CD24 expression has been extensively used as a breast CSC marker. Early studies demonstrated that as few as 100 $CD44^{High}/CD24^{Low}$ cells were able to form tumors in mice, and this population of cells possesses the ability to self-renew and differentiate [258, 364]. Previous work demonstrated that treatment with OSM past 3

days resulted in a significant shift towards the CSC population. In our study we determined the $CD44^{High}/CD24^{Low}$ CSC population frequency at an earlier time point (24 hours) which may explain why we did not see a shift in the $CD44^{High}/CD24^{Low}$ CSC population. Our data suggest that neither autocrine nor short-term paracrine OSM alters the $CD44^{High}/CD24^{Low}$ population in ER+ breast cancer cells; however, as noted above, we cannot definitively conclude that constitutive OSM expression, potentially in combination with some other unknown factor, does not promote the $CD44^{High}/CD24^{Low}$ CSC phenotype. Interestingly, our data suggest that OSM may promote dissemination and metastasis through elevated CD44 expression, but further studies are needed to elucidate whether OSM directly or indirectly acts through other factors to elicit changes in the $CD44^{High}/CD24^{Low}$ CSC population.

Other biomarkers like ALDH1 [364, 365, 367, 368] and CD133 [367, 369] also serve as markers for breast CSCs. ALDH1 expression is linked to drug resistance [370] and poor clinical outcomes in patients [371-373]. CD133 was identified in human breast cancer cell lines to promote higher proliferative rates [374, 375], increased colony formation [367, 374], and tumor initiation [376, 377] when isolated from triple negative breast cancer ($ALDH1^{+}/CD44^{+}/CD24^{-}$) and ER-/HER2+ tumors ($CD44^{+}/CD49^{+}$). In this study, we found that OSM overexpression did not alter *CD133* or *ALDH1A1* expression in ER+ breast cancer cells, but functional studies are necessary to determine OSM role in other CSC properties.

In conclusion, paracrine OSM stimulates CD44 expression, but the impact of paracrine or autocrine OSM on the $CD44^{High}/CD24^{Low}$ CSC population remains unclear. However, our data indicate that OSM reduces or has no effect on CSC-associated genes, including *CD133* and *ALDH1A1*. Taken together, these data indicate that the ability of OSM to promote dissemination of ER+ breast cancer cells to the bone [350], and to promote bone colonization [241], may be in part due to elevated CD44 expression, but additional studies are required to confirm this hypothesis. Continued study of OSM and its role in breast cancer pathogenesis may aid the discovery of new molecular mechanisms and therapeutic targets to prevent breast cancer metastasis.

# CHAPTER V

# CONCLUSIONS AND FUTURE DIRECTIONS

## Conclusions

The gp130 cytokine family regulates a plethora of biological processes across multiple organs and systems. Many of these processes impact bone remodeling, cancer progression, metastatic outgrowth, pluripotency, and stem-like properties. Out of the gp130 cytokine family, our data demonstrate that OSM is the strongest inducer of downstream signal activation in breast cancer cells and promotes the dissemination of ER+ breast tumor cells to the bone marrow. We also demonstrated for the first time that the gp130 cytokine CNTF activates downstream signaling pathways in ER+ breast cancer. Together these findings shed light on the role of these cytokines in tumor dormancy and breast cancer metastasis. As a result, the work presented in this dissertation has sought to elucidate the role of the gp130 cytokines in breast cancer pathogenesis, tumor dormancy and CSC properties.

LIFR is a breast cancer metastasis suppressor [49, 50, 201] and promotes tumor dormancy of MCF7 breast cancer cells in the bone [50]. Downregulation of LIFR results in increased osteolytic bone destruction and increased breast cancer dissemination to the bone. However, the signals that regulate dormancy downstream of LIFR are not well defined. Because LIFR is a member of a larger cytokine family [185], we thought that the dormancy-related actions of LIFR were mediate by the cytokines that form a complex with it. LIF, OSM and CNTF all require at least one subunit of LIFR [150, 185, 308, 335, 378] to activate downstream signaling. In addition, LIF, OSM, and CNTF are all produced and present in the bone microenvironment [142, 185, 379], making the bone marrow an ideal location for bone disseminated tumor cells to remain dormant if they express LIFR. However, our findings demonstrated some complexity with our initial hypothesis.

We were surprised to find that upregulation of OSM in ER+ breast cancer cells, resulted in an increase in bone disseminated tumor cells, with a moderate increase in overall tumor growth. However, our findings are consistent with previous work that demonstrated OSM induced metastatic characteristics [239-242] of ER+ breast cancer

including EMT [255, 328, 366]. Other groups have also shown that reduction in OSM expression reduced spontaneous metastasis to the spine and decreased osteolytic bone destruction follow intratibial inoculations [241]. Our findings also demonstrate that when compared to ER+ cell lines, ER- breast cancer cell lines significantly downregulate expression of the gp130 cytokine specific receptors (LIFR, OSMR, CNTFR). This suggests that loss of the gp130 cytokine specific receptors may be associated with more aggressive disease. However, this data coupled with our findings showing LIF, OSM and CNTF stimulation on ER+ breast cancer cells activate various pro-tumorigenic pathways but are also associated with better survival outcomes in ER+ breast cancer patients, demonstrates the complexity and paradoxical effects of the gp130 cytokines and receptors.

In order to determine the mechanism by which OSM promotes bone dissemination, we examined whether OSM signaling induced stemness. CSCs are well documented to increase metastatic potential and tumor-initiating properties in breast cancer [31, 32, 35, 257, 261, 338, 345, 364, 380]. OSM specifically did not promote the expansion of $CD44^{High}/CD24^{Low}$ cells, identified and accepted as CSCs [258]. However, OSM stimulation and constitutive expression elevated CD44 expression which is consistent with previous work [255]. It has been well documented that expression of CD44 is associated with cancer progression and upregulation of pro-angiogenic factors and enhances the efficiency of metastasis for breast cancer cells [345, 351, 354, 356, 357, 359, 360, 362, 363, 366], suggesting that OSM-induced CD44 expression may be a potential mechanism for the enhanced tumor dissemination to bone. Taken together, further work is needed to elucidate more functions of the gp130 cytokine family in breast cancer and tumor dormancy and the work presented here raises additional questions and avenues for further research.

Our work demonstrates that the gp130 cytokines activate a wide range of signaling pathways in ER+ breast cancer. We also found that OSM promotes bone dissemination, which is further supported by our data indicating that autocrine and paracrine OSM promotes expression of CD44 and activates several pro-tumorigenic pathways. Thus, our data collectively indicate that OSM promotes metastasis. Surprisingly, survival data demonstrates that patients with ER+ tumors and high OSM expression have increased

DMFS, however this is reversed in ER- tumors, where high OSM expression in patients with ER- tumors corresponds to worse DMFS. We propose that in ER+ tumors, OSM promotes dissemination to the bone marrow by activating CD44 and other pro-tumorigenic pathways in the primary tumor. However, once the tumor cells have disseminated to bone, we propose that high OSM promotes tumor dormancy in the bone marrow. We further postulate that this is due to OSM activation of STAT3 signaling, which we demonstrate is robustly activated by OSM in ER+ tumor cells. While STAT3 is typically thought of as a pro-tumorigenic pathway, STAT3 has been identified as a pro-dormancy factor for bone-disseminated ER+ tumor cells by multiple groups [50, 223]. In ER- tumors, we propose that high OSM expression promotes metastasis, similar to ER+ tumors, through activation of pro-tumorigenic signaling pathways, which is consistent with previously published work in the 4T1 mouse mammary carcinoma model [241, 242]. Once the tumor cells have disseminated to bone, it appears that OSM expression may further promote their progression, but the mechanism for this remains unclear. STAT3 is still activated by OSM in ER- breast cancer cells, but it is unclear whether STAT3 plays a similar pro-dormancy role for ER- breast cancer cells. Given that OSM regulates ER expression, it is plausible that there are significant differences in how OSM signals and regulates tumor cell behavior between ER+ and ER- breast cancer cells.

**Future Directions**

***What is the role for OSMR in tumor progression and dormancy?*** In the previous chapters we focused on effects of gp130 cytokine stimulation and the constitutive expression of OSM. We also examined whether OSM and LIF activate downstream signaling in breast cancer cells when LIFR is knocked down. Previous reports demonstrated that in highly metastatic breast cancer cell lines like the MDA-MB-231, LIFR is non-functional [50] when stimulated with recombinant LIF. Inactive or downregulation of LIFR could be a mechanism that aggressive tumor cells utilize to disseminate to and colonize the bone marrow. However, our data demonstrate that these cells respond to OSM stimulation resulting in both robust phosphorylated STAT3 and activation of its downstream mediator SOCS3. Our findings confirm this effect in the MDA-MB-231b cells (Figure 11E, F, H). Importantly, our data further confirm that LIFR is required for LIF

signaling in ER+ breast cancer cell lines, but not for OSM signaling (Figure 12). Since OSM can activate STAT3, AKT, ERK and Src signaling in ER+ breast cancer cells, these effects may also be mediated through OSMR. In breast cancer patients, high OSMR expression was associated with increased RFS in both ER+ and ER- breast cancer patients (Figure 24, 25), but in GSE14548 (Figure 27) higher OSMR expression was found in patients with more invasive disease. Previous studies have not determined if OSMR is required for downstream signaling activation by OSM; however, further studies should be conducted to determine the role OSMR may have in tumor dormancy.

***What are the potential mechanisms by which OSM promotes bone dissemination of ER+ breast cancer cells?*** We demonstrate that constitutive OSM expression and recombinant cytokine treatment increases the number of $CD44^{+}$ cells within the parent population of ER+ breast cancer cells (MCF7 and T47D). Several groups have demonstrated that CD44 expression is correlated with increased tumorigenic potential and metastatic characteristics of breast cancer, thus highlighting a potential mechanism for OSM-mediated bone dissemination. Our data further demonstrate that OSM activates and downregulates a wide range of pro-tumorigenic signaling pathways in ER+ breast cancer cells, including PI3K-AKT, MAPK-ERK, STAT3, mTOR, and Src signaling. In our study, OSM significantly downregulates expression of pro-apoptotic proteins Bim and BAK (Figure 18D), and previous reports have shown Bim and BAK expression is associated with a favorable prognosis [381, 382](ref). OSM may therefore promote bone dissemination through downregulation of Bim and BAK, and upregulation of pro-tumorigenic pathways. We found it interesting that LIF, OSM and CNTF activated $Src^{Y527}$. It's connection to the gp130 cytokines is unknown, but previous work demonstrated that increased $Src^{Y527}$ results in increased bone and lung dissemination in TNBC cell lines and is associated with reduced overall patient survival. Thus, the question remains, what is causing the increased bone dissemination from OSM upregulation? Our findings shed some light on this matter, but further studies need to be conducted to determine the exact mechanism behind OSM bone trophic effects.

***If LIFR promotes tumor dormancy and acts as a breast tumor suppressor, what does it mean if OSM has pro-tumorigenic effects?*** OSM can signal through LIFR, but many of the signaling effects and *in vivo* outcomes that arise from high OSM levels are contradictory to LIFR's pro-dormancy and tumor suppressive functions. From our study, OSM expression is beneficial for long-term patient outcomes (Figure 24, 25) and potently activates downstream STAT3, which is part of an ER+ dormancy signature [223]. A large body of work has demonstrated STAT3's pro-tumorigenic role in the primary site, but recent work has shown STAT3 to be important regulating tumor dormancy. STAT3 knockdown in MCF7 breast cancer cells phenocopied LIFR knockdown [50], further supporting a pro-dormancy role for STAT3 in ER+ breast cancer. OSM is also able to signal through its cytokine specific receptor, OSMR. However, more work is needed to discern if the pro-tumorigenic effects of OSM are through OSMR, and whether LIFR contributes to these effects in breast cancer.

**Concluding remarks**

The work presented in this dissertation sheds light on the complex and nuanced roles for the gp130 cytokines in breast cancer progression, metastasis, tumor dormancy and pluripotency. Our work demonstrates that OSM promotes bone dissemination of ER+ breast cancer, but further studies are needed to determine the full mechanism behind these actions. While OSM activates a wide range of pro-tumorigenic pathways, it also robustly activates STAT3, a pro-dormancy factor in the metastatic site. As a result, we propose that OSM promotes metastasis through activation of pro-tumorigenic pathways but may also promote dormancy in bone-disseminated tumor cells through activation of STAT3. In addition, we highlight novel signaling pathways previously unknown to be activated by CNTF, which may be important for tumor cell entry and exit from dormancy in the bone marrow, where CNTF, OSM, and other gp130 cytokines are abundantly expressed. Taken together, the gp130 cytokine family has distinct functions that are important in a wide range of biological processes. Continued study of the cytokine family may reveal distinct and novel ways to target bone metastases and manipulate the dormancy status of breast tumor cells in the bone.

REFERENCES


1. Siegel, R.L., et al., *Cancer Statistics, 2021.* CA Cancer J Clin, 2021. **71**(1): p. 7-33.
2. Helbig, G., et al., *NF-kappaB promotes breast cancer cell migration and metastasis by inducing the expression of the chemokine receptor CXCR4.* J Biol Chem, 2003. **278**(24): p. 21631-8.
3. Howlader, N., et al., *Differences in Breast Cancer Survival by Molecular Subtypes in the United States.* Cancer Epidemiology Biomarkers & Prevention, 2018. **27**(6): p. 619.
4. Ross, J.S., et al., *The Her-2/neu gene and protein in breast cancer 2003: biomarker and target of therapy.* Oncologist, 2003. **8**(4): p. 307-25.
5. Yager, J.D. and N.E. Davidson, *Estrogen carcinogenesis in breast cancer.* N Engl J Med, 2006. **354**(3): p. 270-82.
6. Gomis, R.R. and S. Gawrzak, *Tumor cell dormancy.* Molecular Oncology, 2017. **11**(1): p. 62-78.
7. Wei, B., et al., *Bone metastasis is strongly associated with estrogen receptor-positive/progesterone receptor-negative breast carcinomas.* Hum Pathol, 2008. **39**(12): p. 1809-15.
8. Han, H.H., et al., *Estrogen Receptor Status Predicts Late-Onset Skeletal Recurrence in Breast Cancer Patients.* Medicine (Baltimore), 2016. **95**(8): p. e2909.
9. Savci-Heijink, C.D., et al., *Retrospective analysis of metastatic behaviour of breast cancer subtypes.* Breast Cancer Res Treat, 2015. **150**(3): p. 547-57.
10. Dasgupta, A., A.R. Lim, and C.M. Ghajar, *Circulating and disseminated tumor cells: harbingers or initiators of metastasis?* Molecular Oncology, 2017. **11**(1): p. 40-61.
11. Sosa, M.S., P. Bragado, and J.A. Aguirre-Ghiso, *Mechanisms of disseminated cancer cell dormancy: an awakening field.* Nature Reviews Cancer, 2014. **14**: p. 611.
12. Aguirre-Ghiso, J.A., *Models, mechanisms and clinical evidence for cancer dormancy.* Nature reviews. Cancer, 2007. **7**(11): p. 834-846.
13. Goss, P.E. and A.F. Chambers, *Does tumour dormancy offer a therapeutic target?* Nat Rev Cancer, 2010. **10**(12): p. 871-7.
14. Recasens, A. and L. Munoz, *Targeting Cancer Cell Dormancy.* Trends in Pharmacological Sciences, 2019. **40**(2): p. 128-141.

15. Conejo-Garcia, J.R., et al., *Tumor-infiltrating dendritic cell precursors recruited by a beta-defensin contribute to vasculogenesis under the influence of Vegf-A.* Nat Med, 2004. **10**(9): p. 950-8.
16. Gao, D., et al., *Endothelial progenitor cells control the angiogenic switch in mouse lung metastasis.* Science, 2008. **319**(5860): p. 195-8.
17. Lyden, D., et al., *Impaired recruitment of bone-marrow-derived endothelial and hematopoietic precursor cells blocks tumor angiogenesis and growth.* Nat Med, 2001. **7**(11): p. 1194-201.
18. Straume, O., et al., *Suppression of heat shock protein 27 induces long-term dormancy in human breast cancer.* Proceedings of the National Academy of Sciences of the United States of America, 2012. **109**(22): p. 8699-8704.
19. Ghajar, C.M., et al., *The perivascular niche regulates breast tumour dormancy.* Nature cell biology, 2013. **15**(7): p. 807-817.
20. Lawler, J., *Thrombospondin-1 as an endogenous inhibitor of angiogenesis and tumor growth.* J Cell Mol Med, 2002. **6**(1): p. 1-12.
21. Malladi, S., et al., *Metastatic Latency and Immune Evasion through Autocrine Inhibition of WNT.* Cell, 2016. **165**(1): p. 45-60.
22. Koebel, C.M., et al., *Adaptive immunity maintains occult cancer in an equilibrium state.* Nature, 2007. **450**(7171): p. 903-7.
23. Muller, M., et al., *EblacZ tumor dormancy in bone marrow and lymph nodes: active control of proliferating tumor cells by CD8+ immune T cells.* Cancer Res, 1998. **58**(23): p. 5439-46.
24. Feuerer, M., et al., *Enrichment of memory T cells and other profound immunological changes in the bone marrow from untreated breast cancer patients.* Int J Cancer, 2001. **92**(1): p. 96-105.
25. Shankaran, V., et al., *IFNgamma and lymphocytes prevent primary tumour development and shape tumour immunogenicity.* Nature, 2001. **410**(6832): p. 1107-11.
26. Eyles, J., et al., *Tumor cells disseminate early, but immunosurveillance limits metastatic outgrowth, in a mouse model of melanoma.* The Journal of clinical investigation, 2010. **120**(6): p. 2030-2039.
27. Gabrilovich, D.I. and S. Nagaraj, *Myeloid-derived suppressor cells as regulators of the immune system.* Nat Rev Immunol, 2009. **9**(3): p. 162-74.
28. Sceneay, J., M.J. Smyth, and A. Möller, *The pre-metastatic niche: finding common ground.* Cancer and Metastasis Reviews, 2013. **32**(3): p. 449-464.

29. Ghajar, C.M., *Metastasis prevention by targeting the dormant niche.* Nature reviews. Cancer, 2015. **15**(4): p. 238-247.
30. Debeb, B.G., W. Xu, and W.A. Woodward, *Radiation resistance of breast cancer stem cells: understanding the clinical framework.* J Mammary Gland Biol Neoplasia, 2009. **14**(1): p. 11-7.
31. Pinto, C.A., et al., *Breast cancer stem cells and epithelial mesenchymal plasticity – Implications for chemoresistance.* Cancer Letters, 2013. **341**(1): p. 56-62.
32. Bai, X., et al., *Cancer stem cell in breast cancer therapeutic resistance.* Cancer Treatment Reviews, 2018. **69**: p. 152-163.
33. Prieto-Vila, M., et al., *Drug Resistance Driven by Cancer Stem Cells and Their Niche.* International Journal of Molecular Sciences, 2017. **18**(12).
34. Price, T.T., et al., *Dormant breast cancer micrometastases reside in specific bone marrow niches that regulate their transit to and from bone.* Sci Transl Med, 2016. **8**(340): p. 340ra73.
35. Roato, I. and R. Ferracini, *Cancer Stem Cells, Bone and Tumor Microenvironment: Key Players in Bone Metastases.* Cancers (Basel), 2018. **10**(2).
36. Muz, B., et al., *The role of hypoxia in cancer progression, angiogenesis, metastasis, and resistance to therapy.* Hypoxia (Auckland, N.Z.), 2015. **3**: p. 83-92.
37. Naumov, G.N., L.A. Akslen, and J. Folkman, *Role of angiogenesis in human tumor dormancy: animal models of the angiogenic switch.* Cell Cycle, 2006. **5**(16): p. 1779-87.
38. Naumov, G.N., et al., *A Model of Human Tumor Dormancy: An Angiogenic Switch From the Nonangiogenic Phenotype.* JNCI: Journal of the National Cancer Institute, 2006. **98**(5): p. 316-325.
39. Semenza, G.L., *Targeting HIF-1 for cancer therapy.* Nat Rev Cancer, 2003. **3**(10): p. 721-32.
40. Woelfle, U., et al., *Molecular signature associated with bone marrow micrometastasis in human breast cancer.* Cancer Res, 2003. **63**(18): p. 5679-84.
41. Liao, D., et al., *Hypoxia-inducible factor-1alpha is a key regulator of metastasis in a transgenic model of cancer initiation and progression.* Cancer Res, 2007. **67**(2): p. 563-72.
42. Büchler, P., et al., *Transcriptional regulation of urokinase-type plasminogen activator receptor by hypoxia-inducible factor 1 is crucial for invasion of pancreatic and liver cancer.* Neoplasia (New York, N.Y.), 2009. **11**(2): p. 196-206.

43. Chaturvedi, P., et al., *Hypoxia-inducible factor-dependent breast cancer-mesenchymal stem cell bidirectional signaling promotes metastasis.* The Journal of clinical investigation, 2013. **123**(1): p. 189-205.
44. Erler, J.T., et al., *Lysyl oxidase is essential for hypoxia-induced metastasis.* Nature, 2006. **440**(7088): p. 1222-1226.
45. Finger, E.C., et al., *Hypoxic induction of AKAP12 variant 2 shifts PKA-mediated protein phosphorylation to enhance migration and metastasis of melanoma cells.* Proceedings of the National Academy of Sciences of the United States of America, 2015. **112**(14): p. 4441-4446.
46. Yang, M.H., et al., *Direct regulation of TWIST by HIF-1alpha promotes metastasis.* Nat Cell Biol, 2008. **10**(3): p. 295-305.
47. Oladipupo, S., et al., *VEGF is essential for hypoxia-inducible factor-mediated neovascularization but dispensable for endothelial sprouting.* Proceedings of the National Academy of Sciences of the United States of America, 2011. **108**(32): p. 13264-13269.
48. Tsuzuki, Y., et al., *Vascular Endothelial Growth Factor (VEGF) Modulation by Targeting Hypoxia-inducible Factor-1α → Hypoxia Response Element → VEGF Cascade Differentially Regulates Vascular Response and Growth Rate in Tumors.* 2000. **60**(22): p. 6248-6252.
49. Chen, D., et al., *LIFR is a breast cancer metastasis suppressor upstream of the Hippo-YAP pathway and a prognostic marker.* Nat Med, 2012. **18**(10): p. 1511-7.
50. Johnson, Rachelle W., et al., *Induction of LIFR confers a dormancy phenotype in breast cancer cells disseminated to the bone marrow.* Nature Cell Biology, 2016. **18**: p. 1078.
51. Wong, C.C.-L., et al., *Inhibitors of hypoxia-inducible factor 1 block breast cancer metastatic niche formation and lung metastasis.* Journal of molecular medicine (Berlin, Germany), 2012. **90**(7): p. 803-815.
52. Erler, J.T., et al., *Hypoxia-induced lysyl oxidase is a critical mediator of bone marrow cell recruitment to form the premetastatic niche.* Cancer cell, 2009. **15**(1): p. 35-44.
53. Kagan, H.M. and W. Li, *Lysyl oxidase: properties, specificity, and biological roles inside and outside of the cell.* J Cell Biochem, 2003. **88**(4): p. 660-72.
54. Fluegen, G., et al., *Phenotypic heterogeneity of disseminated tumour cells is preset by primary tumour hypoxic microenvironments.* Nature cell biology, 2017. **19**(2): p. 120-132.
55. Sosa, M.S., et al., *NR2F1 controls tumour cell dormancy via SOX9- and RARβ-driven quiescence programmes.* Nature communications, 2015. **6**: p. 6170-6170.

56. Thompson, V.C., et al., *A gene signature identified using a mouse model of androgen receptor-dependent prostate cancer predicts biochemical relapse in human disease.* Int J Cancer, 2012. **131**(3): p. 662-72.
57. Bragado, P., et al., *TGF-β2 dictates disseminated tumour cell fate in target organs through TGF-β-RIII and p38α/β signalling.* Nature cell biology, 2013. **15**(11): p. 1351-1361.
58. Adam, A.P., et al., *Computational identification of a p38SAPK-regulated transcription factor network required for tumor cell quiescence.* Cancer Res, 2009. **69**(14): p. 5664-72.
59. Teng, M.W., et al., *Immune-mediated dormancy: an equilibrium with cancer.* J Leukoc Biol, 2008. **84**(4): p. 988-93.
60. Yeh, A.C. and S. Ramaswamy, *Mechanisms of Cancer Cell Dormancy--Another Hallmark of Cancer?* Cancer research, 2015. **75**(23): p. 5014-5022.
61. Wang, H.-f., et al., *Targeting Immune-Mediated Dormancy: A Promising Treatment of Cancer.* 2019. **9**(498).
62. Dunn, G.P., L.J. Old, and R.D. Schreiber, *The immunobiology of cancer immunosurveillance and immunoediting.* Immunity, 2004. **21**(2): p. 137-48.
63. Lan, Q., et al., *Type I interferon/IRF7 axis instigates chemotherapy-induced immunological dormancy in breast cancer.* Oncogene, 2019. **38**(15): p. 2814-2829.
64. Bidwell, B.N., et al., *Silencing of Irf7 pathways in breast cancer cells promotes bone metastasis through immune escape.* Nature Medicine, 2012. **18**(8): p. 1224-1231.
65. Farrar, J.D., et al., *Cancer Dormancy. VII. A Regulatory Role for CD8<sup>+</sup> T Cells and IFN-γ in Establishing and Maintaining the Tumor-Dormant State.* 1999. **162**(5): p. 2842-2849.
66. Chan, C.J., et al., *The receptors CD96 and CD226 oppose each other in the regulation of natural killer cell functions.* Nat Immunol, 2014. **15**(5): p. 431-8.
67. Blake, S.J., et al., *Suppression of Metastases Using a New Lymphocyte Checkpoint Target for Cancer Immunotherapy.* 2016. **6**(4): p. 446-459.
68. Müller-Hermelink, N., et al., *TNFR1 Signaling and IFN-γ Signaling Determine whether T Cells Induce Tumor Dormancy or Promote Multistage Carcinogenesis.* Cancer Cell, 2008. **13**(6): p. 507-518.
69. Romagnani, P., et al., *CXC chemokines: the regulatory link between inflammation and angiogenesis.* Trends in Immunology, 2004. **25**(4): p. 201-209.
70. Huang, B., et al., *Osteoblasts secrete Cxcl9 to regulate angiogenesis in bone.* Nature communications, 2016. **7**: p. 13885-13885.

71. Zhang, R., et al., *Combination of MIG (CXCL9) chemokine gene therapy with low-dose cisplatin improves therapeutic efficacy against murine carcinoma.* Gene Ther, 2006. **13**(17): p. 1263-71.
72. Arenberg, D.A., et al., *Improved survival in tumor-bearing SCID mice treated with interferon-gamma-inducible protein 10 (IP-10/CXCL10).* Cancer Immunol Immunother, 2001. **50**(10): p. 533-8.
73. Pan, J., et al., *CXCR3/CXCR3 ligand biological axis impairs RENCA tumor growth by a mechanism of immunoangiostasis.* J Immunol, 2006. **176**(3): p. 1456-64.
74. Feldman, A.L., et al., *Retroviral gene transfer of interferon-inducible protein 10 inhibits growth of human melanoma xenografts.* Int J Cancer, 2002. **99**(1): p. 149-53.
75. Barash, U., et al., *Heparanase enhances myeloma progression via CXCL10 downregulation.* Leukemia, 2014. **28**(11): p. 2178-87.
76. Wang, X., et al., *A novel recombinant protein of IP10-EGFRvIIIscFv and CD8(+) cytotoxic T lymphocytes synergistically inhibits the growth of implanted glioma in mice.* Cancer Immunol Immunother, 2013. **62**(7): p. 1261-72.
77. Mosser, D.M. and J.P. Edwards, *Exploring the full spectrum of macrophage activation.* Nat Rev Immunol, 2008. **8**(12): p. 958-69.
78. Martin-Fontecha, A., et al., *Induced recruitment of NK cells to lymph nodes provides IFN-gamma for T(H)1 priming.* Nat Immunol, 2004. **5**(12): p. 1260-5.
79. Schoenborn, J.R. and C.B. Wilson, *Regulation of interferon-gamma during innate and adaptive immune responses.* Adv Immunol, 2007. **96**: p. 41-101.
80. Inamoto, S., et al., *Loss of SMAD4 Promotes Colorectal Cancer Progression by Accumulation of Myeloid-Derived Suppressor Cells through the CCL15-CCR1 Chemokine Axis.* Clin Cancer Res, 2016. **22**(2): p. 492-501.
81. Ibrahim, M.L., et al., *Myeloid-Derived Suppressor Cells Produce IL-10 to Elicit DNMT3b-Dependent IRF8 Silencing to Promote Colitis-Associated Colon Tumorigenesis.* Cell Rep, 2018. **25**(11): p. 3036-3046.e6.
82. Deng, L., et al., *Accumulation of foxp3+ T regulatory cells in draining lymph nodes correlates with disease progression and immune suppression in colorectal cancer patients.* Clin Cancer Res, 2010. **16**(16): p. 4105-12.
83. Sampath, S., et al., *Combined modality radiation therapy promotes tolerogenic myeloid cell populations and STAT3-related gene expression in head and neck cancer patients.* Oncotarget, 2018. **9**(13): p. 11279-11290.

84. Lang, S., et al., *Clinical relevance and suppressive capacity of human MDSC subsets.* 2018: p. clincanres.3726.2017.
85. Schuler, P.J., et al., *Effects of adjuvant chemoradiotherapy on the frequency and function of regulatory T cells in patients with head and neck cancer.* Clin Cancer Res, 2013. **19**(23): p. 6585-96.
86. Mabuchi, S., et al., *Myeloid-derived suppressor cells and their role in gynecological malignancies.* Tumor Biology, 2018. **40**(7): p. 1010428318776485.
87. Baert, T., et al., *Myeloid Derived Suppressor Cells: Key Drivers of Immunosuppression in Ovarian Cancer.* 2019. **10**(1273).
88. Curiel, T.J., et al., *Specific recruitment of regulatory T cells in ovarian carcinoma fosters immune privilege and predicts reduced survival.* Nat Med, 2004. **10**(9): p. 942-9.
89. Wang, L., et al., *Increased myeloid-derived suppressor cells in gastric cancer correlate with cancer stage and plasma S100A8/A9 proinflammatory proteins.* J Immunol, 2013. **190**(2): p. 794-804.
90. Mizukami, Y., et al., *CCL17 and CCL22 chemokines within tumor microenvironment are related to accumulation of Foxp3+ regulatory T cells in gastric cancer.* Int J Cancer, 2008. **122**(10): p. 2286-93.
91. Plitas, G., et al., *Regulatory T Cells Exhibit Distinct Features in Human Breast Cancer.* Immunity, 2016. **45**(5): p. 1122-1134.
92. Zhu, H., et al., *CXCR2(+) MDSCs promote breast cancer progression by inducing EMT and activated T cell exhaustion.* Oncotarget, 2017. **8**(70): p. 114554-114567.
93. Clever, D., et al., *Oxygen Sensing by T Cells Establishes an Immunologically Tolerant Metastatic Niche.* Cell, 2016. **166**(5): p. 1117-1131.e14.
94. Krall, J.A., et al., *The systemic response to surgery triggers the outgrowth of distant immune-controlled tumors in mouse models of dormancy.* Science translational medicine, 2018. **10**(436): p. eaan3464.
95. Yang, L., et al., *Abrogation of TGF beta signaling in mammary carcinomas recruits Gr-1+CD11b+ myeloid cells that promote metastasis.* Cancer cell, 2008. **13**(1): p. 23-35.
96. Yang, L., et al., *Expansion of myeloid immune suppressor Gr+CD11b+ cells in tumor-bearing host directly promotes tumor angiogenesis.* Cancer Cell, 2004. **6**(4): p. 409-21.
97. Headley, M.B., et al., *Visualization of immediate immune responses to pioneer metastatic cells in the lung.* Nature, 2016. **531**(7595): p. 513-517.
98. Albrengues, J., et al., *Neutrophil extracellular traps produced during inflammation awaken dormant cancer cells in mice.* 2018. **361**(6409): p. eaao4227.

99. Hanahan, D. and J. Folkman, *Patterns and emerging mechanisms of the angiogenic switch during tumorigenesis.* Cell, 1996. **86**(3): p. 353-64.
100. Folkman, J., *Tumor angiogenesis: therapeutic implications.* N Engl J Med, 1971. **285**(21): p. 1182-6.
101. Carmeliet, P., et al., *Abnormal blood vessel development and lethality in embryos lacking a single VEGF allele.* Nature, 1996. **380**(6573): p. 435-9.
102. Ferrara, N., et al., *Heterozygous embryonic lethality induced by targeted inactivation of the VEGF gene.* Nature, 1996. **380**(6573): p. 439-42.
103. Lee, S., et al., *Autocrine VEGF signaling is required for vascular homeostasis.* Cell, 2007. **130**(4): p. 691-703.
104. Weinstat-Saslow, D.L., et al., *Transfection of thrombospondin 1 complementary DNA into a human breast carcinoma cell line reduces primary tumor growth, metastatic potential, and angiogenesis.* Cancer Res, 1994. **54**(24): p. 6504-11.
105. Aicher, A., et al., *Essential role of endothelial nitric oxide synthase for mobilization of stem and progenitor cells.* Nat Med, 2003. **9**(11): p. 1370-6.
106. Koistinen, P., et al., *Regulation of the acute myeloid leukemia cell line OCI/AML-2 by endothelial nitric oxide synthase under the control of a vascular endothelial growth factor signaling system.* Leukemia, 2001. **15**(9): p. 1433-41.
107. Dias, S., et al., *Inhibition of both paracrine and autocrine VEGF/ VEGFR-2 signaling pathways is essential to induce long-term remission of xenotransplanted human leukemias.* Proc Natl Acad Sci U S A, 2001. **98**(19): p. 10857-62.
108. Dias, S., et al., *Autocrine stimulation of VEGFR-2 activates human leukemic cell growth and migration.* The Journal of clinical investigation, 2000. **106**(4): p. 511-521.
109. Pirtskhalaishvili, G. and J.B. Nelson, *Endothelium-derived factors as paracrine mediators of prostate cancer progression.* Prostate, 2000. **44**(1): p. 77-87.
110. Macedo, F., et al., *Bone Metastases: An Overview.* Oncology reviews, 2017. **11**(1): p. 321-321.
111. Johnson, R.W. and L.J. Suva, *Hallmarks of Bone Metastasis.* Calcif Tissue Int, 2017.
112. Croucher, P.I., M.M. McDonald, and T.J. Martin, *Bone metastasis: the importance of the neighbourhood.* Nature Reviews Cancer, 2016. **16**: p. 373.
113. Zhang, J., et al., *Identification of the haematopoietic stem cell niche and control of the niche size.* Nature, 2003. **425**: p. 836.

114. Butler, J.M., H. Kobayashi, and S. Rafii, *Instructive role of the vascular niche in promoting tumour growth and tissue repair by angiocrine factors.* Nature reviews. Cancer, 2010. **10**(2): p. 138-146.
115. Méndez-Ferrer, S., et al., *Mesenchymal and haematopoietic stem cells form a unique bone marrow niche.* Nature, 2010. **466**(7308): p. 829-834.
116. Ding, L., et al., *Endothelial and perivascular cells maintain haematopoietic stem cells.* Nature, 2012. **481**(7382): p. 457-62.
117. Crane, G.M., E. Jeffery, and S.J. Morrison, *Adult haematopoietic stem cell niches.* Nature Reviews Immunology, 2017. **17**: p. 573.
118. Ikuta, K. and I.L. Weissman, *Evidence that hematopoietic stem cells express mouse c-kit but do not depend on steel factor for their generation.* Proc Natl Acad Sci U S A, 1992. **89**(4): p. 1502-6.
119. Sugiyama, T., et al., *Maintenance of the Hematopoietic Stem Cell Pool by CXCL12-CXCR4 Chemokine Signaling in Bone Marrow Stromal Cell Niches.* Immunity, 2006. **25**(6): p. 977-988.
120. Omatsu, Y., et al., *The essential functions of adipo-osteogenic progenitors as the hematopoietic stem and progenitor cell niche.* Immunity, 2010. **33**(3): p. 387-99.
121. Nie, Y., Y.C. Han, and Y.R. Zou, *CXCR4 is required for the quiescence of primitive hematopoietic cells.* J Exp Med, 2008. **205**(4): p. 777-83.
122. Tzeng, Y.S., et al., *Loss of Cxcl12/Sdf-1 in adult mice decreases the quiescent state of hematopoietic stem/progenitor cells and alters the pattern of hematopoietic regeneration after myelosuppression.* Blood, 2011. **117**(2): p. 429-39.
123. Varnum-Finney, B., et al., *Notch2 governs the rate of generation of mouse long- and short-term repopulating stem cells.* J Clin Invest, 2011. **121**(3): p. 1207-16.
124. Duncan, A.W., et al., *Integration of Notch and Wnt signaling in hematopoietic stem cell maintenance.* Nature Immunology, 2005. **6**: p. 314.
125. Bernad, A., et al., *Interleukin-6 is required in vivo for the regulation of stem cells and committed progenitors of the hematopoietic system.* Immunity, 1994. **1**(9): p. 725-31.
126. Winkler, I.G., et al., *Vascular niche E-selectin regulates hematopoietic stem cell dormancy, self renewal and chemoresistance.* Nat Med, 2012. **18**(11): p. 1651-7.
127. Chatterjee, S., B. Behnam Azad, and S. Nimmagadda, *Chapter Two - The Intricate Role of CXCR4 in Cancer*, in *Advances in Cancer Research*, M.G. Pomper and P.B. Fisher, Editors. 2014, Academic Press. p. 31-82.

128. Corcoran, K.E., et al., *Mesenchymal stem cells in early entry of breast cancer into bone marrow.* PLoS One, 2008. **3**(6): p. e2563.
129. Taichman, R.S., et al., *Use of the stromal cell-derived factor-1/CXCR4 pathway in prostate cancer metastasis to bone.* Cancer Res, 2002. **62**(6): p. 1832-7.
130. Muller, A., et al., *Involvement of chemokine receptors in breast cancer metastasis.* Nature, 2001. **410**(6824): p. 50-6.
131. Azab, A.K., et al., *CXCR4 inhibitor AMD3100 disrupts the interaction of multiple myeloma cells with the bone marrow microenvironment and enhances their sensitivity to therapy.* Blood, 2009. **113**(18): p. 4341-51.
132. Xiang, J., et al., *CXCR4 Protein Epitope Mimetic Antagonist POL5551 Disrupts Metastasis and Enhances Chemotherapy Effect in Triple-Negative Breast Cancer.* Mol Cancer Ther, 2015. **14**(11): p. 2473-85.
133. Domanska, U.M., et al., *CXCR4 inhibition with AMD3100 sensitizes prostate cancer to docetaxel chemotherapy.* Neoplasia, 2012. **14**(8): p. 709-18.
134. Wang, H., et al., *The osteogenic niche promotes early-stage bone colonization of disseminated breast cancer cells.* Cancer Cell, 2015. **27**(2): p. 193-210.
135. Shiozawa, Y., et al., *Human prostate cancer metastases target the hematopoietic stem cell niche to establish footholds in mouse bone marrow.* J Clin Invest, 2011. **121**(4): p. 1298-312.
136. Sterling, J.A. and S.A. Guelcher, *Bone structural components regulating sites of tumor metastasis.* Curr Osteoporos Rep, 2011. **9**(2): p. 89-95.
137. Johnson, R.W., M.E. Sowder, and A.J. Giaccia, *Hypoxia and Bone Metastatic Disease.* Curr Osteoporos Rep, 2017. **15**(4): p. 231-238.
138. Mundy, G.R., *Mechanisms of bone metastasis.* Cancer, 1997. **80**(8 Suppl): p. 1546-56.
139. Johnson, R.W., et al., *Parathyroid Hormone-Related Protein Negatively Regulates Tumor Cell Dormancy Genes in a PTHR1/Cyclic AMP-Independent Manner.* Frontiers in endocrinology, 2018. **9**: p. 241-241.
140. Turner, M.D., et al., *Cytokines and chemokines: At the crossroads of cell signalling and inflammatory disease.* Biochimica et Biophysica Acta (BBA) - Molecular Cell Research, 2014. **1843**(11): p. 2563-2582.
141. Zheng, Y., et al., *Targeting IL-6 and RANKL signaling inhibits prostate cancer growth in bone.* Clinical & Experimental Metastasis, 2014. **31**(8): p. 921-933.

142. Sims, N.A., *Cell-specific paracrine actions of IL-6 family cytokines from bone, marrow and muscle that control bone formation and resorption.* The International Journal of Biochemistry & Cell Biology, 2016. **79**(Supplement C): p. 14-23.
143. Wang, X., et al., *Structural Biology of Shared Cytokine Receptors.* Annual Review of Immunology, 2009. **27**(1): p. 29-60.
144. Yoshida, K., et al., *Targeted disruption of gp130, a common signal transducer for the interleukin 6 family of cytokines, leads to myocardial and hematological disorders.* Proceedings of the National Academy of Sciences, 1996. **93**(1): p. 407-411.
145. Shin, H.-I., et al., *gp130-Mediated Signaling Is Necessary for Normal Osteoblastic Function in Vivo and in Vitro.* Endocrinology, 2004. **145**(3): p. 1376-1385.
146. Kawasaki, K., et al., *Osteoclasts Are Present in gp130-Deficient Mice*.* Endocrinology, 1997. **138**(11): p. 4959-4965.
147. Boulanger, M.J., et al., *Hexameric Structure and Assembly of the Interleukin-6/IL-6 α-Receptor/gp130 Complex.* Science, 2003. **300**(5628): p. 2101-2104.
148. Taga, T. and T. Kishimoto, *gp130 AND THE INTERLEUKIN-6 FAMILY OF CYTOKINES.* Annual Review of Immunology, 1997. **15**(1): p. 797-819.
149. Robledo, O., et al., *Signaling of the Cardiotrophin-1 Receptor: EVIDENCE FOR A THIRD RECEPTOR COMPONENT.* Journal of Biological Chemistry, 1997. **272**(8): p. 4855-4863.
150. Mosley, B., et al., *Dual Oncostatin M (OSM) Receptors: CLONING AND CHARACTERIZATION OF AN ALTERNATIVE SIGNALING SUBUNIT CONFERRING OSM-SPECIFIC RECEPTOR ACTIVATION.* Journal of Biological Chemistry, 1996. **271**(51): p. 32635-32643.
151. Pflanz, S., et al., *WSX-1 and glycoprotein 130 constitute a signal-transducing receptor for IL-27.* J Immunol, 2004. **172**(4): p. 2225-31.
152. Garbers, C., et al., *An interleukin-6 receptor-dependent molecular switch mediates signal transduction of the IL-27 cytokine subunit p28 (IL-30) via a gp130 protein receptor homodimer.* J Biol Chem, 2013. **288**(6): p. 4346-54.
153. Kourko, O., et al., *IL-27, IL-30, and IL-35: A Cytokine Triumvirate in Cancer.* Front Oncol, 2019. **9**: p. 969.
154. Stahl, N., et al., *Association and activation of Jak-Tyk kinases by CNTF-LIF-OSM-IL-6 beta receptor components.* Science, 1994. **263**(5143): p. 92-5.
155. Takahashi-Tezuka, M., et al., *Gab1 acts as an adapter molecule linking the cytokine receptor gp130 to ERK mitogen-activated protein kinase.* Mol Cell Biol, 1998. **18**(7): p. 4109-17.

156. Oh, H., et al., *Activation of phosphatidylinositol 3-kinase through glycoprotein 130 induces protein kinase B and p70 S6 kinase phosphorylation in cardiac myocytes.* J Biol Chem, 1998. **273**(16): p. 9703-10.
157. Fahmi, A., et al., *p42/p44-MAPK and PI3K are sufficient for IL-6 family cytokines/gp130 to signal to hypertrophy and survival in cardiomyocytes in the absence of JAK/STAT activation.* Cell Signal, 2013. **25**(4): p. 898-909.
158. Walker, E.C., et al., *Murine Oncostatin M Acts via Leukemia Inhibitory Factor Receptor to Phosphorylate Signal Transducer and Activator of Transcription 3 (STAT3) but Not STAT1, an Effect That Protects Bone Mass.* J Biol Chem, 2016. **291**(41): p. 21703-21716.
159. Rose, T.M. and A.G. Bruce, *Oncostatin M is a member of a cytokine family that includes leukemia-inhibitory factor, granulocyte colony-stimulating factor, and interleukin 6.* Proc Natl Acad Sci U S A, 1991. **88**(19): p. 8641-5.
160. Sims, N.A. and J.H. Gooi, *Bone remodeling: Multiple cellular interactions required for coupling of bone formation and resorption.* Seminars in Cell & Developmental Biology, 2008. **19**(5): p. 444-451.
161. Bellido, T., et al., *Activation of the Janus Kinase/STAT (Signal Transducer and Activator of Transcription) Signal Transduction Pathway by Interleukin-6-Type Cytokines Promotes Osteoblast Differentiation*.* Endocrinology, 1997. **138**(9): p. 3666-3676.
162. Walker, E.C., et al., *Oncostatin M promotes bone formation independently of resorption when signaling through leukemia inhibitory factor receptor in mice.* J Clin Invest, 2010. **120**(2): p. 582-92.
163. Walker, E.C., et al., *Cardiotrophin-1 Is an Osteoclast-Derived Stimulus of Bone Formation Required for Normal Bone Remodeling.* Journal of Bone and Mineral Research, 2008. **23**(12): p. 2025-2032.
164. Metcalf, D. and D.P. Gearing, *Fatal syndrome in mice engrafted with cells producing high levels of the leukemia inhibitory factor.* Proc Natl Acad Sci U S A, 1989. **86**(15): p. 5948-52.
165. McGregor, N.E., et al., *IL-6 exhibits both cis- and trans-signaling in osteocytes and osteoblasts, but only trans-signaling promotes bone formation and osteoclastogenesis.* 2019. **294**(19): p. 7850-7863.
166. Ishimi, Y., et al., *IL-6 is produced by osteoblasts and induces bone resorption.* J Immunol, 1990. **145**(10): p. 3297-303.

167. Liang, J.D., et al., *Immunohistochemical Localization of Selected Early Response Genes Expressed in Trabecular Bone of Young Rats Given hPTH 1-34.* Calcified Tissue International, 1999. **65**(5): p. 369-373.
168. Romas, E., et al., *The role of gp130-mediated signals in osteoclast development: regulation of interleukin 11 production by osteoblasts and distribution of its receptor in bone marrow cultures.* J Exp Med, 1996. **183**(6): p. 2581-91.
169. Allan, E.H., et al., *Osteoblasts display receptors for and responses to leukemia-inhibitory factor.* Journal of Cellular Physiology, 1990. **145**(1): p. 110-119.
170. Ishimi, Y., et al., *Leukemia inhibitory factor/differentiation-stimulating factor (LIF/D-factor): regulation of its production and possible roles in bone metabolism.* J Cell Physiol, 1992. **152**(1): p. 71-8.
171. Liu, F., J.E. Aubin, and L. Malaval, *Expression of leukemia inhibitory factor (LIF)/interleukin-6 family cytokines and receptors during in vitro osteogenesis: differential regulation by dexamethasone and LIF.* Bone, 2002. **31**(1): p. 212-9.
172. McGregor, N.E., et al., *Ciliary neurotrophic factor inhibits bone formation and plays a sex-specific role in bone growth and remodeling.* Calcif Tissue Int, 2010. **86**(3): p. 261-70.
173. Hunt, L.C. and J. White, *The Role of Leukemia Inhibitory Factor Receptor Signaling in Skeletal Muscle Growth, Injury and Disease*, in *Growth Factors and Cytokines in Skeletal Muscle Development, Growth, Regeneration and Disease*, J. White and G. Smythe, Editors. 2016, Springer International Publishing: Cham. p. 45-59.
174. Pedersen, B.K. and M.A. Febbraio, *Muscle as an Endocrine Organ: Focus on Muscle-Derived Interleukin-6.* Physiological Reviews, 2008. **88**(4): p. 1379-1406.
175. Johnson, R.W., et al., *Myokines (muscle-derived cytokines and chemokines) including ciliary neurotrophic factor (CNTF) inhibit osteoblast differentiation.* Bone, 2014. **64**: p. 47-56.
176. Li, X., et al., *Targeted deletion of the sclerostin gene in mice results in increased bone formation and bone strength.* J Bone Miner Res, 2008. **23**(6): p. 860-9.
177. Ware, C.B., et al., *Targeted disruption of the low-affinity leukemia inhibitory factor receptor gene causes placental, skeletal, neural and metabolic defects and results in perinatal death.* Development, 1995. **121**(5): p. 1283-99.
178. Poulton, I.J., et al., *Contrasting roles of leukemia inhibitory factor in murine bone development and remodeling involve region-specific changes in vascularization.* Journal of Bone and Mineral Research, 2012. **27**(3): p. 586-595.

179. Sims, N.A., et al., *Interleukin-11 receptor signaling is required for normal bone remodeling.* J Bone Miner Res, 2005. **20**(7): p. 1093-102.
180. Johnson, R.W., et al., *The Primary Function of gp130 Signaling in Osteoblasts Is To Maintain Bone Formation and Strength, Rather Than Promote Osteoclast Formation.* Journal of Bone and Mineral Research, 2014. **29**(6): p. 1492-1505.
181. Tamura, T., et al., *Soluble interleukin-6 receptor triggers osteoclast formation by interleukin 6.* Proceedings of the National Academy of Sciences, 1993. **90**(24): p. 11924-11928.
182. Richards, C.D., et al., *Stimulation of osteoclast differentiation in vitro by mouse oncostatin M, leukaemia inhibitory factor, cardiotrophin-1 and interleukin 6: synergy with dexamethasone.* Cytokine, 2000. **12**(6): p. 613-21.
183. Palmqvist, P., et al., *IL-6, leukemia inhibitory factor, and oncostatin M stimulate bone resorption and regulate the expression of receptor activator of NF-kappa B ligand, osteoprotegerin, and receptor activator of NF-kappa B in mouse calvariae.* J Immunol, 2002. **169**(6): p. 3353-62.
184. Horwood, N.J., et al., *Osteotropic agents regulate the expression of osteoclast differentiation factor and osteoprotegerin in osteoblastic stromal cells.* Endocrinology, 1998. **139**(11): p. 4743-6.
185. Sims, N.A. and N.C. Walsh, *GP130 cytokines and bone remodelling in health and disease.* BMB Rep, 2010. **43**(8): p. 513-23.
186. Johnson, R.W., et al., *Glycoprotein130 (Gp130)/interleukin-6 (IL-6) signalling in osteoclasts promotes bone formation in periosteal and trabecular bone.* Bone, 2015. **81**: p. 343-351.
187. Douglas, A.M., et al., *Expression and function of members of the cytokine receptor superfamily on breast cancer cells.* Oncogene, 1997. **14**: p. 661.
188. Nathan, R.W., C.M. Leigh, and H.W. Peter, *Oncostatin M suppresses oestrogen receptor-α expression and is associated with poor outcome in human breast cancer.* Endocrine-Related Cancer, 2012. **19**(2): p. 181-195.
189. Selander, K.S., et al., *Inhibition of gp130 signaling in breast cancer blocks constitutive activation of Stat3 and inhibits in vivo malignancy.* Cancer Res, 2004. **64**(19): p. 6924-33.
190. Perou, C.M., et al., *Molecular portraits of human breast tumours.* Nature, 2000. **406**(6797): p. 747-52.
191. Boyle, P., *Triple-negative breast cancer: epidemiological considerations and recommendations.* Ann Oncol, 2012. **23 Suppl 6**: p. vi7-12.

192. Allred, D.C., P. Brown, and D. Medina, *The origins of estrogen receptor alpha-positive and estrogen receptor alpha-negative human breast cancer.* Breast cancer research : BCR, 2004. **6**(6): p. 240-245.
193. Pauletti, G., et al., *Detection and quantitation of HER-2/neu gene amplification in human breast cancer archival material using fluorescence in situ hybridization.* Oncogene, 1996. **13**(1): p. 63-72.
194. Barkan, D., et al., *Inhibition of metastatic outgrowth from single dormant tumor cells by targeting the cytoskeleton.* Cancer research, 2008. **68**(15): p. 6241-6250.
195. Won, H.S., et al., *Soluble interleukin-6 receptor is a prognostic marker for relapse-free survival in estrogen receptor-positive breast cancer.* Cancer Invest, 2013. **31**(8): p. 516-21.
196. Li, H., et al., *Drug design targeting protein-protein interactions (PPIs) using multiple ligand simultaneous docking (MLSD) and drug repositioning: discovery of raloxifene and bazedoxifene as novel inhibitors of IL-6/GP130 interface.* J Med Chem, 2014. **57**(3): p. 632-41.
197. Hartman, Z.C., et al., *Growth of triple-negative breast cancer cells relies upon coordinate autocrine expression of the proinflammatory cytokines IL-6 and IL-8.* Cancer research, 2013. **73**(11): p. 3470-3480.
198. Hartman, Z.C., et al., *HER2 overexpression elicits a proinflammatory IL-6 autocrine signaling loop that is critical for tumorigenesis.* Cancer research, 2011. **71**(13): p. 4380-4391.
199. Korkaya, H., et al., *Activation of an IL6 inflammatory loop mediates trastuzumab resistance in HER2+ breast cancer by expanding the cancer stem cell population.* Mol Cell, 2012. **47**(4): p. 570-84.
200. Dhingra, K., et al., *Expression of leukemia inhibitory factor and its receptor in breast cancer: A potential autocrine and paracrine growth regulatory mechanism.* Breast Cancer Research and Treatment, 1998. **48**(2): p. 165-174.
201. Li, Y., et al., *A mandatory role of nuclear PAK4-LIFR axis in breast-to-bone metastasis of ERα-positive breast cancer cells.* Oncogene, 2019. **38**(6): p. 808-821.
202. Danforth, D.N., Jr. and M.K. Sgagias, *Interleukin-1 alpha and interleukin-6 act additively to inhibit growth of MCF-7 breast cancer cells in vitro.* Cancer Res, 1993. **53**(7): p. 1538-45.
203. Morinaga, Y., et al., *Contribution of IL-6 to the antiproliferative effect of IL-1 and tumor necrosis factor on tumor cell lines.* 1989. **143**(11): p. 3538-3542.

204. Chiu, J.J., M.K. Sgagias, and K.H. Cowan, *Interleukin 6 acts as a paracrine growth factor in human mammary carcinoma cell lines.* Clin Cancer Res, 1996. **2**(1): p. 215-21.
205. Tamm, I., et al., *Interleukin 6 decreases cell-cell association and increases motility of ductal breast carcinoma cells.* J Exp Med, 1989. **170**(5): p. 1649-69.
206. Asgeirsson, K.S., et al., *The effects of IL-6 on cell adhesion and e-cadherin expression in breast cancer.* Cytokine, 1998. **10**(9): p. 720-8.
207. Badache, A. and N.E. Hynes, *Interleukin 6 inhibits proliferation and, in cooperation with an epidermal growth factor receptor autocrine loop, increases migration of T47D breast cancer cells.* Cancer Res, 2001. **61**(1): p. 383-91.
208. Johnston, P.G., et al., *Identification of a Protein Factor Secreted by 3T3-L1 Preadipocytes Inhibitory for the Human MCF-7 Breast Cancer Cell Line.* Cancer Research, 1992. **52**(24): p. 6860-6865.
209. Jiang, X.P., et al., *Down-regulation of expression of interleukin-6 and its receptor results in growth inhibition of MCF-7 breast cancer cells.* Anticancer Res, 2011. **31**(9): p. 2899-906.
210. Nugoli, M., et al., *Genetic variability in MCF-7 sublines: evidence of rapid genomic and RNA expression profile modifications.* BMC Cancer, 2003. **3**(1): p. 13.
211. Studebaker, A.W., et al., *Fibroblasts Isolated from Common Sites of Breast Cancer Metastasis Enhance Cancer Cell Growth Rates and Invasiveness in an Interleukin-6–Dependent Manner.* Cancer Research, 2008. **68**(21): p. 9087-9095.
212. Taguchi, Y., et al., *Interleukin-6-type cytokines stimulate mesenchymal progenitor differentiation toward the osteoblastic lineage.* Proc Assoc Am Physicians, 1998. **110**(6): p. 559-74.
213. Wu, Q., et al., *IL-6 Enhances Osteocyte-Mediated Osteoclastogenesis by Promoting JAK2 and RANKL Activity In Vitro.* Cell Physiol Biochem, 2017. **41**(4): p. 1360-1369.
214. Bussard, K.M., D.J. Venzon, and A.M. Mastro, *Osteoblasts are a major source of inflammatory cytokines in the tumor microenvironment of bone metastatic breast cancer.* Journal of Cellular Biochemistry, 2010. **111**(5): p. 1138-1148.
215. Zheng, Y., et al., *Direct Crosstalk Between Cancer and Osteoblast Lineage Cells Fuels Metastatic Growth in Bone via Auto-Amplification of IL-6 and RANKL Signaling Pathways.* Journal of Bone and Mineral Research, 2014. **29**(9): p. 1938-1949.
216. Campbell, J.P., et al., *Stimulation of Host Bone Marrow Stromal Cells by Sympathetic Nerves Promotes Breast Cancer Bone Metastasis in Mice.* PLOS Biology, 2012. **10**(7): p. e1001363.

217. Luo, X., et al., *Stromal-Initiated Changes in the Bone Promote Metastatic Niche Development.* Cell Reports, 2016. **14**(1): p. 82-92.
218. Di Carlo, E., *Interleukin-30: A novel microenvironmental hallmark of prostate cancer progression.* Oncoimmunology, 2014. **3**(1): p. e27618.
219. Di Meo, S., et al., *Interleukin-30 expression in prostate cancer and its draining lymph nodes correlates with advanced grade and stage.* Clin Cancer Res, 2014. **20**(3): p. 585-94.
220. Airoldi, I., et al., *Interleukin-30 Promotes Breast Cancer Growth and Progression.* Cancer Res, 2016. **76**(21): p. 6218-6229.
221. Iorns, E., et al., *Whole genome in vivo RNAi screening identifies the leukemia inhibitory factor receptor as a novel breast tumor suppressor.* Breast Cancer Res Treat, 2012. **135**(1): p. 79-91.
222. Zeng, H., et al., *Feedback Activation of Leukemia Inhibitory Factor Receptor Limits Response to Histone Deacetylase Inhibitors in Breast Cancer.* Cancer Cell, 2016. **30**(3): p. 459-473.
223. Kim, R.S., et al., *Dormancy signatures and metastasis in estrogen receptor positive and negative breast cancer.* PloS one, 2012. **7**(4): p. e35569-e35569.
224. Thomas, R.J., et al., *Breast Cancer Cells Interact with Osteoblasts to Support Osteoclast Formation1.* Endocrinology, 1999. **140**(10): p. 4451-4458.
225. Woosley, A.N., et al., *TGFβ promotes breast cancer stem cell self-renewal through an ILEI/LIFR signaling axis.* Oncogene, 2019.
226. Wang, X.J., et al., *Opposing Roles of Acetylation and Phosphorylation in LIFR-Dependent Self-Renewal Growth Signaling in Mouse Embryonic Stem Cells.* Cell Rep, 2017. **18**(4): p. 933-946.
227. Schiemann, W.P., et al., *Phosphorylation of the human leukemia inhibitory factor (LIF) receptor by mitogen-activated protein kinase and the regulation of LIF receptor function by heterologous receptor activation.* 1995. **92**(12): p. 5361-5365.
228. Estrov, Z., et al., *Leukemia Inhibitory Factor Binds to Human Breast Cancer Cells and Stimulates Their Proliferation.* Journal of Interferon & Cytokine Research, 1995. **15**(10): p. 905-913.
229. Kellokumpu-Lehtinen, P., et al., *Leukemia-inhibitory factor stimulates breast, kidney and prostate cancer cell proliferation by paracrine and autocrine pathways.* Int J Cancer, 1996. **66**(4): p. 515-9.

230. Li, X., et al., *LIF promotes tumorigenesis and metastasis of breast cancer through the AKT-mTOR pathway.* Oncotarget, 2014. **5**(3): p. 788-801.
231. Douglas, A.M., et al., *Oncostatin M induces the differentiation of breast cancer cells.* International Journal of Cancer, 1998. **75**(1): p. 64-73.
232. Franken, N.A.P., et al., *Clonogenic assay of cells in vitro.* Nature Protocols, 2006. **1**: p. 2315.
233. Liu, J., et al., *Oncostatin M-specific receptor mediates inhibition of breast cancer cell growth and down-regulation of the c-myc proto-oncogene.* Cell Growth Differ, 1997. **8**(6): p. 667-676.
234. Grant, S.L., et al., *Oncostatin M and Leukemia Inhibitory Factor Regulate the Growth of Normal Human Breast Epithelial Cells.* Growth Factors, 2001. **19**(3): p. 153-162.
235. Li, C., et al., *Oncostatin M–induced growth inhibition and morphological changes of MDA-MB231 breast cancer cells are abolished by blocking the MEK/ERK signaling pathway.* Breast Cancer Research and Treatment, 2001. **66**(2): p. 111-121.
236. Liu, J., et al., *ONCOSTATIN M-SPECIFIC RECEPTOR EXPRESSION AND FUNCTION IN REGULATING CELL PROLIFERATION OF NORMAL AND MALIGNANT MAMMARY EPITHELIAL CELLS.* Cytokine, 1998. **10**(4): p. 295-302.
237. West, N.R., J.I. Murray, and P.H. Watson, *Oncostatin-M promotes phenotypic changes associated with mesenchymal and stem cell-like differentiation in breast cancer.* Oncogene, 2013. **33**: p. 1485.
238. Underhill-Day, N. and J.K. Heath, *Oncostatin M (OSM) cytostasis of breast tumor cells: characterization of an OSM receptor beta-specific kernel.* Cancer Res, 2006. **66**(22): p. 10891-901.
239. Jorcyk, C.L., R.G. Holzer, and R.E. Ryan, *Oncostatin M induces cell detachment and enhances the metastatic capacity of T-47D human breast carcinoma cells.* Cytokine, 2006. **33**(6): p. 323-336.
240. Tawara, K., et al., *HIGH expression of OSM and IL-6 are associated with decreased breast cancer survival: synergistic induction of IL-6 secretion by OSM and IL-1β.* Oncotarget, 2019. **10**(21): p. 2068-2085.
241. Bolin, C., et al., *Oncostatin M Promotes Mammary Tumor Metastasis to Bone and Osteolytic Bone Degradation.* Genes & Cancer, 2012. **3**(2): p. 117-130.
242. Tawara, K., et al., *OSM potentiates preintravasation events, increases CTC counts, and promotes breast cancer metastasis to the lung.* Breast Cancer Res, 2018. **20**(1): p. 53.

243. Johnson, D.E., R.A. O'Keefe, and J.R. Grandis, *Targeting the IL-6/JAK/STAT3 signalling axis in cancer.* Nature Reviews Clinical Oncology, 2018. **15**(4): p. 234-248.
244. Lapeire, L., et al., *Cancer-associated adipose tissue promotes breast cancer progression by paracrine oncostatin M and Jak/STAT3 signaling.* Cancer Res, 2014. **74**(23): p. 6806-19.
245. Tawara, K., et al., *Co-Expression of VEGF and IL-6 Family Cytokines is Associated with Decreased Survival in HER2 Negative Breast Cancer Patients: Subtype-Specific IL-6 Family Cytokine-Mediated VEGF Secretion.* Transl Oncol, 2019. **12**(2): p. 245-255.
246. Garbers, C., et al., *Plasticity and cross-talk of Interleukin 6-type cytokines.* Cytokine & Growth Factor Reviews, 2012. **23**(3): p. 85-97.
247. Boulanger, M.J. and K.C. Garcia, *Shared Cytokine Signaling Receptors: Structural Insights from the Gp130 System*, in *Advances in Protein Chemistry*. 2004, Academic Press. p. 107-146.
248. Huynh, J., et al., *Therapeutically exploiting STAT3 activity in cancer — using tissue repair as a road map.* Nature Reviews Cancer, 2019. **19**(2): p. 82-96.
249. Leslie, K., et al., *Differential interleukin-6/Stat3 signaling as a function of cellular context mediates Ras-induced transformation.* Breast Cancer Research, 2010. **12**(5): p. R80.
250. Liang, F., et al., *The crosstalk between STAT3 and p53/RAS signaling controls cancer cell metastasis and cisplatin resistance via the Slug/MAPK/PI3K/AKT-mediated regulation of EMT and autophagy.* Oncogenesis, 2019. **8**(10): p. 59.
251. Sullivan, N.J., et al., *Interleukin-6 induces an epithelial-mesenchymal transition phenotype in human breast cancer cells.* Oncogene, 2009. **28**(33): p. 2940-7.
252. Tawara, K., J.T. Oxford, and C.L. Jorcyk, *Clinical significance of interleukin (IL)-6 in cancer metastasis to bone: potential of anti-IL-6 therapies.* Cancer management and research, 2011. **3**: p. 177-189.
253. Sansone, P., et al., *IL-6 triggers malignant features in mammospheres from human ductal breast carcinoma and normal mammary gland.* J Clin Invest, 2007. **117**(12): p. 3988-4002.
254. Kujawski, M., et al., *Stat3 mediates myeloid cell-dependent tumor angiogenesis in mice.* J Clin Invest, 2008. **118**(10): p. 3367-77.
255. Junk, D.J., et al., *Oncostatin M promotes cancer cell plasticity through cooperative STAT3-SMAD3 signaling.* Oncogene, 2017. **36**(28): p. 4001-4013.
256. Viswanadhapalli, S., et al., *EC359: A First-in-Class Small-Molecule Inhibitor for Targeting Oncogenic LIFR Signaling in Triple-Negative Breast Cancer.* Mol Cancer Ther, 2019. **18**(8): p. 1341-1354.

257. Kleffel, S. and T. Schatton, *Tumor Dormancy and Cancer Stem Cells: Two Sides of the Same Coin?*, in *Systems Biology of Tumor Dormancy*, H. Enderling, N. Almog, and L. Hlatky, Editors. 2013, Springer New York: New York, NY. p. 145-179.
258. Al-Hajj, M., et al., *Prospective identification of tumorigenic breast cancer cells.* Proc Natl Acad Sci U S A, 2003. **100**(7): p. 3983-8.
259. Sheridan, C., et al., *CD44+/CD24-breast cancer cells exhibit enhanced invasive properties: an early step necessary for metastasis.* Breast Cancer Research, 2006. **8**(5): p. R59.
260. Patel, L.R., et al., *Mechanisms of cancer cell metastasis to the bone: a multistep process.* Future Oncol, 2011. **7**(11): p. 1285-97.
261. Ayob, A.Z. and T.S. Ramasamy, *Cancer stem cells as key drivers of tumour progression.* J Biomed Sci, 2018. **25**(1): p. 20.
262. Phillips, T.M., W.H. McBride, and F. Pajonk, *The Response of CD24 −/low /CD44 + Breast Cancer–Initiating Cells to Radiation.* JNCI: Journal of the National Cancer Institute, 2006. **98**(24): p. 1777-1785.
263. Li, X., et al., *Intrinsic Resistance of Tumorigenic Breast Cancer Cells to Chemotherapy.* JNCI: Journal of the National Cancer Institute, 2008. **100**(9): p. 672-679.
264. Moitra, K., H. Lou, and M. Dean, *Multidrug Efflux Pumps and Cancer Stem Cells: Insights Into Multidrug Resistance and Therapeutic Development.* Clinical Pharmacology & Therapeutics, 2011. **89**(4): p. 491-502.
265. Scheel, C., et al., *Paracrine and autocrine signals induce and maintain mesenchymal and stem cell states in the breast.* Cell, 2011. **145**(6): p. 926-40.
266. Dontu, G., et al., *Role of Notch signaling in cell-fate determination of human mammary stem/progenitor cells.* Breast Cancer Res, 2004. **6**(6): p. R605-15.
267. Liu, S., et al., *Hedgehog signaling and Bmi-1 regulate self-renewal of normal and malignant human mammary stem cells.* Cancer Res, 2006. **66**(12): p. 6063-71.
268. Zardawi, S.J., et al., *Dysregulation of Hedgehog, Wnt and Notch signalling pathways in breast cancer.* Histol Histopathol, 2009. **24**(3): p. 385-98.
269. Boulanger, C.A., K.-U. Wagner, and G.H. Smith, *Parity-induced mouse mammary epithelial cells are pluripotent, self-renewing and sensitive to TGF-β1 expression.* Oncogene, 2004. **24**: p. 552.
270. Clarke, R.B., et al., *A putative human breast stem cell population is enriched for steroid receptor-positive cells.* Developmental Biology, 2005. **277**(2): p. 443-456.

271. Dontu, G., et al., *In vitro propagation and transcriptional profiling of human mammary stem/progenitor cells.* Genes Dev, 2003. **17**(10): p. 1253-70.
272. Kritikou, E.A., et al., *A dual, non-redundant, role for LIF as a regulator of development and STAT3-mediated cell death in mammary gland.* Development, 2003. **130**(15): p. 3459-3468.
273. Mukherjee, S., et al., *Hedgehog signaling and response to cyclopamine differ in epithelial and stromal cells in benign breast and breast cancer.* Cancer Biol Ther, 2006. **5**(6): p. 674-83.
274. Ernst, M., et al., *The Carboxyl-terminal Domains of gp130-related Cytokine Receptors Are Necessary for Suppressing Embryonic Stem Cell Differentiation: INVOLVEMENT OF STAT3.* Journal of Biological Chemistry, 1999. **274**(14): p. 9729-9737.
275. Hirai, H., P. Karian, and N. Kikyo, *Regulation of embryonic stem cell self-renewal and pluripotency by leukaemia inhibitory factor.* Biochem J, 2011. **438**(1): p. 11-23.
276. Bourillot, P.Y., et al., *Novel STAT3 target genes exert distinct roles in the inhibition of mesoderm and endoderm differentiation in cooperation with Nanog.* Stem Cells, 2009. **27**(8): p. 1760-71.
277. Yoshida, K., et al., *Maintenance of the pluripotential phenotype of embryonic stem cells through direct activation of gp130 signalling pathways.* Mechanisms of Development, 1994. **45**(2): p. 163-171.
278. Matsuda, T., et al., *STAT3 activation is sufficient to maintain an undifferentiated state of mouse embryonic stem cells.* The EMBO Journal, 1999. **18**(15): p. 4261-4269.
279. Niwa, H., et al., *Self-renewal of pluripotent embryonic stem cells is mediated via activation of STAT3.* Genes Dev, 1998. **12**(13): p. 2048-60.
280. Conover, J.C., et al., *Ciliary neurotrophic factor maintains the pluripotentiality of embryonic stem cells.* Development, 1993. **119**(3): p. 559-65.
281. Rose, T.M., et al., *Oncostatin M (OSM) inhibits the differentiation of pluripotent embryonic stem cells in vitro.* Cytokine, 1994. **6**(1): p. 48-54.
282. Pennica, D., et al., *Cardiotrophin-1. Biological activities and binding to the leukemia inhibitory factor receptor/gp130 signaling complex.* J Biol Chem, 1995. **270**(18): p. 10915-22.
283. Shi, Y., et al., *Targeting LIF-mediated paracrine interaction for pancreatic cancer therapy and monitoring.* Nature, 2019. **569**(7754): p. 131-135.

284. Doherty, M.R., et al., *The opposing effects of interferon-beta and oncostatin-M as regulators of cancer stem cell plasticity in triple-negative breast cancer.* Breast Cancer Research, 2019. **21**(1): p. 54.
285. Clements, M.E. and R.W. Johnson, *PREX1 drives spontaneous bone dissemination of ER+ breast cancer cells.* Oncogene, 2020. **39**(6): p. 1318-1334.
286. Guise, T.A., et al., *Evidence for a causal role of parathyroid hormone-related protein in the pathogenesis of human breast cancer-mediated osteolysis.* J Clin Invest, 1996. **98**(7): p. 1544-9.
287. Johnson, R.W., et al., *Induction of LIFR confers a dormancy phenotype in breast cancer cells disseminated to the bone marrow.* Nat Cell Biol, 2016. **18**(10): p. 1078-1089.
288. Johnson, R.W., et al., *TGF-beta promotion of Gli2-induced expression of parathyroid hormone-related protein, an important osteolytic factor in bone metastasis, is independent of canonical Hedgehog signaling.* Cancer Res, 2011. **71**(3): p. 822-31.
289. Kusuma, N., et al., *Integrin-dependent response to laminin-511 regulates breast tumor cell invasion and metastasis.* Int J Cancer, 2012. **130**(3): p. 555-66.
290. Sowder, M.E. and R.W. Johnson, *Enrichment and detection of bone disseminated tumor cells in models of low tumor burden.* Scientific Reports, 2018. **8**(1): p. 14299.
291. Poillet, L., et al., *QSOX1 inhibits autophagic flux in breast cancer cells.* PLoS One, 2014. **9**(1): p. e86641.
292. Oki, T., et al., *A novel cell-cycle-indicator, mVenus-p27K-, identifies quiescent cells and visualizes G0-G1 transition.* Sci Rep, 2014. **4**: p. 4012.
293. Johnson, R.W., et al., *The Primary Function of gp130 Signaling in Osteoblasts Is To Maintain Bone Formation and Strength, Rather Than Promote Osteoclast Formation.* Journal of Bone and Mineral Research, 2014. **29**(6): p. 1492-1505.
294. Győrffy, B., et al., *An online survival analysis tool to rapidly assess the effect of 22,277 genes on breast cancer prognosis using microarray data of 1,809 patients.* Breast Cancer Research and Treatment, 2010. **123**(3): p. 725-731.
295. Lánczky, A., et al., *miRpower: a web-tool to validate survival-associated miRNAs utilizing expression data from 2178 breast cancer patients.* Breast Cancer Research and Treatment, 2016. **160**(3): p. 439-446.
296. Győrffy, B. and R. Schäfer, *Meta-analysis of gene expression profiles related to relapse-free survival in 1,079 breast cancer patients.* Breast Cancer Research and Treatment, 2009. **118**(3): p. 433-441.

297. Győrffy, B., et al., *TP53 mutation-correlated genes predict the risk of tumor relapse and identify MPS1 as a potential therapeutic kinase in TP53-mutated breast cancers.* 2014. **8**(3): p. 508-519.
298. Mihály, Z., et al., *A meta-analysis of gene expression-based biomarkers predicting outcome after tamoxifen treatment in breast cancer.* Breast Cancer Research and Treatment, 2013. **140**(2): p. 219-232.
299. Győrffy, B., et al., *RecurrenceOnline: an online analysis tool to determine breast cancer recurrence and hormone receptor status using microarray data.* Breast Cancer Research and Treatment, 2012. **132**(3): p. 1025-1034.
300. Li, Q., et al., *Jetset: selecting the optimal microarray probe set to represent a gene.* BMC Bioinformatics, 2011. **12**(1): p. 474.
301. Ma, X.J., et al., *Gene expression profiling of the tumor microenvironment during breast cancer progression.* Breast Cancer Res, 2009. **11**(1): p. R7.
302. Colak, D., et al., *Age-specific gene expression signatures for breast tumors and cross-species conserved potential cancer progression markers in young women.* PloS one, 2013. **8**(5): p. e63204-e63204.
303. Kuchuk, I., et al., *Incidence, consequences and treatment of bone metastases in breast cancer patients—Experience from a single cancer centre.* Journal of Bone Oncology, 2013. **2**(4): p. 137-144.
304. Coleman, R.E., *Metastatic bone disease: clinical features, pathophysiology and treatment strategies.* Cancer Treatment Reviews, 2001. **27**(3): p. 165-176.
305. Croucher, P.I., M.M. McDonald, and T.J. Martin, *Bone metastasis: the importance of the neighbourhood.* Nat Rev Cancer, 2016. **16**(6): p. 373-86.
306. Salvador, F., A. Llorente, and R.R. Gomis, *From latency to overt bone metastasis in breast cancer: potential for treatment and prevention.* J Pathol, 2019. **249**(1): p. 6-18.
307. Kim, R.S., et al., *Dormancy signatures and metastasis in estrogen receptor positive and negative breast cancer.* PLoS One, 2012. **7**(4): p. e35569.
308. Davis, S., et al., *LIFR beta and gp130 as heterodimerizing signal transducers of the tripartite CNTF receptor.* Science, 1993. **260**(5115): p. 1805-8.
309. Allan, E.H., et al., *Osteoblasts display receptors for and responses to leukemia-inhibitory factor.* J Cell Physiol, 1990. **145**(1): p. 110-9.
310. Lapeire, L., et al., *Cancer-associated adipose tissue promotes breast cancer progression by paracrine oncostatin M and Jak/STAT3 signaling.* Cancer Res, 2014. **74**(23): p. 6806-19.

311. Matsuda, T., et al., *STAT3 activation is sufficient to maintain an undifferentiated state of mouse embryonic stem cells.* Embo j, 1999. **18**(15): p. 4261-9.
312. Li, C., et al., *Oncostatin M-induced growth inhibition and morphological changes of MDA-MB231 breast cancer cells are abolished by blocking the MEK/ERK signaling pathway.* Breast Cancer Res Treat, 2001. **66**(2): p. 111-21.
313. Borowsky, A.D., et al., *Syngeneic mouse mammary carcinoma cell lines: two closely related cell lines with divergent metastatic behavior.* Clin Exp Metastasis, 2005. **22**(1): p. 47-59.
314. Barkan, D., et al., *Inhibition of metastatic outgrowth from single dormant tumor cells by targeting the cytoskeleton.* Cancer Res, 2008. **68**(15): p. 6241-50.
315. Boulanger, M.J., et al., *Hexameric structure and assembly of the interleukin-6/IL-6 alpha-receptor/gp130 complex.* Science, 2003. **300**(5628): p. 2101-4.
316. Taga, T. and T. Kishimoto, *Gp130 and the interleukin-6 family of cytokines.* Annu Rev Immunol, 1997. **15**: p. 797-819.
317. Yin, T., et al., *Involvement of IL-6 signal transducer gp130 in IL-11-mediated signal transduction.* The Journal of Immunology, 1993. **151**(5): p. 2555.
318. West, N.R., *Coordination of Immune-Stroma Crosstalk by IL-6 Family Cytokines.* 2019. **10**(1093).
319. Mosley, B., et al., *Dual oncostatin M (OSM) receptors. Cloning and characterization of an alternative signaling subunit conferring OSM-specific receptor activation.* J Biol Chem, 1996. **271**(51): p. 32635-43.
320. West, N.R., L.C. Murphy, and P.H. Watson, *Oncostatin M suppresses oestrogen receptor-α expression and is associated with poor outcome in human breast cancer.* Endocr Relat Cancer, 2012. **19**(2): p. 181-95.
321. Schröder, J., et al., *Treatment and pattern of bone metastases in 1094 patients with advanced breast cancer – Results from the prospective German Tumour Registry Breast Cancer cohort study.* European Journal of Cancer, 2017. **79**: p. 139-148.
322. Wang, Z., et al., *lncRNA Epigenetic Landscape Analysis Identifies EPIC1 as an Oncogenic lncRNA that Interacts with MYC and Promotes Cell-Cycle Progression in Cancer.* Cancer Cell, 2018. **33**(4): p. 706-720.e9.
323. Bjorge, J., et al., *Simultaneous siRNA Targeting of Src and Downstream Signaling Molecules Inhibit Tumor Formation and Metastasis of a Human Model Breast Cancer Cell Line.* PloS one, 2011. **6**: p. e19309.

324. Chiu, J.-H., et al., *Role of estrogen receptors and Src signaling in mechanisms of bone metastasis by estrogen receptor positive breast cancers.* Journal of Translational Medicine, 2017. **15**(1): p. 97.
325. Defilippi, P., P. Di Stefano, and S. Cabodi, *p130Cas: a versatile scaffold in signaling networks.* Trends Cell Biol, 2006. **16**(5): p. 257-63.
326. Finn, R.S., *Targeting Src in breast cancer.* Annals of Oncology, 2008. **19**(8): p. 1379-1386.
327. Campbell, J.P., et al., *Models of bone metastasis.* J Vis Exp, 2012(67): p. e4260.
328. West, N.R., J.I. Murray, and P.H. Watson, *Oncostatin-M promotes phenotypic changes associated with mesenchymal and stem cell-like differentiation in breast cancer.* Oncogene, 2014. **33**(12): p. 1485-94.
329. Chong, Y.P., et al., *Endogenous and synthetic inhibitors of the Src-family protein tyrosine kinases.* Biochim Biophys Acta, 2005. **1754**(1-2): p. 210-20.
330. Xu, W., et al., *Crystal structures of c-Src reveal features of its autoinhibitory mechanism.* Mol Cell, 1999. **3**(5): p. 629-38.
331. Cowan-Jacob, S.W., et al., *The crystal structure of a c-Src complex in an active conformation suggests possible steps in c-Src activation.* Structure, 2005. **13**(6): p. 861-71.
332. Myoui, A., et al., *C-Src Tyrosine Kinase Activity Is Associated with Tumor Colonization in Bone and Lung in an Animal Model of Human Breast Cancer Metastasis.* Cancer Research, 2003. **63**(16): p. 5028.
333. Kanomata, N., et al., *Clinicopathological significance of Y416Src and Y527Src expression in breast cancer.* J Clin Pathol, 2011. **64**(7): p. 578-86.
334. Zhang, L., et al., *c-Src expression is predictive of poor prognosis in breast cancer patients with bone metastasis, but not in patients with visceral metastasis.* Apmis, 2012. **120**(7): p. 549-57.
335. Sleeman, M.W., et al., *The ciliary neurotrophic factor and its receptor, CNTFRα.* Pharmaceutica Acta Helvetiae, 2000. **74**(2): p. 265-272.
336. Sowder, M.E. and R.W. Johnson, *Bone as a Preferential Site for Metastasis.* JBMR Plus, 2019. **3**(3): p. e10126.
337. Allocca, G., et al., *The bone metastasis niche in breast cancer: potential overlap with the haematopoietic stem cell niche in vivo.* Journal of Bone Oncology, 2019. **17**: p. 100244.
338. Patel, P. and E. Chen, *Cancer stem cells, tumor dormancy, and metastasis.* 2012. **3**(125).
339. Jo, M., et al., *Cell signaling by urokinase-type plasminogen activator receptor induces stem cell-like properties in breast cancer cells.* Cancer Res, 2010. **70**(21): p. 8948-58.

340. Almog, N., *Molecular mechanisms underlying tumor dormancy.* Cancer Lett, 2010. **294**(2): p. 139-46.
341. Ali, H.R., et al., *Cancer stem cell markers in breast cancer: pathological, clinical and prognostic significance.* Breast Cancer Research, 2011. **13**(6): p. R118.
342. Thakur, R., et al., *Inhibition of STAT3, FAK and Src mediated signaling reduces cancer stem cell load, tumorigenic potential and metastasis in breast cancer.* Scientific Reports, 2015. **5**(1): p. 10194.
343. Yue, Z., et al., *LGR4 modulates breast cancer initiation, metastasis, and cancer stem cells.* Faseb j, 2018. **32**(5): p. 2422-2437.
344. Fico, F. and A. Santamaria-Martínez, *TGFBI modulates tumour hypoxia and promotes breast cancer metastasis.* Mol Oncol, 2020. **14**(12): p. 3198-3210.
345. Hu, J., et al., *A CD44v+ subpopulation of breast cancer stem-like cells with enhanced lung metastasis capacity.* Cell Death & Disease, 2017. **8**(3): p. e2679-e2679.
346. Butti, R., et al., *Breast cancer stem cells: Biology and therapeutic implications.* The International Journal of Biochemistry & Cell Biology, 2019. **107**: p. 38-52.
347. Duru, N., et al., *HER2-Associated Radioresistance of Breast Cancer Stem Cells Isolated from HER2-Negative Breast Cancer Cells.* 2012. **18**(24): p. 6634-6647.
348. Wang, Q.-E., *DNA damage responses in cancer stem cells: Implications for cancer therapeutic strategies.* World journal of biological chemistry, 2015. **6**(3): p. 57-64.
349. Ye, X., et al., *Oncostatin M Maintains Naïve Pluripotency of mESCs by Tetraploid Embryo Complementation (TEC) Assay.* Frontiers in Cell and Developmental Biology, 2021. **9**: p. 1341.
350. Omokehinde, T., A. Jotte, and R.W. Johnson, *gp130 Cytokines Activate Novel Signaling Pathways and Alter Bone Dissemination in ER+ Breast Cancer Cells.* J Bone Miner Res, 2021.
351. Senbanjo, L.T. and M.A. Chellaiah, *CD44: A Multifunctional Cell Surface Adhesion Receptor Is a Regulator of Progression and Metastasis of Cancer Cells.* 2017. **5**(18).
352. Ponta, H., L. Sherman, and P.A. Herrlich, *CD44: From adhesion molecules to signalling regulators.* Nature Reviews Molecular Cell Biology, 2003. **4**(1): p. 33-45.
353. Okamoto, I., et al., *CD44 cleavage induced by a membrane-associated metalloprotease plays a critical role in tumor cell migration.* Oncogene, 1999. **18**(7): p. 1435-1446.
354. Chen, C., et al., *The biology and role of CD44 in cancer progression: therapeutic implications.* Journal of Hematology & Oncology, 2018. **11**(1): p. 64.

355. Subramaniam, V., et al., *CD44 regulates cell migration in human colon cancer cells via Lyn kinase and AKT phosphorylation.* Exp Mol Pathol, 2007. **83**(2): p. 207-15.
356. Nam, K., et al., *CD44 regulates cell proliferation, migration, and invasion via modulation of c-Src transcription in human breast cancer cells.* Cell Signal, 2015. **27**(9): p. 1882-94.
357. Jang, J.H., et al., *Breast Cancer Cell-Derived Soluble CD44 Promotes Tumor Progression by Triggering Macrophage IL1β Production.* Cancer Res, 2020. **80**(6): p. 1342-1356.
358. Chen, C., et al., *The biology and role of CD44 in cancer progression: therapeutic implications.* J Hematol Oncol, 2018. **11**(1): p. 64.
359. Sun, H., et al., *CD44+/CD24- breast cancer cells isolated from MCF-7 cultures exhibit enhanced angiogenic properties.* Clin Transl Oncol, 2013. **15**(1): p. 46-54.
360. Paulis, Y.W.J., et al., *CD44 enhances tumor aggressiveness by promoting tumor cell plasticity.* Oncotarget, 2015. **6**(23): p. 19634-19646.
361. Prasad, C.P., et al., *WNT5A signaling impairs breast cancer cell migration and invasion via mechanisms independent of the epithelial-mesenchymal transition.* Journal of Experimental & Clinical Cancer Research, 2016. **35**(1): p. 144.
362. Bellerby, R., et al., *Overexpression of Specific CD44 Isoforms Is Associated with Aggressive Cell Features in Acquired Endocrine Resistance.* Front Oncol, 2016. **6**: p. 145.
363. McFarlane, S., et al., *CD44 increases the efficiency of distant metastasis of breast cancer.* Oncotarget, 2015. **6**(13): p. 11465-76.
364. Li, W., et al., *Unraveling the roles of CD44/CD24 and ALDH1 as cancer stem cell markers in tumorigenesis and metastasis.* Sci Rep, 2017. **7**(1): p. 13856.
365. Liu, S., et al., *Breast cancer stem cells transition between epithelial and mesenchymal states reflective of their normal counterparts.* Stem Cell Reports, 2014. **2**(1): p. 78-91.
366. Covert, H., et al., *OSM-induced CD44 contributes to breast cancer metastatic potential through cell detachment but not epithelial-mesenchymal transition.* Cancer management and research, 2019. **11**: p. 7721-7737.
367. Croker, A.K., et al., *High aldehyde dehydrogenase and expression of cancer stem cell markers selects for breast cancer cells with enhanced malignant and metastatic ability.* J Cell Mol Med, 2009. **13**(8b): p. 2236-52.
368. Croker, A.K. and A.L. Allan, *Inhibition of aldehyde dehydrogenase (ALDH) activity reduces chemotherapy and radiation resistance of stem-like ALDHhiCD44⁺ human breast cancer cells.* Breast Cancer Res Treat, 2012. **133**(1): p. 75-87.
369. Liu, T.J., et al., *CD133+ cells with cancer stem cell characteristics associates with vasculogenic mimicry in triple-negative breast cancer.* Oncogene, 2013. **32**(5): p. 544-553.

370. Moreb, J.S., et al., *The enzymatic activity of human aldehyde dehydrogenases 1A2 and 2 (ALDH1A2 and ALDH2) is detected by Aldefluor, inhibited by diethylaminobenzaldehyde and has significant effects on cell proliferation and drug resistance.* Chemico-Biological Interactions, 2012. **195**(1): p. 52-60.
371. Demir, H., et al., *Prognostic value of aldehyde dehydrogenase 1 (ALDH1) in invasive breast carcinomas.* Bosn J Basic Med Sci, 2018. **18**(4): p. 313-319.
372. Liu, Y., et al., *ALDH1A1 expression correlates with clinicopathologic features and poor prognosis of breast cancer patients: a systematic review and meta-analysis.* BMC Cancer, 2014. **14**(1): p. 444.
373. Ma, F., et al., *Aldehyde dehydrogenase 1 (ALDH1) expression is an independent prognostic factor in triple negative breast cancer (TNBC).* Medicine, 2017. **96**(14): p. e6561-e6561.
374. Wright, M.H., et al., *Brca1 breast tumors contain distinct CD44+/CD24- and CD133+ cells with cancer stem cell characteristics.* Breast Cancer Res, 2008. **10**(1): p. R10.
375. Brugnoli, F., et al., *In triple negative breast tumor cells, PLC-β2 promotes the conversion of CD133high to CD133low phenotype and reduces the CD133-related invasiveness.* Mol Cancer, 2013. **12**: p. 165.
376. Liou, G.-Y., *CD133 as a regulator of cancer metastasis through the cancer stem cells.* The international journal of biochemistry & cell biology, 2019. **106**: p. 1-7.
377. Meyer, M.J., et al., *CD44posCD49fhiCD133/2hi defines xenograft-initiating cells in estrogen receptor-negative breast cancer.* Cancer Res, 2010. **70**(11): p. 4624-33.
378. Boulton, T.G., N. Stahl, and G.D. Yancopoulos, *Ciliary neurotrophic factor/leukemia inhibitory factor/interleukin 6/oncostatin M family of cytokines induces tyrosine phosphorylation of a common set of proteins overlapping those induced by other cytokines and growth factors.* Journal of Biological Chemistry, 1994. **269**(15): p. 11648-55.
379. Sims, N.A. and J.M. Quinn, *Osteoimmunology: oncostatin M as a pleiotropic regulator of bone formation and resorption in health and disease.* Bonekey Rep, 2014. **3**: p. 527.
380. Bao, B., et al., *Overview of cancer stem cells (CSCs) and mechanisms of their regulation: implications for cancer therapy.* Curr Protoc Pharmacol, 2013. **Chapter 14**: p. Unit 14.25.
381. Akiyama, T., C.R. Dass, and P.F.M. Choong, *Bim-targeted cancer therapy: A link between drug action and underlying molecular changes.* Molecular Cancer Therapeutics, 2009. **8**(12): p. 3173.

382. Luo, Y., et al., *High Bak Expression Is Associated with a Favorable Prognosis in Breast Cancer and Sensitizes Breast Cancer Cells to Paclitaxel.* PLoS One, 2015. **10**(9): p. e0138955.